NOS1-mediated Regulation of Macrophage IL-1β and CD40: Mechanisms and Therapeutic Implications in Atherosclerosis

Ph.D. Thesis

By

KUNDAN SOLANKI

MEHTA FAMILY SCHOOL OF BIOSCIENCES AND BIOMEDICAL ENGINEERING

INDIAN INSTITUTE OF TECHNOLOGY INDORE

DECEMBER 2025

NOS1-mediated Regulation of Macrophage IL-1β and CD40: Mechanisms and Therapeutic Implications in Atherosclerosis

A THESIS

Submitted in partial fulfillment of the
requirements for the award of the degree
of
DOCTOR OF PHILOSOPHY

by
KUNDAN SOLANKI

MEHTA FAMILY SCHOOL OF BIOSCIENCES AND BIOMEDICAL ENGINEERING

INDIAN INSTITUTE OF TECHNOLOGY INDORE
DECEMBER 2025

INDIAN INSTITUTE OF TECHNOLOGY INDORE

I hereby certify that the work which is being presented in the thesis entitled **NOS1-mediated Regulation of Macrophage IL-1β and CD40: Mechanisms and Therapeutic Implications in Atherosclerosis** in the partial fulfillment of the requirements for the award of the degree of **DOCTOR OF PHILOSOPHY** and submitted in the **Mehta Family School of Biosciences and Biomedical Engineering, Indian Institute of Technology Indore**, is an authentic record of my own work carried out during the time period from **December 2020** to **December 2025** under the supervision of **Prof. Mirza S. Baig, Professor, Mehta Family School of Biosciences and Biomedical Engineering, Indian Institute of Technology Indore**.

The matter presented in this thesis has not been submitted by me for the award of any other degree of this or any other institute.

14-05-2026

Signature of the student with date
(KUNDAN SOLANKI)

This is to certify that the above statement made by the candidate is correct to the best of my/our knowledge.

14-5-26

Signature of Thesis Supervisor #1 with date
(PROF. MIRZA S. BAIG)

Signature of Thesis Supervisor #2 with date
(NAME OF THESIS SUPERVISOR)

Mr. Kundan Solanki has successfully given his/her Ph.D. Oral Examination held on **14-05-2026**

14-5-26

Signature of Thesis Supervisor #1 with date
(PROF. MIRZA S. BAIG)

Signature of Thesis Supervisor #2 with date
(NAME OF THESIS SUPERVISOR)

ACKNOWLEDGEMENT

As every beautiful chapter comes to an end, this is the ending of one of the chapters of my life. The work required tremendous level of patience, perseverance, resilience and I am grateful to the God and myself for successfully completing this chapter of my life. Before enrolling into PhD program, I was aware of the strength and resilience it would require to complete it, but the difficulties were much higher than expected. This chapter of my life taught me life lessons which I would have never learned if I had not completed the program. It built enough strength in me to tackle the life problems in future. I would like to acknowledge some of the members who played an active role during this period, without which the journey would not be easier.

Foremost, I would like to acknowledge my supervisor Prof. Mirza S. Baig for his guidance and support during the PhD program. I would like to thank and acknowledge my PSPC members Dr. Parimal Kar and Prof. Kiran Bala mam for their support and valuable insights for my PhD project. I would also like to thank the DPGC Convener and Head of the Department for supporting me and providing me guidance during my difficult phase of the research journey. I also share my sincere gratitude to all the faculty members of the Mehta Family School of Biosciences and Biomedical Engineering for providing me valuable guidance during my research program. I extend my sincere gratitude to staff of BSBE office for providing me the necessary research support and in documentation process. Further, I would like to acknowledge the confocal microscopy facility at the Sophisticated Instrumentation Centre (SIC), IIT Indore for providing me the technical and analytical support for my work. Special thanks go to Dr. Ravindra Kumar for his technical support and helping in the analysis of my results.

I would also like to thank the lab members, my friends and colleagues who played an instrumental role during my journey. I would like to thank my senior Dr. Sajjan Rajpoot for providing me necessary guidance to

navigate through this phase of my life and helping with the technical and non-technical stuff. My sincere gratitude goes to Dr. Anjali Roy for helping with the experimental work whenever I felt stuck in the research. I would like to acknowledge my other lab members Mr. Khandu Wadhonkar, Mr. Pramod Patidar, Mr. Rajat Atre, Mr. Sk Rameez Raza, Ms. Krishma Bajaj, Mr. Shubham Kumar Behera, Mr. Anil Prajapati, Ms. Shreya Bharti, Mr. Rohit Saha, Mr. Manvir and Mr. Evans Akimat for providing their valuable suggestions and inputs in my research. My special thanks go to Mr. Shubham Kumar Behera for providing me his helping hand in my experimental work. My thanks go to all the current and past MSc students and interns in my lab who helped me with their necessary inputs and guidance during this journey. My sincere thanks go to Mr. Lateefur Rahman Khan for his valuable support in documentation process so that we could focus on our research. His guidance and wisdom played an instrumental role during this journey. I would also like to acknowledge Ms. Bushra for providing us her helping hand in the same process. I would also like to extend my thanks to my friends and colleagues Dr. Krishna Singh, Mr. Rahul Chaudhari and Mrs. Raveena Dhore. These three individuals played a crucial role during my research journey by providing their words of wisdom and motivating and inspiring me during this journey. I was fortunate to have friends like them who constantly encouraged me in pursuing my research goals.

I would like this opportunity to give my sincere thanks and gratitude to my mentor Dr. Tanmoy Bhowmick who provided and helped me with the necessary inputs during this research journey. His words of wisdom and guidance drove me forward and inspired me to attain my desired goals.

Lastly, I would like to provide my sincere thanks and gratitude to my parents and my family for their encouragement and support during this journey. Words would not be enough to show my gratitude to my mom, Dad and my brothers. They were actively involved in every phase of this journey with me. Their constant words of encouragement, wisdom and belief in me motivated me to keep on my pursuit of achieving my

objectives and instilled in me the attitude of never giving up. The journey would be incomplete without acknowledging my fiancé. She was the main pillar who supported and encouraged me during this research journey. Her wisdom and guidance helped me navigate through this phase. Her belief in me instilled positive attitude in me to tackle various challenges during the journey. My special thanks also go to my in-laws who believed in me and supported me during this journey.

At last, I would like to bow my head and sincerely thanks and express my gratitude to almighty god. His blessings and guidance helped me in navigating during this phase of my life. Lastly, I sincerely apologise if I have missed to acknowledge anyone. Your guidance and wisdom were instrumental in my research journey.

I am grateful for completing this journey and excited to venture what lies ahead in future.

-KUNDAN SOLANKI

DEDICATED TO MY BELOVED PARENTS AND MY FIANCÉ

SYNOPSIS

1. Background and Rationale for the study:

Atherosclerosis is a chronic inflammatory disease of the arterial vessel wall and remains the leading cause of morbidity and mortality worldwide. The pathogenesis of the disease is complex, involving endothelial dysfunction and a persistent inflammatory response driven by immune cells, particularly macrophages [1]. Macrophage plays a dual role in the disease pathogenesis, by initially clearing lipids to form foam cells, but subsequently contributing to the instability of the plaque by release of proinflammatory mediators [2].

The inflammatory cascade within the atherosclerotic plaque is tightly regulated by various signalling molecules. Among these, the pro-inflammatory cytokine Interleukin-1 beta (IL-1β) and the co-stimulatory molecule CD40, along with its ligand CD40L, are recognised as a critical driver for the disease progression. IL-1β, in particular, promotes endothelial activation, recruitment of leukocyte, and plaque rupture, while the CD40-40L axis mediates the cross-talk between immune cells and endothelial cells, further amplifying the inflammatory and thrombotic environment [3,4]

Nitric Oxide Synthases (NOSs) are a family of enzymes that produce Nitric Oxide (NO), a crucial signalling molecule in the cardiovascular system. Neuronal Nitric Oxide Synthase (NOS1, or nNOS) is typically associated with the neuronal function but is increasingly recognized for its non-neuronal roles, including immune regulation [5]. The present study is based on the hypothesis that NOS1-mediated signalling in macrophages may act as a key regulatory mechanism in generating the inflammatory phenotype, specifically by controlling the expression of key molecules such as IL-1β and the CD40 receptor. Understanding this regulatory mechanism is crucial for identifying novel therapeutic targets that

can serve as stabilizers of atherosclerotic plaques and prevent adverse cardiovascular events.

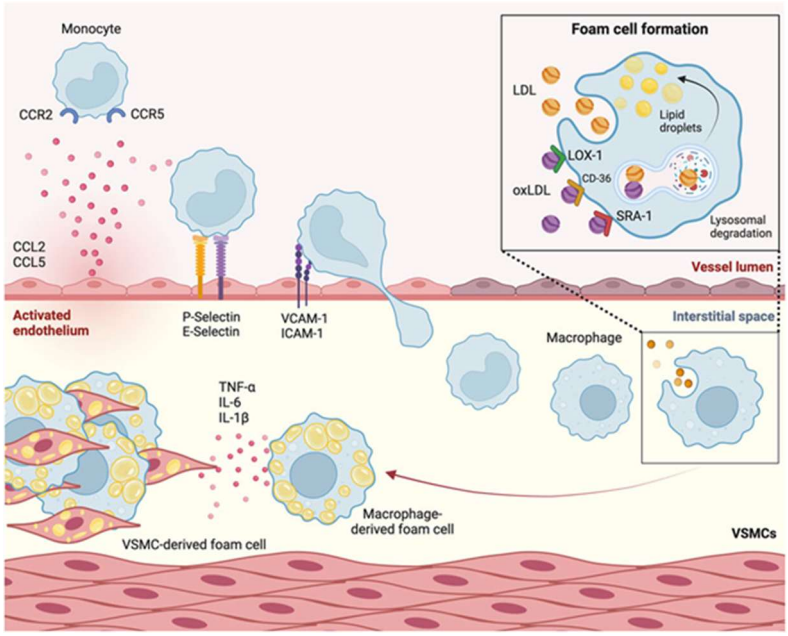

Annink, Maxim E., et al Frontiers in Cell and Developmental Biology 12 (2024): 1446758

Structure of the Synopsis

This synopsis summarises the proposed research work, which is structured into three main aims. The first aim investigates the fundamental role of NOS1 in macrophage foam cell formation and expression of inflammatory markers. The second aim explores the downstream effects of NOS1-regulated IL-1β on the functioning of the endothelial cell. The third aim focuses on the therapeutic aspects by identifying small molecule inhibitors and peptide/peptidomimetics targeting the IL-1β/IL-1R1 and CD40/CD40L signalling axes. The synopsis is organised as follows: **Section 2** presents the current review of the literature in the field; **Section 3** details the research gap and hypothesis; **Section 4** specifies the research objectives; **Section 5** provides the structure of the chapters; **Section 6** provides a chapter-wise summary of the proposed thesis and **Section 7** lists the references for the study.

2. Review of literature

2.1. Macrophage polarisation and foam cell formation in Atherosclerosis

The transformation of macrophages into lipid-laden foam cells is a hallmark of atherosclerosis progression. The process is driven by the unregulated uptake of modified lipoproteins, primarily oxidised low-density lipoproteins (oxLDL). Macrophages within the plaque exist in two different states, mainly pro-inflammatory (M1) and anti-inflammatory (M2). The M1 phenotype is characterised by high expression of pro-inflammatory cytokines such as IL-1β, which is detrimental to the stability of the plaque. The literature strongly supports that modulating the macrophage phenotype is a promising strategy for atherosclerosis therapy[2].

2.2. Role of IL-1β and CD40-40L dyad:

Interleukin-1 beta (IL-1β): IL-1β is a potent pro-inflammatory cytokine whose activity is tightly controlled by the inflammasome complex. Its binding to the IL-1 Receptor Type 1 (IL-1R1) on the endothelial cells and other immune cells initiates a signalling cascade, including the MAPK and NF-κB pathways, thereby leading to the increase in vascular permeability and inflammation. Clinical trials, such as the CANTOS trial which targeted IL-1β, have validated the therapeutic potential of this pathway in reducing the risk of cardiovascular disease [3]

CD40-40L Interaction: The CD40-40L dyad is a critical mediator for the activation of B-cell and T-cell, but its role in innate immunity and vascular inflammation is equally significant. CD40 is expressed on the macrophages, endothelial cells, and smooth muscle cells, while CD40L is expressed on the activated T-cells and platelets. Their interaction promotes the

release of matrix metalloproteinases (MMPs) and tissue factors thereby contributing to the plaque erosion and thrombosis [4].

2.3. The Emerging Role of NOS1 in Macrophage Biology

While endothelial NOS (eNOS) and inducible NOS (iNOS) are well-studied in the context of vascular biology and inflammation, the role of neuronal NOS (NOS1) in macrophage-driven atherosclerosis is less understood. Preliminary evidence suggests that NOS1 is expressed in macrophages and may be involved in the regulation of the inflammatory responses [6]. The phosphorylation and activation of NOS1 could serve as a novel regulatory checkpoint for the inflammatory mediators, bridging the gap between cellular stress and production of cytokine [5]. The current literature lacks a definitive mechanistic link between the NOS1 activation and the downstream regulation of IL-1β and CD40 expression in the macrophages.

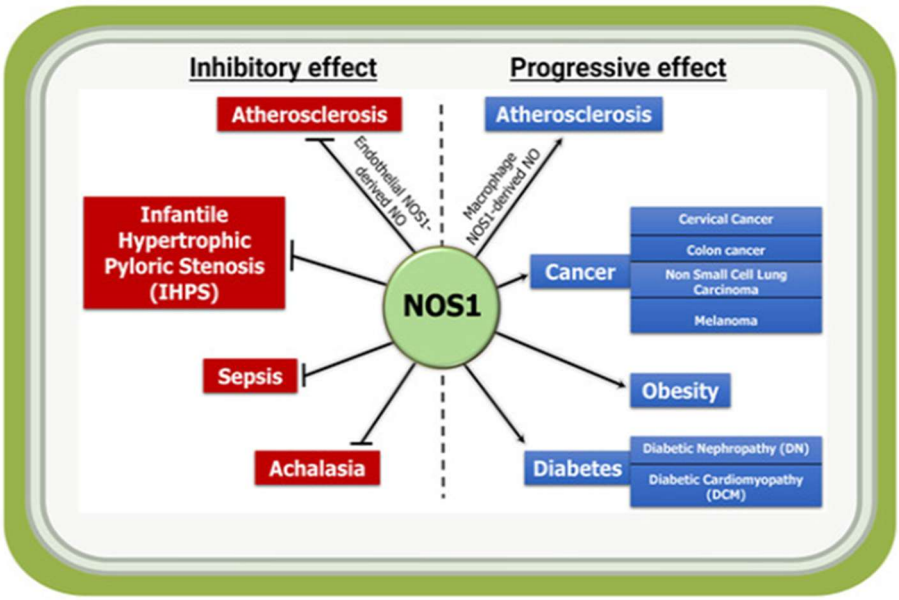

Solanki, K.S. et. al. PeerJ. 2022, 10:e13651

3. Research Gap and Hypothesis

3.1. Research Gap

Despite extensive research, a critical gap remains in the understanding of the upstream regulatory mechanisms that control the simultaneous expression of the key inflammatory mediators such as IL-1β and CD40 in the atherosclerotic macrophages. Also, targeting NOS1 is not beneficial as it plays important role in functioning of brain as well in maintaining the general physiology of heart, kidney and of gastrointestinal tract. Therefore, targeting the molecules expressed through NOS1 can be seen as a better therapeutic approach. As a result, there lies following research gaps:

1. The precise role of NOS1 in macrophage foam cell formation and the subsequent activation of inflammatory response is not fully elucidated.
2. The mechanistic link between NOS1 activation and the expression of IL-1β and CD40 in macrophages remains unknown.
3. There is a lack of targeted therapeutic interventions that specifically modulate the IL-1β/IL-1R1 and CD40/CD40L pathways.

3.2. Hypothesis

Therefore, the current hypothesis is: **NOS1-mediated signalling in macrophages acts as a key regulatory mechanism promoting the pro-inflammatory phenotype by upregulating the expression of IL-1β and CD40 receptor, and the therapeutic intervention targeting the IL-1β/IL-1R1 and CD40/CD40L interactions can effectively mitigate the vascular inflammation and endothelial dysfunction in atherosclerosis**

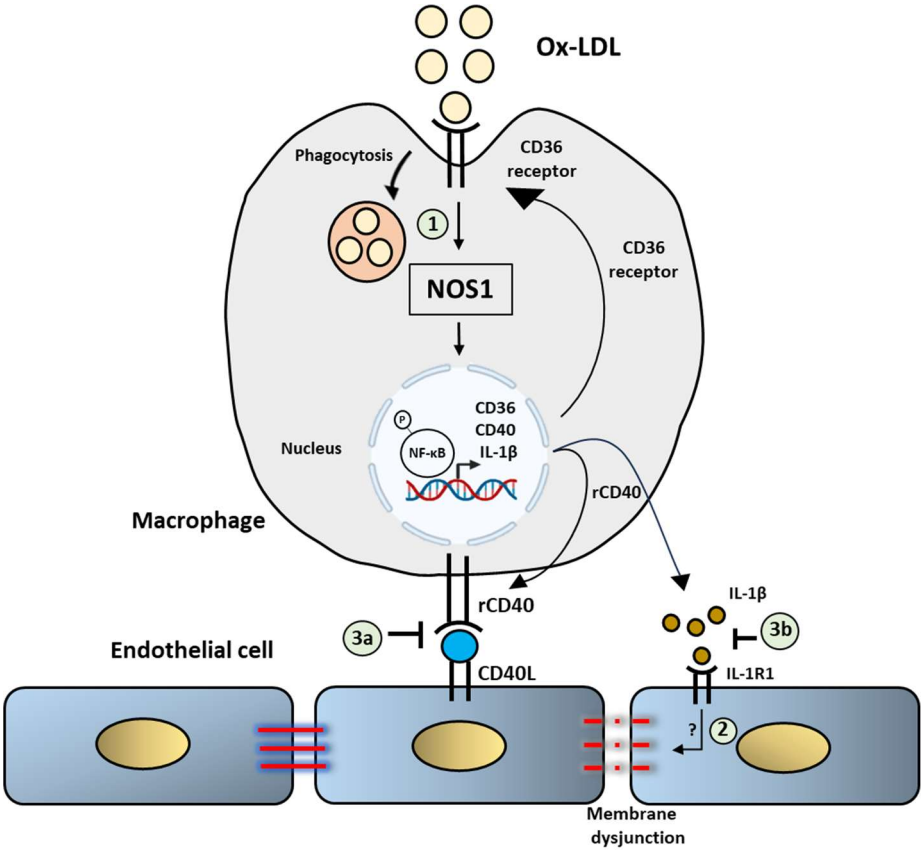

4. Scope and Objectives of the Study

The overall goal of this research is to elucidate the NOS1-mediated inflammatory pathway in macrophages and endothelial cells and to develop therapeutic strategies against key inflammatory molecules.

To study this, following objectives were accomplished:

Aim 1: To study the role of NOS1 in foam cell formation and expression of inflammatory markers in macrophage.

- 1.1. Investigating the effect of NOS1 modulation (activation/inhibition) on macrophage foam cell formation using Oil Red O (ORO) staining.

- 1.2. Quantifying the expression of pro-inflammatory cytokines (e.g., IL-1β, TNF-α) and the levels of NOS1 phosphorylation and nitric oxide production in macrophage.

Aim 2: To study the effect of NOS1 mediated activation of IL-1β on the endothelial cell.

- 2.1. Characterising the effect of OxLDL-stimulated conditioned media from macrophage on the endothelial cell permeability by analysing junction proteins and Transendothelial Electrical Resistance (TEER) analysis.
- 2.2. Determining the IL-1β mediated molecular mechanism leading to the endothelial dysfunction, focusing on the activation of MAPK and NF-κB signalling axis.

Aim 3: To design a therapeutic intervention by targeting key inflammatory modulators involved in atherosclerosis

- 3.1. To identify/repurpose a therapeutic molecule(s) against the IL-1β-IL-1R1 interaction on the endothelial cells using in-silico screening and in-vitro validation.
- 3.2. To identify peptide/peptidomimetics as a therapeutic intervention against the CD40-40L interaction using molecular docking, molecular dynamics (MD) simulations and ADMET analysis.

5. Summary of the chapters:

The complete research work is structured into the following chapters:

Chapter 1: Introduction

Chapter 1 provides the introductory context of the thesis. The chapter provides a comprehensive overview of the atherosclerosis pathogenesis, focusing on the crucial role of macrophage-mediated inflammatory response, foam cell formation and endothelial dysfunction. It also discusses about the role of reactive oxygen species and reactive nitrogen species in atherosclerosis and in macrophages.

Chapter 2: Literature review

The current chapter discuss about the Nitric Oxide synthase (NOS) and different types of NOS. Regulation and expression of Nitric Oxide synthase 1 (NOS1) is also discussed. Furthermore, it discusses about the role of NOS1 in different diseases such as Cancer, Diabetes, Obesity and other inflammatory diseases. The chapter further discusses about the role of IL-1β and CD40-40L interaction in atherosclerosis. It concludes by discussing the role of macrophage CD36 in atherosclerosis.

Chapter 3: Role of NOS1 in macrophage inflammatory phenotype and foam cell formation

This chapter presents the experimental findings addressing the Aim 1, focusing on the role of NOS1 activation in macrophage stimulated by OxLDL. It highlights the finding that NOS1 activity is directly correlated with the foam cell formation and subsequent activation of inflammatory response. Key results highlight the upregulation of pro-inflammatory cytokines such as IL-1β and TNF-α in response to

OxLDL-stimulated macrophage. A clear correlation with the production of pro-inflammatory cytokines and phosphorylation of NOS1 with simultaneous production of nitric oxide was detected. The chapter establishes the importance of NOS1 as a novel upstream regulator of macrophage-driven inflammation in disease progression.

Chapter 4: NOS1 mediated IL-1β activation and small molecule inhibitors targeting IL-1β and IL-1R1 interaction

This chapter addresses the findings related to Aim 2, investigating the downstream effect of NOS1-regulated IL-1β on the endothelial cells. Treatment of the recombinant IL-1β on the endothelial cell led to significant decrease in the Transendothelial Electrical Resistance (TEER) measurement and in the VE-Cadherin expression. Identification of the molecular mechanism shows that IL-1β triggers endothelial dysfunction through robust activation of key signalling pathways, specifically MAPK and NF-κB. This chapter also addresses the computational and experimental findings from Aim 3.1. In-silico screening, ADMET analysis and MD simulations data identified two drugs: Lomitapide and Radotinib as a potent small molecule inhibitor for the IL-1β-IL-1R1 interaction. It includes molecular docking and MM-PBSA analysis, followed by the in-vitro validation showing that the identified compounds significantly supress the IL-1β-induced signalling axis and restore the endothelial function, thereby confirming their therapeutic potential.

Chapter 5: Design/Identification of Peptide/Peptidomimetics inhibitors targeting the CD40-40L interaction

This chapter focuses on the work from Aim 3.2., highlighting the design and/or identification of novel therapeutic entities against the CD40-40L axis. The chapter includes designing of the peptide

inhibitor (p-KGYY) followed by the docking, ADMET analysis and MD simulation with the receptor. This was followed by the identification of peptidomimetics inhibitor and its derivatives to increase the therapeutic potential against the receptor. Further, ADMET analysis justified the identification of the peptidomimetic derivatives as a promising lead compound to target the CD40-40L signalling axis.

Chapter 6: Summary, Conclusions and Future Directions

This chapter provides the summary of the major findings across all the experimental chapters. It confirms the central hypothesis that the NOS1/IL-1β/CD40 signalling axis is a critical target for atherosclerosis. The chapter discusses the limitations of the in-silico and in-vitro studies and proposes future research directions, primarily focusing on the in-vivo validation and clinical translation of the identified therapeutic candidates.

6. References:

[1] P. Libby, J.E. Buring, L. Badimon, G.K. Hansson, J. Deanfield, M.S. Bittencourt, L. Tokgözoğlu, E.F. Lewis, Atherosclerosis, Nat Rev Dis Primers 5 (2019) 56. https://doi.org/10.1038/s41572-019-0106-z.

[2] P. Hou, J. Fang, Z. Liu, Y. Shi, M. Agostini, F. Bernassola, P. Bove, E. Candi, V. Rovella, G. Sica, Q. Sun, Y. Wang, M. Scimeca, M. Federici, A. Mauriello, G. Melino, Macrophage polarization and metabolism in atherosclerosis, Cell Death Dis 14 (2023) 691. https://doi.org/10.1038/s41419-023-06206-z.

[3] P. Libby, Interleukin-1 Beta as a Target for Atherosclerosis Therapy, Journal of the American College of Cardiology 70 (2017) 2278–2289. https://doi.org/10.1016/j.jacc.2017.09.028.

[4] L.A. Bosmans, L. Bosch, P.J.H. Kusters, E. Lutgens, T.T.P. Seijkens, The CD40-CD40L Dyad as Immunotherapeutic Target in Cardiovascular Disease, J. of Cardiovasc. Trans. Res. 14 (2021) 13–22. https://doi.org/10.1007/s12265-020-09994-3.

[5] K. Solanki, S. Rajpoot, E.E. Bezsonov, A.N. Orekhov, R. Saluja, A. Wary, C. Axen, K. Wary, M.S. Baig, The expanding roles of neuronal nitric oxide synthase (NOS1), PeerJ 10 (2022) e13651. https://doi.org/10.7717/peerj.13651.

[6] A. Roy, U. Saqib, K. Wary, M.S. Baig, Macrophage neuronal nitric oxide synthase (NOS1) controls the inflammatory response and foam cell formation in atherosclerosis, International Immunopharmacology 83 (2020) 106382. https://doi.org/10.1016/j.intimp.2020.106382.

List of Publications

- **Thesis**

1. **Solanki K,** Rajpoot S, Bezsonov EE, Orekhov AN, Saluja R, Wary A, Axen C, Wary K, Baig MS. The expanding roles of neuronal nitric oxide synthase (NOS1). *PeerJ.* 2022 Jul 7;10: e13651. doi: 10.7717/peerj.13651.

2. **Solanki K,** Kumar A, Khan MS, Karthikeyan S, Atre R, Zhang KYJ, Bezsonov E, Abukhov AG, Baig MS. Novel peptide inhibitors targeting CD40 and CD40L interaction: A potential for atherosclerosis therapy. *Current Res in Struc Biology*. 2023; 6:100110. doi: 10.1016/j.crstbi.2023.100110

3. **Solanki K**, Atre R, Sharma R, Bezsonov E, Baig MS. Small Molecule Inhibitors Targeting Endothelial IL-1β Receptor (IL-1R1): A Novel Approach to Atherosclerosis Therapy. *Austin J Pharmacol Ther*. 2023; 11(1): 1170

4. **Solanki, K**., Bezsonov, E., Orekhov, A., Parihar, S. P., Vaja, S., White, F. A., Obukhov, A. G., & Baig, M. S. (2024). Effect of reactive oxygen, nitrogen, and sulfur species on signaling pathways in atherosclerosis. *Vascular pharmacology*, *154*, 107282. https://doi.org/10.1016/j.vph.2024.107282

5. **Solanki, K**., Raja SkR., Samanta, S., Shishira, PS., Roy A., Kar, P., Biswas, S., Ramkumar, KM., Baig, MS., Modulating IL-1β-induced pro-atherogenic endothelial responses through drug repurposing. *Immunopharmacology*. 2026; 34(4):1-16. https://doi.org/10.1007/s10787-026-02229-y

- **Others:**

1. Li J, Wang Y, **Solanki K**, Atre R, Lavrijsen M, Pan Q, Baig MS, Li P. Nirmatrelvir exerts distinct antiviral potency against different human coronaviruses. Antiviral Res. 2023 Feb 14; 211:105555

2. Rajpoot S*, **Solanki K***, Kumar A, Zhang KYJ, Pullamsetti SS, Savai R, Faisal SM, Pan Q, Baig MS. In-Silico Design of a Novel Tridecapeptide Targeting Spike Protein of SARS-CoV-2 Variants of Concern. Int J Pept Res Ther. 2022;28(1):28. doi: 10.1007/s10989-021-10339-0. Epub 2021 Dec 13.

   *(*Contributed equally)*

3. Baig, M.S., Rajpoot, S., Ohishi, T., Savai, R., Seidel, S., Kamennaya, N.A., Bezsonov, E.E., Orekhov, A.N., Mahajan, P., **Solanki, K**. and Saqib, U., 2022. Anti-lung cancer properties of cyanobacterial bioactive compounds. Archives of Microbiology, 204(10), p.603

4. **Solanki K***, Rajpoot S*, Kumar A, J Zhang KY, Ohishi T, Hirani N, Wadhonkar K, Patidar P, Pan Q, Baig MS. Structural analysis of spike proteins from SARS-CoV-2 variants of concern highlighting their functional alterations. Future virology. 2022 Oct 1;17(10):723-32.

   *(*Contributed equally)*

5. Wang, Y., Li, P., **Solanki, K.,** Li, Y., Ma, Z., Peppelenbosch, M. P., Baig, M. S., & Pan, Q. (2021). Viral polymerase binding and broad-spectrum antiviral activity of molnupiravir against human seasonal coronaviruses. *Virology*, *564*, 33–38.

6. Atre, R., Sharma, R., Vadim, G., **Solanki, K**., Wadhonkar, K., Singh, N., Patidar, P., Khabiya, R., Samaur, H., Banerjee, S., & Baig, M. S. (2023). The indispensability of macrophage adaptor

proteins in chronic inflammatory diseases. International immunopharmacology, 119, 110176. (IF: 5.7)

7. Hussain, S., Sabiruddin, K., Patidar, P., **Solanki, K.,** & Baig, M. S. (2024). In vitro bioactivity and biocompatibility behaviour of atmospheric plasma sprayed Indian clam seashell derived hydroxyapatite coating on Ti-alloy. *Journal of Alloys and Compounds*, *976*, 173132.

List of Figures

Chapter 1. Introduction

Chapter 2: Literature review

Chapter 4: NOS1 mediated IL-1β activation and small molecule inhibitors targeting IL-1β and IL-1R1 interaction

LIST OF TABLES

NOMENCLATURE

Da- Kilo Dalton

μg/ml- Microgram per millilitre

ng/ml- Nanogram per millilitre

μM- Micro molar

U/ml- Unit per millilitre

°C- Centigrade

%- Percentage

min- Minutes

h- Hour

mM- Milli molar

μg- Microgram

ACRONMYS

CVD – cardiovascular disease

CAD- coronary artery disease

PAD- peripheral arterial disease

CVA- cerebrovascular accidents

ASCVD- atherosclerotic cardiovascular diseases

MI- myocardial infarction

LDL- low-density lipoproteins

ECM- extracellular matrix proteins

VCAM-1- vascular cell adhesion molecule

ICAM-1- inter-cellular adhesion molecule

IFN-γ- interferon-gamma

LPS- lipopolysaccharides

iNOS- inducible nitric oxide synthase

NO- nitric oxide

TGF-β- transforming growth factor-beta

SRA- scavenger receptor type A

SREBP- sterol-regulatory element binding pathway

ACAT- acyl-CoA: cholesterol ester transferase

IL-1β- Interleukin-1 beta

IL-1R1- interleukin-1 receptor type 1

IL-1RAcP- interleukin-1 receptor accessory protein

IRAK- interleukin-1 receptor-associated kinases

MAPK- mitogen-activated protein kinases

VSMC- vascular smooth muscle cells

APC- antigen presenting cells

PARP- poly-ADP-ribose polymerase

SOD- Superoxide dismutase

nNOS- neuronal nitric oxide synthase

NOS1- nitric oxide synthase-1

eNOS- endothelial NOS

NOS3- nitric oxide synthase-3

EC- endothelial cell

ORF- open reading frame

TF- transcription factor

KLF2/KLF4- Kruppel Like Factor-2 and -4

HRE- Hypoxia Response Element

GFP- green fluorescent protein

TNF- tumor necrosis factor

SER- smooth endoplasmic reticulum

LTCC- L-type Ca^{2+} channel

RyR- ryanodine receptor

XOR- Xanthine oxido-reductase

CIMT- carotid intima-media thickness

SNP- single nucleotide polymorphism

TEER- Transendothelial Electrical Resistance

MD- molecular dynamics

DNA-PK- DNA-dependent protein kinase

ABCG2- adenosine triphosphate (ATP)-binding cassette sub-family G member 2

IFN- interferon

ISG- interferon-stimulated genes

PBMC- peripheral blood mononuclear cells

HDAC2- Histone deacetylase 2

NSCLC- non- small cell lung carcinoma

ROS- reactive oxygen species

SIRT3- Sirtuin 3

DM- Diabetes mellitus

GFR- glomerular filtration rate

DN- Diabetes nephropathy

TGF- tubuloglomerular feedback

SMTC- S-methyl-l-thiocitrulline

DCM- diabetic cardiomyopathy

BH4- tetrahydrobiopterin

7-NI- 7-nitroindazole

IHPS- Infantile hypertrophic pyloric stenosis

Ox-LDL- oxidised low-density lipoprotein

qPCR- quantitative polymerase chain reaction

BSA- bovine serum albumin

RIPA- radioimmunoprecipitation

HUVEC- human umbilical vein endothelial cell

PDB- Protein data bank

GAFF2- General Amber Force Field 2

PME- particle mesh Ewald

MM-PBSA- molecular mechanics Poisson–Boltzmann surface area

MTT- 3-(4,5-dimethylthiazol-2-yl)-2,5-diphenyltetrazolium bromide

RoG- radius of gyration

RMSD- root mean square deviation

RMSF- root mean square fluctuation

SASA- Solvent accessible surface area

CML- chronic myeloid leukemia

TKI- tyrosine kinase inhibitor

ApoB- Apolipoprotein B

CD40R- Cluster of differentiation 40 receptor

CD40L- Cluster of differentiation 40 ligand

PPI- protein-protein interactions

DILI- Drug-induced liver injury

Table of Contents

CHAPTER 1

INTRODUCTION

1.1. Atherosclerosis

Atherosclerosis is a chronic inflammatory disease in which plaque builds up inside the wall of the arteries. It is the main driving force behind cardiovascular disease (CVD) and vascular diseases such as coronary artery disease (CAD), peripheral arterial disease (PAD), cerebrovascular accidents (CVAs), aortic atherosclerotic disease, and others [1]. Collectively, these diseases are termed as atherosclerotic cardiovascular diseases (ASCVD). ASCVD is the leading cause of death worldwide [2]. The main component of the disease formation is the accumulation of lipid and inflammation of the large arteries, which eventually may lead to its clinical complications, such as myocardial infarction (MI) and stroke [3]. Atherosclerotic lesions are characterized by lifelong accumulation and transformation of lipids, inflammatory cells, smooth muscles cells, and necrotic cell debris in the intimal space underneath the endothelial cell monolayer that line the interior vessel wall [3]. Overtime, lesions can become unstable which leads to its rupture resulting in the formation of local clot and obstructing the blood flow in the large arteries, thereby leading to MI. Alternatively, the clot can escape the heart and travel towards brain where it may cause stroke. [3]

Over the last few decades, there has been increased awareness regarding the importance of inflammation and activation of inflammatory process in the development of atherosclerosis. Immune cells such as monocytes, T-cells and B- cells plays an important role in the development of the disease. Both innate and adaptive immunity has found be play a central role in the pathogenesis of the disease progression. [4]

1.2. Process of atherosclerosis development:

1.2.1. Retention and modification of lipoproteins:

The initial step in the development of atherosclerosis is the accumulation of low-density lipoproteins (LDL) that becomes accumulated in the subendothelial space by adhering to the

extracellular matrix proteins (ECM) rich in proteoglycans. Permeability to the endothelial cell results in the accumulation of the LDL inside the lumen. Once inside the sub-intimal space, LDL undergo modification and becomes aggregated and /or oxidised. The aggregated LDL undergoes pinocytosis or phagocytosis by the immune cells present in the subendothelial space. The presence of reactive oxygen species and enzymes such as lipoxygenases and myeloperoxidase modify the phospholipid and protein component of the LDL particle, thereby leading to their uptake by the scavenger receptor present on the immune cells. [3]

1.2.2. Recruitment of monocytes and its differentiation into macrophages

Various stimuli such as dyslipidaemia, smoking, hypertension, viruses and abnormal blood flow lead to endothelial damage. In the presence of damaging stimuli, the endothelium responds by upregulating the transcriptional factor NF-κB and releasing a series of factors that enhance the adhesion of leukocytes on the endothelium such as E-selectin, vascular and inter-cellular adhesion molecules (VCAM-1 and ICAM-1), as well as pro-coagulant factors. Rolling leukocytes adhere to the endothelium and penetrate beneath the endothelial layer to reach the subintimal space. Modified LDL are taken up by tissue resident dendritic cells and macrophages in the arterial lumen. Expression of ICAM-1 on the endothelium leads to monocytes attachment which then migrate to the intima. In the subendothelial space, monocyte differentiate into macrophage and engulf modified LDL, thereby leading to storage of cholesterol inside as lipid droplets and giving macrophage a foam-like appearance. Production of foam cells further leads to release of cytokines and chemokines leading to further recruitment of immune cells, and activating the inflammatory response. [3]

1.3. Role of macrophage in disease pathogenesis

Macrophages are crucial components of the immune system with diverse functions in both innate and adaptive immunity. Macrophages are present in various tissues throughout the body and act as a sentinel cell by surveying their microenvironment for the presence of cellular debris and pathogens. Upon encountering the foreign particles, macrophage undergoes phagocytosis which engulf the foreign pathogens inside the cells. Macrophage secrete a range of cytokines and chemokines that modulate the inflammation and recruit other immune cells to the site of infection or injury [5].

Based on their activation state, macrophages can be broadly classified into two main subtypes: classically activated M1 macrophages and alternatively activated M2 macrophages. M1 macrophages are classically activated by proinflammatory cytokines such as interferon-gamma (IFN-γ) and lipopolysaccharides (LPS). They produce high level of proinflammatory cytokines such as IL-1β, TNF-α and IL-6. M1 macrophages also produces high level of inducible nitric oxide synthase (iNOS), which produces high level of nitric oxide (NO) that contribute to tissue damage and oxidative stress [6]. M1 macrophages are located in the shoulder region of the atherosclerotic plaque, where they are exposed to proinflammatory stimuli and contribute to plaque destabilization by promoting degradation of matrix and formation of necrotic core. [7] M2 macrophages, on the other hand, are alternatively activated by anti-inflammatory cytokines such as interleukin-4 (IL-4) and IL-13. They produce high levels of anti-inflammatory cytokines such as IL-10, and transforming growth factor-beta (TGF-β). M2 macrophages also express scavenger receptors such as CD206 and CD163, which are involved in phagocytosis of apoptotic cells and debris. M2 macrophages are located at the

core region of the atherosclerotic plaque, where they contribute to the tissue repair and resolution of inflammation by promoting angiogenesis and fibrosis [5]

Local proliferation of macrophage contributes to ~87% of the macrophages accumulated in the advanced atherosclerotic lesions [8]. Foam cell formation occurs by uptake of oxidized LDL via scavenger receptors, notably type A scavenger receptor (SRA) and a member of type B family, CD36. Once ingested, the cholesteryl esters of the lipoproteins are hydrolyzed in the late endosome to cholesterol, also referred as free cholesterol, and fatty acids. Late endosomal free cholesterol is trafficked to peripheral cellular sites by late endosomal proteins NPC1 and NPC2. Delivery of free cholesterol to the endoplasmic reticulum (ER) has important roles in downregulating the LDL receptors and endogenous cholesterol synthesis by suppressing the sterol-regulatory element binding pathway (SREBP). The free cholesterol undergoes re-esterification to cholesteryl fatty acid esters by the ER enzyme acyl-CoA: cholesterol ester transferase (ACAT), thereby leading to foam cell appearance. Defects in function of ACAT or processes involved in cholesterol efflux from the cells leads to free cholesterol-induced cytotoxicity and may promote death of macrophage in advanced lesion [9]

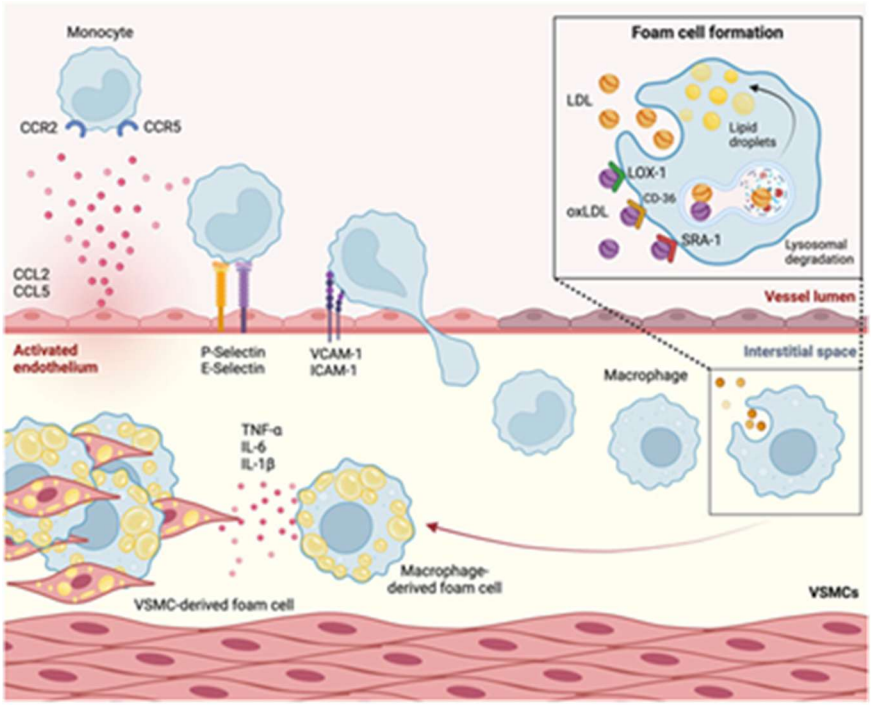

Figure 1.1. Overview of the role of macrophage in foam cell formation and disease progression (Image courtesy: *Annink, Maxim E., et al Frontiers in Cell and Developmental Biology 12 (2024): 1446758*)

1.4. Role of Reactive oxygen species and reactive nitrogen species in Atherosclerosis

Reactive oxygen species (ROS) and reactive nitrogen species (RNS) play an important role in the induction of inflammatory response, facilitating atherosclerosis progression [10,11]. Uncontrolled production and release of ROS and RNS are especially dangerous [12]. Thus, the regulation of ROS and RNS is important for limiting disease progression. Specifically, ROS and RNS activate multiple inflammatory signaling cascades, promoting macrophage transformation into foam cells [13]. Whereas elevated ROS and RNS act as an atherogenic agents.

The atherogenic procession involves multiple cell types, i.e., endothelial cells (ECs), smooth muscle cells (SMC), and immune cells such as macrophages [14]. The levels of

intracellular and extracellular ROS in these cells play an important role in vascular homeostasis and the development of atherosclerosis [15]. Importantly, it should be noted that at low physiological concentrations, ROS is required for cellular functions such as differentiation, migration, senescence, growth, and apoptosis [16]. Thus, ROS may play the role of a second messenger under physiological conditions. Conversely, the high concentration of ROS may contribute to endothelial dysfunction, leading to senescence and activation of inflammatory response in the endothelium. This in turn leads to the development of atherosclerosis [17].

It was proposed that oxidative stress triggers the onset of atherosclerosis by inducing early endothelial cell activation, endothelial permeability, glycocalyx disruption, and myeloid and progenitor stem cell activation [17]. Many important signaling pathways are activated or modulated by ROS, such as GPCR, Notch, MAPK, JAK-STAT, NF-κB, and PI3K/Akt [18–22]. Enzymes such as superoxide dismutase (SOD), catalase, and heme-oxygenase-1 (HO-1) play an important role in scavenging ROS, thereby reducing its harmful effect [23]. Oxidative stress manifests when the production of ROS overcomes the ROS scavenging capacity of cells [23].

Peroxynitrite ($ONOO^-$) is one of the major RNS and is involved in atherogenesis [24]. Formation of $ONOO^-$ is detrimental to NO generation because it leads to the uncoupling of eNOS and endothelial dysfunction [25]. $ONOO^-$ can modify the components of LDL, including lipids and proteins [26–28]. $ONOO^-$ oxidizes the eNOS cofactor tetrahydrobiopterin (BH4) to BH2 [27] as well as the zinc-thiolase cluster present in eNOS [29]. This leads to the uncoupling of eNOS and the generation of O_2^- instead of NO, further promoting oxidative stress and disease progression. $ONOO^-$ also interacts with guanylate cyclase (GC)

which is expressed in smooth muscle cells. GC plays an important role in smooth muscle cell relaxation. $ONOO^-$-dependent inhibition of GC disrupts the signal transduction pathway which is critical for smooth muscle cell relaxation. As a result, NO may be unable to relax smooth muscle cells in the presence of $ONOO^-$ [30]. Thus, formation of $ONOO^-$ results in facilitating atherosclerosis by regulating important molecules involved in maintaining vascular homeostasis.

1.5. Effect of ROS and RNS in macrophage:

NOS1-derived NO was found to play an important role in CD36 mediated ox-LDL uptake and foam cell formation [31]. Further, NOS1-derived NO was also found to induce the ox-LDL-mediated pro-inflammatory cytokines expression [31]. Interestingly, normal LDL was not able to induce the pro-inflammatory cytokine expression [32]. Expression of proinflammatory cytokines is mediated through IKKβ dependent phosphorylation and degradation of IκBα and subsequent translocation of p65 subunit into the nucleus [33]. Interestingly, NOS1-derived NO mediated p65 activation did not involve the degradation of IκBα. Instead, IκBα was S-nitrosylated at putative cysteine residue involved in its interaction with the p50/p65 heterodimer [31]. The S-nitrosylation of the putative IκBα residue released its interaction with the p50/p65 heterodimer, leading to its translocation into the nucleus [31]. There are five putative cysteine residues in the structure of IκBα, among which Cys-215 is known to mediate the interaction of IκBα with the p50/p65 heterodimer [34–36]. The author suggested that Cys-215 was the site which was S-nitrosylated by NOS1-derived NO leading to its translocation into the nucleus [31].

Cholesterol crystals found in atherosclerotic plaques induce ROS production in macrophages via xanthine oxidase and NADPH oxidase [37]. ROS production in turn is involved in CD36 upregulation [38]. Kolta et al revealed that in macrophages, ROS activates the Bruton's tyrosine kinase (BTK) that causes tyrosine phosphorylation of the transcriptional co-activator p300, a histone acetyltransferase. The phosphorylated p300, in turn, acetylates STAT1 [38]. The authors found that the acetylated STAT1 interacts with PPARγ, and the complex of acetylated STAT1 and PPARγ is more potent in increasing CD36 expression compared to PPARγ alone [38]. Thus, cholesterol crystals stimulate ROS production in macrophages, and the ROS-BTK-p300-dependent formation of the complex of acetylated STAT1 and PPARγ upregulates proatherogenic CD36 expression, promoting foam cell formation [38].

1.6. Nitric Oxide Synthase:

The NOS enzymes are primarily responsible for oxidizing L-arginine to L-citrulline in presence of co-factors, secondarily release biologically active NO free radical as a by-product. According to their abundance or the tissue type in which they were first discovered, three main NOS enzymes have been described; (a) neuronal NOS (nNOS or NOS1), (b) inducible NOS (iNOS or NOS2), and (c) endothelial NOS (eNOS or NOS3) [39]. In addition, there are five different isoforms of NOS1 proteins that are products of alternatively spliced NOS1 mRNAs: NOS1-α, μ, β, γ, and NOS1-2.

NOS1 is constitutively expressed in specific neurons of the brain. Although highly enriched in brain tissues, immunohistochemical analysis showed the occurrence of NOS1 in kidney macula densa (MD), pancreatic islet, vascular smooth muscle cells, spinal cord, adrenal glands, and in peripheral nitrergic nerves [40]. In mammals, NOS1 is highly enriched in

skeletal muscles. As NOS1 is found in particulate and soluble fractions, and localizes to different intracellular compartments, therefore predict its multiple functions in tissue microenvironment [41]. However, the underlying molecular mechanisms are crucially unknown.

1.7. Research Gap and Hypothesis

1.7.1. Research Gap:

Despite extensive research, a critical gap remains in the understanding of the upstream regulatory mechanisms that control the simultaneous expression of the key inflammatory mediators such as IL-1β and CD40 in the atherosclerotic macrophages. Also, targeting NOS1 is not beneficial as it plays important role in functioning of brain as well in maintaining the general physiology of heart, kidney and of gastrointestinal tract. Therefore, targeting the molecules expressed through NOS1 can be seen as a better therapeutic approach. As a result, there lies following research gaps:

1. The precise role of NOS1 in macrophage foam cell formation and the subsequent activation of inflammatory response is not fully elucidated.

2. The mechanistic link between NOS1 activation and the expression of IL-1β and CD40 in macrophages remains unknown.

3. There is a lack of targeted therapeutic interventions that specifically modulate the IL-1β/IL-1R1 and CD40/CD40L pathways.

1.7.2. Hypothesis:

Therefore, the current hypothesis is: NOS1-mediated signalling in macrophages acts as a key regulatory mechanism promoting the pro-inflammatory phenotype by upregulating the expression of IL-1β and CD40 receptor, and the therapeutic intervention targeting the IL-1β/IL-1R1 and CD40/CD40L interactions can effectively mitigate the vascular inflammation and endothelial dysfunction in atherosclerosis

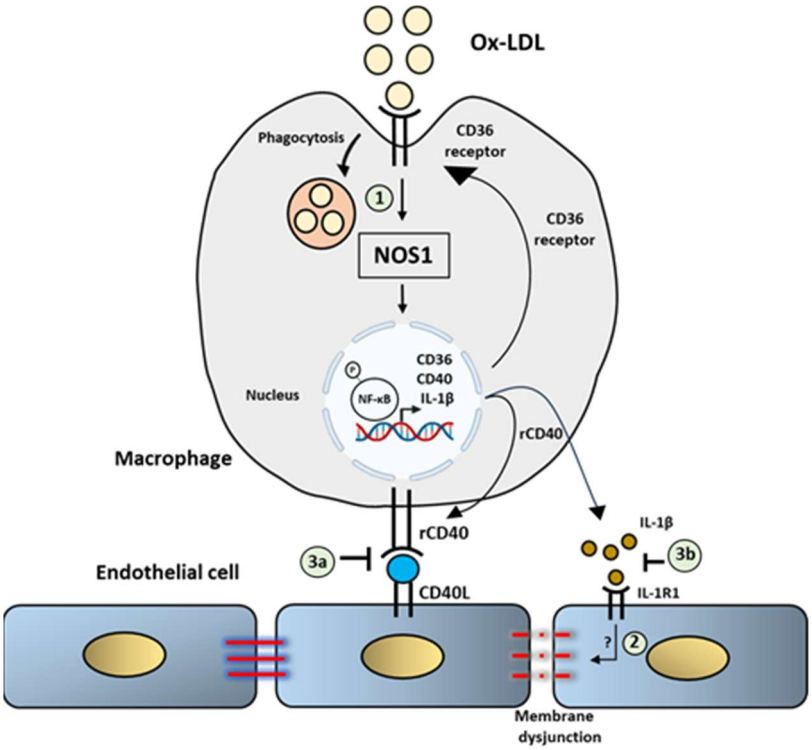

1.8. Scope and Objectives of the Study

The overall goal of this research is to elucidate the NOS1-mediated inflammatory pathway in macrophages and endothelial cells and to develop therapeutic strategies against key inflammatory molecules.

To study this, following objectives were accomplished:

Aim 1: To study the role of NOS1 in foam cell formation and expression of inflammatory markers in macrophage.

•**1.1.** Investigating the effect of NOS1 modulation (activation/inhibition) on macrophage foam cell formation using Oil Red O (ORO) staining.

• **1.2**. Quantifying the expression of pro-inflammatory cytokines (e.g., IL-1β, TNF-α) and the levels of NOS1 phosphorylation and nitric oxide production in macrophage.

Aim 2: To study the effect of NOS1 mediated activation of IL-1β on the endothelial cell.

•**2.1.** Characterizing the effect of OxLDL-stimulated conditioned media from macrophage on the endothelial cell permeability by analyzing junction proteins and Transendothelial Electrical Resistance (TEER) analysis.

• **2.2**. Determining the IL-1β mediated molecular mechanism leading to the endothelial dysfunction, focusing on the activation of MAPK and NF-κB signalling axis.

Aim 3: To design a therapeutic intervention by targeting key inflammatory modulators involved in atherosclerosis

•**3.1.** To identify/repurpose a therapeutic molecule(s) against the IL-1β-IL-1R1 interaction on the endothelial cells using in-silico screening and in-vitro validation.

•**3.2.** To identify peptide/peptidomimetics as a therapeutic intervention against the CD40-40L interaction using molecular docking, molecular dynamics (MD) simulations and ADMET analysis.

1.9. Structure of the Chapters:

Chapter 1- Introduction and Literature Review

Chapter 2- Literature Review

Chapter 3- Role of NOS1 in different diseases and in Macrophage inflammatory phenotype and Foam cell formation

Chapter 4- NOS1-mediated IL-1β signalling and Endothelial dysfunction and identification of small molecule inhibitors targeting IL-1β-IL-1R1 interaction

Chapter 5- Novel peptide inhibitors targeting CD40 and CD40L interaction: a potential for atherosclerosis therapy

Chapter 6- Summary, Conclusions and Future directions

1.10. Bibliography:

[1] V. Tasouli-Drakou, I. Ogurek, T. Shaikh, M. Ringor, M.V. DiCaro, K. Lei, Atherosclerosis: A Comprehensive Review of Molecular Factors and Mechanisms, IJMS 26 (2025) 1364. https://doi.org/10.3390/ijms26031364.

[2] J. Fan, T. Watanabe, Atherosclerosis: Known and unknown, Pathology International 72 (2022) 151–160. https://doi.org/10.1111/pin.13202.

[3] P. Raggi, J. Genest, J.T. Giles, K.J. Rayner, G. Dwivedi, R.S. Beanlands, M. Gupta, Role of inflammation in the pathogenesis of atherosclerosis and therapeutic interventions, Atherosclerosis 276 (2018) 98–108. https://doi.org/10.1016/j.atherosclerosis.2018.07.014.

[4] R.R.S. Packard, A.H. Lichtman, P. Libby, Innate and adaptive immunity in atherosclerosis, Semin Immunopathol 31 (2009) 5–22. https://doi.org/10.1007/s00281-009-0153-8.

[5] P. Theofilis, E. Oikonomou, K. Tsioufis, D. Tousoulis, The Role of Macrophages in Atherosclerosis: Pathophysiologic Mechanisms and Treatment Considerations, IJMS 24 (2023) 9568. https://doi.org/10.3390/ijms24119568.

[6] Z. Strizova, I. Benesova, R. Bartolini, R. Novysedlak, E. Cecrdlova, L.K. Foley, I. Striz, M1/M2 macrophages and their overlaps – myth or reality?, Clinical Science 137 (2023) 1067–1093. https://doi.org/10.1042/CS20220531.

[7] P. Lin, H.-H. Ji, Y.-J. Li, S.-D. Guo, Macrophage Plasticity and Atherosclerosis Therapy, Front. Mol. Biosci. 8 (2021) 679797. https://doi.org/10.3389/fmolb.2021.679797.

[8] L. Farahi, S.K. Sinha, A.J. Lusis, Roles of Macrophages in Atherogenesis, Front. Pharmacol. 12 (2021) 785220. https://doi.org/10.3389/fphar.2021.785220.

[9] P. Hou, J. Fang, Z. Liu, Y. Shi, M. Agostini, F. Bernassola, P. Bove, E. Candi, V. Rovella, G. Sica, Q. Sun, Y. Wang, M. Scimeca, M. Federici, A. Mauriello, G. Melino, Macrophage polarization and

metabolism in atherosclerosis, Cell Death Dis 14 (2023) 691. https://doi.org/10.1038/s41419-023-06206-z.

[10] C. Leeuwenburgh, M.M. Hardy, S.L. Hazen, P. Wagner, S. Oh-ishi, U.P. Steinbrecher, J.W. Heinecke, Reactive Nitrogen Intermediates Promote Low Density Lipoprotein Oxidation in Human Atherosclerotic Intima, Journal of Biological Chemistry 272 (1997) 1433–1436. https://doi.org/10.1074/jbc.272.3.1433.

[11] W.N. Nowak, J. Deng, X.Z. Ruan, Q. Xu, Reactive Oxygen Species Generation and Atherosclerosis, ATVB 37 (2017). https://doi.org/10.1161/ATVBAHA.117.309228.

[12] S. Di Meo, T.T. Reed, P. Venditti, V.M. Victor, Role of ROS and RNS Sources in Physiological and Pathological Conditions, Oxidative Medicine and Cellular Longevity 2016 (2016) 1245049. https://doi.org/10.1155/2016/1245049.

[13] X. Yang, Y. Li, Y. Li, X. Ren, X. Zhang, D. Hu, Y. Gao, Y. Xing, H. Shang, Oxidative Stress-Mediated Atherosclerosis: Mechanisms and Therapies, Front. Physiol. 8 (2017) 600. https://doi.org/10.3389/fphys.2017.00600.

[14] M. Liu, S. Samant, C.H. Vasa, R.M. Pedrigi, U.M. Oguz, S. Ryu, T. Wei, D.R. Anderson, D.K. Agrawal, Y.S. Chatzizisis, Co-culture models of endothelial cells, macrophages, and vascular smooth muscle cells for the study of the natural history of atherosclerosis, PLoS ONE 18 (2023) e0280385. https://doi.org/10.1371/journal.pone.0280385.

[15] D. Burtenshaw, M. Kitching, E.M. Redmond, I.L. Megson, P.A. Cahill, Reactive Oxygen Species (ROS), Intimal Thickening, and Subclinical Atherosclerotic Disease, Front. Cardiovasc. Med. 6 (2019) 89. https://doi.org/10.3389/fcvm.2019.00089.

[16] K.M. Holmström, T. Finkel, Cellular mechanisms and physiological consequences of redox-dependent signalling, Nat Rev Mol Cell Biol 15 (2014) 411–421. https://doi.org/10.1038/nrm3801.

[17] M.M. Elahi, Y.X. Kong, B.M. Matata, Oxidative Stress as a Mediator of Cardiovascular Disease, Oxidative Medicine and

Cellular Longevity 2 (2009) 259–269. https://doi.org/10.4161/oxim.2.5.9441.

[18] M. Ushio-Fukai, Vascular signaling through G protein-coupled receptors: new concepts:, Current Opinion in Nephrology and Hypertension 18 (2009) 153–159. https://doi.org/10.1097/MNH.0b013e3283252efe.

[19] C. Caliceti, P. Nigro, P. Rizzo, R. Ferrari, ROS, Notch, and Wnt Signaling Pathways: Crosstalk between Three Major Regulators of Cardiovascular Biology, BioMed Research International 2014 (2014) 1–8. https://doi.org/10.1155/2014/318714.

[20] R.J. Duhé, Redox regulation of Janus kinase: The elephant in the room, JAK-STAT 2 (2013) e26141. https://doi.org/10.4161/jkst.26141.

[21] M.J. Morgan, Z. Liu, Crosstalk of reactive oxygen species and NF-κB signaling, Cell Res 21 (2011) 103–115. https://doi.org/10.1038/cr.2010.178.

[22] N. Koundouros, G. Poulogiannis, Phosphoinositide 3-Kinase/Akt Signaling and Redox Metabolism in Cancer, Front. Oncol. 8 (2018) 160. https://doi.org/10.3389/fonc.2018.00160.

[23] J.C. Juarez, M. Manuia, M.E. Burnett, O. Betancourt, B. Boivin, D.E. Shaw, N.K. Tonks, A.P. Mazar, F. Doñate, Superoxide dismutase 1 (SOD1) is essential for H_2O_2 -mediated oxidation and inactivation of phosphatases in growth factor signaling, Proc. Natl. Acad. Sci. U.S.A. 105 (2008) 7147–7152. https://doi.org/10.1073/pnas.0709451105.

[24] D. Salisbury, U. Bronas, Reactive Oxygen and Nitrogen Species: Impact on Endothelial Dysfunction, Nursing Research 64 (2015) 53–66. https://doi.org/10.1097/NNR.0000000000000068.

[25] U. Förstermann, A. Mülsch, E. Böhme, R. Busse, Stimulation of soluble guanylate cyclase by an acetylcholine-induced endothelium-derived factor from rabbit and canine arteries., Circulation Research 58 (1986) 531–538. https://doi.org/10.1161/01.RES.58.4.531.

[26] J.S. Beckman, W.H. Koppenol, Nitric oxide, superoxide, and peroxynitrite: the good, the bad, and ugly, American Journal of Physiology-Cell Physiology 271 (1996) C1424–C1437. https://doi.org/10.1152/ajpcell.1996.271.5.C1424.

[27] S. Milstien, Z. Katusic, Oxidation of Tetrahydrobiopterin by Peroxynitrite: Implications for Vascular Endothelial Function, Biochemical and Biophysical Research Communications 263 (1999) 681–684. https://doi.org/10.1006/bbrc.1999.1422.

[28] V.M. Darley-usmar, N. Hogg, V.J. O'leary, M.T. Wilson, S. Moncada, The Simultaneous Generation of Superoxide and Nitric Oxide Can Initiate Lipid Peroxidation in Human Low Density Lipoprotein, Free Radical Research Communications 17 (1992) 9–20. https://doi.org/10.3109/10715769209061085.

[29] M.-H. Zou, C. Shi, R.A. Cohen, Oxidation of the zinc-thiolate complex and uncoupling of endothelial nitric oxide synthase by peroxynitrite, J. Clin. Invest. 109 (2002) 817–826. https://doi.org/10.1172/JCI0214442.

[30] M. Bassil, Y. Li, M.B. Anand-Srivastava, Peroxynitrite inhibits the expression of G_i α protein and adenylyl cyclase signaling in vascular smooth muscle cells, American Journal of Physiology-Heart and Circulatory Physiology 294 (2008) H775–H784. https://doi.org/10.1152/ajpheart.00841.2007.

[31] A. Roy, U. Saqib, K. Wary, M.S. Baig, Macrophage neuronal nitric oxide synthase (NOS1) controls the inflammatory response and foam cell formation in atherosclerosis, International Immunopharmacology 83 (2020) 106382. https://doi.org/10.1016/j.intimp.2020.106382.

[32] A. Roy, S. Banerjee, U. Saqib, M.S. Baig, NOS1-derived nitric oxide facilitates macrophage uptake of low-density lipoprotein, J of Cellular Biochemistry 120 (2019) 11593–11603. https://doi.org/10.1002/jcb.28439.

[33] E.B. Traenckner, H.L. Pahl, T. Henkel, K.N. Schmidt, S. Wilk, P.A. Baeuerle, Phosphorylation of human I kappa B-alpha on serines 32 and 36 controls I kappa B-alpha proteolysis and NF-kappa B

activation in response to diverse stimuli., The EMBO Journal 14 (1995) 2876–2883. https://doi.org/10.1002/j.1460-2075.1995.tb07287.x.

[34] B. Manavalan, S. Basith, Y.-M. Choi, G. Lee, S. Choi, Structure-Function Relationship of Cytoplasmic and Nuclear IκB Proteins: An In Silico Analysis, PLoS ONE 5 (2010) e15782. https://doi.org/10.1371/journal.pone.0015782.

[35] S.-C. Sue, H.J. Dyson, Interaction of the IκBα C-terminal PEST Sequence with NF-κB: Insights into the Inhibition of NF-κB DNA Binding by IκBα, Journal of Molecular Biology 388 (2009) 824–838. https://doi.org/10.1016/j.jmb.2009.03.048.

[36] C.B. Phelps, L.L. Sengchanthalangsy, T. Huxford, G. Ghosh, Mechanism of IκBα Binding to NF-κB Dimers, Journal of Biological Chemistry 275 (2000) 29840–29846. https://doi.org/10.1074/jbc.M004899200.

[37] P. Pichavaram, A.M. Mani, N.K. Singh, G.N. Rao, Cholesterol crystals promote endothelial cell and monocyte interactions via H2O2-mediated PP2A inhibition, NFκB activation and ICAM1 and VCAM1 expression, Redox Biology 24 (2019) 101180. https://doi.org/10.1016/j.redox.2019.101180.

[38] S. Kotla, N.K. Singh, G.N. Rao, ROS via BTK-p300-STAT1-PPARγ signaling activation mediates cholesterol crystals-induced CD36 expression and foam cell formation, Redox Biology 11 (2017) 350–364. https://doi.org/10.1016/j.redox.2016.12.005.

[39] J.T. Mattila, A.C. Thomas, Nitric Oxide Synthase: Non-Canonical Expression Patterns, Front. Immunol. 5 (2014). https://doi.org/10.3389/fimmu.2014.00478.

[40] A.V. Hall, H. Antoniou, Y. Wang, A.H. Cheung, A.M. Arbus, S.L. Olson, W.C. Lu, C.L. Kau, P.A. Marsden, Structural organization of the human neuronal nitric oxide synthase gene (NOS1), Journal of Biological Chemistry 269 (1994) 33082–33090. https://doi.org/10.1016/S0021-9258(20)30099-5.

[41] L. Zhou, D.-Y. Zhu, Neuronal nitric oxide synthase: Structure, subcellular localization, regulation, and clinical implications,

Nitric Oxide 20 (2009) 223–230. https://doi.org/10.1016/j.niox.2009.03.001.

CHAPTER 2

LITERATURE REVIEW

The current chapter discuss about the Nitric Oxide synthase (NOS) and different types of NOS. Regulation and expression of Nitric Oxide synthase 1 (NOS1) is also discussed. Furthermore, it discusses about the role of NOS1 in different diseases such as Cancer, Diabetes, Obesity and other inflammatory diseases. The chapter further discusses about the role of IL-1β and CD40-40L interaction in atherosclerosis. It concludes by discussing the role of macrophage CD36 in atherosclerosis.

2.1. Nitric Oxide Synthase

The NOS enzymes are primarily responsible for oxidizing L-arginine to L-citrulline in presence of co-factors, secondarily release biologically active NO free radical as a by-product [1]. As a highly membrane permeable free radical, NO can modify significant number of molecular targets. Therefore, NO has the ability to regulate diverse biological activities within cells and tissues. As NO can modify cysteine residue(s) via the redox-based mechanism, therefore, it controls myriads of cellular responses by activating NO-sensitive guanylyl cyclase; transcriptional and translational activities, for example, by interacting with iron-responsive elements; and post-translational modifications, such as ADP ribosylation [2]. Further, NO free radicals (NO^{*}) can collide with superoxide anion (O_2^{-*}) to form peroxynitrite ($ONOO^{-}$) intracellularly. Peroxynitrite ($ONOO^{-}$) species is equally a highly reactive molecule that can stimulate or modify biological processes including oxidative damage, nitration, peroxidation of lipids, and S-nitrosylation of proteins, lipids, and DNAs, while also generating nitryl and hydroxyl species [3]. Additionally, $ONOO^{-}$ can induce DNA single-strand breaks thereby activate poly-ADP-ribose polymerase (PARP). Superoxide dismutase (SOD) competes with O_2^{-*} in reacting with NO^{*} to form $ONOO^{-}$. Under most physiological conditions NO occurs at a sub-micromolar concentration [4]; however, due

to the rate constant of $ONOO^-$ formation being a few orders of magnitude higher than that of SOD-mediated H_2O_2 formation by O_2^-, $ONOO^-$ is always present even with high expression of SOD, and the formation of $ONOO^-$ gradually increase with increasing production of NO^* by NOS [5]. The compartmentalized action of NO in the tissue microenvironment is diverse and complex. As NO and most of its downstream products are highly reactive and readily diffusible, therefore, it is not surprising to find involvement of NO in many pathophysiological states.

According to their abundance or the tissue type in which they were first discovered, three main NOS enzymes have been described; (a) neuronal NOS (nNOS or NOS1), (b) inducible NOS (iNOS or NOS2), and (c) endothelial NOS (eNOS or NOS3) [6]. In addition, there are five different isoforms of NOS1 proteins that are products of alternatively spliced NOS1 mRNAs: NOS1-α, μ, β, γ, and NOS1-2 [7]. With regards to their expression and localization, NOS2 is not constitutively expressed in cells, but its expression can be induced by infection, bacterial lipopolysaccharide (LPS), cytokines, and other agonists [8]. Although primarily identified in macrophages, the expression of the enzyme can be stimulated in many cell types or tissues, provided that appropriate stimuli are used. NOS3 is highly enriched in endothelial cells (ECs), responsible for the synthesis of NO to exert vasodilation and to regulate the flow of blood throughout the body. However, this enzyme has also been detected in cardiac myocytes, platelets, certain brain neurons, syncytiotrophoblasts of the human placenta, and kidney tubular epithelial cells [9]. NOS1 is constitutively expressed in specific neurons of the brain. Although highly enriched in brain tissues, immunohistochemical analysis showed the occurrence of NOS1 in kidney macula densa (MD), pancreatic islet, vascular smooth muscle cells, spinal cord, adrenal glands, and in peripheral

nitrergic nerves [10]. In mammals, NOS1 is highly enriched in skeletal muscles. As NOS1 is found in particulate and soluble fractions, and localizes to different intracellular compartments, therefore predict its multiple functions in tissue microenvironment [11]. However, the underlying molecular mechanisms are crucially unknown.

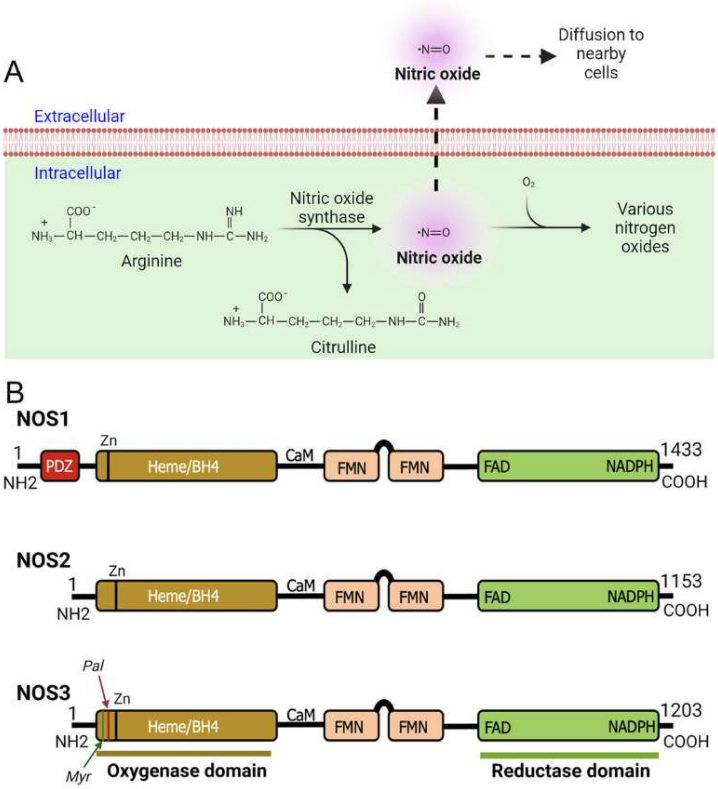

Figure 2.1. Production of nitric oxide (NO) and functional domains of human NOS1, NOS2, and NOS3. (A) Production of nitric oxide (NO). NOS converts L-arginine to L-citrulline in presence of nicotinamide adenine dinucleotide phosphate (NADPH) and oxygen to produce highly diffusible NO free radical in the tissue microenvironment. (B) Functional domains of human NOS1, NOS2, and NOS3. NOS1 harbors a PDZ domain at the NH2-terminus. The oxygenase and reductase domains are as shown. The oxygenase domain contains heme and tetrahydrobiopterin (BH4) interacting sites, whereas the reductase domain contains interacting sites for FMN,

FAD, and NADPH; the FMN domain connects to the oxygenase domain via a calmodulin-binding (CaM) domain. The NOS1 and NOS3 proteins contain an autoinhibition segment that interrupts the FMN domain, while NOS2 lacks. Myristoylation (Myr), palmitoylation (Palm), zinc-ligating (Zn) positions are as shown.

2.2.Regulation of expression of NOS1

The human *NOS1* gene located at the chromosome 12q24.2 and is made of 29 exons, 28 introns, and these DNA elements are interspersed over 250 Kb genome. The open reading frame (ORF) of *NOS1* is composed of 4,302 base pairs, and the translation starts at exon-2 and stops at exon-28, thereby give rise to 1,434 amino acid polypeptide species. The *NOS1* gene can produce several alternatively spliced mRNA transcripts. Moreover, literature survey shows complex transcriptional regulation of *NOS1* gene as described below.

The enhancers, promoters and boundary elements (chromatin insulators) spread across the genome can fine-tune the expression of genes. These three major elements can titrate the levels of gene expression precisely, in temporo-spatial manner in response to specific signals. A promoter of gene usually represents a region of a genome that allows for the recruitment of DNA binding transcription factors (TFs) including epigenetic modifiers, where the activities of RNA polymerase facilitate the transcription of a gene. These promoter DNA sequences are located at the 5′ end (upstream) of the transcription initiation site (TSS), but could also be located downstream of TSS. TFs can be positive or negative regulators of gene transcription, however, the promoters, the TSS and the key TFs collaborate, thereby fine tune to regulate the activities of RNA polymerase. Additionally, the promoter DNA sequences can be found in both in forward and in reverse orientations.

The TFs including the epigenetic modifiers could directly or indirectly regulate the expression of human *NOS1* is not clearly understood. Inspection of 5′ region of the human NOS1-promoter and enhancer suggest that the expression of this gene could be regulated by several TFs, *e.g.*, AP-2, TCF/LEF1, CREB/ATF/c-Fos, Ets, p53, and NF-kappa B-like sequences [10]. In addition, we observed that there are also at least 2 Kruppel Like Factor-2 and -4 (KLF2/KLF4) recognition sites (CACCC) in the human *NOS1*-promoter/enhancer-500 bp upstream of TSS and at least 11 binding sites +3.5 kb downstream of exon-1, thereby increasing the complexity of transcriptional regulation of *NOS1* gene by KLF4/KLF2 [12]. We also found putative binding sites for OCT4, Hypoxia Response Element (HRE) and Sox2. Additional levels of regulation of NOS1 expression are likely due to SNPs and polymorphic loci. Nevertheless, the NOS1-promoter driven green fluorescent protein (GFP) or *Lac-Z* reporter transgenic mice lines should be used with which to study the regulated expression of NOS1 in several pathophysiological setting. The neuronal specific functions of NOS1 are documented very well; however, in the following sections, we highlight the neglected roles of NOS1 in non-neuronal disease settings.

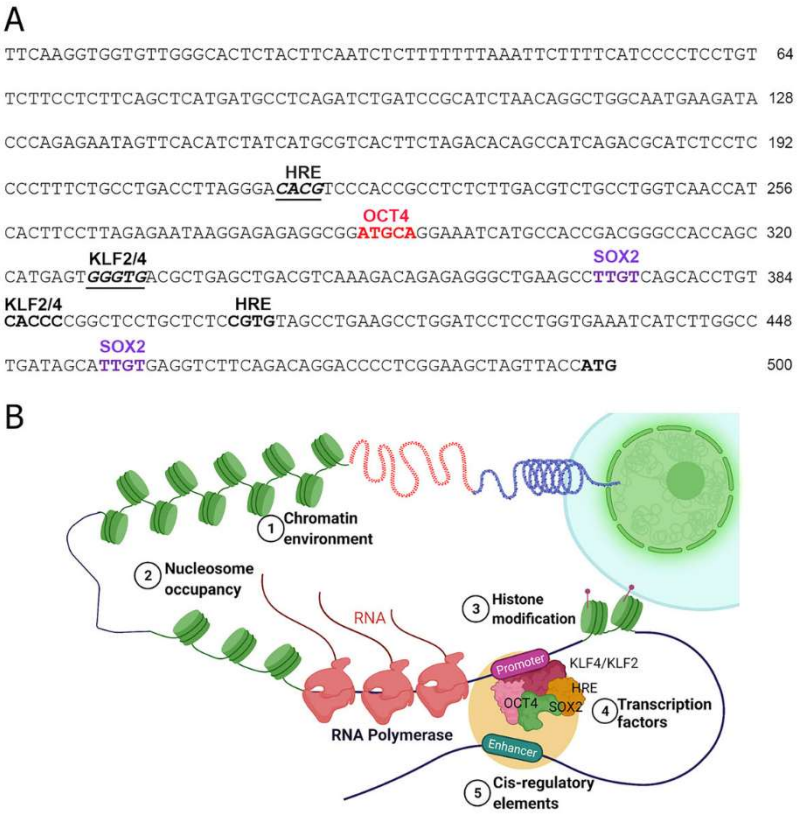

Figure 2.2: Transcriptional regulation of NOS1. (A) Nucleotide sequence of the human NOS1-promoter of -500 bp upstream of the transcription start site (TSS) ATG as shown. The locations of putative binding sites for KLF2/KLF4, Hypoxia Response Element (HRE), OCT4, and SOX2 are indicated. (B) Hypothetical diagram of transcriptional regulation of NOS1 and the potential roles of epigenetic mediators KLF2/KLF4, HRE, OCT4, and SOX2. Epigenetic mediator-induced expression of NOS1 gene could occur prior to the appearance of genomic instability, thereafter mutation and/or deletion of critical genes could drive tumor cell proliferation, resist apoptosis, together alter NOS1 expression. Additionally, SNPs and polymorphic loci in cis-regulating elements (e.g., enhancer) could up-or downregulate NOS1 expression. Expression of NOS1 gene could be measured by RT-PCR, epigenetic modifications by DNA methylation assays or by chromatin immunoprecipitation (ChiP) experiments.

2.3. Role of NOS1 in different diseases:

2.3.1. Roles of NOS1 and NO in cardiovascular disease

The NO is a fundamental modifier of wealth of biological processes in the heart and in the vasculature [13]. Owing to its fast reaction kinetics, the roles of NO in different circumstances, at best, is contradictory. For instance, in the vasculature, it acts as a vasodilator for smooth muscle cells and an anti-platelet aggregator for platelets, whereas in cardiomyocytes, it acts as a pro-apoptotic or necrotic if present in excessive amount [13]. Thus, the biological effect of NO can oscillate, subject to which NOS polypeptide species is engaged and the bioavailability of NO.

The effector molecules downstream of NO include ion channels found in the membrane, enzymes, and several key proteins in the mitochondria, cytosol and nuclear compartment [14,15]. All three NOS isoforms are abundant in the heart and in atherosclerotic plaques [16] and have addressed the expression of NOS isoforms in normal and during the progression of atherosclerotic lesions. NOS3 found in quiescent blood vessels is expressed by ECs, where it maintains basal physiological functions. NOS3 expression does not decrease appreciably in early lesions but is significantly decreased in advanced lesions in the EC overlying the atherosclerotic lesion; whereas NOS1 and NOS2 are expressed in early and advanced lesions in macrophages, ECs, and mesenchymal-appearing intimal cells, but not found in a normal quiescent vasculature. The expression of NOS2 was confirmed by immunohistochemical staining, while *in situ* hybridization did not detect its mRNA, suggesting that mRNA level was below the detection limit [17]. In mice the loss of NOS2 gene is atheroprotective, conversely, NOS3 provided atheroprotective effect in ApoE$^{-/-}$ [18,19]. Thus, it can be surmised that NOS2 acts as a pro-atherogenic agent, while

NOS3 acts as an atheroprotective agent. Although, there are points and counterpoints regarding the role of NOS1 in atherosclerosis, studies have found that NOS1 acts as an anti-atherogenic agent, which was evident by increased plaque formation and mortality in ApoE/nNOSα double knockout mice [19]. Additionally, $NOS1^{-/-}$ increased the mortality of $ApoE^{-/-}$ mice [20]. Reportedly, macrophage NOS1-derived NO mediated the uptake of ox-LDL and foam cell formation with the subsequent expression of adhesion molecules on the endothelial wall, thereby enhancing the inflammatory process [21,22]. Chakrabarti et. al. studied the effect of NOS1 by tumor necrosis factor (TNF) stimulation in ECs [23]. Accordingly, NOS1-knockdown or inhibition by L-NPA (a selective inhibitor of NOS1) enhanced the inflammatory response by elevating expression of vascular cell adhesion molecule (VCAM)-1, IL-2, and IL-8. NOS1 inhibition also increased the expression of GM-CSF, which plays a major role in the biology of leukocyte production and maturation in bone marrow. NOS1 inhibition did not increase the expression of intercellular cell adhesion molecule-1 (ICAM-1) and anti-inflammatory cytokines IFN-γ and IL-10, suggesting a paradoxical role of NOS1 in ECs. NOS1 inhibition did not alter the mRNA level of VCAM-1, suggesting a posttranscriptional regulatory role of NOS1 in ECs [23]. NOS1-derived H_2O_2 had been described as an important vasodilator in ECs, and a reduction in NOS1 expression has been shown to lead to EC-dysfunction in $ApoE^{-/-}$ mice through decrease in H_2O_2 level and subsequently decreased vasodilation [24]. Ox-LDL reduced NOS1 expression and increased NOS-Ser^{852} phosphorylation, thereby uncoupling of NOS1 with a subsequent decrease in NO and H_2O_2 level in ECs, thus generating oxidative stress. Impairment of H_2O_2 production in ECs by ox-LDL activated c-Jun and c-Fos, which mediate elaboration of inflammatory cytokines [25,26]. Notably, NOS1 mediated the interaction between ECs and macrophages in the

early stage of atherosclerosis. CD40 ligand is expressed on macrophages by ox-LDL activated NOS1. Macrophage secretes soluble factors and increases the expression of the CD40 receptor on ECs. Interaction between CD40-40L generates an inflammatory response and leads to EC-dysfunction [21]. A study of myocyte hypertrophy and ventricular stiffness revealed an increased response in $NOS1^{-/-}$ in the progression of both [20], thus signifying the beneficial effect of NOS1 on myocyte hypertrophy. As the (a) expression of NOS1 was found in early and advanced atherosclerotic plaques [16] and (b) the concentration of NO determines the pro-or anti-inflammatory processes, studies explaining the role of NOS1-derived NO in early and advanced atherosclerotic plaque by modulating the concentration of NO and its subsequent effect on atherosclerosis plaque could help clarify the role of NOS1-derived NO in these processes. However, laboratory animal experiments have their own limitations as these experiments are often carried out in inbred strains of mice coupled with restrictive dietary regiments.

NOS1 is localized on the membrane vesicles of the smooth endoplasmic reticulum (SER) in cardiac muscles that modulate contractility of cardiac muscle and regulation of intracellular Ca^{2+} movement [7]. NOS1-derived NO inhibited Ca^{2+} influx into cardiomyocyte *via* regulation on L-type Ca^{2+} channel (LTCC) present on the cell membrane. It increased Ca^{2+} reabsorption in the SER by increasing phospholamblan phosphorylation and regulating the release of Ca^{2+} from the SER through S-nitrosylation of the ryanodine receptor (RyR) Ca^{2+} release channel present on the SER [7]. *NOS1* gene deletion decreased the S-nitrosylation of RyR. However, these contrasting results suggest the ability of NOS1 in regulating the excitation-contraction (EC) coupling response in cardiomyocytes. Enhanced contraction and relaxation in left-ventricular cardiomyocytes in $NOS1^{-/-}$ mice compared to wild-

type mice have been documented [27], which was subsequently confirmed by others [28–30], although some studies demonstrated otherwise [20]. This signifies presence of other variable factors, which could modify the NOS1-derived physiological responses, *e.g.*, temperature modulated NOS1 behavior on EC coupling [31]. Temperature has been known to modulate NO production by affecting NOS activity [32]. Impairment in Ca^{2+} handling, such as Ca^{2+} leak, contribute to impairment in contractibility by depleting Ca^{2+} storage in the SER. Xanthine oxidase (XOR) and NOS1 have been shown to co-localize on the SER in proximity to RyR2. NOS1-derived NO mediates the inhibitory effect on XOR and thus regulates RyR2, and a decrease in NOS1 leads to a rise in the generation of superoxide anion [33] and the dysregulation of RyR2-mediated Ca^{2+} release. In wild-type cardiomyocytes, a reduction in temperature increased Ca^{2+} leak due to increased ROS generation through XOR activity and NOS1 uncoupling, therefore decreasing the S-nitrosylation of RyR2 and affecting the contractibility of myocardium. Every time NO collides with superoxide anion, this event generates peroxynitrite, which induces more damage to RyR2 compared to ROS [33]. Mice that lack denitrosylation machinery ($GSNOR^{-/-}$) showed reversed cooling-induced ROS generation and calcium leak. In a $NOS1^{-/-}$ mice model, higher temperature (>30 °C) increased Ca^{2+} leak and elevated ROS [31]. Therefore, this observation indicated that the effect of NOS1 on cellular activity cannot be studied by modulating the intrinsic parameters only, as extrinsic factors could also be a major player.

Further complicating the picture, epigenetic modification in the NOS gene and in the promoter/enhancer regions could also modulate disease states, because such modification can alter gene expression, generation and bioavailability of NO in the cells and tissues. Methylation of the NOS1 gene plays an

essential role in atherogenesis in children [34]. The methylation pattern of 16 CpG loci located within NOS1, NOS2A, NOS3, ARG1, and ARG2 genes was analysed in 377 children, with a history of carotid intima-media thickness (CIMT), and linear regression was plotted with CIMT measurement. CIMT was found to increase by 1.2 μm for every 1% increase in the average DNA methylation of the NOS1 gene ($p = 0.02$) [34]. Methylation patterns on the non-CpG island and their correlation to CIMT were addressed as well, in which the subject with high mean methylation on the non-CpG island of the NOS1 gene had a 15.8 μm higher measurement of CIMT ($p = 0.004$). Although extrapolation of this study's findings on larger cohorts would clarify the correlation of CIMT with NOS1 methylation status, the findings on these subjects signify the importance of epigenetic modification on NOS1 gene. In addition, the occurrence of single nucleotide polymorphism (SNP) in NOS1 genome has been suggested to elevate the risk of cardiovascular disease, for example, in coronary heart disease and in hypertension [35]. In a total of 3,351 individuals (560 cases of coronary heart disease (CHD) and 2,791 controls in which 1,158 individuals were hypertensive) genotyped for 58 SNPs in NOS genes, the presence of NOS1 SNP rs3782218 showed a positive correlation with disease pathogenesis in both cases of CHD and hypertension, whereas another NOS1 SNP (rs2682826) showed a positive correlation with CHD but not with hypertension [36]. Thus, early detection of these SNPs in individuals can serve as an effective marker for the pathogenesis of CHD and hypertension, leading to early treatment. Sudden cardiac death caused by abrupt decline of heart function within 1 h of the onset of these symptoms [37]. In this regard, coronary artery disease is likely the main driver of sudden cardiac death, and most deaths harbor genetic variations [38]. For example, SNP in NOS1 adaptor protein (NOS1AP; also known as CAPON) was linked with QT prolongation phenomena (delayed ventricular

repolarization) in the general population and increased sudden death in patients with type 1 QT [39,40]. NOS1AP is expressed in the cardiac myocyte, which interacts with NOS1 to suppress the sarcolemma L-type calcium channel (LTCC) *via* the S-nitrosylation, thereby enhance Iκr current, accelerating cardiac repolarization [41]. Analysis of SNP in NOS1AP could serve as an indicative marker for the estimation of potential sudden cardiac death and for early treatment in patients. Nevertheless, genetic experiments with mouse model mimicking human SNPs with the use of CRISPR/Cas9 technology, thereby introducing precise SNP variations analogous to human counterparts, might be useful in determining the precise roles of SNPs in the above-described cardiovascular diseases. SNPs that are found within the promoter/enhancer regions have been hypothesized to increase or decrease or even create a new binding site for TFs, thereby controlling RNA-polymerase activities to turn on the transcription of downstream target genes. Careful genetic and biochemical studies are needed to address such possibilities.

2.3.2. Role of NOS1 in Cancer:

The roles of NO in cancer, at best, represent crucially important unknowns. For example, low levels (<100 nM) of NO are thought to enhance tumor progression and metastasis, while high levels (>300 nM) of NO induce cell cycle arrest, senescence, and apoptosis [42]. All three NOS have the potential to either inhibit or promote cancer growth by adjusting the level of NO. Accumulation of NOS1-derived NO in various types of cancer cells seemingly plays a crucial role in tumor progression, however, mechanistic details are far from understood [43]. NO can modify the DNA damage and repair mechanisms in tumor by upregulating p53, poly (ADP-ribose) polymerase (PARP), and DNA-dependent protein kinase (DNA-PK), thereby modulating the cellular apoptosis [44]. In the following sections,

we describe the cellular mechanisms governed by NOS1 in the progression of a subset of tumors.

2.3.2.1.Cervical cancer

Cervical cancer is the fourth most common form of cancer that occur in women [45]. In these patients, the expression of adenosine triphosphate (ATP)-binding cassette sub-family G member 2 (ABCG2) correlates strongly with anti-neoplastic drug resistance and migratory/invasive cancer cell phenotypes [46]. Accordingly, the mRNA expression of NOS1 and ABCG2 were analyzed in 40 human cervical cancer tissues and 20 control tissues [47]. The expression levels of NOS1 and ABCG2 mRNAs increased compared to the normal control group with a mean difference of 2.63 and 2.02 times, respectively ($p < 0.05$), and therefore strongly correlate (r-value, 1.246; $p = 0.014$). In an experiment, NOS1-depletion decreased ABCG2 protein level, in contrast, ABCG2-depletion did not change the NOS1 protein level, indicating that NOS1 is upstream of ABCG2 in cervical cancer cells. In their study, NOS1-depletion significantly decreased the proliferation and increased the apoptosis of cervical cancer cells ($p < 0.05$), suggesting pro-life roles of NOS1 in cervical cancer [47]. In a separate study, a positive correlation was reported between ABCG2 and NOS1 expression in cisplatin-induced chemoresistance in ovarian cancer [48]. Thus, delineating the signaling cascade involved in the regulation of ABCG2 by NOS1 would unravel clearer mechanism into the specific role of NOS1 in cervical cancer cells, which could be an effective target in the management of cervical cancer.

2.3.2.2.Melanoma

Perturbation of immune system is a hallmark of neoplastic transformation. For example, type I interferon (IFN) dysfunction allows for immune escape and tumor metastasis. In contrast,

constitutive activation of IFN signaling affords increased immune surveillance against cancer [49]. STAT1 phosphorylation by IFNα activates the intrinsic signaling cascade, which activates the expression of interferon-stimulated genes (ISGs) [50]. In melanoma as well as colon and breast carcinoma, exposure to peripheral blood mononuclear cells (PBMC) with IFN-α ex vivo, activated ISGs, reduced phosphorylation of STAT-1 and decreased immune response, which was due to decreased expression of ISGs [50,51]. Studies identifying the link between the genetics of cancer patients and its effect on IFN signaling in PBMC can help in predicting the clinical outcome in the patient due to modulation in immunosurveillance. Analysis of the transcription level of the genes in different melanoma patients dictated that a decrease in IFN signaling in PBMC correlates with amplification of NOS1 locus and its expression in melanoma cells [52]. The same research group further addressed the mechanism of action of NOS1 in the suppression of IFN signaling in melanoma cells [53]. Histone deacetylase 2 (HDAC2) plays a key role in the expression of ISGs at the transcriptional level, as HDAC2-knockdown decreases the response to IFNα [54]. Accordingly, NOS1 mediated S-nitrosylation of HDAC2 at Cys-262 and -274 [55]. In a controlled experiment, HDAC2 deacetylated H4K16, thereby recruiting RNA polymerase II to the promoter and lead to expression of ISGs in melanoma cells. In this study, NOS1 decreased the IFNα response by S-nitrosylating HDAC2 at position Cys262/Cys274 [55]. S-nitrosylation of HDAC2 by NOS1 decreased the binding of HDAC2 to STAT1, thereby reduced HDAC2 recruitment to the promoter of ISGs, subsequently decreased deacetylation of H4K16. A mutant form of HDAC2 (Cys262/Cys274) that cannot be nitrosylated, reversed NOS1-mediated ISG inhibition, reduced NOS1-induced lung metastasis, and inhibited tumor-homing lymphocytes in a mouse model of melanoma [53]. Thus, NOS1

mediated repression of ISGs through HDAC S-nitrosylation serves as a novel pathway in the progression of melanoma, and studies identifying the targets of NOS1 would help in understanding the cellular mechanism and in designing better immunotherapeutic strategies to target melanoma.

2.3.2.3. Non-small cell lung carcinoma (NSCLC)

The lung tumors such as NSCLC, lung adenocarcinoma, and lung squamous cell carcinoma, together add up to 80% of the lung cancer incidences [56]. A hallmark of tumor microenvironment is the accumulation of stromal fibroblasts, by interacting with tumor cells, these cells can accelerate tumor growth and metastasis [57,58]. Chemo-attractant cytokines, called the chemokines control cellular behavior such as cell migration during organogenesis and immune surveillance [59]. CXCL14 (C-X-C Motif Chemokine Ligand 14) is expressed in various types of cancer and in stromal cells [60,61]. The specific role of CXCL14 is likely context dependent, in that it can promote or regress depending upon which cell type expresses the ligand. For instance, when expressed by the stromal fibroblasts, it showed a tumor-promoting effect [62], in contrast, it acted as an antitumor when expressed by carcinoma cells [63]. Immunohistochemical combined with morphometric analyses were conducted to address the relevance of expression and correlation of CXCL14 and NOS1 in Stage I–IIIA NSCLC patients. In their analyses, CXCL14 was expressed by stromal fibroblasts as well as in cancer cells, while NOS1 was seen only in cancer cells, but not in stromal fibroblast. However, NOS1 level in cancer cells was strongly associated with CXCL14 level in stromal fibroblasts, showing a decrease in progression-free survival (PFS) and overall survival (OS) [58]. While CXCL14-expressing fibroblasts promoted the growth of prostate tumors by NOS1 secretion; in NCSLC, the expression of CXCL14 and NOS1 served as surrogate markers of cancer progression [64].

Thus, more research is warranted to understand how CXCL14 in stromal fibroblasts modulates the level of NOS1 expression in relation to NSCLC disease states. In addition, it would be a rewarding endeavor to carry-out loss- and gain-of-function experiments, thereby titrating down- or up- the levels of CXCL14 to address how CXCL14 levels in stromal cells alters the fate of NSCLC. Indeed, if CXCL14 is required for tumor growth and metastasis, CXCL14 neutralizing antibody could have therapeutic use in the treatment of NSCLC.

2.3.2.4.Colon cancer

The N-terminus of the NOS1 protein harbors a PDZ (PSD-95/Dlg/ZO-1) domain, which mediates its subcellular localization [65]. In their study, NOS1 protein translocated to mitochondria through Hsp90, as geldanamycin (C-terminal inhibitor of Hsp90) treatment inhibited mitochondrial localization. The mitochondria produced reactive oxygen species (ROS) in response to cisplatin, which mediated apoptotic pathway through the release of Cytochrome-c. Additionally, overexpression of mitochondrial NOS1 (mNOS1) inhibited the formation of superoxide anions and the expression of Cytochrome-c after cisplatin treatment. Thus, mNOS inhibits cisplatin-induced apoptosis via mitochondrial ROS suppression [66]. Superoxide dismutase 2 (SOD2) helps in the removal of mitochondrial superoxide [67]. Anticancer drugs increase ROS production to a toxic level in cells, thus mediating tumor cell death [68]. Sirtuin 3 (SIRT3) maintains mitochondrial ROS below toxic level, thereby optimizing tumor cell survival and proliferative mechanism. Enhanced SIRT3 activity enhanced cancer cell resistance to radiation, as well as by chemotherapeutic drugs [69]. mNOS1 increased SIRT3 activity, thereby attenuating mitochondrial superoxide- and cisplatin-induced apoptosis [66]. Thus, Hsp90 induced translocation of mNOS1 to the mitochondria, accordingly enhanced SIRT3

activity to decrease cisplatin-induced ROS generation, suppressed intrinsic apoptosis pathway and promoted tumor growth [66]. Thus, NOS1 limits the magnitude of toxicity of superoxide in mitochondria, thereby providing survival advantage. However, sophisticated cellular and molecular experiments are needed to determine the roles of NOS1 and NO signaling in colon cancer progression.

2.3.3. Role of NOS1 in diabetes

Diabetes mellitus (DM) is a metabolic syndrome defined by chronic hyperglycemia occurring owing to defects in insulin secretion or action mechanisms, or a combination of both [70]. The magnitude and kinetics of hyperglycemia can give rise to EC dysfunction and blood vessel complications. These complications are, (a) microvascular: diabetic kidney disease, retinopathy, and neuropathy; and (b) macrovascular: coronary artery disease, peripheral vascular disease, and stroke, that are linked with morbidity and mortality events in diabetic patients [71]. One of the underlying factors in vascular pathophysiology is NO, where hyperglycemia has a major impact [72,73]. Additionally, the incidences of DM have been linked with alterations in NO-mediated vasomotor dysfunction [74]. NO function has been shown to regulate systemic and local hemodynamics [75]. NOS1-derived NO in MD cells and its role in the regulation of glomerular hemodynamic and renal dysfunctions is of great interest to nephrologists; accordingly, several studies reported NOS1-mediated NO in controlling the DM disease states [75]. Diabetes nephropathy (DN) represents one of the main chronic complications associated with T1DM and T2DMs, together represent the leading causes of renal failure, defined by an increased glomerular filtration rate (GFR), perfusion, and renal hypertrophy [76]. Although the role of NOS1-derived NO is not fully elucidated as it relates to pathogenesis of glomerular hyperfiltration in diabetes, a few

studies have delineated its significance and the underlying biological mechanism. A recent study reported a SGLT1 (Sodium-Glucose Cotransporter 1)-NOS1-TGF signaling axis mediating acute hyperglycemia-associated glomerular hyperfiltration, where NOS1 and SGLT1 may prove to be key therapeutic targets [76]. This mechanism suggests that acute hyperglycemia-induced hyperfiltration increases luminal glucose at MD, leading to an increase in the expression and activity of NOS1 via SGTL1, thus blunting the tubuloglomerular feedback (TGF) response and promoting glomerular hyperfiltration. The authors observed that in both mice and human renal cortices, high glucose upregulated NOS1 level and increased phosphorylation of NOS1 at Ser1417. Interestingly, MD-NOS1 knockout showed no defect in NO generation and effect upon glucose addition to the MD perfusate, as well as no significant TGF response after glucose addition to tubular perfusate. Eventually, acute hyperglycemia-induced elevation in GFR was significantly attenuated, which suggests the key role of NOS1 in mediating glucose-induced hyperfiltration [76]. As discussed above the NOS1-mediated NO production is a major factor in the pathogenesis of renal hemodynamic changes in the early course of diabetes and considered it as the major denominator in the NO mechanisms in this pathology [77]. In their previous study, the inhibition of NOS1 by the administration of S-methyl-l-thiocitrulline (SMTC) both in control and experimentally induced diabetic rats increased blood pressure, but not in normal rats; additionally, diabetic rats showed elevated renal hemodynamic response, suggesting diabetic rats are more sensitive to this inhibition [74]. Subsequently, these authors reported that STZ-induced diabetic rats have increased the number of NOS1-positive cells; and in these rats SMTC administration normalized the elevated GFR in diabetic rats but had no effect on non-diabetic rats, defining the NOS1-specific role in renal hemodynamics in diabetes [78].

Additionally, the same group of authors published a separate study to analyze the nephroprotective role of NOS1 and addressed the progression of renal injury in terms of proteinuria and glomerular sclerosis in uninephrectomized diabetic and non-diabetic rats [77]. This time, the long-term impact of the NOS1-selective inhibitor SMTC was assessed, revealing a modest effect where the renal injury was delayed in diabetic mice, whereas no beneficial effects were observed in normal rats; rather, it increased glomerulosclerosis. Further, SMTC-treated diabetic rats displayed a reduction in weight gain [77]. However, cyclooxygenase-2 (COX-2) expression and activity increase in renal injury, and its action has been implicated in the pathophysiology of such conditions, while NOS1 derived NO in MD is reported as one of the COX-2 activators [79]. Thus, NOS1 inhibition can modulate COX-2 activity to provide therapeutic benefits in conditions such as proteinuria and glomerulosclerosis. However, SMTC inhibition of NOS1 had no effect in COX-2 level in the renal cortex, and this finding does not represent the COX-2 role in mediating the beneficial effect via NOS1 inhibition in diabetic rats; nevertheless, the effect of the NOS1-COX-2 axis during nephropathy cannot be excluded [77].

Excluding DN, the role of NOS1 has also been studied in diabetic cardiomyopathy (DCM). DCM is characterized by cardiac muscle dysfunction and change in cardiomyocyte architecture, caused mostly due to altered glucose metabolism homeostasis, characterized by cardiac muscle contractility dysfunction [80]. As diabetes progresses, systolic dysfunction develops, the cardiac muscle deteriorates, and the production of oxidative stress increases. An increase in oxygen species is directly proportional to NOS uncoupling, which can be reversed for NOS1, upon treatment with cofactor tetrahydrobiopterin (BH4) and sepiapterin, thereby reconfiguring the production of

superoxide rather than NO [81]. T1DM predicts adverse cardiovascular events, e.g., the incidence of heart failure is 2–3 fold higher in diabetic than in normal cohorts [82]. Reduction of myocyte and cardiac contractility is the hallmark of DCM [83]. Due to NOS1 activity in the regulation of RyR2 S-nitrosylation [84], β-adrenergic in the heart, and preventing cardiac dysfunction [85], and the roles of NOS1-derived NO in DCM has been reported. Increased NO concentration could develop EC-dysfunction and atherosclerotic complications in DM; however, it may precipitate into insulin resistance. In one study, NOS1 knockout showed insulin resistance, hypertension, and dyslipidemia [86]. The subsequent hyperglycemia, hyperlipidemia, and insulin resistance, together, augmented oxidative stress in the diabetic cardiac muscles. In diabetic vascular and cardiomyopathy, the oxidation of NOS cofactor BH_4 and dysfunctional activity of NOS are known. In a recent study, an increase in cardiac muscle BH_4 prevented and reversed left ventricular remodeling and systolic dysfunction associated with diabetes, via a mechanism whereby NOS1-derived NO mediated an increase in insulin-independent myocardial glucose absorption and consumption [87].

Independent studies have reported that in DCM, NOS1-derived NO mediates the effect of the β3-adrenoceptor (β3-AR) being involved in an altered positive ionotropic activity to β-adrenoceptor agonist stimulation [88,89]. NOS1 also exerts a crucial role in the mechanism of this disease by the β3-AR-NOS1-RyR2 specific pathway. Inhibition of NOS1 leads to normalization of adverse conditions. In cardiomyocytes, NOS1 is coupled to β3-AR/caveolin3 (Cav3) complex present in the sarcolemma. NOS1 translocation from the sarcoplasmic reticulum (SR) to Sarcolemma caveolae decreased the nitrosylation of RyR2 and activated to release uncontrolled Ca2+ induced arrhythmias [90]. Regular exercise plus insulin

treatment has been regarded as an effective therapy for avoiding the complications of type 1 diabetes (T1DM) [91]. Combined insulin treatment with exercise training was studied on diabetic male Wistar rats for 8 weeks to deduce its effect on baseline heart physiology and NOS1, β3-AR, and RyR2 signaling pathways. Experiments were conducted in four diabetic rodent cohorts: (1) with no treatment, (2) with insulin treatment, (3) trained with exercise, and (4) trained with exercise that received insulin. The diabetic control group showed decreased basal systolic and diastolic cardiac function, and RyR2 expression, with increased β3-AR and NOS1 expression. However, combined treatment in Group 4 did not display normalized diastolic pressure but showed normalized systolic pressure and induced increased RyR2 expression, and this effect was higher than in Group-2 and -3 rodents. Complete normalization of β3-AR and downregulation of NOS1 were observed in all three treatment cohorts [92].

Polymorphism in NOS1 in DM and the genetic variant of NOS1 have been reported. For example, common variation in NOS1AP loci is associated with T2DM in African American and Caucasian cohorts; specifically, the study found that variation in NOS1AP rs12742393 was strongly linked with susceptibility to T2DM [93]. Analyses of 79 SNPs in a group of Shanghai Chinese subjects comprised of 1,691 diabetic and 1,720 normal individuals, an association between NOS1AP SNP rs12742393 and T2DM were observed. Although this variant locus may not be a clinically relevant to T2DM incidence, its effect cannot be neglected [94]. Nevertheless, the roles of SNPs are far from clear, therefore, novel techniques are needed to address the roles of SNPs, not only in cardiovascular disease and diabetes, but also in many neglected diseases as well.

2.3.4. Role of NOS1 in Obesity

Obesity is a major health concern worldwide as risks for hypertension, diabetes, metabolic syndrome, and stroke are increased in these patients [95]. Sedentary lifestyle and genetic variations are considered main drivers of obesity [96]. In this regard, obesity is associated with an imbalance of energy, where the consumption of calories is higher than those required by bodily processes [97]. The homeostatic steady state between energy consumption and expenditure is complicated, likely modulated by several factors, however, understanding underlying mechanism of this metabolic disorder and its key players is crucial. To this end, NO is likely to be a proximal cause of obesity [97], as obese rodents and human cells reportedly have elevated levels of BH2, an oxidized form of BH4. BH4 deficiency is a major factor in the EC damage and dysfunction that occur during obesity, which uncouples the ability of NOS1 to superoxide generation [97,98]. The underlying facts of NOS1-derived NO in obesity are described as drivers of hyperphagia, a phenomenon in which individuals desire to increase food intake [97]. Mice cohort receiving a high-fat diet had an increase in NOS1 in their aortas, and the induction of NOS1 was demonstrated to be due to leptin stimulation [97]. Interestingly, a study stated that leptin deficiency decreases the expression of NOS1 and NO, with an increase in xanthine oxidoreductase (XOR) activity and oxidative stress, thus mediating imbalance in nitroso-redox generation and generating myocardium dysfunction in obesity. Mice lacking leptin (ob/ob) develop cardiac hypertrophy, increased apoptosis of cardiac muscle cells, and decreased survival. Nitrate and nitrite production were reduced in myocardium of ob/ob mice. Leptin treatment restored NOS1 protein in ob/ob mice. The ratio of GSH/GSSG was decreased, suggesting an increase in oxidative stress in ob/ob

mice [99]. In another study, the production NOS1 increased, but decreased catalytic activity of NOS1 in pancreatic beta-cell hyperactivity, in insulin-resistant rats and islets of obese human individuals. Islets from Zucker fa/fa rats showed increased sensitivity to glucose, with subsequent utilization and oxidation. These results in the hypersecretion of insulin due to the fatty acid esterification resulting from increased glucose responsiveness in beta cells [100]. Therefore, these studies suggested that 50–70% of the variation in body weight can be attributed to genetic variation. In a Korean population, three SNPs (rs2293048, rs9658490, and rs4766843) were described in the NOS1 gene; two of which (rs2293048 and rs9658490) showed close association with obesity. A total of six haplotypes among the SNPs of NOS1 (CCG, CGA, TCA, TCG, TGG, and CCG, and TCG and TGG) were associated with increased susceptibility to obesity [101]. Therefore, NOS1 in the regulation of obesity warrants more in-depth studies to reveal the significance of NOS1-derived NO in relation to obese subjects

2.3.5. Role of NOS1 in other inflammatory diseases

In addition to the above-mentioned diseases, the role of NOS1-derived NO has also been described in other pathologies, such as sepsis, achalasia, and infantile hypertrophic pyloric stenosis. NO modulates leukocytes activities and the response of the immune system to infection, sepsis, or septic shock [102]. NOS1 also occurs in the epithelium and microvasculature of the gastrointestinal tract [103], in the myocytes of skeletal muscle, in the bronchial epithelium [104], in mast cells and neutrophils [105]. During sterile peritonitis, $NOS1^{-/-}$ mice displayed increased rolling of leukocytes and adhesion to the post-capillary venule endothelium and its subsequent migration to the peritoneal cavity. Although $NOS1^{-/-}$ mice displayed increased migration of leukocytes in chemical peritonitis and live bacterial

peritonitis, a genetic deficiency in NOS1 lead to increased mortality [106], indicating its pro-life function.

In a mouse model sepsis, increased elaboration of proinflammatory cytokines TNF-α, IL-1β, IL-12, and IL-17 were reported [107]. NO plays a pivotal role during sepsis, exemplified by hypotension (low blood pressure) or hypo-responsiveness (decrease in the response to vasoconstrictors). NOS1 and soluble guanylate cyclase are expressed at high levels in vascular tissue during sepsis, and the blockade of NOS1 inhibits cGMP production, indicating a physical interaction between the two. Pharmacological blockade of NOS1 by 7-nitroindazole (7-NI) or S-methyl-L-thiocitrulline (SMTC) decreased hypo-responsiveness and increased vasoconstriction in a mouse model. Thus, inhibiting NOS1 may help to increase the effect of vasopressors during the late sepsis [108]. In contrast, NOS1-derived NO regulated downstream signaling and cytokine expression in macrophages [102]. This investigation suggested that NOS1-derived NO plays an early role and targets the SOCS1 protein, leading to its degradation. SOCS1 is mainly responsible for the proteasomal degradation of the TIRAP protein, which eventually disrupts TLR-mediated inflammatory signaling and inactivate TF NF-κB. However, the inhibition of SOCS1 by NOS1-derived NO activated NF-κB mediated elaboration of pro-inflammatory cytokines [102,109]. Therefore, it is conceivable that the complete ablation of NOS1 could alter signaling pathways at several cellular and molecular levels in the tissue microenvironment.

Achalasia is a rare disorder, wherein a patient experience trouble passing food or liquid from the esophagus into the stomach. Reduced peristaltic action of the esophagus emerges as smooth muscles fail to relax, thereby causing the lower esophageal sphincter to remain closed, inhibiting the passage of food [110].

NO activity can delay the contraction of the distal esophagus and relaxing the lower esophageal sphincter to allow peristaltic action [111]. A study of the genetic polymorphism of NOS correlated with the presence of nNOS29 C/T with achalasia [112]. NOS1 C/T allelic variant in exon 29 that resides in the untranslated region of the gene likely alters the NOS1 mRNA stability [113]. Thus, the loss of NOS1 predicts poor prognosis of achalasia. Analysis of two siblings with infant-onset achalasia displayed bilateral premature stop codon in the NOS1 gene, which resulted in defects in folding, cofactor binding, and NO production, suggesting the importance of NOS1-derived NO in the prevention of achalasia [114]. Nevertheless, additional studies in aged populations should provide a clearer insight into its role in achalasia.

Infantile hypertrophic pyloric stenosis (IHPS) results from hypertrophy (increase in cell size) of the pyloric muscle and is the most common disease of the gastrointestinal tract in infants [115]. NOS1 is the main source of NO in the gut [116] and plays a major role as a neurotransmitter in the gastrointestinal tract, causing relaxation of smooth muscle of the tract [103]. Genetic disequilibrium of the NOS1 variant locus has been found to pose a susceptibility to IHPS [117]. Genetic analysis of the NOS1 gene conducted in IHPS patients revealed two different mutations, (a) one between the 21st and 22nd exomes, which affected splicing, and (b) another at the 3′ untranslated region, which affects the binding of TFs. The first variant decreased the mRNA expression of NOS1 in IHPS patients [118]. However, there are contrasting results for NOS1 polymorphisms in IHPS patients. Genetic analysis of the NOS1 gene in IHPS patients found 19 polymorphisms in the NOS1 coding region but found no statistically significant correlation with IHPS [119]. SNP at −84 G/A on the promoter of NOS1 exon 1c (rs41279104) has been correlated with an increased risk for the development of

IHPS, with a 30% decrease in NOS1 expression in 16 IHPS patients [120], although no such correlation was found in 54 familial and 28 sporadic cases of IHPS [121], suggesting that the expression of NOS1 in IHPS is regulated by different factors other than SNPs. The −84 G/A polymorphism of NOS1 with IHPS was correlated in Caucasian subjects but was not found in the Chinese population, suggesting that genetic heterogeneity in different populations also plays a crucial role [122]. Differences across population subjects in allelic frequency and linkage disequilibrium also allow for contrasting results. Analyses of DNAs obtained from three Swedish families with multiple affected members did not correlate with NOS1 locus [123]; however, a study of 37 Swedish vs 31 British families with IHPS suggested positive correlation [124]. The major limitation of all studies was the limited number of subjects used. Study on larger samples with individuals from different races might help rule out the possibility of genetic heterogeneity due to different populations and direct us in analysing the other factors responsible for NOS1 expression in IHPS. As discussed above, the mechanisms by which SNPs regulate gene expression constitute a large gap. To address this crucial gap, new technologies are required to fully elucidate the exact roles of SNPs in normal and disease settings.

2.4.Conclusion:

At the basal state, the NOS1 is the sole producer of NO in the brain, and involved in learning and memory development, and modulating synaptic plasticity. As NOS1 can be detected in non-neuronal tissues and organs including in cardiovascular disease, cancer, diabetes, and obesity, therefore, we attempted to provide an overview of the roles of NOS1 in several pathologies to understand the importance of this molecule in different tissue and organ systems. The biological roles of NO in higher organism relies on its basal-state bioavailability and its temporo-

spatial concentration. The organ- and cell type-specific NO production can also add to the complexity in signaling activities. Additionally, organelle specific localization or mis-localization could produce signaling cross-talks and unexpected phenotypes. However, the real workings of NOS1 mediated NO-modified proteins and how they transmit and modulate signaling mechanisms remain unknown.

Although found in a subset of tumors, NOS1 is not an oncogene or a tumor suppressor gene; in other words, NOS1 inhibition or activation in tumor cells may not inhibit the tumor cell proliferation. Conversely, whether the overexpression of NOS1 could transform NIH-3T3 fibroblast cells or the knockdown of NOS1 in tumor cells induce apoptosis, remain unknown. Thus, the precise role of NOS1 in tumor progression is not completely understood. Nevertheless, altered expression or misexpression of NOS1 and NO production thereby signaling cross-talks are likely to define pathophysiological states. Cell-specific NOS1 gene knockouts studies are expected to clarify its exact function. Additionally, the use of small molecule agonist or antagonist for NOS1 and NO in combination with other tools that mediate downstream effect on e.g., NF-κB constitute a potential application for NOS1 mediated interventions in the complications associated with NO produced by NOS1.

Thus, the expression of NOS1 outside the brain in regulating many pathological states can no longer be neglected. Therefore, sophisticated experiments delineating the signaling pathways and molecules regulated by NOS1-derived NO in non-neuronal tissues are needed. As the personalized medicine becomes more clinically relevant in combating certain ailments, elucidation of the complexity of NO signaling pathway will remain a topic of basic research. We feel that continued research on NOS1 in various pathophysiological situations will synthesize new

knowledge as well as to identify therapeutic targets. State of the art techniques including bioelectronics to generate NO in vivo, assay for transposase-accessible chromatin with sequencing (ATAC-Seq), single-cell RNA-seq and biochemical methods combined with computational approaches will be required to address this problem more effectively.

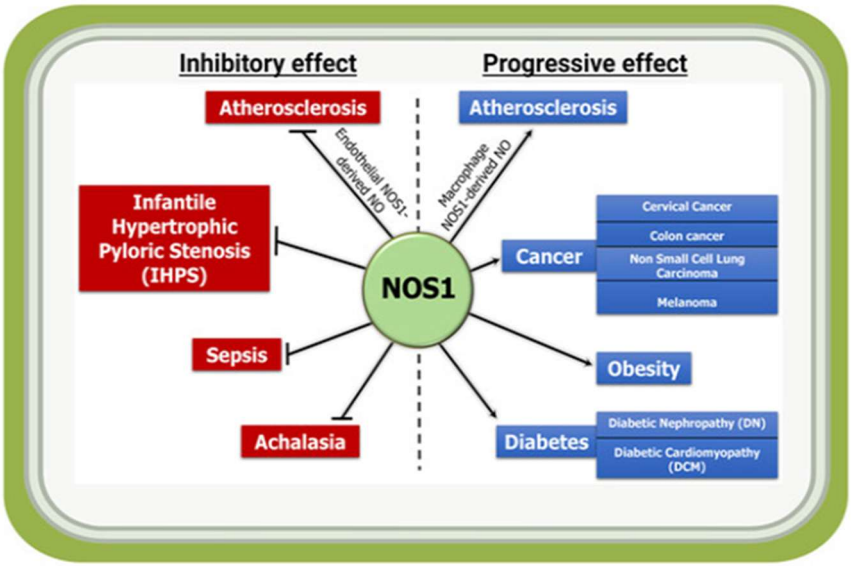

Figure 2.3. Inflammatory and anti-inflammatory activities of NOS1-derived NO in indicated diseases. NOS1-mediated production of NO acts as an inflammatory molecule and mediates the progression of disease such as macrophage NOS1-driven atherosclerosis, and in a subset of cancer, obesity and diabetes; while it acts as a protector in conditions such as endothelial NOS1-driven atherosclerosis, infantile hypertrophic pyloric stenosis (IHPS), sepsis and achalasia**.**

2.5. Macrophage mediated activation of IL-1β and CD40 receptor:

2.5.1. Macrophage mediated activation of IL-1β:

Among the cytokines involved, interleukin-1 beta (IL-1β) is one of the most potent inflammatory mediators produced by macrophages within the arterial wall [125]. IL-1β is synthesized as an inactive precursor (pro-IL-1β) and requires dual regulation—transcriptional priming and inflammasome activation—for its maturation. This tight control reflects the powerful downstream effects of IL-1β signaling in vascular tissues [126].

IL-1β Production Pathway:

IL-1β generation in macrophages involves two signals. Signal 1 (priming) occurs through PRRs such as TLR2 and TLR4 activated by oxLDL, cholesterol crystals, saturated fatty acids, or endothelial debris. This activates the MyD88/NF-κB pathway, inducing transcription of pro-IL-1β and inflammasome components (e.g., NLRP3). Signal 2 (activation) is triggered by cholesterol crystals, mitochondrial ROS, ATP-induced potassium efflux, lysosomal rupture, and ER stress. These initiate assembly of the NLRP3 inflammasome, recruitment of ASC, and activation of caspase-1, which cleaves pro-IL-1β to active IL-1β, enabling secretion [127,128].

Effects on Endothelial Cells:

Macrophage-derived IL-1β is one of the earliest cytokines that disrupt endothelial homeostasis. It downregulates VE-cadherin and tight-junction proteins, increasing vascular permeability and facilitating LDL infiltration and leukocyte entry into the intima.

IL-1β also induces adhesion molecules (VCAM-1, ICAM-1, E-selectin), enhancing monocyte adhesion and transendothelial migration. Through NF-κB activation, endothelial cells under IL-1β stimulation produce CCL2, IL-8, and CXCL1, which recruit monocytes. IL-1β further stimulates NOX-derived ROS production, reducing NO bioavailability and worsening endothelial dysfunction—hallmarks of early atherogenesis [129–131].

Monocyte Recruitment and Myelopoiesis:

IL-1β plays a significant role in monocyte influx. It induces CCL2, CCL5, and CXCL1, forming chemotactic gradients for $CCR2^{+}$ monocytes [132]. IL-1β also activates adhesion molecules on endothelial cells, enabling firm monocyte attachment [133]. Additionally, IL-1β increases systemic myelopoiesis by stimulating bone marrow progenitors, expanding circulating monocyte pools available for lesion recruitment [134].

Foam Cell Formation and Lipid Metabolism:

Within plaques, IL-1β enhances macrophage lipid uptake by upregulating scavenger receptors such as CD36, SR-A1, and LOX-1. Simultaneously, it suppresses ABCA1 and ABCG1, impairing cholesterol efflux and promoting foam cell formation. IL-1β shifts macrophage metabolism toward glycolysis via HIF-1α stabilization, supporting a pro-inflammatory phenotype that maintains chronic plaque inflammation [135,136].

Inflammatory Amplification:

IL-1β acts upstream in inflammatory networks. It sustains NF-κB and AP-1 activation, inducing TNF-α, IL-6, GM-CSF, and further IL-1β transcription, forming a feed-forward cycle [137]. IL-1β also enhances NLRP3 expression, reinforcing inflammasome activity. Additionally, IL-1β promotes Th1 recruitment and activation, increasing IFN-γ levels within plaques, which further amplifies macrophage inflammatory responses [138].

Pathological Consequences of IL-1β in Plaque Progression, Destabilization, and Clinical Relevance

Macrophage-derived IL-1β contributes significantly to plaque progression and the development of unstable, rupture-prone lesions. Its effects extend across extracellular matrix remodeling, necrotic core expansion, smooth muscle cell (SMC) phenotype modulation, and promotion of thrombosis.

Extracellular Matrix Degradation and Fibrous Cap Weakening:

IL-1β stimulates macrophages and SMCs to secrete matrix metalloproteinases (MMP-1, MMP-3, MMP-9, MMP-12), which degrade collagen and elastin in the fibrous cap. This weakens structural stability and increases susceptibility to plaque rupture [139]. IL-1β also upregulates cathepsins and suppresses collagen synthesis, compounding the weakening of the fibrous cap [140].

Cell Death, Necrotic Core Expansion, and Defective Efferocytosis:

IL-1β promotes macrophage apoptosis and secondary necrosis, contributing to necrotic core expansion. Oxidative stress induced by IL-1β further disrupts efferocytosis, impairing clearance of apoptotic cells. Accumulation of necrotic debris creates a pro-thrombotic lipid core, a defining feature of advanced atherosclerosis.

Smooth Muscle Cell Modulation:

IL-1β induces SMCs to shift from a contractile to a synthetic, inflammatory phenotype. These SMCs proliferate and migrate into the intima, where they secrete extracellular matrix components and inflammatory cytokines [141]. Although SMC-driven matrix production initially contributes to plaque stability, chronic IL-1β signaling reduces SMC contractile protein expression and promotes detrimental matrix remodeling.

Thrombogenicity and Plaque Rupture:

IL-1β upregulates tissue factor on macrophages and endothelial cells, strongly promoting thrombogenicity. In advanced plaques, high IL-1β levels correlate with thin fibrous caps, large necrotic cores, and high tissue factor expression—features that facilitate acute thrombus formation upon plaque rupture, leading to myocardial infarction or stroke [142].

Human Studies and Clinical Evidence:

Human atherosclerotic plaques consistently show high IL-1β expression in macrophage-rich regions, with strong correlations to necrotic core size and markers of plaque instability. Genetic

polymorphisms in IL1B, NLRP3, and IL1R1 genes are associated with increased cardiovascular risk. The most compelling evidence comes from the CANTOS trial, where selective IL-1β inhibition with canakinumab significantly reduced recurrent cardiovascular events independent of lipid lowering. IL-1β blockade decreased IL-6 and hsCRP levels, confirming the cytokine's upstream regulatory role in systemic and vascular inflammation [143].

Therapeutic Implications:

The pathogenic role of IL-1β highlights it as a prime therapeutic target. Existing agents such as canakinumab and anakinra demonstrate cardiovascular benefits but carry risks of increased infection due to systemic immunosuppression [144]. Thus, emerging strategies aim for macrophage-specific IL-1β suppression, such as nanoparticle-mediated delivery of IL-1β siRNA, inhibition of macrophage-specific inflammasome activation, and metabolic reprogramming to reduce IL-1β production. These approaches aim to retain the anti-atherosclerotic benefits of IL-1β inhibition while minimizing systemic side effects.

Conclusion:

Macrophage-derived IL-1β is a central inflammatory mediator that acts at nearly every step of atherosclerosis—from endothelial dysfunction and monocyte recruitment to foam cell formation, plaque expansion, and final plaque destabilization. Its role as an upstream cytokine driving sustained inflammatory signaling, coupled with strong clinical evidence from IL-1β inhibition trials, establishes IL-1β as a causal and therapeutically actionable driver of atherosclerotic disease. Targeted modulation

of macrophage IL-1β offers a promising avenue for future cardiovascular therapies.

2.5.2. Macrophage mediated activation of CD40 receptor and CD40-40L interaction:

The CD40–CD40 ligand (CD40L) signaling axis is a central immunoregulatory mechanism that profoundly influences the initiation, progression, and destabilization of atherosclerotic plaques. CD40 belongs to the tumor necrosis factor receptor (TNFR) superfamily and is primarily expressed on macrophages, dendritic cells, endothelial cells, and vascular smooth muscle cells within atherosclerotic lesions. Its ligand, CD40L (also known as CD154), is predominantly expressed on activated T cells and platelets but can also be found on endothelial cells and some macrophage subsets. In the context of atherosclerosis, the macrophage–T cell interaction mediated through CD40–CD40L represents a powerful inflammatory and immunomodulatory pathway that amplifies lesion inflammation, supports foam cell formation, drives matrix degradation, and contributes to plaque instability [145,146].

CD40 Expression on Macrophages and Its Induction in Atherosclerosis

In healthy tissues, macrophage CD40 expression is relatively low. However, in atherosclerotic plaques, macrophages are exposed to a variety of pro-inflammatory stimuli including oxidized LDL (oxLDL), cholesterol crystals, toll-like receptor (TLR) ligands, interferon-γ (IFN-γ), and tumor necrosis factor-α (TNF-α). These signals markedly upregulate CD40 transcription and surface expression [147]. Activated plaque macrophages display high levels of CD40 especially in lipid-rich and shoulder

regions of plaques—areas known to be prone to rupture [148]. Additionally, circulating monocytes from patients with coronary artery disease show increased CD40 expression even before entering the lesion, reflecting systemic priming. Macrophage polarization also influences CD40 expression; M1 (classically activated) macrophages exhibit higher CD40 levels compared to M2 macrophages, linking CD40 signaling to pro-inflammatory macrophage phenotypes associated with unstable plaque morphology [149].

Mechanisms of CD40 Activation by CD40L in the Atherosclerotic Microenvironment

CD40 is activated through interaction with CD40L, which is expressed primarily on $CD4^+$ T helper cells, especially Th1 cells that infiltrate atherosclerotic lesions [150]. Platelets, which are abundant at sites of endothelial injury and arterial shear stress, are also a major source of soluble and membrane-bound CD40L. Engagement of CD40 with CD40L leads to receptor trimerization and recruitment of TNF receptor-associated factors (TRAFs), particularly TRAF2, TRAF3, TRAF5, and TRAF6. These adaptor proteins initiate downstream signaling cascades including NF-κB, MAPK (p38, JNK, ERK), and PI3K/Akt pathways [151]. In macrophages, CD40–CD40L signaling generates a potent transcriptional response involving upregulation of inflammatory cytokines, chemokines, matrix metalloproteinases (MMPs), costimulatory molecules, and genes that regulate lipid uptake and antigen presentation [152].

In the plaque microenvironment, the interaction between $CD40^+$ macrophages and $CD40L^+$ T cells occurs within defined microdomains, particularly in regions of high cellularity and antigen presentation. These immune synapse–like interactions sustain chronic macrophage activation. Moreover, platelets

adhering to dysfunctional endothelium or aggregated within damaged plaques express high levels of CD40L, providing an abundant and sustained ligand source that activates CD40 signaling even in the absence of T cells [153].

CD40–CD40L Signaling in Macrophage-Driven Inflammation

CD40 ligation induces macrophages to produce a broad array of pro-inflammatory cytokines and chemokines including IL-1β, TNF-α, IL-6, CCL2 (MCP-1), CCL5, CXCL9, and CXCL10. These molecules recruit additional monocytes, T cells, and dendritic cells to the lesion, creating a highly inflamed microenvironment that supports plaque expansion. CD40 signaling also enhances NLRP3 inflammasome priming by activating NF-κB, further promoting IL-1β maturation and secretion. This positions CD40 as an upstream amplifier of inflammasome-mediated inflammation [154].

Additionally, CD40 drives expression of costimulatory molecules such as CD80 and CD86, which enhance antigen presentation and T cell activation. This creates a bidirectional reinforcement loop: activated T cells provide more CD40L, which further activates macrophages, resulting in persistent inflammation. This loop is a key mechanism underlying the chronicity of atherosclerosis.

CD40–CD40L Effects on Lipid Handling and Foam Cell Formation

CD40 engagement alters macrophage lipid metabolism in ways that promote foam cell formation. CD40 signaling increases the expression of scavenger receptors including CD36, SR-A1, and LOX-1, enhancing uptake of oxidized and modified LDL

particles. The pathway also suppresses cholesterol efflux transporters ABCA1 and ABCG1 through NF-κB and JNK-mediated repression, reducing cholesterol removal and encouraging intracellular lipid accumulation [155]. These events accelerate foam cell formation, a hallmark of early and progressive atherosclerotic plaques. Moreover, CD40 activation increases macrophage metabolic reprogramming toward glycolysis, which supports sustained inflammatory cytokine production and survival of foam cells within the hypoxic plaque environment [156]. This metabolic adaptation contributes to the persistence of inflammatory macrophages and the growth of necrotic cores.

CD40–CD40L in Smooth Muscle Cell Modulation and Endothelial Dysfunction

Macrophage-derived cytokines generated via CD40 signaling strongly influence endothelial cells (ECs) and vascular smooth muscle cells (SMCs). On endothelial cells, CD40 activation increases expression of adhesion molecules (VCAM-1, ICAM-1, E-selectin) and enhances endothelial permeability. This promotes further monocyte recruitment and LDL entry into the intima [157]. Exposure to soluble mediators downstream of CD40 activation also induces oxidative stress, reduces nitric oxide bioavailability, and amplifies endothelial dysfunction.

In SMCs, CD40 signaling promotes a phenotypic shift from a contractile to an inflammatory/synthetic phenotype. SMCs exposed to CD40L or macrophage-derived cytokines migrate into the intima, proliferate, and produce extracellular matrix components. While this initially contributes to plaque stability, chronic CD40-mediated inflammation increases SMC production of MMPs and reduces collagen synthesis, ultimately weakening the fibrous cap [158].

CD40–CD40L and Matrix Degradation, Fibrous Cap Thinning, and Plaque Destabilization

One of the most significant consequences of CD40–CD40L activation is the induction of matrix metalloproteinases (MMP-1, MMP-3, MMP-9, MMP-12) and cathepsins (Cathepsin S, K, L) in macrophages and SMCs [159]. These proteases degrade collagen, elastin, and basement membrane components within the fibrous cap, contributing to thinning and weakening of plaque structure. TRAF6-dependent activation via CD40 is particularly important in MMP induction. The imbalance between ECM synthesis and degradation driven by CD40–CD40L is a defining feature of unstable plaques [159]. Additionally, CD40 signaling enhances macrophage apoptosis, which contributes to enlargement of the necrotic core [160]. Inefficient efferocytosis in advanced plaques means these apoptotic cells undergo secondary necrosis, releasing cellular debris and pro-thrombotic lipid content. This further destabilizes plaques.

CD40–CD40L and Thrombogenicity

Beyond inflammation and matrix degradation, CD40–CD40L signaling promotes thrombosis [161]. CD40L on activated platelets promotes platelet aggregation and stabilization of thrombi [162]. CD40 activation on endothelial cells and macrophages induces tissue factor expression, the primary initiator of the coagulation cascade [163]. In vulnerable plaques, elevated tissue factor levels markedly increase the risk of thrombosis upon plaque disruption. Furthermore, soluble CD40L released by activated platelets amplifies thrombus formation independently of classic coagulation factors [164].

Clinical Evidence Supporting the Role of CD40–CD40L in Atherosclerosis

Human atherosclerotic plaques show high CD40 expression in macrophage-rich regions and elevated CD40L expression on infiltrating T cells and platelet aggregates [165]. Serum levels of soluble CD40L correlate with plaque burden, degree of inflammation, and risk of acute coronary events. Genetic studies indicate that polymorphisms in CD40 or CD40L modulate susceptibility to atherosclerosis and cardiovascular disease severity [166]. Importantly, experimental models show that disruption of CD40–CD40L interactions reduces plaque size, inflammation, and vulnerability [167].

Therapeutic Implications and Selective Targeting Strategies

Given its central role, CD40–CD40L is considered a promising therapeutic target [167]. However, systemic blockade of CD40L caused thrombotic complications in clinical trials due to CD40L's role on platelets [168]. Therefore, recent strategies aim to selectively inhibit CD40–TRAF6 interactions while preserving TRAF2/3 pathways essential for immune homeostasis [169]. Blocking specific CD40 signaling arms reduces inflammation and plaque progression without causing immunosuppression [169]. Another promising avenue is nanoparticle-mediated delivery of CD40 siRNA to plaque macrophages, which selectively suppresses CD40 expression in atherosclerotic lesions without affecting systemic immunity.

Conclusion

The CD40–CD40L interaction is a master regulator of immune-mediated inflammation in atherosclerosis. Macrophage activation through CD40 signaling promotes lipid accumulation, cytokine production, endothelial dysfunction, extracellular matrix degradation, and plaque instability, while simultaneously increasing thrombogenic potential. Its upstream positioning in inflammatory signaling networks makes CD40–CD40L an attractive therapeutic target, but selective, macrophage-specific approaches are necessary to avoid systemic adverse effects. The pathway's multifaceted involvement across inflammation, immunity, metabolism, and thrombosis underscores its importance as a driver of atherosclerotic disease.

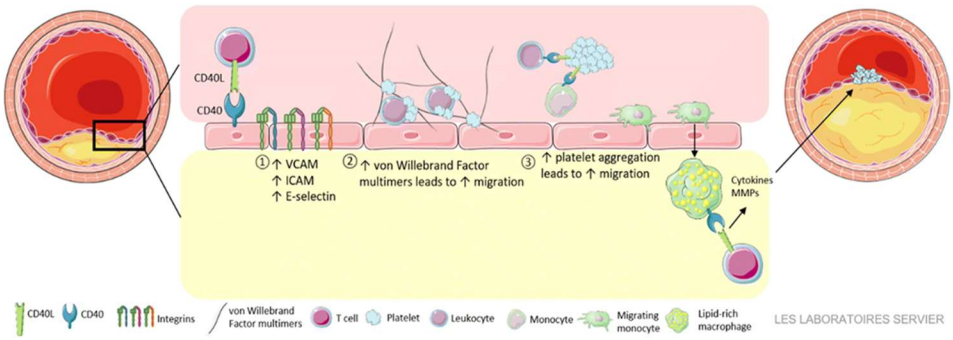

Figure 2.4. Role of CD40 receptor and ligand in atherosclerosis. (Image Courtesy: Bosmans, L.A. et al. J. of Cardiovasc. Trans. Res. 14, 13–22 (2021). https://doi.org/10.1007/s12265-020-09994-3)

2.6.Role of CD36 in Atherosclerosis:

Macrophage CD36 is a multifunctional scavenger receptor that plays a central and highly influential role in lipid uptake, inflammatory activation, metabolic programming, and plaque destabilization in atherosclerosis [170]. CD36, an 88-kDa transmembrane glycoprotein of the class B scavenger receptor family, is abundantly expressed on macrophages within atherosclerotic plaques, particularly in lipid-rich and necrotic core regions. Its expression is tightly regulated by transcription factors such as PPARγ, LXRα, NF-κB, and STAT1, and is strongly induced by atherogenic stimuli including oxidized LDL (oxLDL), saturated fatty acids, advanced glycation end products, hypoxia, and inflammatory cytokines like IL-1β and TNF-α [171]. Circulating monocytes from individuals with metabolic syndrome or diabetes show elevated CD36 even before entering the arterial intima, indicating systemic priming and heightened susceptibility to foam cell formation [172].

CD36 is one of the principal receptors responsible for the internalization of oxLDL and other modified lipoproteins such as acetylated LDL and oxidized phospholipids [173]. Upon ligand binding, CD36 initiates actin-dependent endocytosis that leads to cholesterol ester accumulation and foam cell formation. This lipid loading is amplified by metabolic adaptations: CD36 signaling suppresses cholesterol efflux transporters ABCA1 and ABCG1 while increasing the activity of ACAT1, promoting intracellular esterification and storage of cholesterol [174]. In addition to direct lipid uptake, CD36 activation induces mitochondrial dysfunction and reactive oxygen species (ROS) generation, which enhances oxidative stress and further increases the pool of oxidized lipids within the plaque [175]. Foam cells formed through CD36-mediated processes not only

accumulate lipids but also secrete pro-inflammatory cytokines, chemokines, and proteases that contribute to the amplification of local inflammation.

Beyond lipid uptake, CD36 serves an essential role as a pattern-recognition receptor linking metabolic signals to innate immune activation [171]. Binding of oxLDL or oxidized phospholipids causes CD36 to form complexes with TLR4 and TLR6, leading to MyD88-dependent activation of NF-κB, AP-1, and MAPK pathways [176]. This culminates in the production of inflammatory mediators such as IL-1β, TNF-α, IL-6, CCL2, and CXCL10. CD36 signaling also primes the NLRP3 inflammasome by upregulating inflammatory gene expression, while cholesterol crystal accumulation drives the second activation signal, triggering caspase-1–mediated processing of IL-1β and IL-18 [177]. Through this mechanism, CD36 integrates metabolic stress with inflammatory amplification, positioning it as a major driver of sustained inflammation within atherosclerotic plaques. Cytokines released downstream of CD36 activation also enhance endothelial adhesion molecule expression such as VCAM-1 and ICAM-1, facilitating recruitment of additional monocytes into the intima [178]. Thus, CD36 participates in a self-reinforcing cycle of immune activation and leukocyte infiltration.

CD36 also contributes to efferocytosis, the process by which macrophages clear apoptotic cells, through recognition of oxidized phosphatidylserine on dying cells [179]. However, the lipid-rich, inflammatory conditions of advanced plaques impair this beneficial function. Excessive oxLDL uptake via CD36 promotes ER stress, mitochondrial dysfunction, and apoptosis in macrophages [180]. Because efferocytosis becomes defective in

late-stage plaques, apoptotic macrophages undergo secondary necrosis, releasing cellular debris, proteases, and lipid material. This contributes to necrotic core expansion, increased inflammation, and heightened plaque vulnerability. Thus, CD36 has a dual role in cell clearance—facilitating efferocytosis in controlled environments but contributing to defective clearance and necrotic core enlargement during chronic lipid overload.

The effects of CD36 activation extend beyond macrophages to the vascular wall. Macrophage-derived cytokines and ROS impair endothelial function by reducing nitric oxide bioavailability and increasing endothelial permeability, allowing further LDL and monocyte entry into the intima [181]. CD36-driven inflammatory signaling also influences smooth muscle cells (SMCs), promoting their migration from the media to the intima and shifting them toward a synthetic, pro-inflammatory phenotype [182]. These SMCs contribute to extracellular matrix remodeling but eventually participate in fibrous cap thinning due to increased matrix metalloproteinase secretion under inflammatory conditions. Platelets express CD36 as well, and CD36 activation enhances platelet aggregation and thrombosis [183]. Interactions between $CD36^{+}$ platelets and macrophages within the plaque further elevate inflammatory signaling and create a highly pro-thrombotic environment [184].

Given its multifaceted role in lipid uptake, inflammation, cell death, and plaque destabilization, CD36 is an attractive therapeutic target in atherosclerosis [184]. Experimental models demonstrate that genetic deletion or pharmacological inhibition of CD36 reduces foam cell formation, plaque burden, and inflammatory cytokine production [184]. Therapeutic strategies include blocking CD36 with antibodies, inhibiting downstream

signaling, suppressing CD36 transcription, or delivering CD36-targeted siRNA encapsulated in nanoparticles to plaque macrophages [185]. However, systemic inhibition of CD36 may carry risks because of its roles in fatty acid uptake, metabolism, taste signaling, and platelet function. Therefore, macrophage-selective targeting strategies are being developed to exploit the therapeutic benefits of CD36 inhibition while minimizing unwanted systemic effects.

In summary, macrophage CD36 is a central orchestrator of atherogenesis, integrating lipid uptake with inflammatory signaling and contributing to foam cell formation, inflammasome activation, necrotic core expansion, endothelial dysfunction, and thrombosis. Through its ability to couple metabolic stress with innate immune activation, CD36 drives the chronic inflammatory environment characteristic of atherosclerotic plaques. Understanding the diverse roles and regulatory mechanisms of CD36 provides important insights for therapeutic strategies aimed at reducing macrophage-driven inflammation and improving plaque stability in cardiovascular disease.

2.7. Bibliography:

[1] S.M. Morris, Enzymes of Arginine Metabolism, The Journal of Nutrition 134 (2004) 2743S-2747S. https://doi.org/10.1093/jn/134.10.2743S.

[2] J.V. Esplugues, NO as a signalling molecule in the nervous system, British J Pharmacology 135 (2002) 1079–1095. https://doi.org/10.1038/sj.bjp.0704569.

[3] P. Ferdinandy, R. Schulz, Nitric oxide, superoxide, and peroxynitrite in myocardial ischaemia-reperfusion injury and preconditioning, British J Pharmacology 138 (2003) 532–543. https://doi.org/10.1038/sj.bjp.0705080.

[4] S. Moncada, E.A. Higgs, Nitric Oxide and the Vascular Endothelium, in: S. Moncada, A. Higgs (Eds.), The Vascular Endothelium I, Springer Berlin Heidelberg, Berlin, Heidelberg, 2006: pp. 213–254. https://doi.org/10.1007/3-540-32967-6_7.

[5] R. Radi, Oxygen radicals, nitric oxide, and peroxynitrite: Redox pathways in molecular medicine, Proc. Natl. Acad. Sci. U.S.A. 115 (2018) 5839–5848. https://doi.org/10.1073/pnas.1804932115.

[6] J.T. Mattila, A.C. Thomas, Nitric Oxide Synthase: Non-Canonical Expression Patterns, Front. Immunol. 5 (2014). https://doi.org/10.3389/fimmu.2014.00478.

[7] R. Carnicer, M.J. Crabtree, V. Sivakumaran, B. Casadei, D.A. Kass, Nitric Oxide Synthases in Heart Failure, Antioxidants & Redox Signaling 18 (2013) 1078–1099. https://doi.org/10.1089/ars.2012.4824.

[8] R.A. Frost, G.J. Nystrom, C.H. Lang, Lipopolysaccharide stimulates nitric oxide synthase-2 expression in murine skeletal muscle and C_2 C_{12} myoblasts via Toll-like receptor-4 and c-Jun NH_2 -terminal kinase pathways, American Journal of Physiology-Cell Physiology 287 (2004) C1605–C1615. https://doi.org/10.1152/ajpcell.00010.2004.

[9] U. Forstermann, W.C. Sessa, Nitric oxide synthases: regulation and function, European Heart Journal 33 (2012) 829–837. https://doi.org/10.1093/eurheartj/ehr304.

[10] A.V. Hall, H. Antoniou, Y. Wang, A.H. Cheung, A.M. Arbus, S.L. Olson, W.C. Lu, C.L. Kau, P.A. Marsden, Structural organization of the human neuronal nitric oxide synthase gene (NOS1), Journal of Biological Chemistry 269 (1994) 33082–33090. https://doi.org/10.1016/S0021-9258(20)30099-5.

[11] L. Zhou, D.-Y. Zhu, Neuronal nitric oxide synthase: Structure, subcellular localization, regulation, and clinical implications, Nitric Oxide 20 (2009) 223–230. https://doi.org/10.1016/j.niox.2009.03.001.

[12] P. Zhang, P. Basu, L.C. Redmond, P.E. Morris, J.W. Rupon, G.D. Ginder, J.A. Lloyd, A functional screen for Krüppel-like factors that regulate the human γ-globin gene through the CACCC promoter element, Blood Cells, Molecules, and Diseases 35 (2005) 227–235. https://doi.org/10.1016/j.bcmd.2005.04.009.

[13] H. Strijdom, N. Chamane, A. Lochner, Nitric oxide in the cardiovascular system: a simple molecule with complex actions, Cardiovasc J Afr 20 (2009) 303–310.

[14] C. Villanueva, C. Giulivi, Subcellular and cellular locations of nitric oxide synthase isoforms as determinants of health and disease, Free Radical Biology and Medicine 49 (2010) 307–316. https://doi.org/10.1016/j.freeradbiomed.2010.04.004.

[15] Y.H. Zhang, Nitric oxide signalling and neuronal nitric oxide synthase in the heart under stress, F1000Res 6 (2017) 742. https://doi.org/10.12688/f1000research.10128.1.

[16] J.N. Wilcox, R.R. Subramanian, C.L. Sundell, W.R. Tracey, J.S. Pollock, D.G. Harrison, P.A. Marsden, Expression of Multiple Isoforms of Nitric Oxide Synthase in Normal and Atherosclerotic Vessels, ATVB 17 (1997) 2479–2488. https://doi.org/10.1161/01.ATV.17.11.2479.

[17] A. Weisz, S. Oguchi, L. Cicatiello, H. Esumi, Dual mechanism for the control of inducible-type NO synthase gene expression in macrophages during activation by interferon-gamma and bacterial lipopolysaccharide. Transcriptional and post-transcriptional regulation, J Biol Chem 269 (1994) 8324–8333.

[18] P.J. Kuhlencordt, R. Gyurko, F. Han, M. Scherrer-Crosbie, T.H. Aretz, R. Hajjar, M.H. Picard, P.L. Huang, Accelerated Atherosclerosis, Aortic Aneurysm Formation, and Ischemic Heart Disease in Apolipoprotein E/Endothelial Nitric Oxide Synthase Double-Knockout Mice, Circulation 104 (2001) 448–454. https://doi.org/10.1161/hc2901.091399.

[19] P. Ponnuswamy, A. Schröttle, E. Ostermeier, S. Grüner, P.L. Huang, G. Ertl, U. Hoffmann, B. Nieswandt, P.J. Kuhlencordt, eNOS Protects from Atherosclerosis Despite Relevant Superoxide Production by the Enzyme in apoE−/− Mice, PLoS ONE 7 (2012) e30193. https://doi.org/10.1371/journal.pone.0030193.

[20] L. Barouch, Combined loss of neuronal and endothelial nitric oxide synthase causes premature mortality and age-related hypertrophic cardiac remodeling in mice, Journal of Molecular and Cellular Cardiology 35 (2003) 637–644. https://doi.org/10.1016/S0022-2828(03)00079-8.

[21] A. Roy, U. Saqib, M.S. Baig, NOS1-mediated macrophage and endothelial cell interaction in the progression of atherosclerosis, Cell Biology International 45 (2021) 1191–1201. https://doi.org/10.1002/cbin.11558.

[22] A. Roy, S. Banerjee, U. Saqib, M.S. Baig, NOS1-derived nitric oxide facilitates macrophage uptake of low-density lipoprotein, J of Cellular Biochemistry 120 (2019) 11593–11603. https://doi.org/10.1002/jcb.28439.

[23] S. Chakrabarti, C.K. Chan, Y. Jiang, S.T. Davidge, Neuronal nitric oxide synthase regulates endothelial inflammation, Journal of

Leukocyte Biology 91 (2012) 947–956. https://doi.org/10.1189/jlb.1011513.

[24] L. Capettini, S. Cortes, J. Silva, J. Alvarez-Leite, V. Lemos, Decreased production of neuronal NOS-derived hydrogen peroxide contributes to endothelial dysfunction in atherosclerosis, British J Pharmacology 164 (2011) 1738–1748. https://doi.org/10.1111/j.1476-5381.2011.01500.x.

[25] J.M. Navia-Pelaez, G.P. Campos-Mota, J.C. Araujo De Souza, E.C. Aguilar, N. Stergiopulos, J.I. Alvarez-Leite, L.S.A. Capettini, nNOS uncoupling by oxidized LDL: Implications in atherosclerosis, Free Radical Biology and Medicine 113 (2017) 335–346. https://doi.org/10.1016/j.freeradbiomed.2017.09.018.

[26] J.M. Navia-Pelaez, G.P. Campos, J.C. Araujo-Souza, N. Stergiopulos, L.S.A. Capettini, Modulation of nNOS ser852 phosphorylation and translocation by PKA/PP1 pathway in endothelial cells, Nitric Oxide 72 (2018) 52–58. https://doi.org/10.1016/j.niox.2017.11.007.

[27] E.A. Ashley, C.E. Sears, S.M. Bryant, H.C. Watkins, B. Casadei, Cardiac Nitric Oxide Synthase 1 Regulates Basal and β-Adrenergic Contractility in Murine Ventricular Myocytes, Circulation 105 (2002) 3011–3016. https://doi.org/10.1161/01.CIR.0000019516.31040.2D.

[28] C.E. Sears, S.M. Bryant, E.A. Ashley, C.A. Lygate, S. Rakovic, H.L. Wallis, S. Neubauer, D.A. Terrar, B. Casadei, Cardiac Neuronal Nitric Oxide Synthase Isoform Regulates Myocardial Contraction and Calcium Handling, Circulation Research 92 (2003). https://doi.org/10.1161/01.RES.0000064585.95749.6D.

[29] D. Dawson, C.A. Lygate, M.-H. Zhang, K. Hulbert, S. Neubauer, B. Casadei, *nNOS* Gene Deletion Exacerbates Pathological Left Ventricular Remodeling and Functional Deterioration After Myocardial Infarction, Circulation 112 (2005) 3729–3737. https://doi.org/10.1161/CIRCULATIONAHA.105.539437.

[30] D.E. Burger, X. Lu, M. Lei, F.-L. Xiang, L. Hammoud, M. Jiang, H. Wang, D.L. Jones, S.M. Sims, Q. Feng, Neuronal Nitric Oxide Synthase Protects Against Myocardial Infarction-Induced Ventricular Arrhythmia and Mortality in Mice, Circulation 120 (2009) 1345–1354. https://doi.org/10.1161/CIRCULATIONAHA.108.846402.

[31] R.A. Dulce, V. Mayo, E.B. Rangel, W. Balkan, J.M. Hare, Interaction Between Neuronal Nitric Oxide Synthase Signaling and Temperature Influences Sarcoplasmic Reticulum Calcium Leak: Role of Nitroso–Redox Balance, Circulation Research 116 (2015) 46–55. https://doi.org/10.1161/CIRCRESAHA.116.305172.

[32] G. Venturini, M. Colasanti, E. Fioravanti, A. Bianchini, P. Ascenzi, Direct Effect of Temperature on the Catalytic Activity of Nitric Oxide Synthases Types I, II, and III, Nitric Oxide 3 (1999) 375–382. https://doi.org/10.1006/niox.1999.0250.

[33] S.A. Khan, K. Lee, K.M. Minhas, D.R. Gonzalez, S.V.Y. Raju, A.D. Tejani, D. Li, D.E. Berkowitz, J.M. Hare, Neuronal nitric oxide synthase negatively regulates xanthine oxidoreductase inhibition of cardiac excitation-contraction coupling, Proc. Natl. Acad. Sci. U.S.A. 101 (2004) 15944–15948. https://doi.org/10.1073/pnas.0404136101.

[34] C.V. Breton, C. Park, K. Siegmund, W.J. Gauderman, L. Whitfield-Maxwell, H.N. Hodis, E. Avol, F.D. Gilliland, *NOS1* Methylation and Carotid Artery Intima-Media Thickness in Children, Circ Cardiovasc Genet 7 (2014) 116–122. https://doi.org/10.1161/CIRCGENETICS.113.000320.

[35] S. Fiatal, R. Ádány, Application of Single-Nucleotide Polymorphism-Related Risk Estimates in Identification of Increased Genetic Susceptibility to Cardiovascular Diseases: A Literature Review, Front. Public Health 5 (2018) 358. https://doi.org/10.3389/fpubh.2017.00358.

[36] A. Levinsson, A.-C. Olin, L. Björck, A. Rosengren, F. Nyberg, Nitric oxide synthase (NOS) single nucleotide polymorphisms are

associated with coronary heart disease and hypertension in the INTERGENE study, Nitric Oxide 39 (2014) 1–7. https://doi.org/10.1016/j.niox.2014.03.164.

[37] J.D. Sara, M.F. Eleid, R. Gulati, D.R. Holmes, Sudden Cardiac Death From the Perspective of Coronary Artery Disease, Mayo Clinic Proceedings 89 (2014) 1685–1698. https://doi.org/10.1016/j.mayocp.2014.08.022.

[38] K.-C. Chang, T. Sasano, Y.-C. Wang, S.K.S. Huang, Nitric Oxide Synthase 1 Adaptor Protein, an Emerging New Genetic Marker for QT Prolongation and Sudden Cardiac Death, Acta Cardiol Sin 29 (2013) 217–225.

[39] W.H.L. Kao, D.E. Arking, W. Post, T.D. Rea, N. Sotoodehnia, R.J. Prineas, B. Bishe, B.Q. Doan, E. Boerwinkle, B.M. Psaty, G.F. Tomaselli, J. Coresh, D.S. Siscovick, E. Marbán, P.M. Spooner, G.L. Burke, A. Chakravarti, Genetic Variations in Nitric Oxide Synthase 1 Adaptor Protein Are Associated With Sudden Cardiac Death in US White Community-Based Populations, Circulation 119 (2009) 940–951. https://doi.org/10.1161/CIRCULATIONAHA.108.791723.

[40] M. Tomás, C. Napolitano, L. De Giuli, R. Bloise, I. Subirana, A. Malovini, R. Bellazzi, D.E. Arking, E. Marban, A. Chakravarti, P.M. Spooner, S.G. Priori, Polymorphisms in the NOS1APGene Modulate QT Interval Duration and Risk of Arrhythmias in the Long QT Syndrome, Journal of the American College of Cardiology 55 (2010) 2745–2752. https://doi.org/10.1016/j.jacc.2009.12.065.

[41] A.V. Treuer, D.R. Gonzalez, NOS1AP Modulates Intracellular Ca2+ in Cardiac Myocytes and is Up-Regulated in Dystrophic Cardiomyopathy, Biophysical Journal 106 (2014) 116a. https://doi.org/10.1016/j.bpj.2013.11.700.

[42] S. Korde Choudhari, M. Chaudhary, S. Bagde, A.R. Gadbail, V. Joshi, Nitric oxide and cancer: a review, World J Surg Onc 11 (2013) 118. https://doi.org/10.1186/1477-7819-11-118.

[43] R. Hamaoka, Y. Yaginuma, T. Takahashi, J. Fujii, M. Koizumi, H.G. Seo, Y. Hatanaka, K. Hashizume, K. Ii, J. Miyagawa, T. Hanafusa, Y. Matsuzawa, M. Ishikawa, N. Taniguchi, Different expression patterns of nitric oxide synthase isozymes in various gynecological cancers, J Cancer Res Clin Oncol 125 (1999) 321. https://doi.org/10.1007/s004320050281.

[44] W. Xu, L.Z. Liu, M. Loizidou, M. Ahmed, I.G. Charles, The role of nitric oxide in cancer, Cell Res 12 (2002) 311–320. https://doi.org/10.1038/sj.cr.7290133.

[45] S. Vaccarella, S. Franceschi, G. Engholm, S. Lönnberg, S. Khan, F. Bray, 50 years of screening in the Nordic countries: quantifying the effects on cervical cancer incidence, Br J Cancer 111 (2014) 965–969. https://doi.org/10.1038/bjc.2014.362.

[46] R.W. Robey, O. Polgar, J. Deeken, K.W. To, S.E. Bates, ABCG2: determining its relevance in clinical drug resistance, Cancer Metastasis Rev 26 (2007) 39–57. https://doi.org/10.1007/s10555-007-9042-6.

[47] M. Ding, H. Zhang, L. Liu, R. Liang, Effect of NOS1 regulating ABCG2 expression on proliferation and apoptosis of cervical cancer cells, Oncol Lett (2018). https://doi.org/10.3892/ol.2018.9786.

[48] X. Li, Z. Zou, J. Tang, Y. Zheng, Y. Liu, Y. Luo, Q. Liu, Y. Wang, NOS1 upregulates ABCG2 expression contributing to DDP chemoresistance in ovarian cancer cells, Oncol Lett (2018). https://doi.org/10.3892/ol.2018.9787.

[49] M. Budhwani, R. Mazzieri, R. Dolcetti, Plasticity of Type I Interferon-Mediated Responses in Cancer Therapy: From Anti-tumor Immunity to Resistance, Front. Oncol. 8 (2018) 322. https://doi.org/10.3389/fonc.2018.00322.

[50] R.J. Critchley-Thorne, N. Yan, S. Nacu, J. Weber, S.P. Holmes, P.P. Lee, Down-Regulation of the Interferon Signaling Pathway in T Lymphocytes from Patients with Metastatic Melanoma, PLoS Med 4 (2007) e176. https://doi.org/10.1371/journal.pmed.0040176.

[51] R.J. Critchley-Thorne, D.L. Simons, N. Yan, A.K. Miyahira, F.M. Dirbas, D.L. Johnson, S.M. Swetter, R.W. Carlson, G.A. Fisher, A. Koong, S. Holmes, P.P. Lee, Impaired interferon signaling is a common immune defect in human cancer, Proc. Natl. Acad. Sci. U.S.A. 106 (2009) 9010–9015. https://doi.org/10.1073/pnas.0901329106.

[52] Q. Liu, S. Tomei, M.L. Ascierto, V. De Giorgi, D. Bedognetti, C. Dai, L. Uccellini, T. Spivey, Z. Pos, J. Thomas, J. Reinboth, D. Murtas, Q. Zhang, L. Chouchane, G.R. Weiss, C.L. Slingluff, P.P. Lee, S.A. Rosenberg, H. Alter, K. Yao, E. Wang, F.M. Marincola, Melanoma NOS1 expression promotes dysfunctional IFN signaling, J. Clin. Invest. 124 (2014) 2147–2159. https://doi.org/10.1172/JCI69611.

[53] P. Xu, S. Ye, K. Li, M. Huang, Q. Wang, S. Zeng, X. Chen, W. Gao, J. Chen, Q. Zhang, Z. Zhong, Y. Lin, Z. Rong, Y. Xu, B. Hao, A. Peng, M. Ouyang, Q. Liu, NOS1 inhibits the interferon response of cancer cells by S-nitrosylation of HDAC2, J Exp Clin Cancer Res 38 (2019) 483. https://doi.org/10.1186/s13046-019-1448-9.

[54] L. Icardi, K. De Bosscher, J. Tavernier, The HAT/HDAC interplay: Multilevel control of STAT signaling, Cytokine & Growth Factor Reviews 23 (2012) 283–291. https://doi.org/10.1016/j.cytogfr.2012.08.002.

[55] A. Nott, P.M. Watson, J.D. Robinson, L. Crepaldi, A. Riccio, S-nitrosylation of histone deacetylase 2 induces chromatin remodelling in neurons, Nature 455 (2008) 411–415. https://doi.org/10.1038/nature07238.

[56] P. Goldstraw, D. Ball, J.R. Jett, T. Le Chevalier, E. Lim, A.G. Nicholson, F.A. Shepherd, Non-small-cell lung cancer, The Lancet 378 (2011) 1727–1740. https://doi.org/10.1016/S0140-6736(10)62101-0.

[57] D.F. Quail, J.A. Joyce, Microenvironmental regulation of tumor progression and metastasis, Nat Med 19 (2013) 1423–1437. https://doi.org/10.1038/nm.3394.

[58] X. Ji, Z. Shen, B. Zhao, X. Yuan, X. Zhu, CXCL14 and NOS1 expression in specimens from patients with stage I–IIIA nonsmall cell lung cancer after curative resection, Medicine 97 (2018) e0101. https://doi.org/10.1097/MD.0000000000010101.

[59] J.S. Song, C.M. Kang, H.H. Kang, H.K. Yoon, Y.K. Kim, K.H. Kim, H.S. Moon, S.H. Park, Inhibitory effect of CXC chemokine receptor 4 antagonist AMD3100 on bleomycin induced murine pulmonary fibrosis, Exp Mol Med 42 (2010) 465. https://doi.org/10.3858/emm.2010.42.6.048.

[60] M.N. Wente, C. Mayer, M.M. Gaida, C.W. Michalski, T. Giese, F. Bergmann, N.A. Giese, M.W. Büchler, H. Friess, CXCL14 expression and potential function in pancreatic cancer, Cancer Letters 259 (2008) 209–217. https://doi.org/10.1016/j.canlet.2007.10.021.

[61] C.G. Kleer, N. Bloushtain-Qimron, Y.-H. Chen, D. Carrasco, M. Hu, J. Yao, S.-K. Kraeft, L.C. Collins, M.S. Sabel, P. Argani, R. Gelman, S.J. Schnitt, I.E. Krop, K. Polyak, Epithelial and Stromal Cathepsin K and CXCL14 Expression in Breast Tumor Progression, Clinical Cancer Research 14 (2008) 5357–5367. https://doi.org/10.1158/1078-0432.CCR-08-0732.

[62] M. Augsten, C. Hägglöf, E. Olsson, C. Stolz, P. Tsagozis, T. Levchenko, M.J. Frederick, Å. Borg, P. Micke, L. Egevad, A. Östman, CXCL14 is an autocrine growth factor for fibroblasts and acts as a multi-modal stimulator of prostate tumor growth, Proc. Natl. Acad. Sci. U.S.A. 106 (2009) 3414–3419. https://doi.org/10.1073/pnas.0813144106.

[63] X.-L. Gu, Z.-L. Ou, F.-J. Lin, X.-L. Yang, J.-M. Luo, Z.-Z. Shen, Z.-M. Shao, Expression of CXCL14 and its anticancer role in breast cancer, Breast Cancer Res Treat 135 (2012) 725–735. https://doi.org/10.1007/s10549-012-2206-2.

[64] M. Augsten, E. Sjöberg, O. Frings, S.U. Vorrink, J. Frijhoff, E. Olsson, Å. Borg, A. Östman, Cancer-Associated Fibroblasts Expressing CXCL14 Rely upon NOS1-Derived Nitric Oxide Signaling for Their

Tumor-Supporting Properties, Cancer Research 74 (2014) 2999–3010. https://doi.org/10.1158/0008-5472.CAN-13-2740.

[65] L. Zhou, D.-Y. Zhu, Neuronal nitric oxide synthase: Structure, subcellular localization, regulation, and clinical implications, Nitric Oxide 20 (2009) 223–230. https://doi.org/10.1016/j.niox.2009.03.001.

[66] Q. Wang, S. Ye, X. Chen, P. Xu, K. Li, S. Zeng, M. Huang, W. Gao, J. Chen, Q. Zhang, Z. Zhong, Q. Liu, Mitochondrial NOS1 suppresses apoptosis in colon cancer cells through increasing SIRT3 activity, Biochemical and Biophysical Research Communications 515 (2019) 517–523. https://doi.org/10.1016/j.bbrc.2019.05.114.

[67] Y. Wang, R. Branicky, A. Noë, S. Hekimi, Superoxide dismutases: Dual roles in controlling ROS damage and regulating ROS signaling, Journal of Cell Biology 217 (2018) 1915–1928. https://doi.org/10.1083/jcb.201708007.

[68] V. Aggarwal, H. Tuli, A. Varol, F. Thakral, M. Yerer, K. Sak, M. Varol, A. Jain, Md. Khan, G. Sethi, Role of Reactive Oxygen Species in Cancer Progression: Molecular Mechanisms and Recent Advancements, Biomolecules 9 (2019) 735. https://doi.org/10.3390/biom9110735.

[69] R. Liu, M. Fan, D. Candas, L. Qin, X. Zhang, A. Eldridge, J.X. Zou, T. Zhang, S. Juma, C. Jin, R.F. Li, J. Perks, L.-Q. Sun, A.T.M. Vaughan, C.-X. Hai, D.R. Gius, J.J. Li, CDK1-Mediated SIRT3 Activation Enhances Mitochondrial Function and Tumor Radioresistance, Molecular Cancer Therapeutics 14 (2015) 2090–2102. https://doi.org/10.1158/1535-7163.MCT-15-0017.

[70] American Diabetes Association, 2. Classification and Diagnosis of Diabetes, Diabetes Care 38 (2015) S8–S16. https://doi.org/10.2337/dc15-S005.

[71] T.S. Assmann, L.A. Brondani, A.P. Bouças, J. Rheinheimer, B.M. De Souza, L.H. Canani, A.C. Bauer, D. Crispim, Nitric oxide levels in patients with diabetes mellitus: A systematic review and meta-

analysis, Nitric Oxide 61 (2016) 1–9. https://doi.org/10.1016/j.niox.2016.09.009.

[72] S. Yamagishi, T. Matsui, Nitric oxide, a janus-faced therapeutic target for diabetic microangiopathy—Friend or foe?, Pharmacological Research 64 (2011) 187–194. https://doi.org/10.1016/j.phrs.2011.05.009.

[73] C. Heltianu, C. Guja, Role of Nitric Oxide Synthase Family in Diabetic Neuropathy, J Diabetes Metab 01 (2012). https://doi.org/10.4172/2155-6156.S5-002.

[74] R. Komers, J.N. Lindsley, T.T. Oyama, K.M. Allison, S. Anderson, Role of neuronal nitric oxide synthase (NOS1) in the pathogenesis of renal hemodynamic changes in diabetes, American Journal of Physiology-Renal Physiology 279 (2000) F573–F583. https://doi.org/10.1152/ajprenal.2000.279.3.F573.

[75] M. Khamaisi, S. Keynan, M. Bursztyn, R. Dahan, E. Reinhartz, H. Ovadia, I. Raz, Role of Renal Nitric Oxide Synthase in Diabetic Kidney Disease during the Chronic Phase of Diabetes, Nephron Physiol 102 (2006) p72–p80. https://doi.org/10.1159/000089946.

[76] J. Zhang, J. Wei, S. Jiang, L. Xu, L. Wang, F. Cheng, J. Buggs, H. Koepsell, V. Vallon, R. Liu, Macula Densa SGLT1-NOS1-Tubuloglomerular Feedback Pathway, a New Mechanism for Glomerular Hyperfiltration during Hyperglycemia, JASN 30 (2019) 578–593. https://doi.org/10.1681/ASN.2018080844.

[77] R. Komers, J.N. Lindsley, T.T. Oyama, S. Anderson, Effects of long-term inhibition of neuronal nitric oxide synthase (NOS1) in uninephrectomized diabetic rats, Nitric Oxide 11 (2004) 147–155. https://doi.org/10.1016/j.niox.2004.08.005.

[78] R. Komers, T.T. Oyama, J.G. Chapman, K.M. Allison, S. Anderson, Effects of Systemic Inhibition of Neuronal Nitric Oxide Synthase in Diabetic Rats, Hypertension 35 (2000) 655–661. https://doi.org/10.1161/01.HYP.35.2.655.

[79] H.-F. Cheng, J.-L. Wang, M.-Z. Zhang, James.A. McKanna, R.C. Harris, Nitric oxide regulates renal cortical cyclooxygenase-2 expression, American Journal of Physiology-Renal Physiology 279 (2000) F122–F129. https://doi.org/10.1152/ajprenal.2000.279.1.F122.

[80] J.M. Pappachan, G.I. Varughese, R. Sriraman, G. Arunagirinathan, Diabetic cardiomyopathy: Pathophysiology, diagnostic evaluation and management, WJD 4 (2013) 177. https://doi.org/10.4239/wjd.v4.i5.177.

[81] D.M. Ansley, B. Wang, Oxidative stress and myocardial injury in the diabetic heart, The Journal of Pathology 229 (2013) 232–241. https://doi.org/10.1002/path.4113.

[82] G.M. Rosano, Clinical Academic Group Cardiovascular, St George's Hospital NHS Trust Medical School, London, UK, C. Vitale, Department of Medical Sciences, IRCCS San Raffaele, Rome, Italy, P. Seferovic, Department of Cardiology, University of Belgrade, Belgrade, Serbia, Heart Failure in Patients with Diabetes Mellitus, Cardiac Failure Review 03 (2017) 52. https://doi.org/10.15420/cfr.2016:20:2.

[83] J. Amour, X. Loyer, M. Le Guen, N. Mabrouk, J.-S. David, E. Camors, N. Carusio, B. Vivien, R. Andriantsitohaina, C. Heymes, B. Riou, Altered Contractile Response due to Increased β3-Adrenoceptor Stimulation in Diabetic Cardiomyopathy: The Role of Nitric Oxide Synthase 1–derived Nitric Oxide, Anesthesiology 107 (2007) 452–460. https://doi.org/10.1097/01.anes.0000278909.40408.24.

[84] H. Wang, S. Viatchenko-Karpinski, J. Sun, I. Györke, N.A. Benkusky, M.J. Kohr, H.H. Valdivia, E. Murphy, S. Györke, M.T. Ziolo, Regulation of myocyte contraction via neuronal nitric oxide synthase: role of ryanodine receptor *S* -nitrosylation, The Journal of Physiology 588 (2010) 2905–2917. https://doi.org/10.1113/jphysiol.2010.192617.

[85] E.A. Ashley, C.E. Sears, S.M. Bryant, H.C. Watkins, B. Casadei, Cardiac Nitric Oxide Synthase 1 Regulates Basal and β-Adrenergic

Contractility in Murine Ventricular Myocytes, Circulation 105 (2002) 3011–3016. https://doi.org/10.1161/01.CIR.0000019516.31040.2D.

[86] H. Duplain, R. Burcelin, C. Sartori, S. Cook, M. Egli, M. Lepori, P. Vollenweider, T. Pedrazzini, P. Nicod, B. Thorens, U. Scherrer, Insulin Resistance, Hyperlipidemia, and Hypertension in Mice Lacking Endothelial Nitric Oxide Synthase, Circulation 104 (2001) 342–345. https://doi.org/10.1161/01.CIR.104.3.342.

[87] R. Carnicer, D. Duglan, K. Ziberna, A. Recalde, S. Reilly, J.N. Simon, S. Mafrici, R. Arya, E. Roselló-Lletí, S. Chuaiphichai, D. Tyler, C.A. Lygate, K.M. Channon, B. Casadei, BH4 Increases nNOS Activity and Preserves Left Ventricular Function in Diabetes, Circulation Research 128 (2021) 585–601. https://doi.org/10.1161/CIRCRESAHA.120.316656.

[88] A. Birenbaum, A. Tesse, X. Loyer, P. Michelet, R. Andriantsitohaina, C. Heymes, B. Riou, J. Amour, Involvement of β3-Adrenoceptor in Altered β-Adrenergic Response in Senescent Heart: Role of Nitric Oxide Synthase 1–derived Nitric Oxide, Anesthesiology 109 (2008) 1045–1053. https://doi.org/10.1097/ALN.0b013e31818d7e5a.

[89] A.L. Moens, R. Yang, V.L. Watts, L.A. Barouch, Beta 3-adrenoreceptor regulation of nitric oxide in the cardiovascular system, Journal of Molecular and Cellular Cardiology 48 (2010) 1088–1095. https://doi.org/10.1016/j.yjmcc.2010.02.011.

[90] D.R. Gonzalez, F. Beigi, A.V. Treuer, J.M. Hare, Deficient ryanodine receptor *S* -nitrosylation increases sarcoplasmic reticulum calcium leak and arrhythmogenesis in cardiomyocytes, Proc. Natl. Acad. Sci. U.S.A. 104 (2007) 20612–20617. https://doi.org/10.1073/pnas.0706796104.

[91] E.A. Gulve, Exercise and Glycemic Control in Diabetes: Benefits, Challenges, and Adjustments to Pharmacotherapy, Physical Therapy 88 (2008) 1297–1321. https://doi.org/10.2522/ptj.20080114.

[92] S. Le Douairon Lahaye, A. Rebillard, M.S. Zguira, L. Malardé, B. Saïag, A. Gratas-Delamarche, F. Carré, F.R. Bekono, Effects of exercise training combined with insulin treatment on cardiac NOS1 signaling pathways in type 1 diabetic rats, Mol Cell Biochem 347 (2011) 53–62. https://doi.org/10.1007/s11010-010-0611-6.

[93] T. Wang, Y. Wang, D. Lv, J. Song, Q. Lu, X. Gao, F. Zhang, H. Guo, W. Li, X. Yin, Effects of *NOS 1 AP* rs12742393 Polymorphism on Repaglinide Response in Chinese Patients with Type 2 Diabetes Mellitus, Pharmacotherapy 34 (2014) 131–139. https://doi.org/10.1002/phar.1379.

[94] C. Hu, C. Wang, R. Zhang, M.C. Ng, Y. Bao, C. Wang, W.Y. So, R.C. Ma, X. Ma, J.C. Chan, K. Xiang, W. Jia, Association of genetic variants of NOS1AP with type 2 diabetes in a Chinese population, Diabetologia 53 (2010) 290–298. https://doi.org/10.1007/s00125-009-1594-2.

[95] S.H. Ma, B.-Y. Park, J.J. Yang, E.-J. Jung, Y. Yeo, Y. Whang, S.-H. Chang, H.-R. Shin, D. Kang, K.-Y. Yoo, S.K. Park, Interaction of Body Mass Index and Diabetes as Modifiers of Cardiovascular Mortality in a Cohort Study, J Prev Med Public Health 45 (2012) 394–401. https://doi.org/10.3961/jpmph.2012.45.6.394.

[96] F.T. Yazdi, S.M. Clee, D. Meyre, Obesity genetics in mouse and human: back and forth, and back again, PeerJ 3 (2015) e856. https://doi.org/10.7717/peerj.856.

[97] B.E. Sansbury, B.G. Hill, Regulation of obesity and insulin resistance by nitric oxide, Free Radical Biology and Medicine 73 (2014) 383–399. https://doi.org/10.1016/j.freeradbiomed.2014.05.016.

[98] H. Ding, C.R. Triggle, Endothelial dysfunction in diabetes: multiple targets for treatment, Pflugers Arch - Eur J Physiol 459 (2010) 977–994. https://doi.org/10.1007/s00424-010-0807-3.

[99] R.M. Saraiva, K.M. Minhas, M. Zheng, E. Pitz, A. Treuer, D. Gonzalez, K.H. Schuleri, K.M. Vandegaer, L.A. Barouch, J.M. Hare,

Reduced neuronal nitric oxide synthase expression contributes to cardiac oxidative stress and nitroso-redox imbalance in ob/ob mice, Nitric Oxide 16 (2007) 331–338. https://doi.org/10.1016/j.niox.2006.12.001.

[100] K. Mezghenna, P. Pomiès, A. Chalançon, F. Castex, J. Leroy, N. Niclauss, B. Nadal, L. Cambier, C. Cazevieille, P. Petit, R. Gomis, T. Berney, R. Gross, A.D. Lajoix, Increased neuronal nitric oxide synthase dimerisation is involved in rat and human pancreatic beta cell hyperactivity in obesity, Diabetologia 54 (2011) 2856–2866. https://doi.org/10.1007/s00125-011-2264-8.

[101] H.K. Park, S.K. Kim, O.Y. Kwon, J.-H. Chung, S.-K. Lee, Analysis between nitric oxide synthase 1 (NOS1) and risk of obesity, Mol. Cell. Toxicol. 12 (2016) 217–222. https://doi.org/10.1007/s13273-016-0026-x.

[102] M.S. Baig, S.V. Zaichick, M. Mao, A.L. De Abreu, F.R. Bakhshi, P.C. Hart, U. Saqib, J. Deng, S. Chatterjee, M.L. Block, S.M. Vogel, A.B. Malik, M.E.L. Consolaro, J.W. Christman, R.D. Minshall, B.N. Gantner, M.G. Bonini, NOS1-derived nitric oxide promotes NF-κB transcriptional activity through inhibition of suppressor of cytokine signaling-1, Journal of Experimental Medicine 212 (2015) 1725–1738. https://doi.org/10.1084/jem.20140654.

[103] T. Takahashi, Pathophysiological significance of neuronal nitric oxide synthase in the gastrointestinal tract, Journal of Gastroenterology 38 (2003) 421–430. https://doi.org/10.1007/s00535-003-1094-y.

[104] J. Shan, P. Carbonara, N. Karp, M. Tulic, Q. Hamid, D.H. Eidelman, Localization and distribution of NOS1 in murine airways, Nitric Oxide 17 (2007) 25–32. https://doi.org/10.1016/j.niox.2007.05.001.

[105] T. Yoshimura, T.C. Moon, C.D. St. Laurent, L. Puttagunta, K. Chung, E. Wright, M. Yoshikawa, H. Moriyama, A.D. Befus, Expression of nitric oxide synthases in leukocytes in nasal polyps, Annals of

Allergy, Asthma & Immunology 108 (2012) 172-177.e2. https://doi.org/10.1016/j.anai.2011.12.013.

[106] X. Cui, V. Besch, A. Khaibullina, A. Hergen, M. Quezado, P. Eichacker, Z.M.N. Quezado, Neuronal nitric oxide synthase deficiency decreases survival in bacterial peritonitis and sepsis, Intensive Care Med 33 (2007) 1993–2003. https://doi.org/10.1007/s00134-007-0814-9.

[107] W. Schulte, J. Bernhagen, R. Bucala, Cytokines in Sepsis: Potent Immunoregulators and Potential Therapeutic Targets—An Updated View, Mediators of Inflammation 2013 (2013) 1–16. https://doi.org/10.1155/2013/165974.

[108] G.M. Nardi, K. Scheschowitsch, D. Ammar, S.K. De Oliveira, T.B. Arruda, J. Assreuy, Neuronal Nitric Oxide Synthase and Its Interaction With Soluble Guanylate Cyclase Is a Key Factor for the Vascular Dysfunction of Experimental Sepsis*:, Critical Care Medicine 42 (2014) e391–e400. https://doi.org/10.1097/CCM.0000000000000301.

[109] S. Rajpoot, K.K. Wary, R. Ibbott, D. Liu, U. Saqib, T.L.M. Thurston, M.S. Baig, TIRAP in the Mechanism of Inflammation, Front. Immunol. 12 (2021) 697588. https://doi.org/10.3389/fimmu.2021.697588.

[110] J.E. Pandolfino, A.J. Gawron, Achalasia: A Systematic Review, JAMA 313 (2015) 1841. https://doi.org/10.1001/jama.2015.2996.

[111] U.C. Ghoshal, Pathogenesis of achalasia cardia, WJG 18 (2012) 3050. https://doi.org/10.3748/wjg.v18.i24.3050.

[112] R. Singh, U.C. Ghoshal, A. Misra, B. Mittal, Achalasia Is Associated With eNOS4a4a, iNOS22GA, and nNOS29TT Genotypes: A Case-control Study, J Neurogastroenterol Motil 21 (2015) 380–389. https://doi.org/10.5056/jnm14123.

[113] C. Levecque, Association between Parkinson's disease and polymorphisms in the nNOS and iNOS genes in a community-based

case-control study, Human Molecular Genetics 12 (2003) 79–86. https://doi.org/10.1093/hmg/ddg009.

[114] E. Shteyer, S. Edvardson, S.L. Wynia-Smith, C.L. Pierri, T. Zangen, S. Hashavya, M. Begin, B. Yaacov, Y. Cinamon, B.Z. Koplewitz, A. Vromen, O. Elpeleg, B.C. Smith, Truncating Mutation in the Nitric Oxide Synthase 1 Gene Is Associated With Infantile Achalasia, Gastroenterology 148 (2015) 533-536.e4. https://doi.org/10.1053/j.gastro.2014.11.044.

[115] R. Galea, E. Said, Infantile Hypertrophic Pyloric Stenosis: An Epidemiological Review, Neonatal Network 37 (2018) 197–204. https://doi.org/10.1891/0730-0832.37.4.197.

[116] D. Saur, H. Paehge, V. Schusdziarra, H. Allescher, Distinct expression of splice variants of neuronal nitric oxide synthase in the human gastrointestinal tract, Gastroenterology 118 (2000) 849–858. https://doi.org/10.1016/S0016-5085(00)70171-5.

[117] E. Chung, D. Curtis, G. Chen, P.A. Marsden, R. Twells, W. Xu, M. Gardiner, Genetic evidence for the neuronal nitric oxide synthase gene (NOS1) as a susceptibility locus for infantile pyloric stenosis, Am J Hum Genet 58 (1996) 363–370.

[118] J. Jabłoński, I. Drozdz, M. Borowiec, W. Fendler, W. Młynarski, M. Lewandowska, E. Andrzejewska, Mutations of NOS1 and MLN regulatory sequences are a potential cause of infantile hypertrophic pyloric stenosis, Arch Med Sci Civil Dis 1 (2016) 79–80. https://doi.org/10.5114/amscd.2016.62218.

[119] A. Serra, K. Schuchardt, J. Genuneit, C. Leriche, G. Fitze, Genomic variants in the coding region of neuronal nitric oxide synthase (NOS1) in infantile hypertrophic pyloric stenosis, Journal of Pediatric Surgery 46 (2011) 1903–1908. https://doi.org/10.1016/j.jpedsurg.2011.05.021.

[120] D. Saur, J.-M. Vanderwinden, B. Seidler, R.M. Schmid, M.-H. De Laet, H.-D. Allescher, Single-nucleotide promoter polymorphism

alters transcription of neuronal nitric oxide synthase exon 1c in infantile hypertrophic pyloric stenosis, Proc. Natl. Acad. Sci. U.S.A. 101 (2004) 1662–1667. https://doi.org/10.1073/pnas.0305473101.

[121] K. Lagerstedt-Robinson, A. Svenningsson, A. Nordenskjöld, No association between a promoter NOS1 polymorphism (rs41279104) and Infantile Hypertrophic Pyloric Stenosis, J Hum Genet 54 (2009) 706–708. https://doi.org/10.1038/jhg.2009.101.

[122] X. Miao, M.-M. Garcia-Barceló, M. So, W. Tang, X. Dong, B. Wang, J. Mao, E.S. Ngan, Y. Chen, V.C. Lui, K.K. Wong, L. Liu, P.K. Tam, Lack of association between nNOS −84G>A polymorphism and risk of infantile hypertrophic pyloric stenosis in a Chinese population, Journal of Pediatric Surgery 45 (2010) 709–713. https://doi.org/10.1016/j.jpedsurg.2009.07.067.

[123] C. Söderhäll, A. Nordenskjöld, Neuronal nitric oxide synthase, nNOS, is not linked to infantile hypertrophic pyloric stenosis in three families, Clinical Genetics 53 (1998) 421–422. https://doi.org/10.1111/j.1399-0004.1998.tb02758.x.

[124] A. Svenningsson, C. Söderhäll, S. Persson, F. Lundberg, H. Luthman, E. Chung, M. Gardiner, I. Kockum, A. Nordenskjöld, Genome-wide linkage analysis in families with infantile hypertrophic pyloric stenosis indicates novel susceptibility loci, J Hum Genet 57 (2012) 115–121. https://doi.org/10.1038/jhg.2011.137.

[125] J. Galea, J. Armstrong, P. Gadsdon, H. Holden, S.E. Francis, C.M. Holt, Interleukin-1β in Coronary Arteries of Patients With Ischemic Heart Disease, ATVB 16 (1996) 1000–1006. https://doi.org/10.1161/01.ATV.16.8.1000.

[126] G. Lopez-Castejon, D. Brough, Understanding the mechanism of IL-1β secretion, Cytokine & Growth Factor Reviews 22 (2011) 189–195. https://doi.org/10.1016/j.cytogfr.2011.10.001.

[127] T. Køllgaard, C. Enevold, K. Bendtzen, P.R. Hansen, M. Givskov, P. Holmstrup, C.H. Nielsen, Cholesterol crystals enhance

TLR2- and TLR4-mediated pro-inflammatory cytokine responses of monocytes to the proatherogenic oral bacterium Porphyromonas gingivalis, PLoS ONE 12 (2017) e0172773. https://doi.org/10.1371/journal.pone.0172773.

[128] N.V. Mushenkova, E.E. Bezsonov, V.A. Orekhova, T.V. Popkova, A.V. Starodubova, A.N. Orekhov, Recognition of Oxidized Lipids by Macrophages and Its Role in Atherosclerosis Development, Biomedicines 9 (2021) 915. https://doi.org/10.3390/biomedicines9080915.

[129] M. Puhlmann, D.M. Weinreich, J.M. Farma, N.M. Carroll, E.M. Turner, H.R. Alexander, Interleukin-1β induced vascular permeability is dependent on induction of endothelial Tissue Factor (TF) activity, J Transl Med 3 (2005) 37. https://doi.org/10.1186/1479-5876-3-37.

[130] T. Xia, J. Yu, M. Du, X. Chen, C. Wang, R. Li, Vascular endothelial cell injury: causes, molecular mechanisms, and treatments, MedComm 6 (2025) e70057. https://doi.org/10.1002/mco2.70057.

[131] S. Xiong, Z. Hong, L.S. Huang, Y. Tsukasaki, S. Nepal, A. Di, M. Zhong, W. Wu, Z. Ye, X. Gao, G.N. Rao, D. Mehta, J. Rehman, A.B. Malik, IL-1β suppression of VE-cadherin transcription underlies sepsis-induced inflammatory lung injury, Journal of Clinical Investigation 130 (2020) 3684–3698. https://doi.org/10.1172/JCI136908.

[132] B.R. Evans, A. Yerly, E.P.C. Van Der Vorst, I. Baumgartner, S.M. Bernhard, M. Schindewolf, Y. Döring, Inflammatory Mediators in Atherosclerotic Vascular Remodeling, Front. Cardiovasc. Med. 9 (2022) 868934. https://doi.org/10.3389/fcvm.2022.868934.

[133] S. Kukreti, K. Konstantopoulos, C.W. Smith, L.V. McIntire, Molecular Mechanisms of Monocyte Adhesion to Interleukin-1β–Stimulated Endothelial Cells Under Physiologic Flow Conditions, Blood 89 (1997) 4104–4111. https://doi.org/10.1182/blood.V89.11.4104.

[134] D. Flores-Gomez, W. Hobo, D. Van Ens, E.L. Kessler, B. Novakovic, N.P.M. Schaap, W.H.C. Rijnen, L.A.B. Joosten, M.G. Netea, N.P. Riksen, S. Bekkering, Interleukin-1β induces trained innate immunity in human hematopoietic progenitor cells in vitro, Stem Cell Reports 19 (2024) 1651–1664. https://doi.org/10.1016/j.stemcr.2024.09.004.

[135] A. Remmerie, C.L. Scott, Macrophages and lipid metabolism, Cellular Immunology 330 (2018) 27–42. https://doi.org/10.1016/j.cellimm.2018.01.020.

[136] P. Hou, J. Fang, Z. Liu, Y. Shi, M. Agostini, F. Bernassola, P. Bove, E. Candi, V. Rovella, G. Sica, Q. Sun, Y. Wang, M. Scimeca, M. Federici, A. Mauriello, G. Melino, Macrophage polarization and metabolism in atherosclerosis, Cell Death Dis 14 (2023) 691. https://doi.org/10.1038/s41419-023-06206-z.

[137] J. Rex, A. Lutz, L.E. Faletti, U. Albrecht, M. Thomas, J.G. Bode, C. Borner, O. Sawodny, I. Merfort, IL-1β and TNFα Differentially Influence NF-κB Activity and FasL-Induced Apoptosis in Primary Murine Hepatocytes During LPS-Induced Inflammation, Front. Physiol. 10 (2019) 117. https://doi.org/10.3389/fphys.2019.00117.

[138] K. Pyrillou, L.C. Burzynski, M.C.H. Clarke, Alternative Pathways of IL-1 Activation, and Its Role in Health and Disease, Front. Immunol. 11 (2020) 613170. https://doi.org/10.3389/fimmu.2020.613170.

[139] B. Song, Y. Bie, H. Feng, B. Xie, M. Liu, F. Zhao, Inflammatory factors driving atherosclerotic plaque progression new insights, Journal of Translational Internal Medicine 10 (2022) 36–47. https://doi.org/10.2478/jtim-2022-0012.

[140] H. Xiao, A.-M. Ji, Z.-L. Li, X.-D. Song, D. Su, A.-H. Chen, Interleukin-1β inhibits collagen synthesis and promotes its decomposition in cultured cardiac fibroblasts, Sheng Li Xue Bao 60 (2008) 355–361.

[141] M.R. Alexander, M. Murgai, C.W. Moehle, G.K. Owens, Interleukin-1β modulates smooth muscle cell phenotype to a distinct inflammatory state relative to PDGF-DD via NF-κB-dependent mechanisms, Physiological Genomics 44 (2012) 417–429. https://doi.org/10.1152/physiolgenomics.00160.2011.

[142] H. Yoshida, J. Russell, E.Y. Senchenkova, L.D. Almeida Paula, D.N. Granger, Interleukin-1β Mediates the Extra-Intestinal Thrombosis Associated with Experimental Colitis, The American Journal of Pathology 177 (2010) 2774–2781. https://doi.org/10.2353/ajpath.2010.100205.

[143] C. Weber, P. Von Hundelshausen, CANTOS Trial Validates the Inflammatory Pathogenesis of Atherosclerosis: Setting the Stage for a New Chapter in Therapeutic Targeting, Circulation Research 121 (2017) 1119–1121. https://doi.org/10.1161/CIRCRESAHA.117.311984.

[144] P.M. Ridker, B.M. Everett, T. Thuren, J.G. MacFadyen, W.H. Chang, C. Ballantyne, F. Fonseca, J. Nicolau, W. Koenig, S.D. Anker, J.J.P. Kastelein, J.H. Cornel, P. Pais, D. Pella, J. Genest, R. Cifkova, A. Lorenzatti, T. Forster, Z. Kobalava, L. Vida-Simiti, M. Flather, H. Shimokawa, H. Ogawa, M. Dellborg, P.R.F. Rossi, R.P.T. Troquay, P. Libby, R.J. Glynn, Antiinflammatory Therapy with Canakinumab for Atherosclerotic Disease, N Engl J Med 377 (2017) 1119–1131. https://doi.org/10.1056/NEJMoa1707914.

[145] J. Luo, J. Zhang, Y. Xie, M. Wu, Z. Wang, D. Ma, TNF superfamily molecules in atherosclerosis: mechanistic insights and therapeutic translation, Front. Immunol. 16 (2025) 1629577. https://doi.org/10.3389/fimmu.2025.1629577.

[146] R.P. Phipps, Atherosclerosis: The emerging role of inflammation and the CD40–CD40 ligand system, Proc. Natl. Acad. Sci. U.S.A. 97 (2000) 6930–6932. https://doi.org/10.1073/pnas.97.13.6930.

[147] L. Farahi, S.K. Sinha, A.J. Lusis, Roles of Macrophages in Atherogenesis, Front. Pharmacol. 12 (2021) 785220. https://doi.org/10.3389/fphar.2021.785220.

[148] P. Aukrust, F. Müller, T. Ueland, T. Berget, E. Aaser, A. Brunsvig, N.O. Solum, K. Forfang, S.S. Frøland, L. Gullestad, Enhanced Levels of Soluble and Membrane-Bound CD40 Ligand in Patients With Unstable Angina: Possible Reflection of T Lymphocyte and Platelet Involvement in the Pathogenesis of Acute Coronary Syndromes, Circulation 100 (1999) 614–620. https://doi.org/10.1161/01.CIR.100.6.614.

[149] J.L. Johnson, A.C. Newby, Macrophage heterogeneity in atherosclerotic plaques:, Current Opinion in Lipidology 20 (2009) 370–378. https://doi.org/10.1097/MOL.0b013e3283309848.

[150] S. Tian, Y. Wang, J. Wan, M. Yang, Z. Fu, Co-stimulators CD40-CD40L, a potential immune-therapy target for atherosclerosis: A review, Medicine 103 (2024) e37718. https://doi.org/10.1097/MD.0000000000037718.

[151] R. Elgueta, M.J. Benson, V.C. De Vries, A. Wasiuk, Y. Guo, R.J. Noelle, Molecular mechanism and function of CD40/CD40L engagement in the immune system, Immunological Reviews 229 (2009) 152–172. https://doi.org/10.1111/j.1600-065X.2009.00782.x.

[152] E.N. Benveniste, V.T. Nguyen, D.R. Wesemann, Molecular regulation of CD40 gene expression in macrophages and microglia, Brain, Behavior, and Immunity 18 (2004) 7–12. https://doi.org/10.1016/j.bbi.2003.09.001.

[153] D. Lievens, W. Eijgelaar, E. Biessen, M. Daemen, E. Lutgens, The multi-functionality of CD40L and its receptor CD40 in atherosclerosis, Thromb Haemost 102 (2009) 206–214. https://doi.org/10.1160/TH09-01-0029.

[154] R. Alonaizan, Molecular regulation of NLRP3 inflammasome activation during parasitic infection, Bioscience Reports 44 (2024) BSR20231918. https://doi.org/10.1042/BSR20231918.

[155] K. Malekmohammad, E.E. Bezsonov, M. Rafieian-Kopaei, Role of Lipid Accumulation and Inflammation in Atherosclerosis: Focus on Molecular and Cellular Mechanisms, Front. Cardiovasc. Med. 8 (2021) 707529. https://doi.org/10.3389/fcvm.2021.707529.

[156] P.-S. Liu, Y.-T. Chen, X. Li, P.-C. Hsueh, S.-F. Tzeng, H. Chen, P.-Z. Shi, X. Xie, S. Parik, M. Planque, S.-M. Fendt, P.-C. Ho, CD40 signal rewires fatty acid and glutamine metabolism for stimulating macrophage anti-tumorigenic functions, Nat Immunol 24 (2023) 452–462. https://doi.org/10.1038/s41590-023-01430-3.

[157] K.M. Omari, K. Dorovini-Zis, CD40 expressed by human brain endothelial cells regulates CD4+ T cell adhesion to endothelium, Journal of Neuroimmunology 134 (2003) 166–178. https://doi.org/10.1016/S0165-5728(02)00423-X.

[158] V.H. Rao, V. Kansal, S. Stoupa, D.K. Agrawal, MMP-1 and MMP-9 regulate epidermal growth factor-dependent collagen loss in human carotid plaque smooth muscle cells, Physiol Rep 2 (2014) e00224. https://doi.org/10.1002/phy2.224.

[159] M. Wu, Y.-G. Li, The expression of CD40-CD40L and activities of matrix metalloproteinases in atherosclerotic rats, Mol Cell Biochem 282 (2006) 141–146. https://doi.org/10.1007/s11010-006-1741-8.

[160] U. Schönbeck, P. Libby, CD40 Signaling and Plaque Instability, Circulation Research 89 (2001) 1092–1103. https://doi.org/10.1161/hh2401.101272.

[161] P.J.H. Kusters, T.T.P. Seijkens, L. Beckers, D. Lievens, H. Winkels, V. De Waard, A. Duijvestijn, M. Lindquist Liljeqvist, J. Roy, A. Daugherty, A. Newby, N. Gerdes, E. Lutgens, CD40L Deficiency Protects Against Aneurysm Formation, ATVB 38 (2018) 1076–1085. https://doi.org/10.1161/ATVBAHA.117.310640.

[162] K. Kojok, S.E. Akoum, M. Mohsen, W. Mourad, Y. Merhi, CD40L Priming of Platelets via NF-κB Activation is CD40- and TAK1-Dependent, JAHA 7 (2018) e03677. https://doi.org/10.1161/JAHA.118.009636.

[163] U. Schönbeck, F. Mach, G.K. Sukhova, M. Herman, P. Graber, M.R. Kehry, P. Libby, CD40 Ligation Induces Tissue Factor Expression in Human Vascular Smooth Muscle Cells, The American Journal of Pathology 156 (2000) 7–14. https://doi.org/10.1016/S0002-9440(10)64699-8.

[164] M.J.E. Kuijpers, N.J.A. Mattheij, L. Cipolla, J.P. Van Geffen, T. Lawrence, M.M.P.C. Donners, L. Boon, D. Lievens, M. Torti, H. Noels, N. Gerdes, J.M.E.M. Cosemans, E. Lutgens, J.W.M. Heemskerk, Platelet CD40L Modulates Thrombus Growth Via Phosphatidylinositol 3-Kinase β, and Not Via CD40 and IκB Kinase α, ATVB 35 (2015) 1374–1381. https://doi.org/10.1161/ATVBAHA.114.305127.

[165] C. Antoniades, C. Bakogiannis, D. Tousoulis, A.S. Antonopoulos, C. Stefanadis, The CD40/CD40 Ligand System, Journal of the American College of Cardiology 54 (2009) 669–677. https://doi.org/10.1016/j.jacc.2009.03.076.

[166] L. Zhou, L. Xie, D. Zheng, N. Li, J. Zhu, S. Wang, B. Li, L. Ye, Genetic Variants of CD40 Gene Are Associated with Coronary Artery Disease and Blood Lipid Levels, BioMed Research International 2016 (2016) 1–8. https://doi.org/10.1155/2016/1693619.

[167] U. Schönbeck, G.K. Sukhova, K. Shimizu, F. Mach, P. Libby, Inhibition of CD40 signaling limits evolution of established atherosclerosis in mice, Proc. Natl. Acad. Sci. U.S.A. 97 (2000) 7458–7463. https://doi.org/10.1073/pnas.97.13.7458.

[168] L. Robles-Carrillo, T. Meyer, M. Hatfield, H. Desai, M. Dávila, F. Langer, M. Amaya, E. Garber, J.L. Francis, Y.-M. Hsu, A. Amirkhosravi, Anti-CD40L Immune Complexes Potently Activate Platelets In Vitro and Cause Thrombosis in FCGR2A Transgenic Mice,

The Journal of Immunology 185 (2010) 1577–1583. https://doi.org/10.4049/jimmunol.0903888.

[169] L. Strohm, H. Ubbens, D. Mihalikova, A. Czarnowski, P. Stamm, M. Molitor, S. Finger, M. Oelze, D. Atzler, P. Wenzel, P. Lurz, T. Münzel, C. Weber, E. Lutgens, A. Daiber, S. Daub, CD40-TRAF6 inhibition suppresses cardiovascular inflammation, oxidative stress and functional complications in a mouse model of arterial hypertension, Redox Biology 80 (2025) 103520. https://doi.org/10.1016/j.redox.2025.103520.

[170] E.A. Podrez, M. Febbraio, N. Sheibani, D. Schmitt, R.L. Silverstein, D.P. Hajjar, P.A. Cohen, W.A. Frazier, H.F. Hoff, S.L. Hazen, Macrophage scavenger receptor CD36 is the major receptor for LDL modified by monocyte-generated reactive nitrogen species, J. Clin. Invest. 105 (2000) 1095–1108. https://doi.org/10.1172/JCI8574.

[171] Y. Chen, J. Zhang, W. Cui, R.L. Silverstein, CD36, a signaling receptor and fatty acid transporter that regulates immune cell metabolism and fate, Journal of Experimental Medicine 219 (2022) e20211314. https://doi.org/10.1084/jem.20211314.

[172] M.J. Sampson, I.R. Davies, S. Braschi, K. Ivory, D.A. Hughes, Increased expression of a scavenger receptor (CD36) in monocytes from subjects with Type 2 diabetes, Atherosclerosis 167 (2003) 129–134. https://doi.org/10.1016/S0021-9150(02)00421-5.

[173] A.C. Nicholson, S. Frieda, A. Pearce, R.L. Silverstein, Oxidized LDL Binds to CD36 on Human Monocyte-Derived Macrophages and Transfected Cell Lines: Evidence Implicating the Lipid Moiety of the Lipoprotein as the Binding Site, ATVB 15 (1995) 269–275. https://doi.org/10.1161/01.ATV.15.2.269.

[174] Y. Duan, K. Gong, S. Xu, F. Zhang, X. Meng, J. Han, Regulation of cholesterol homeostasis in health and diseases: from mechanisms to targeted therapeutics, Sig Transduct Target Ther 7 (2022) 265. https://doi.org/10.1038/s41392-022-01125-5.

[175] Y. Chen, M. Yang, W. Huang, W. Chen, Y. Zhao, M.L. Schulte, P. Volberding, Z. Gerbec, M.T. Zimmermann, A. Zeighami, W. Demos, J. Zhang, D.A. Knaack, B.C. Smith, W. Cui, S. Malarkannan, K. Sodhi, J.I. Shapiro, Z. Xie, D. Sahoo, R.L. Silverstein, Mitochondrial Metabolic Reprogramming by CD36 Signaling Drives Macrophage Inflammatory Responses, Circulation Research 125 (2019) 1087–1102. https://doi.org/10.1161/CIRCRESAHA.119.315833.

[176] F.J. Sheedy, A. Grebe, K.J. Rayner, P. Kalantari, B. Ramkhelawon, S.B. Carpenter, C.E. Becker, H.N. Ediriweera, A.E. Mullick, D.T. Golenbock, L.M. Stuart, E. Latz, K.A. Fitzgerald, K.J. Moore, CD36 coordinates NLRP3 inflammasome activation by facilitating intracellular nucleation of soluble ligands into particulate ligands in sterile inflammation, Nat Immunol 14 (2013) 812–820. https://doi.org/10.1038/ni.2639.

[177] C. Oury, CD36: linking lipids to the NLRP3 inflammasome, atherogenesis and atherothrombosis, Cell Mol Immunol 11 (2014) 8–10. https://doi.org/10.1038/cmi.2013.48.

[178] Y.M. Park, CD36, a scavenger receptor implicated in atherosclerosis, Exp Mol Med 46 (2014) e99–e99. https://doi.org/10.1038/emm.2014.38.

[179] M.E. Greenberg, M. Sun, R. Zhang, M. Febbraio, R. Silverstein, S.L. Hazen, Oxidized phosphatidylserine–CD36 interactions play an essential role in macrophage-dependent phagocytosis of apoptotic cells, The Journal of Experimental Medicine 203 (2006) 2613–2625. https://doi.org/10.1084/jem.20060370.

[180] Y. Chen, M. Yang, W. Huang, W. Chen, Y. Zhao, M.L. Schulte, P. Volberding, Z. Gerbec, M.T. Zimmermann, A. Zeighami, W. Demos, J. Zhang, D.A. Knaack, B.C. Smith, W. Cui, S. Malarkannan, K. Sodhi, J.I. Shapiro, Z. Xie, D. Sahoo, R.L. Silverstein, Mitochondrial Metabolic Reprogramming by CD36 Signaling Drives Macrophage Inflammatory Responses, Circulation Research 125 (2019) 1087–1102. https://doi.org/10.1161/CIRCRESAHA.119.315833.

[181] S. Mundi, M. Massaro, E. Scoditti, M.A. Carluccio, V.W.M. Van Hinsbergh, M.L. Iruela-Arispe, R. De Caterina, Endothelial permeability, LDL deposition, and cardiovascular risk factors—a review, Cardiovascular Research 114 (2018) 35–52. https://doi.org/10.1093/cvr/cvx226.

[182] H. Yue, M. Febbraio, P.A. Klenotic, D.J. Kennedy, Y. Wu, S. Chen, A.F. Gohara, O. Li, A. Belcher, B. Kuang, T.M. McIntyre, R.L. Silverstein, W. Li, CD36 Enhances Vascular Smooth Muscle Cell Proliferation and Development of Neointimal Hyperplasia, ATVB 39 (2019) 263–275. https://doi.org/10.1161/ATVBAHA.118.312186.

[183] A. Ghosh, W. Li, M. Febbraio, R.G. Espinola, K.R. McCrae, E. Cockrell, R.L. Silverstein, Platelet CD36 mediates interactions with endothelial cell–derived microparticles and contributes to thrombosis in mice, J. Clin. Invest. (2008) JCI34904. https://doi.org/10.1172/JCI34904.

[184] M. Yang, R.L. Silverstein, CD36 signaling in vascular redox stress, Free Radical Biology and Medicine 136 (2019) 159–171. https://doi.org/10.1016/j.freeradbiomed.2019.02.021.

[185] C. Yang, L. Mo, G. Zhang, Y. Dai, B. Li, Z. Tan, Y. Guo, S. Lu, Y. Hong, H. He, H. Yang, J. He, Advancements in dual-targeting nanoparticle strategies for enhanced atherosclerosis therapy: Overcoming limitations of single-targeting approaches, Bioactive Materials 55 (2026) 302–333. https://doi.org/10.1016/j.bioactmat.2025.09.023.

CHAPTER 3

Role of NOS1 in Macrophage Inflammatory phenotype and foam cell formation

CHAPTER 3

Role of NOS1 in Macrophage Inflammatory phenotype and foam cell formation

3.1 Graphical Abstract

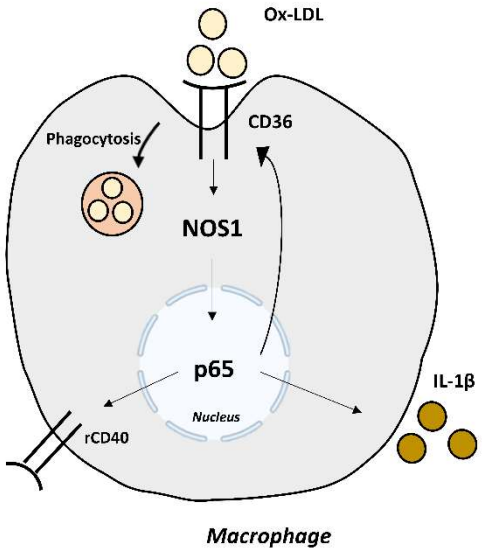

Figure 3.1. NOS1 mediated expression of inflammatory mediators. Figure depicts the Ox-LDL mediated activation of NOS1 further leading to p65 activation and activation of pro-inflammatory mediators such as IL-1β, CD40 and CD36 receptor

3.2. Summary

Atherosclerosis is a chronic inflammatory disease in which plaque buildup inside the wall of the arteries. Macrophage plays an important role in the foam cell formation. Macrophage leads to uptake of Ox-LDL and activate the signalling cascade further leading to the expression of pro-inflammatory cytokines and inflammatory mediators. Inflammatory mediators such as IL-1β, CD40 and CD36 receptor plays an important role in generation of inflammation by mediating uptake of ox-LDL, binding to endothelial cell surface receptor and leading to endothelial permeability. In this context, we explored the role of NOS1 in activation of these inflammatory mediators. The result suggested that ox-LDL led to activation of NOS1. NOS1 further mediated the activation of p65 into the nucleus. Activation of p65 further led to expression of these pro-inflammatory mediators such as IL-1β, CD40 and CD36 receptor. Overall, our study identified the novel role played by NOS1 in mediating the inflammatory process in atherosclerosis.

3.3. Introduction

Atherosclerosis is a chronic inflammatory disease in which plaque build-up in the wall of the artery [1]. Macrophage plays an important role in the pathogenesis of the disease. Activation of macrophage by pro-inflammatory stimulant leads to activation of the inflammatory cascade further leading to disease aggravation [2]. Pro-inflammatory cytokines such as IL-1β and TNF-α plays an important role in the pathogenesis of the disease. Also, expression of inflammatory molecules such as CD36 and CD40 receptor further mediates the pathogenesis of the disease [3]. CD36 receptor is a scavenger receptor which is expressed on the surface of the macrophage. The receptor is involved in the binding to the ox-LDL further leading to its uptake through phagocytosis. Uptake of Ox-LDL leads to activation of inflammatory cascade further leading to disease progression [4]. Expression of CD40 receptor on the macrophage also plays an important role. It is a well-known fact that expression of CD40 receptor leads to binding of the macrophage with the CD40 ligand on the endothelial cells. Binding of CD40-40L interaction leads to adhesion of monocytes and macrophages on to the endothelial cells. It also leads to the expression of cell adhesion molecules such as ICAM-1 and VCAM-1 [5]. Expression of these molecules leads to further recruitment of immune cells at the site of lesion. Binding of immune cells to these receptors present on the endothelial cell leads to adhesion and internalisation of the immune cell inside the intima through chemotaxis. These further aggravates the disease pathogenesis by recruiting high number of inflammatory cells inside the intimal region, thereby leading to substantial increase in the plaque progression [6].

Nitric oxide plays an important role in maintaining the normal vasculature of the arteries as well as in vascular homeostasis [7]. Nitric Oxide synthase (NOS) is an enzyme which helps in the production of Nitric oxide inside the cells. As discussed earlier, there are three different isoforms of NOS: NOS1, NOS2 and NOS3. Role of NOS2 and NOS3 has been well documented in context of disease mechanism.

NOS2 is involved at the later stage of the disease generating NO and nitrosylating different proteins involved in the disease mechanism thereby regulating their functions [7]. NOS3 plays a pleiotropic role in the disease mechanism. High concentration of inflammatory stimulants leads to uncoupling of NOS3 enzyme, thereby generating free radicals of NO which further forms peroxynitrite species ($ONOO^-$) [7]. Peroxynitrite is well known to mediate the progression of inflammatory pathogenesis by reacting with different proteins and modulating their actions [8].

Although the role of NOS2 and NOS3 has been well documented, there lies a significant gap in understanding the role of NOS1 in pathogenesis of atherosclerosis. Thus, our study identified the novel role played by NOS1 in mediating the pro-inflammatory cascade activation in macrophage in response to Ox-LDL treatment. Our study identified that NOS1 plays a central role in mediating the foam cell formation in macrophage and NO generation. This further leads to activation of p65 and downstream expression of pro-inflammatory cytokines and receptors involved in disease progression such as CD36 and CD40 receptor. Thus, the study identified the novel role played by NOS1 in mediating the disease pathogenesis

3.4. Methods:

3.4.1. Cell culture

RAW264.7 cell line was obtained from NCCS, Pune and cultured in RPMI media (11875; Gibco). supplemented with heat-inactivated 10% fetal bovine serum (10270106; Gibco) and 100 U/ml penicillin and 100µg/ml streptomycin (15140122; Gibco). To achieve maximum confluency, the cells were cultured in a humidified incubator with 5% CO_2 at 37˚C. Oxidised LDL was prepared as mentioned earlier [9]. RAW264.7 cells were cultured for 24 hours and treated with oxLDL for 2h. TRIM treatment was done 30 min prior to oxLDL treatment. All oxLDL related study on RAW 264.7 was conducted at 2h timepoint

3.4.2. Nitrite detection

Nitrite detection was done as previously described [10]. Briefly, RAW264.7 cells were treated with OxLDL with indicated time point followed by incubation with 5uM diluted DAF-FM diacetate (D23844; Invitrogen) in serum-free DMEM media for 60 minutes at 37ºC. The cells were then washed with 1X PBS to remove the excess probe. The cells were incubated for an additional 30 minutes to allow complete de-esterification of the intracellular diacetates. Fluorescence was captured at excitation and emission of 495 and 515 nm, respectively, using confocal laser scanning microscope (FV100; Olympus).

3.4.3. Oil Red O Staining

Oil Red O staining was done as previously described [10]. Briefly, RAW264.7 cells were treated with OxLDL with indicated time-point and stained with 0.3% freshly prepared Oil Red O (01391; Sigma Aldrich), for 10 minutes at room temperature followed by washing with 1X PBS to remove the unbound dye. Further, cells were stained and mounted on coverslip with mounting media and DAPI premix solution

(F6057; Sigma-Aldrich). Stained lipids were visualised using confocal laser scanning microscope (FV100; Olympus) and image were captured at 60X magnification.

3.4.4. qRT-PCR

Total RNA was isolated from RAW264.7 by RNAiso Plus reagent (9109; Takara Bio Inc., Shiga, Japan) according to the manufacturer's instructions. The concentration and purity of the isolated RNA was determined using Nanodrop. For cDNA preparation, a total of 1µg of RNA was reverse transcribed using cDNA Synthesis Kit (Takara) according to the manufacturer's instructions. Real-time quantitative PCR (qPCR) was performed using SYBR green master mix (A25742; Applied Biosystems, MA, USA) in StepOnePlus Real-Time PCR Systems (Applied Biosystems). At least three independent sets for the genes GAPDH, CD36, TNF-α and IL-1β were performed. Primer sequences are provided in Supplementary file (**Supplementary table 3.1**). The cycle threshold value was analysed using the $2^{-\Delta\Delta Ct}$ method for the expression of relative cytokines. GAPDH was used as a reference.

3.4.5. Immunofluorescence Staining

Cells were seeded on glass coverslip in 12-well plates. After treatment, cells were fixed with 4% paraformaldehyde for 10 minutes and blocked with 5% BSA for 1 hour. Cells were then incubated overnight at 4ºC with primary antibody against p-NOS1 (PA1-032; Invitrogen) and total-p65 (33-9900; Invitrogen) with dilution of 1:200. After washing, cells were incubated with Rabbit anti-mouse Alexa Fluor 488 secondary antibody (1:1000; Invitrogen) for 1 hour at room temperature in the dark. Nuclei were counterstained with DAPI (F6057, Sigma-Aldrich) and mounted on coverslips. Images were acquired using confocal laser scanning microscope (Olympus, Tokyo, Japan). Mean fluorescence intensity was quantified using ImageJ [11].

3.4.6. Immunoblot

Total protein was extracted from treated cells using radioimmunoprecipitation (RIPA) lysis buffer (Invitrogen) supplemented with protease and phosphatase inhibitors cocktail (Roche). Protein concentrations were determined using the Bradford assay dye reagent (500-0006; Bio Rad). Equal amounts of protein (30-50 ug) were separated by SDS-PAGE on 10% polyacrylamide gels and then transferred overnight onto nitrocellulose membrane (Bio Rad). Membranes were then blocked with 5% BSA in TBST (Tris-buffered saline with 0.1% Tween-20) for 1 hour at room temperature. Membranes were then incubated overnight at 4^{o}C with primary antibodies against total NOS2 (PA3-030A; Invitrogen) and β-actin (sc-47778; Santacruz). After washing, membranes were incubated with appropriate HRP-conjugated secondary antibodies for 1 hour at room temperature. Protein bands were visualised using an enhanced chemiluminescence HRP substrate (Bio Rad) and imaged with Gel documentation system (Image Quant LAS 4000, GE Healthcare, Uppsala, Sweden). Densitometric analysis was performed using ImageJ and normalised to β-actin.

3.4.7. Statistical analysis

All experiments were performed in at least three independent replicates. Data are presented as mean ± SEM. Statistical analysis was performed using GraphPad Prism 8.0.0 for Windows (GraphPad Software, Boston, USA). Differences between groups were analysed using one-way ANOVA followed by Tukey's post-hoc test for multiple comparisons, or unpaired Student's t-test for two group comparisons. A p-value of <0.05 was considered statistically significant. Specific statistical significance levels are indicated in the figures (e.g. *$p<0.05$, **$p<0.01$, ***$p<0.001$, ****$p<0.0001$).

3.5. Results:

3.5.1. OxLDL led to increase in the Nitrite production in RAW264.7 macrophages

To analyse the role of Ox-LDL in the production of Nitrite in the RAW264.7 macrophages, we incubated the cells with Ox-LDL for 2 hr time point. Staining with DAF-FM led to significant increase in the fluorescence intensity in the Ox-LDL treatment condition suggesting that ox-LDL led to increase in the nitrite production at 2-hour time point. To identify that NOS1 is involved in the nitrite production, NOS1 specific inhibitor TRIM (100nM) was incubated in presence of ox-LDL at 2hr time point. The result showed significant decrease in the fluorescence intensity compared to its non-inhibited counterpart. This suggested that the nitrite production in response to Ox-LDL was mediated through NOS1 (**Figure 3.2A**).

3.5.2. OxLDL led to increase in phosphorylation of NOS1 in THP1 macrophages

To check the activation status of NOS1 at the protein level, immunofluorescence staining of p-NOS1-S1417 was done. The cells were treated with Ox-LDL for 2 hrs and then incubated with the antibody against p-NOS1. The Ox-LDL condition showed significant upregulation of p-NOS1 intensity suggesting its activation in response to Ox-LDL. To derive the specificity, treatment with TRIM led to significant downregulation of p-NOS1 intensity suggesting that Ox-LDL induced specific phosphorylation of NOS1. To check specificity of the ox-LDL induced NOS1 activation, activation of other isoform of NOS i.e., NOS2 was analysed. The result suggested no activation of NOS2 at the 2-hr time point, indicating that the effect is due to NOS1 mediated activation (**Figure 3.2B**)

3.5.3. OxLDL led to NOS1-dependent increase in the OxLDL uptake in the macrophage

To check whether activation of NOS1 leads to uptake of Ox-LDL in RAW264.7 macrophage, we incubated the macrophage with ox-LDL for 2 hour and stained the cells with Oil Red O. The ox-LDL treated group showed significant uptake of ox-LDL. To deduce the involvement of NOS1 in lipid uptake, Ox-LDL treatment in presence of TRIM showed significant downregulation of lipid uptake, suggesting that the uptake of lipids is mediated through NOS1 activation (**Figure 3.2C**)

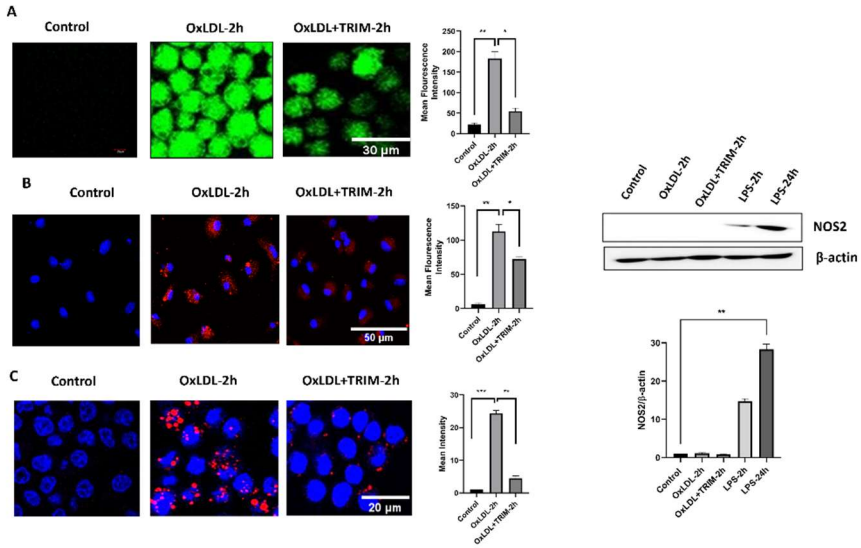

Figure 3.2: Ox-LDL mediated activation of NOS1: A.) NO detection by DAF-FM method, B.) Immunofluorescence analysis of phospho-NOS1 (p-NOS1) ±TRIM and western blot analysis of NOS2. β-actin was used as a loading control. C.) Uptake of Ox-LDL at 2hour time point ± TRIM. Statistical analysis was performed using unpaired two-tailed Student's t-test ($p>0.05$). Data are shown as mean ± SEM. (n=3) (*$p<0.05$, **$p<0.01$, ***$p<0.001$, ****$p<0.0001$)

3.5.4. *NOS1 mediated OxLDL uptake led to increase in p65 translocation into the nucleus*

To analyse the downstream signalling molecule activated by NOS1 in response to ox-LDL, we checked the p65 translocation into the nucleus at the indicated time-point. The result found significant migration of p65 into the nucleus in case of ox-LDL treatment. To see whether the p65 translocation is mediated through NOS1 activation, OxLDL in presence of TRIM showed significant inhibition of p65 translocation into the nucleus. The result suggested that activation of p-NOS1 by ox-LDL led to signalling cascade activation further leading to p65 translocation from the cytoplasm into the nucleus (**Figure 3.3A**).

3.5.5. *NOS1 mediated increase in the pro-inflammatory cytokines and scavenger molecule on the macrophage*

To check whether NOS1-induced p65 translocation leads to activation of pro-inflammatory cytokines, we incubated the macrophage with Ox-LDL for 2-hr time point. After treatment, relative mRNA expression of IL-1β and TNF-α were analysed. The result indicated significant upregulation of IL-1β and TNF-α in response to ox-LDL treatment. Furthermore, treatment with TRIM significantly inhibited the IL-1β and TNF-α mRNA expression in response to ox-LDL suggesting that the cytokines expression is mediated in part through activation of NOS1. Also, similar expression pattern was observed for CD36 receptor on the macrophage, with 24-hr time point showing increased expression and inhibition of expression in presence of TRIM. The result thus suggested that NOS1 mediated activation of CD36 receptor and pro-inflammatory cytokines expression (**Figure 3.3B**).

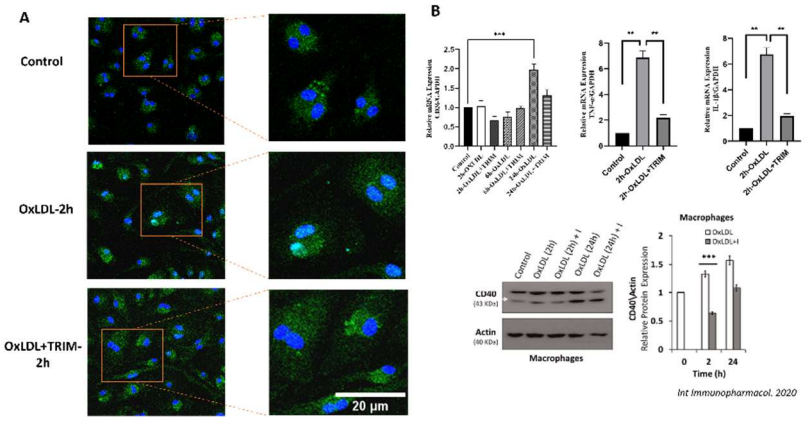

Figure 3.3. Effect of oxLDL on IL-1β expression in RAW264.7 macrophages. A.) Immunofluorescence image of translocation of p65 into the nucleus at 2h time point. (B) Relative mRNA expression of CD36, TNF-α and IL-1β normalized to GAPDH. Immunoblot of CD40 receptor in response to OxLDL ±TRIM. Statistical analysis was performed using unpaired two-tailed Student's t-test ($p>0.05$). Data are shown as mean ± SEM (n=3) (*$p<0.05$, **$p<0.01$, ***$p<0.001$, ****$p<0.0001$)

3.6. Discussion:

The current study focused on the role of macrophage NOS1 in mediating the foam cell formation and activation of downstream signalling molecules leading to activation of pro-inflammatory cytokines and CD36 receptor. Treatment with Ox-LDL led to significant upregulation of nitrite formation followed by lipid uptake in the macrophage. The specificity of NOS1 activation was detected through immunofluorescence staining. NOS1 activation further led to p65 translocation into the nucleus followed by activation of pro-inflammatory cytokines and CD36 receptor.

Foam cell formation by macrophage plays an important role in the pathogenesis of atherosclerosis. Uptake of Ox-LDL by macrophage leads to accumulation of lipids inside the

macrophage, thereby leading to foam cell formation [1]. NO produced by Nitric oxide synthase plays an important physiological role in mediating the disease pathogenesis [7]. In this context, we analysed the role of NOS1 in mediating the foam cell formation and activation of downstream inflammatory molecules leading to disease pathogenesis. Our initial result suggested that NOS1 induced NO production was regulated by ox-LDL treatment. Also, NOS1 led to the upregulation of lipid molecules inside the macrophage leading to foam cell formation. This result suggested that NOS1 plays an important role in the macrophage in the early pathogenesis of the disease.

It is a well-known concept that foam cell formation in the macrophage leads to secretion of pro-inflammatory cytokines by the macrophage such as IL-1β, TNF-α and IL-6 along with other chemokines [3]. Transcription factor p65 plays an important role in the activation of pro-inflammatory cytokines. OxLDL leads to activation of downstream signalling cascade which further mediates activation of p65 and pro-inflammatory cytokines [3]. Our study identified that NOS1 acts an important regulatory molecule mediating the activation and translocation of p65 into the nucleus. Uptake of OxLDL leads to activation of NOS1 which further leads to downstream p65 activation and translocation into the nucleus. Translocation of p65 leads to activation of pro-inflammatory cytokines such as IL-1β and TNF-α as well as scavenger receptor CD36. Expression of CD36 further leads to increased uptake of oxLDL into the macrophage, thereby aggravating the disease pathogenesis. Also, our previous study had identified the expression of CD40 receptor on the macrophage in response to oxLDL stimulation [9]. Interestingly, inhibiting the NOS1 led to decrease in the expression of the CD40 receptor [9]. Overall, these leads to the conclusion that NOS1 is also involved in the expression of CD40 receptor, thereby further aggravating the disease pathogenesis.

Thus, our study identified a novel role of NOS1 in mediating the pathogenesis of atherosclerosis by activating the downstream transcription factor involved in the production of pro-inflammatory cytokines and inflammatory molecules which further leads to disease pathogenesis.

3.7. Conclusion:

Our study identified the novel role of NOS1 in mediating the disease pathogenesis of atherosclerosis in macrophage in response to oxLDL. OxLDL stimulation led to NOS1 activation further leading to activation of p65 and expression of pro-inflammatory cytokines. Other inflammatory molecules such as CD36 and CD40 receptor involved in the disease pathogenesis were also found to be regulated by the NOS1 activation. Thus, regulating the activation of NOS1 and delineating the downstream signalling molecules involved in the activation of inflammatory molecules might provide better understanding of the disease pathogenesis.

3.8. Bibliography

[1] J.L.M. Björkegren, A.J. Lusis, Atherosclerosis: Recent developments, Cell 185 (2022) 1630–1645. https://doi.org/10.1016/j.cell.2022.04.004.

[2] S. Yang, M. Zhao, S. Jia, Macrophage: Key player in the pathogenesis of autoimmune diseases, Front. Immunol. 14 (2023) 1080310. https://doi.org/10.3389/fimmu.2023.1080310.

[3] E. Gusev, A. Sarapultsev, Atherosclerosis and Inflammation: Insights from the Theory of General Pathological Processes, IJMS 24 (2023) 7910. https://doi.org/10.3390/ijms24097910.

[4] Y.M. Park, CD36, a scavenger receptor implicated in atherosclerosis, Exp Mol Med 46 (2014) e99–e99. https://doi.org/10.1038/emm.2014.38.

[5] F. Mach, U. Schönbeck, G.K. Sukhova, T. Bourcier, J.-Y. Bonnefoy, J.S. Pober, P. Libby, Functional CD40 ligand is expressed on human vascular endothelial cells, smooth muscle cells, and macrophages: Implications for CD40–CD40 ligand signaling in atherosclerosis, Proc. Natl. Acad. Sci. U.S.A. 94 (1997) 1931–1936. https://doi.org/10.1073/pnas.94.5.1931.

[6] Z. Chi, A.J. Melendez, Role of Cell Adhesion Molecules and Immune-Cell Migration in the Initiation, Onset and Development of Atherosclerosis, Cell Adhesion & Migration 1 (2007) 171–175. https://doi.org/10.4161/cam.1.4.5321.

[7] J. Loscalzo, Jin, Vascular nitric oxide: formation and function, JBM (2010) 147. https://doi.org/10.2147/JBM.S7000.

[8] R. Radi, Peroxynitrite, a Stealthy Biological Oxidant, Journal of Biological Chemistry 288 (2013) 26464–26472. https://doi.org/10.1074/jbc.R113.472936.

[9] A. Roy, U. Saqib, M.S. Baig, NOS1-mediated macrophage and endothelial cell interaction in the progression of atherosclerosis, Cell Biology International 45 (2021) 1191–1201. https://doi.org/10.1002/cbin.11558.

[10] A. Roy, U. Saqib, K. Wary, M.S. Baig, Macrophage neuronal nitric oxide synthase (NOS1) controls the inflammatory response and foam cell formation in atherosclerosis, International Immunopharmacology 83 (2020) 106382. https://doi.org/10.1016/j.intimp.2020.106382.

[11] C.A. Schneider, W.S. Rasband, K.W. Eliceiri, NIH Image to ImageJ: 25 years of image analysis, Nat Methods 9 (2012) 671–675. https://doi.org/10.1038/nmeth.2089.

CHAPTER 4

NOS1 mediated IL-1β activation and small molecule inhibitors targeting IL-1β and IL-1R1 interaction

CHAPTER 4

NOS1 mediated IL-1β activation and small molecule inhibitors targeting IL-1β and IL-1R1 interaction

4.1. Graphical Abstract

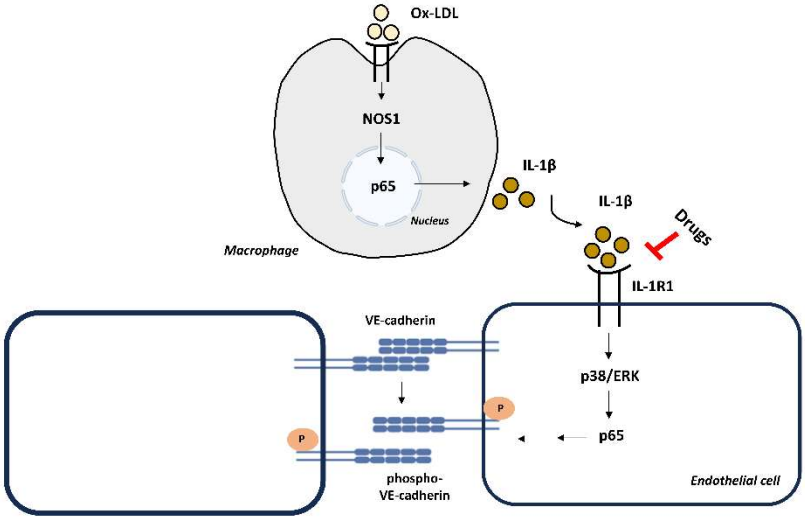

Figure 4.1. NOS1 mediated release of IL-1β and its effect on endothelial cell. Figure depicting the NOS1 mediated release of IL-1β from the macrophage. IL-1β binds to the IL-1R1 receptor on the endothelial cell further activating the MAPK cascade and p65 activation. p65 activation leads to phosphorylation and internalisation of VE-cadherin from the cell surface thereby inducing the membrane permeability

4.2. Summary

Inflammation plays a major role in the progression of atherosclerosis and its complications. Macrophage-derived IL-1β is an important mediator that drives both acute and chronic vascular inflammation. When IL-1β signalling becomes dysregulated, it leads to endothelial damage, plaque instability, and worsening of the disease. Current biologic therapies that block IL-1β are effective but limited by their high cost, need for injection, and potential side effects. Therefore, there is a strong need for new, affordable, and orally available treatments that are safer and easier for patients to use. This study sought to identify and characterize novel small-molecule inhibitors capable of modulating IL-1β signalling, with particular emphasis on its potential to attenuate inflammatory responses and preserve endothelial integrity. We employed a comprehensive strategy integrating in silico virtual screening of the IL-1R1 receptor with in vitro cell-based assays to validate biological efficacy. The screening identified two novel small molecules with favourable binding affinity and stable interaction with IL-1R1. In vitro, these compounds effectively preserved endothelial barrier integrity, as evidenced by the restoration of trans endothelial electrical resistance (TEER). Furthermore, co-treatment with IL-1β maintained VE-cadherin expression and localization in endothelial cells. It also led to downregulation of inflammatory cascade involved in the downregulation of VE-cadherin expression. Taken together, these findings establish the identified small-molecule inhibitors as a promising modulator of IL-1β signalling with demonstrated anti-inflammatory and endothelial-protective effects, supporting its potential utility in mitigating cytokine-driven endothelial dysfunction and disease progression.

4.3. Introduction

Atherosclerosis is a chronic inflammatory disease of the arterial wall and remains the leading cause of morbidity and mortality worldwide. Although traditionally considered a disorder for lipid storage, decades of research have equivocally established that vascular inflammation is a driving force for the initiation, progression and destabilisation of plaque [1]. Among the inflammatory mediators, interleukin-1 beta (IL-1β) has emerged as a central orchestrator of endothelial dysfunction, recruitment of leukocyte and vascular remodelling. Several evidence suggests that dysregulated signalling of IL-1β not only amplifies local vascular inflammation but also systematically contributes to the cardiovascular disease pathogenesis [2,3]

IL-1β is predominantly produced by activated macrophages, monocytes and dendritic cells in response to damage-associated or pathogen-associated molecular patterns. It is well reported that OxLDL plays an important role in activation and release of IL-1β from the macrophage [4]. OxLDL leads to activation of NOS1 at the early stage of the disease [5]. NOS1 activation further leads to proinflammatory signalling cascade activation and release of pro-inflammatory cytokines such as TNF-α and IL-1β from the macrophages [5,6]. Maturation of IL-1β requires assembly of inflammasome and caspase-1-mediated cleavage of pro-IL-1β into its active form [7–9]. IL-1β is then secreted and engages with the interleukin-1 receptor type 1 (IL-1R1) on the endothelial cells, smooth muscle cells, and infiltrating immune cells. This receptor-ligand interaction initiates the recruitment of the IL-1 receptor accessory protein (IL-1RAcP) and downstream adaptor molecules such as MyD88 and IL-1 receptor-associated kinases (IRAK), leading to activation of mitogen-activated protein kinases (MAPK) and NF-κB pathways [10]. These pathways drive the transcription of adhesion molecules (VCAM-1, ICAM-1, E-selectin), chemokines (MCP-1, IL-8), and other cytokines, thereby leading to the infiltration of immune cells into the intima of vascular bed [11]. Also, IL-1β leads to induction of inducible nitric oxide synthase (iNOS) and excessive

production of nitric oxide, which in turn contributes to the oxidative stress and dysfunction of endothelial barrier [12].

Persistent activity of IL-1β is profound in the pathophysiological consequences of atherosclerosis. Exposure of IL-1β to endothelial cells upregulate the adhesion molecules for leukocytes, enhanced recruitment of monocyte to the lesion, further leading to proliferation of smooth muscle, secretion of extracellular matrix proteins, leading to thickening of intima [10,11]. Within the plaque microenvironment, IL-1β amplifies the formation of foam cell and promotes the expression of matrix metalloproteinase, thereby leading to weakened fibrous cap and predisposing plaques to rupture [10]. In line with this, several clinical studies strongly correlate with these mechanistic insights: elevated levels of circulating IL-1β correlate with the cardiovascular events, and the CANTOS trial provided direct evidence for therapeutic blockade of IL-1β with canakinumab leading to significant reduction in recurrent myocardial infarction and cardiovascular-related mortality [13]. Collectively, these findings establish IL-1β as a potential biomarker and mediator of atherosclerosis disease.

Despite the success of biologics targeting IL-1β signalling, important limitations remain. Approved therapies such as anakinra, canakinumab and rilonacept require parenteral administration, are costly to manufacture, and may elicit immunogenic responses with long-term use [14,15]. These challenges lead to constrained accessibility and patient adherence, particularly in resource-limited healthcare systems [14]. Furthermore, the large molecular size of the biologics may restrict their tissue penetration, limiting their ability to act within the atherosclerotic lesions [14]. These shortcomings underscore the urgent need for novel small-molecule inhibitors that can selectively disrupt the IL-1β/IL-1R1 signalling, offer good oral bioavailability and maintain its efficacy at the reduced cost.

Small molecules hold particular promising in addressing these gaps. By virtue of their lower molecular weight, they exhibit favourable

pharmacokinetic properties, improved tissue penetration, and potential for oral delivery- features that would greatly enhance the patient compliance in management of chronic cardiovascular disease [16]. Moreover, rational drug discovery strategies, including structure-based virtual screening and molecular dynamics simulations, now enable identification of compounds capable of targeting specific receptor interfaces or allosteric sites with high precision [17]. In this context, we sought to identify and evaluate novel small-molecule inhibitors with the potential to block IL-1β induced endothelial activation and vascular inflammation. Using in-silico approaches, we screened chemical libraries against IL-1R1 and identified promising candidates capable of interfering with the interaction of IL-1β-IL-1R1. Among these, radotinib, a clinically approved tyrosine kinase inhibitor, and lomitapide, an FDA-approved microsomal triglyceride transfer protein inhibitor, emerged as a strong candidate with favourable binding stability and drug-like properties. Radotinib has been reported to exert anti-inflammatory effects beyond its oncologic indications [18], while lomitapide, a lipid-lowering agent, directly acts on the dyslipidaemia pathway central to atherosclerosis [19].

Our study dealt with the identification of these compounds as an anti-inflammatory potential in reversing the IL-1β induced inflammation activation in endothelial cells (i.e. HUVEC and Ea.hy.926 cells) in context of atherosclerosis. Specifically, we evaluated the ability of these compounds to mitigate the IL-1β induced change in endothelial permeability, cytoskeletal organisation, localisation of VE-cadherin and processes linked to vascular integrity and extravasation of leukocytes. Through this integrated approach, we aim to provide mechanistic and functional evidence of the repurposed small molecules such as radotinib and lomitapide as a viable alternative to biologics in targeting the IL-1β driven vascular inflammation. Such findings would not only advance our understanding of endothelial response to IL-1β but also establish a foundation for developing orally bioavailable, cost-effective therapies for atherosclerosis.

4.4. Materials and methods

4.4.1. Molecular docking and virtual screening

A comprehensive virtual screening approach was employed to identify potential small molecule inhibitors targeting the IL-1R1 receptor. The crystal structure of human IL-1R1 (PDB 4DEP_Chain B) was retrieved from the Protein Data Bank (PDB). Protein preparation involved removal of water molecules, addition of hydrogen atoms and appropriate protonation states using Maestro. A binding site was defined around the known ligand binding pocket of IL-1R1 covering the domain 1 and 2 of the receptor. A library of commercially available FDA approved compounds from ZINC database and natural compounds from IMMPAT library was prepared for docking by generating 3D conformations and assigning partial charges. The compounds were docked using Standard precision (SP) mode in Glide module of Schrodinger [20] and simultaneously processed for docking in AutoDock Vina 1.2.0 [21]. The common compounds were shortlisted based on the higher binding affinity with the receptor in both the docking platforms, followed by binding to the active site residues and having good ADMET properties. The top compounds were further shortlisted based on the binding to at least 50% of the critical residues (6 out of 12 residues) on the IL-1R1 receptor. The top compounds were then selected for MD simulation and MM-PBSA analysis

4.4.2. Molecular Dynamics Simulations

All-atom molecular dynamics simulations and subsequent trajectory analyses were carried out using the AMBER18 [22] software package along with AmberTools19, with the apo form and the docked complexes serving as the starting structures for the simulations. The ff14SB force field was employed to model the amino acid residues [23], whereas ligand parameters were generated using the updated General Amber Force Field (GAFF2) [24]. Partial atomic charges for the ligands were calculated with the Antechamber module of AmberTools19 [25]. The

systems were solvated using the explicit TIP3P water model [26], maintaining a 10 Å buffer from the protein surface. To neutralize the systems and achieve a physiological salt concentration of 0.15 M, appropriate numbers of Na^+ and Cl^- ions were added. The solvated topology and coordinate files were then generated using the LEaP module of AmberTools19. During the simulations, long-range electrostatic interactions were treated using the particle mesh Ewald (PME) method [27], while covalent bonds involving hydrogen atoms were constrained with the SHAKE algorithm [28]. System pressure and temperature were controlled using the Berendsen barostat [29] and the Langevin thermostat [30,31], respectively. A time step of 2 fs was used in all simulations. The initial energy minimization was carried out in two stages. In the first stage, 5000 cycles of steepest descent followed by 5000 cycles of conjugate gradient minimization were performed with the protein and ligand restrained. In the second stage, an unrestrained minimization was conducted using 100 cycles of steepest descent and 900 cycles of the conjugate gradient algorithm. Subsequently, the systems were gradually heated from 0 K to 300 K under the NVT ensemble, followed by a 1 ns equilibration in the NPT ensemble. The production simulations were then carried out for 200 ns under NPT conditions, during which 20,000 snapshots were collected from each trajectory and analysed using the Cpptraj [32] module of AmberTools19. The simulations were performed with GPU acceleration using the pmemd.cuda [33,34] implementation in AMBER18.

4.4.3. Binding Free Energy Calculation using MM/PBSA

Binding free energies were estimated using the molecular mechanics Poisson–Boltzmann surface area (MM/PBSA) method, a widely applied end-point free energy calculation approach [35–38]. For each complex, a total of 2000 snapshots were analysed in the MM/PBSA calculations. In MM/PBSA, the binding free energy is expressed as follows -

$$\Delta G_{bind} = \Delta H - T\Delta S = \Delta E_{vdW} + \Delta E_{elec} + \Delta G_{pol} + G_{np} - T\Delta S \quad (1)$$

Here, the terms ΔE_{vdW}, ΔE_{elec}, ΔG_{pol}, and ΔG_{np} respectively represent the van der Waals, electrostatic, polar solvation, and non-polar solvation components of the binding free energy, which, combined with the entropy contribution -TΔS, give the binding free energy (ΔG_{bind}). Entropy contributions were omitted from our binding free energy analysis due to their substantial computational cost.

4.4.4. Cell culture

The HUVEC primary cells was obtained from AIIMS, Delhi and cultured in Endothelial Cell Growth media (AL517; Himedia) supplemented with heat-inactivated 10% fetal bovine serum (10270106; Gibco) and 100 U/ml penicillin and 100µg/ml streptomycin (15140122; Gibco) plus supplements (AL517; Himedia). The Ea.hy.926 cell line was obtained from BITS Pilani, Hyderabad and grown in Dulbecco Modified Eagle Medium (DMEM) (Gibco) supplemented with heat-inactivated 10% fetal bovine serum (10270106; Gibco) and 100 U/ml penicillin and 100µg/ml streptomycin (15140122; Gibco). To achieve maximum confluency, all cells were cultured in a humidified incubator with 5% CO_2 at 37˚C. Ox-LDL conditioned media was derived from the macrophage as described earlier [39]. Recombinant IL-1β was purchased from Proteintech (HZ-1164). The identified small molecule compounds (Radotinib and Lomitapide) were purchased from Cayman and dissolved in dimethyl sulfoxide (DMSO) for stock solutions, with final DMSO concentrations in the cell culture experiments not exceeding 0.1% (v/v).

4.4.5. Cell culture treatment

For preparation of oxLDL-CM, BMDM were treated with oxLDL for 24 hours. After treatment, supernatant was collected and 50% of CM was treated on the endothelial cell. For drugs related studies, endothelial cells were treated with test compounds 1 hour prior to IL-1β treatment

(10ng/ml). For detection of VE-cadherin and VCAM-1, endothelial cells were treated with IL-1β (10ng/ml) for 12 hours after treatment with drugs. For detection of p65 and MAPK cascade, IL-1β was treated at indicated timepoints 1 hour prior to drugs treatment.

4.4.6. Cell Viability Assay (MTT)

Cell viability was assessed using the 3-(4,5-dimethylthiazol-2-yl)-2,5-diphenyltetrazolium bromide (MTT) assay. HUVEC and EA.hy.926 cells were seeded in 96-well plates at a density of $1*10^4$ cells/well and allowed to adhere overnight. Cells were then pre-treated with various concentrations of test compounds for 24 hours. After the treatment period, MTT solution (0.5mg/ml) was added to each well and incubated for 4 hours at 37^{o}C. The resulting formazan crystals were dissolved in DMSO, and the absorbance was measured at 570 nm using microplate reader. Cell viability was expressed as a percentage relative to the untreated control cells.

4.4.7. Transendothelial permeability assay (TEER)

Endothelial barrier integrity was evaluated by measuring the Transendothelial Electrical Resistance (TEER). For TEER measurements, HUVEC cells were seeded on 12-well plate with 12mm permeable insert supplied with 3μm polycarbonate membrane. Cells were seeded at a density of $1x10^6$ cells/insert and allowed to form a confluent monolayer. Test compounds were added to the apical chamber and incubated for 1 hour prior to IL-1β (10ng/ml) treatment. TEER values were measured using an EVOM volt-ohm meter (MillicellERS-2, Millipore). The voltage was measured by placing the electrode tips between the chambers at pre-determined time intervals

4.4.8. Immunofluorescence Staining

Cells were seeded on glass coverslip in 12-well plates. After treatment, cells were fixed with 4% paraformaldehyde for 10 minutes and blocked with 5% BSA for 1 hour. Cells were then incubated overnight at 4ºC with primary antibody against VE-Cadherin (14-1449-82; Invitrogen), and ZO-1 (33-9100; Invitrogen) with dilution of 1:200. After washing, cells were incubated with Rabbit anti-mouse Alexa Fluor 488 secondary antibody (1:1000; Invitrogen) for 1 hour at room temperature in the dark. Nuclei were counterstained with DAPI (F6057, Sigma-Aldrich) and mounted on coverslips. Images were acquired using confocal laser scanning microscope (Olympus, Tokyo, Japan). Mean fluorescence intensity was quantified using ImageJ [40].

4.4.9. Immunoblot

Total protein was extracted from treated cells using radioimmunoprecipitation (RIPA) lysis buffer (Invitrogen) supplemented with protease and phosphatase inhibitors cocktail (Roche). Protein concentrations were determined using the Bradford assay dye reagent (500-0006; Bio Rad). Equal amounts of protein (30-50 ug) were separated by SDS-PAGE on 10% polyacrylamide gels and then transferred overnight onto nitrocellulose membrane (Bio Rad). Membranes were then blocked with 5% BSA in TBST (Tris-buffered saline with 0.1% Tween-20) for 1 hour at room temperature. Membranes were then incubated overnight at 4ºC with primary antibodies against phospho-p65 (MA5-15160; Invitrogen), total p65 (33-9900; Invitrogen), phospho-ERK (9101S; CST), total ERK (9102S; CST), phospho-p38 (9211S; CST), total p38 (sc-7972; Santa Cruz) and β-actin (sc-47778; Santacruz). After washing, membranes were incubated with appropriate HRP-conjugated secondary antibodies for 1 hour at room temperature. Protein bands were visualised using an enhanced chemiluminescence HRP substrate (Bio Rad) and imaged with Gel documentation system (Image Quant LAS 4000, GE Healthcare,

Uppsala, Sweden). Densitometric analysis was performed using ImageJ and normalised to β-actin.

4.4.10. Statistical analysis

All experiments were performed in at least three independent replicates. Data are presented as mean ± SEM. Statistical analysis was performed using GraphPad Prism 8.0.0 for Windows (GraphPad Software, Boston, USA). Differences between groups were analysed using one-way ANOVA followed by Tukey's post-hoc test for multiple comparisons, or unpaired Student's t-test for two group comparisons. A p-value of <0.05 was considered statistically significant. Specific statistical significance levels are indicated in the figures (e.g. *$p<0.05$, **$p<0.01$, ***$p<0.001$, ****$p<0.0001$).

4.5. Results

4.5.1. Ox-LDL conditioned media from macrophage and recombinant IL-1β leads to decrease in the expression of cell adhesion molecule and increase in the membrane permeability in primary HUVEC cells

To check the effect of soluble factors released by OxLDL-stimulated macrophage on the endothelial integrity, OxLDL stimulated conditioned media (OxLDL-CM) was used on the endothelial cell. Endothelial cell adhesion molecule i.e. VE-Cadherin showed prominent decrease in the surface expression in case of OxLDL-CM compared to control (**Figure 4.2A**). Furthermore, to analyse the effect of recombinant IL-1β on the expression of VE-Cadherin on the cell membrane and its effect on endothelial permeability, HUVEC was stimulated with IL-1β (10ng/ml) and incubated for 12 hours. Treatment with IL-1β significantly decrease the membrane VE-Cadherin expression on the HUVEC cells compared to control (**Figure 4.2B**). Furthermore, effect of IL-1β on the endothelial permeability of HUVEC cells was examined through TEER experiment.

Treatment with IL-1β significantly increased the permeability of HUVEC cells compared to control suggesting the effect of IL-1β on the permeability of HUVEC cells (**Figure 4.2C**). The result signifies the importance of the effect of IL-1β on the endothelial cells, limiting which can ameliorate the susceptibility to the disease.

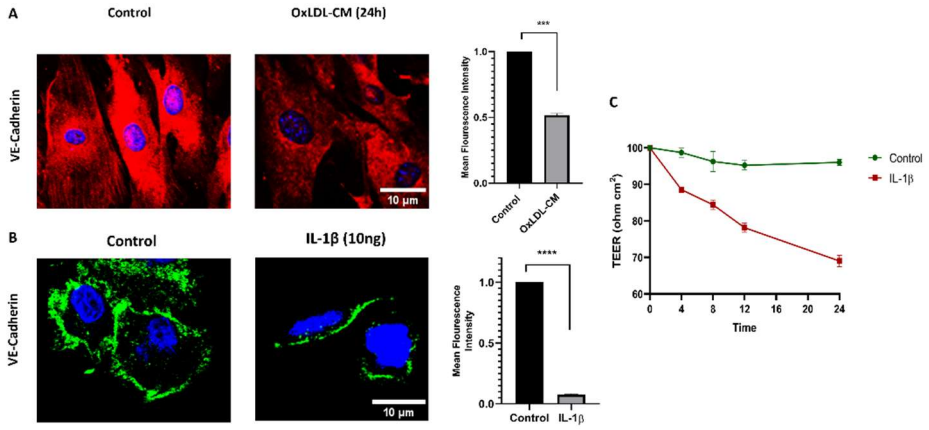

Figure 4.2. Effect of OxLDL-stimulated conditioned media and recombinant IL-1β on the integrity of endothelial junction: A.) Immunofluorescence staining VE-cadherin in primary HUVEC in presence of OxLDL-stimulated conditioned media. B.) Immunofluorescence staining of VE-cadherin in primary HUVEC in presence of recombinant IL-1β. C.) TEER values in HUVEC cells with treatment with IL-1β (10ng/ml). Statistical analysis was performed using unpaired two-tailed Student's t-test ($p>0.05$, $n=3$) (*$p<0.05$, **$p<0.01$, ***$p<0.001$, ****$p<0.0001$)

4.5.2. Recombinant IL-1β leads to activation of p65 and MAPK cascade molecules

To check the expression and activation of p65 and MAPK cascade (p38 and ERK) signalling molecules, recombinant IL-1β (10ng/ml) was treated on primary HUVEC cells and Ea.hy.926 cell line at various time points from 10 mins to 4 hours. The result indicated increase in activation of phospho-p65 at 10mins and 30 mins, indicating the activation of NF-κB signalling molecule (**Figure 4.3A, B**). Moreover,

the activation of phospho-p38 and phospho-ERK was also detected from 10mins up to 4 hours, indicating that IL-1β induced the activation of NF-κB signalling axis through activation of MAPK cascade (**Figure 4.3C**). As p65 is known to regulate VE-cadherin expression, these results signify that IL-1β induces p65 signaling through activation of the MAPK cascade molecules ERK and p38 in HUVEC cells and EAhy926 cells.

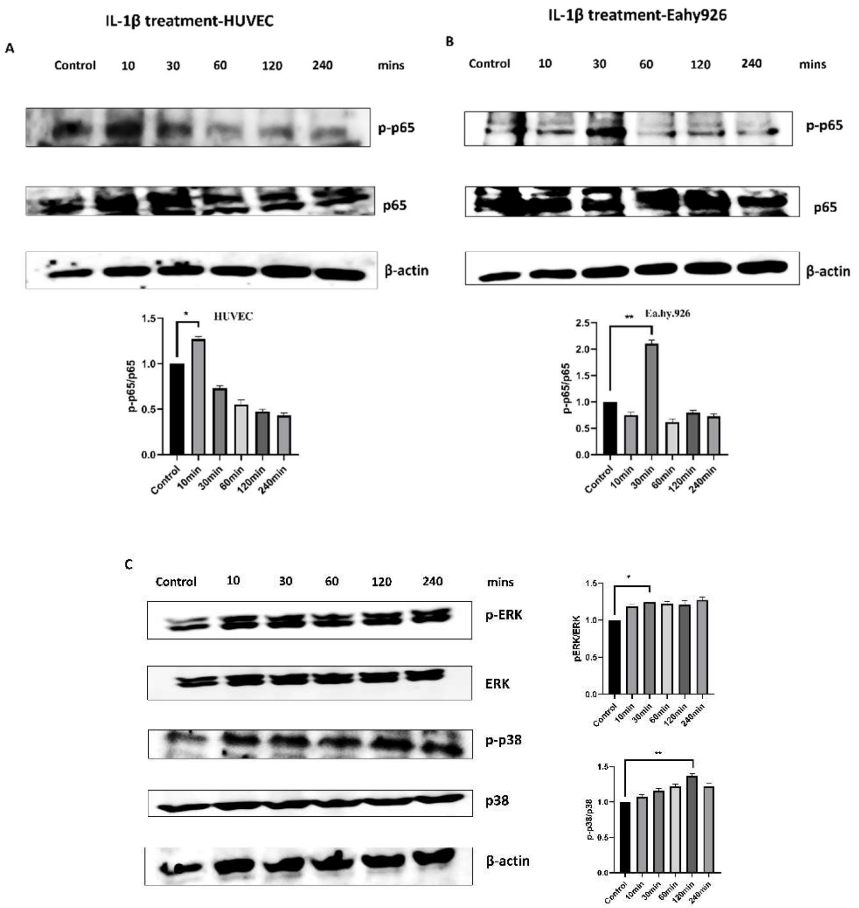

Figure 4.3. Activation of p65, ERK and p38 in response to recombinant IL-1β. Figure depicting the western blot analysis of phospho-p65 and total p65 in primary HUVEC cells (**A**) and Ea.hy.926 cell line (**B**). Figure depicting the western blot analysis of phospho-ERK, total ERK, phospho-p38 and total p38 in Ea.hy.926 cell line in the early time point (10-240mins) (**C**). β-actin is used as control. Statistical analysis was performed using unpaired two-tailed Student's t-test ($p>0.05$, $n=3$) (*$p<0.05$, **$p<0.01$, ***$p<0.001$, ****$p<0.0001$)

4.5.3. Structural analyses reveal key interacting residues in IL-1β/IL-1R1 and IL-1Ra/IL-1R1 binding

Designing a therapeutic inhibitor for the IL-1β/IL-1R1 complex requires understanding of the molecular basis of ligand-receptor interaction. **Figure 4.4** depicts structural analysis of ligand binding interfaces with the receptor. Figure illustrate the three-dimensional structure of IL-1β bound to IL-1R1 receptor (PDB 4DEP). For comparison, crystal structure of IL-1Ra bound to IL-1R1 receptor was used (PDB 1IRA). Table depicts the 4Å interacting residues between the IL-1R1 and both the ligands-IL-1β and IL-1Ra across all the three domains of the IL-1R1 receptor. For instance, in Domain 1, residues like E11, K12, I13, I14, L15, V16, P28, and N30 of IL-1R1 are shown to interact with IL- 1β. Similarly, Domain 2 involves Q108, A109, I110, F111, K112, Q113, K114, L115, G122, V124, P126, Y127, E129, and R163, while Domain 3 includes N204, K205, P206, Q236, L237, S238, D239, I240, Y242, K244, V249, I250, E252, E259, D260, Y261, Y262, S263, R271, L275, K298, T300, and H301. Similarly, IL-1Ra/IL-1R1 revealed key residues in the IL-1R1 receptor involved in binding with the ligand. Critical residues were identified based on the common interacting residues between both the ligands. In total, 12 critical residues- I14, L15, V16, Q108, A109, I110, F111, K112, Q113, V124, P126, and Y127 were identified as crucial residues between IL-1β/IL-1R1 complex, inhibition of which can prevent the binding of IL-1β with the IL-1R1 receptor (**Figure 4.4**). This detailed mapping of interacting residues provides crucial insights into the specific amino acids within the receptor that are essential for recognition and binding of ligand. Henceforth, taking these residues into consideration, libraries of small molecules compounds were screened against the receptor to target the receptor-ligand interaction.

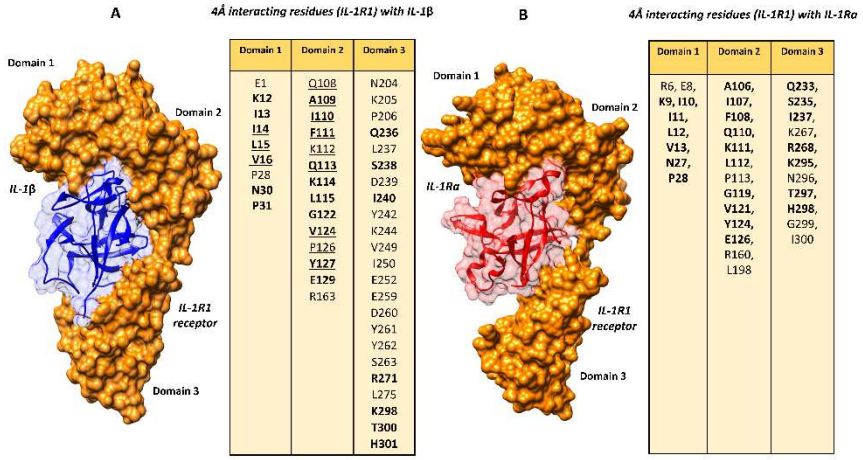

Figure 4.4. In-silico analysis of IL-1β and IL-1Ra interaction with IL-1R1. Structural mapping of residues within 4 Å of the IL-1R1 receptor binding site in complex with (A) IL-1β (PDB 4DEP) and (B) IL-1 receptor antagonist (IL-1Ra) (PDB 1IRA). Critical interacting residues from each receptor domain (Domains 1–3) are highlighted.

4.5.4. Identification of small molecule inhibitors targeting IL-1R1 through in-silico screening

Figure 4.5A depicts the workflow for the in-silico screening strategy employed to identify novel small molecule inhibitors. A combined library consisting of 3203 compounds were used to screen potential inhibitor against the receptor-ligand complex. Initial screening focused on binding affinity of the compound with a threshold of $\Delta G \geq -8.5$kcal/mol, identifying 55 compounds with a dock score ≥ -8.5 kcal/mol. These compounds were then subjected to further analysis for binding to the specific target site on IL-1R1, narrowing the pool to 49 compounds. Subsequently, ADMET analysis further refined to 12 compounds with favourable pharmacokinetic and safety profiles. Further, these 12 compounds were analysed for interacting with at least 50% of the critical residues (6 in total). These further led to total of 2 compounds of which Molecular dynamics (MD) simulations and MM-PBSA (Molecular Mechanics Generalised Born Surface Area) analysis

was done to assess their stability and binding free energies. The binding of both the compounds with the IL-1R1 receptor was analysed which depicted that the compounds bound to the critical residues present in domain 1 and 2 of the receptor (**Figure 4.5B and 4.5C**). Detailed analysis of the binding site residues revealed that both Radotinib and Lomitapide were found to interact with at least 7 residues out of 12 with good dock score, suggesting strong interaction with the receptor. Also, both Radotinib, and Lomitapide showed docked score greater than -9.0 kcal/mol which represents significantly strong affinity with the IL-1R1 receptor. For comparison, anakinra, a known inhibitor for IL-1R1 was docked with the receptor which showed dock score of -6.5kcal/mol, suggesting that the identified compounds hold greater therapeutic potential in comparison to the currently available therapeutic.

4.5.5. Molecular Dynamic Simulation and MM-PBSA analysis provided top compounds with significantly higher stability and binding affinity

All-atom molecular dynamics simulations of 200 ns each were carried out to probe the conformational dynamics of the apo protein and the ligand-bound complexes of radotinib, lomitapide, and the reference compound anakinra. Several stability metrics derived from the trajectories are shown in **Figure 4.5D, E and F** and **Supplementary figure S4.1 and S4.2**, and the last 100 ns averages are reported in **Supplementary Table S4.1**. To assess deviation from the starting production run conformation, the root-mean-square deviation (RMSD), a widely used metric, was computed. Backbone RMSD for the whole protein rose into the ~9–14 Å range across simulations, with stability differences among systems' simulation trajectories, as seen in **Figure S4.1A**. The Radotinib- and Lomitapide-bound complexes showed the most stable RMSD profiles, whereas the apo trajectory displayed prominent mid-run fluctuations, and the Anakinra control system exhibited increased variability near the end. These observations were

also consistent with the high standard deviations of the whole protein's backbone RMSD from the last 100 ns trajectories reported in **Table S4.1** (8.81 ± 2.06 Å for apo and 12.21 ± 2.12 Å for the Anakinra complex). Broadly, as the three structured regions of the protein are linked by loops, the loop segments exhibited comparatively higher fluctuations in the trajectories. To better resolve region-specific deviations, RMSD as well as other metrics were computed separately for residues 6–201 (denoted as domains 1+2) and residues 210–311 (denoted as domain 3). Across systems, the domain-wise RMSD values were smaller in magnitude and overall stable, with only minor variability noted for the Radotinib complex as shown in **Figure 4.5D, S4.1B**. The last 100 ns mean backbone RMSD for domains 1+2 in the Radotinib complex (**Table S4.1**) was slightly elevated relative to the other systems at 2.46 ± 0.21 Å, whereas domain 3 showed comparable average RMSD values across systems. Overall, the whole protein backbone RMSD and the domain-wise RMSD indicated trajectory convergence over the simulated timescale. Further, the binding pocket RMSD was evaluated for the three complexes and is presented in **Figure S4.1D** and **Table S4.1**. For each complex, binding-site residues were defined as those within a 5 Å of the bound ligand. As observed, the control Anakinra complex stabilized at a higher pocket RMSD range, averaging 2.66 ± 0.31 Å, compared with Radotinib (1.40 ± 0.18 Å) and Lomitapide (1.43 ± 0.15 Å), consistent with a more stable binding pocket for the novel inhibitor complexes. Further, residue-wise flexibility was quantified via root-mean-square fluctuation (RMSF), providing per-residue fluctuations for the apo protein and each bound complex. As shown in **Figure S4.1C**, Radotinib and Lomitapide-bound systems exhibited lower RMSF at many protein segments than the apo and Anakinra control, consistent with reduced flexibility in multiple regions, including the binding site. Ligand stability was assessed by tracking the distance between each ligand and its initially defined pocket residues (those within 5 Å of the ligand) over time, as depicted in **Figure S4.1F**. Across all three complexes, the ligands remained confined to the pocket, with pocket-ligand distances staying at approximately 8 Å or less throughout

the simulations. To analyse the conformational stability of the ligands, a ligand heavy atom RMSD–based potential of mean force was further computed by histogramming the RMSD coordinate into 100 bins, assigning the most populated bin(s) as zero energy, and converting other bin populations to relative free energies (**Figure S4.1E**). Each complex displayed a single PMF minimum along the ligand heavy atom RMSD coordinate, with minima centered around approximately 2.2–2.6 Å, and Radotinib and Lomitapide showed slightly broader distributions than the control. Taken together, the analyses indicate that each ligand remained conformationally stable in the binding pocket over the simulation timescale.

Further, to analyse the compactness and solvent accessibility, radius of gyration (RoG) and solvent-accessible surface area (SASA) were evaluated for domains 1+2 and domain 3, with results summarized in **Table S4.1** and **Figure S4.2A, B** for domain 1+2 and **Figures S4.2C, D** for domain 3. Overall, RoG values remained in a similar range across systems. In domains 1+2, the Lomitapide and Anakinra complexes trended slightly lower in RoG toward the end of the simulations relative to the others. SASA over time for domains 1+2 was lower in the complexes than in apo (mean 104.24 ± 2.42 nm^2), consistent with solvent displacement upon binding. Across domains 1+2 and domain 3, the Lomitapide complex exhibited a narrower and lower SASA distribution than the others, suggesting more extensive protein–ligand and intradomain contacts, reduced water exposure in the pocket and nearby regions, and thereby relatively greater complex stability. Ligand–protein binding energetics were evaluated using the molecular mechanics Poisson–Boltzmann surface area (MM/PBSA) approach, an efficient end point method for estimating binding free energies from molecular dynamics trajectories, as shown in **Table S4.2** and **Figure 4.5E**. Table S4.2 shows that the control Anakinra complex had a binding free energy (ΔG_{bind}) of -19.15 kcal/mol, whereas the novel molecules bound more favorably, with Lomitapide at -37.39 kcal/mol and Radotinib at -28.38 kcal/mol, both substantially more negative than the

control. In the MM/PBSA decomposition, the dominant contributors to binding were the van der Waals, electrostatic, and non-polar solvation energy terms of the binding free energy. Both Radotinib (ΔE_{vdW} = -56.76 kcal/mol) and Lomitapide (ΔE_{vdW} = -50.11 kcal/mol) displayed markedly more favorable van der Waals interaction energies, which stabilized their binding. Although the Radotinib complex exhibited the most favorable van der Waals stabilization, its net polar contribution ($\Delta E_{elec} + \Delta G_{pol}$ = 33.68 kcal/mol) was more unfavourable overall, and conversely, the Lomitapide complex ($\Delta E_{elec} + \Delta G_{pol}$ = 18.06 kcal/mol) had the least penalty from the net polar terms, giving the most favorable overall affinity among the three (Control $\Delta E_{elec} + \Delta G_{pol}$ = 28.19 kcal/mol). Overall, the results support Radotinib and Lomitapide as promising IL-1β inhibitor candidates for therapeutic development.

One key stabilizing interaction in protein-ligand binding is hydrogen bonding. The time-series analysis across the trajectories indicates that the Lomitapide complex maintained the lowest H bond counts, implying a lesser role for H bonding in its binding mode (**Figure S4.2E**). Key hydrogen bonding residues included Lys132 (26.79% occupancy) and Asn136 (22.03% occupancy) in the Anakinra complex, Gly122 (16.03% occupancy) in the Radotinib complex, and Glu11 (10.48% occupancy) in the Lomitapide complex (**Table S4.3**). To quantify residue-level contributions to binding, per-residue free energy decomposition was performed for each complex, as shown in **Figure 4.5F, S4.2F** and **Table S4.4**. As summarized in Table S4.4, the Radotinib complex featured notable favorable contributions from Arg25, Tyr127, Ser17, Pro28, and Phe111, each with < -1 kcal/mol energy contribution. The Lomitapide complex shows Tyr261, Ile13, and Pro28 with contributions below -1 kcal/mol, whereas in the Anakinra control, only Hie60 met this threshold. Conversely, unfavorable per residue contributions included Asp23 (G_{total} = 5.32 kcal/mol), Ser18 (G_{total} = 1.04 kcal/mol), and Glu21 (G_{total} = 1.03 kcal/mol) for the Radotinib complex, offsetting some favorable effects. The Anakinra complex showed a sizable penalty from Lys63 (G_{total} = 2.85 kcal/mol), whereas in the Lomitapide complex, only

Glu11 exceeded +1 kcal/mol (G_{total} = 1.35 kcal/mol). Overall, the per-residue energy decomposition offers insights into the binding mechanism and can be leveraged to optimize the compounds or to design new therapeutics.

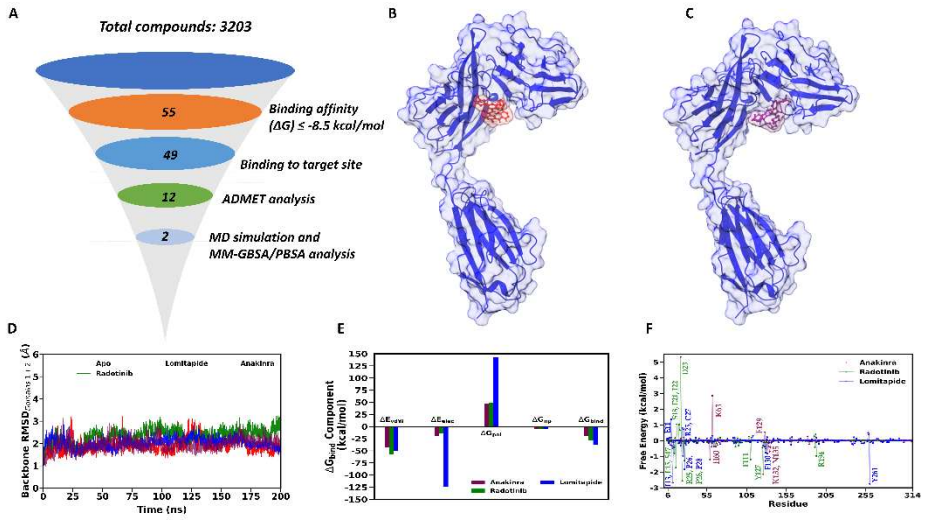

Figure 4.5. In silico screening, Molecular Dynamics and MM-PBSA/GBSA analysis for IL-1β inhibitors. A.) Summary of the virtual screening workflow. B) Schematic representation of the binding of Radotinib with the IL-1R1 receptor. C.) Schematic representation of the binding of Lomitapide with the IL-1R1 receptor. D.) MD simulation for the domain 1 and 2 of the IL-1R1 receptor in presence of IL-1β inhibitors and positive control (Anakinra). E.) MM-PBSA/GBSA analysis for Radotinib and Lomitapide along with positive control. F.) Per-residue free energy decomposition showing contributions of key residues to ligand binding

4.5.6. Both the compounds restore the expression and localisation of VE-Cadherin in IL-1β treated endothelial cells

Adheren junction plays an important role in maintaining the integrity of endothelial barrier. VE-cadherin plays an important role in this regard. Therefore, we investigated the effect of both the compounds on the expression as well as localisation of VE-Cadherin using immunofluorescence. **Figure 4.6** shows the representative

immunofluorescence images for VE-Cadherin in HUVEC under different treatment conditions. VE-cadherin was linearly present on the membrane in control cells, indicating an intact endothelial barrier, whereas stimulation with IL-1β (10ng/ml) shows fragmented and discontinuous staining of VE-cadherin. This suggests the disruption of the integrity of membrane. Co-treatment of Lomitapide (400 and 800nM) and Radotinib (400 and 800nM) with IL-1β (10ng/ml) resulted in restoration of the VE-Cadherin expression on the periphery of the membrane, suggesting recovery of the membrane integrity with the compound treatment. Specifically, both Lomitapide and Radotinib at 800nM showed increased restoration of membrane integrity depicted by the enhanced expression of VE-cadherin on the membrane.

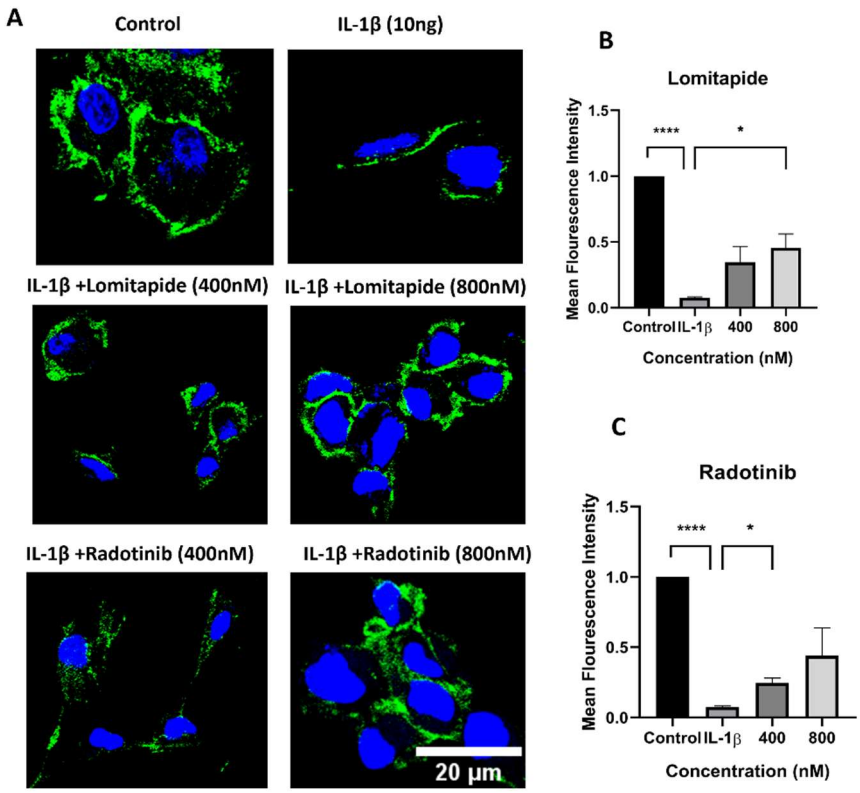

Figure 4.6. Effect of IL-1β and small molecule inhibitors on endothelial junctional integrity. (A) Immunofluorescence staining of VE-cadherin in primary HUVECs under different treatment conditions: untreated control, IL-1β (10 ng/ml), IL-1β + Lomitapide (400 nM, 800 nM), and IL-1β + Radotinib (400 nM, 800 nM). B.) Measurement of fluorescence intensity of Lomitapide. C.) Measurement of fluorescence

intensity of Radotinib. Statistical analysis was performed using unpaired two-tailed Student's t-test ($p>0.05$) Data are shown as mean ± SEM (n=3) (*$p<0.05$, **$p<0.01$, ***$p<0.001$, ****$p<0.0001$)

4.5.7. Both the compounds attenuated IL-1β induced cytotoxicity and preserved the endothelial barrier integrity

To assess the biological effects of the identified compounds, we first investigated its impact on the cell viability and integrity of endothelial barrier. As per the MTT assay results, both the compounds were found to be non-toxic, which is consistent with their status as FDA-approved molecules (**Figure 4.7A, B**). To evaluate the endothelial barrier integrity in response to compounds, Transendothelial Electrical Resistance (TEER) analysis was done in HUVEC cells up to 24 hours. IL-1β treatment (10ng/ml) showed time-dependent decrease in the barrier integrity with 24 hours showing decrease of 24.6% in the barrier integrity. In response, co-treatment of compounds with IL-1β showed significantly increase in the barrier integrity. Specifically, Radotinib at 800nM showed increase of 24.8% of barrier integrity at 24 hours compared to IL-1β treatment. Same result was observed with the co-treatment of lomitapide with IL-1β with 800nM showing an increase of 20.9% of barrier integrity compared to IL-1β alone (**Figure 4.7C, D**). Thus, these findings suggest that both the compound not only showed reduced cytotoxicity but also prevented the IL-1β induced decrease in the integrity of the endothelial barrier.

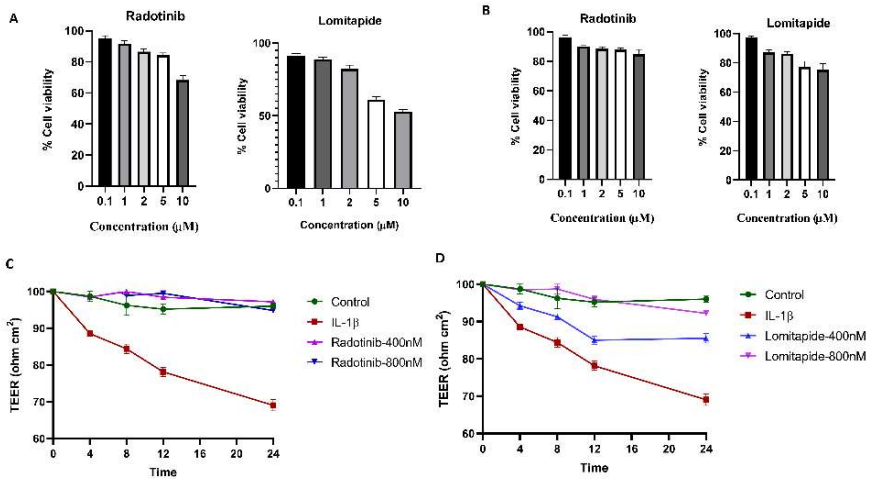

Figure 4.7. Cytotoxicity of selected IL-1R1 inhibitors in endothelial cells and endothelial permeability. MTT assay showing dose-dependent effects of lead compounds on HUVEC primary cell line (A) and EA.hy.926 (B). Data are expressed as percentage cell viability relative to untreated controls. Transendothelial electrical resistance (TEER) measurements of HUVEC monolayers following treatment with IL-1β (10 ng/ml) alone or in combination with Radotinib (400 and 800 nM) (C) or Lomitapide (400 and 800 nM) (D). Statistical analysis was performed using unpaired two-tailed Student's t-test ($p>0.05$, $n=3$). Data are shown as mean ± SEM, with values normalized to untreated control. (*$p<0.05$, **$p<0.01$, ***$p<0.001$, ****$p<0.0001$)

4.5.8. Both the compounds were effective in decreasing the activation of p65 while Radotinib and Lomitapide led to decrease in VCAM-1 and MAPK cascade respectively.

Furthermore, to check the effect of the compounds in reducing the activation of NF-κB signalling axis, the compounds were tested at 400 and 800nM concentration at 30 min time point. Both the compounds showed significant dose-dependent decrease in the phospho-p65 expression. While Radotinib was effective in decreasing the expression of VCAM-1, Lomitapide was effective in decreasing the expression phospho-ERK and phospho-p38 molecules, indicating that Lomitapide might be mediating its effect through inhibition of MAPK cascade and NF-κB signalling axis and Radotinib might be acting through different signalling cascade in decreasing p65 activation and VCAM-1 expression (**Figure 4.8**).

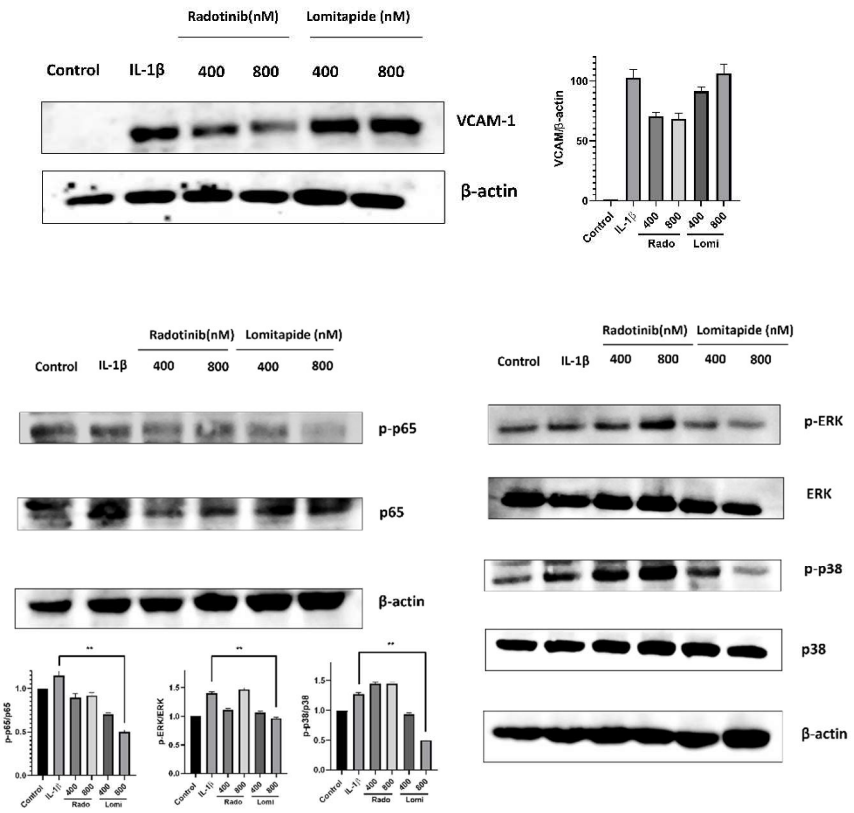

Figure 4.8. Effect of small molecule inhibitors against the activation of VCAM-1, p65 and MAPK Cascade in response to IL-1β. Western blot analysis of effect of drugs on the key signalling molecules such as VCAM1, phospho-p65, phospho-ERK and phospho-p38 in response to Radotinib and Lomitapide in different concentration (400 and 800nM) in presence of IL-1β (10ng/ml). β-actin was used as control. Statistical analysis was performed using unpaired two-tailed Student's t-test ($p>0.05$, n=3). Data are shown as mean ± SEM, with values normalized to untreated control. (*$p<0.05$, **$p<0.01$, ***$p<0.001$, ****$p<0.0001$)

4.6. Discussion

This study identified and characterised novel small-molecule inhibitors targeting the IL-1β signalling pathway, with the objective of reducing the inflammatory responses and preserving the endothelial integrity. By combining in silico analyses with the in vitro validation, we demonstrated that both Radotinib and Lomitapide exhibit significant anti-inflammatory properties. These findings provide new insights into the molecular regulation of IL-1β signalling and open promising therapeutic avenues for inflammatory diseases. Our initial computational screening employed molecular docking and molecular dynamics simulations, which identified Radotinib and Lomitapide as a high-affinity binders for the IL-1R1 receptor. These analyses suggested that the compounds either directly compete with the IL-1β for receptor binding or induce allosteric confirmational changes that disrupt signalling initiation. This computational prediction was further confirmed through cellular assays in human endothelial cell models (HUVEC and EA.hy.926 cell line).

Our initial study found that oxLDL plays an important role in the activation of NOS1 at the early stage of the disease. Activation of NOS1 leads to uptake of OxLDL, which further leads to activation of signalling cascade, p65 translocation into the nucleus and activation of pro-inflammatory cytokines, such as TNF-α and IL-1β. These results align with the previously reported literature that NOS1 plays an active role at early stage of the disease through activation of inflammatory cascade and disease progression [5]. IL-1β, in particular, play a prominent role in mediating the further progression of the disease. OxLDL induced release of IL-1β from the macrophage acts on the IL-1R1 receptor present on the endothelial cell further leading to the activation of signalling cascade and membrane permeability in the endothelial cell, thereby aggravating the disease progression [10,11]. Several literatures supports the notion that IL-1β plays an important role in atherosclerosis disease progression by acting specifically on the endothelial cells [41,42]. Therefore, therapeutic strategy targeting the binding of IL-1β

with the receptor on the endothelial cell can prevent the cytokine-induced permeability in the endothelial cells and can thereby reduce the disease progression. In line with this, other studies had also analysed the IL-1β/IL1R1 receptor complex to design therapeutics to limit the receptor-ligand interaction for mitigating inflammatory cascade activation [43–45]

Our in-silico docking analysis and MD-MMPBSA analyses against the IL-1R1 receptor revealed two compounds binding to the receptor with higher affinity and better stability compared to positive control (Anakinra). Further in-vitro analyses found positive response of the compounds with the endothelial cells. One of the key observations of the effect of compounds on the endothelial cells was the preservation of the endothelial barrier integrity. Endothelial dysfunction, characterised by the loss of junctional proteins leading to increased permeability, is a hallmark of inflammatory diseases [46]. We observed that both Radotinib and Lomitapide restored the Transendothelial electrical resistance (TEER) values and maintained the expression and localisation of VE-Cadherin at the cellular junctions, with cotreatment with IL-1β. This suggests that the compounds prevent disassembly of adheren junctions, thereby protecting against the IL-1β induced vascular permeability. Preservation of endothelial integrity plays a central role in the prevention of diseases such as atherosclerosis, sepsis, and acute respiratory distress syndrome, where vascular leakage contributes to the disease pathology [46].

Regulation of VE-cadherin is highly dependent on the key signalling molecules such as NF-κB, ERK and p38 MAP kinase [47]. p38 MAP kinase plays an important role in the regulation of the VE-cadherin expression on the cell surface [47]. The surface expression of VE-cadherin is highly regulated by the phosphorylation and dephosphorylation of VE-cadherin subunits [48]. In that regard, p38 MAP kinase has been shown to mediate the phosphorylation of VE-cadherin, thereby leading to its disassembly from the membrane and its subsequent degradation [47]. Also, studies have identified that

activation of ERK contributes to the Transendothelial permeability by triggering the dissociation of VE-cadherin/β-catenin complex through β-catenin phosphorylation and VE-cadherin downregulation [49]. Therefore, to identify the activation of these signalling molecules in response to IL-1β treatment leading to VE-cadherin downregulation, protein expression and activation of p65, ERK and p38 were analysed. Our result identified prominent increase in the expression of phospho-p65, phospho-ERK and phospho-p38 in response to IL-1β, suggesting that the resulting activation of signalling molecules might have an effect on the VE-cadherin downregulation in response to IL-1β treatment. Furthermore, to check whether upregulation of VE-cadherin expression in response to drugs treatment is correlated with the inhibition of these signalling molecules, we tested both Radotinib and Lomitapide at different concentrations. The result indicated significant decrease in the level of phospho-p65, phospho-ERK and phospho-p38 in response to Lomitapide in dose-dependent manner. Thus, the results indicated that Lomitapide might act through inhibiting these signalling molecules involved in VE-cadherin downregulation, thereby regaining the junctional permeability in response to IL-1β treatment.

When comparing with the existing literature, our findings extend the current understanding of modulation of IL-1β by therapeutic targets. Currently available therapies targeting the IL-1β signalling such as Anakinra, Canakinumab and Rilonacept neutralise IL-1β or block the IL-1R1 receptor [50]. While showing clinical effectivity, their widespread use is hindered by high cost, parenteral administration, and potential immunogenicity [14,15]. In contrast, small molecule inhibitors offer potential advantages offering good oral bioavailability, lower manufacturing costs, and improved tissue penetration [16]. Both Radotinib and Lomitapide has previously been used for the treatment of diseases such as chronic myeloid leukemia and familial hypercholesterolemia respectively [18,19]. Specifically, Radotinib is a second-generation tyrosine kinase inhibitor (TKI) primarily used in the treatment of chronic myeloid leukemia (CML) [18]. It exerts its action

by selectively binding to the ATP-binding site of the Bcr-Abl kinase, thereby inhibiting its kinase activity and blocking downstream signalling pathway that promote leukemogenesis [18]. Lomitapide is an inhibitor for microsomal triglyceride transfer protein (MTP), which is essential for the assembly of lipoproteins containing Apolipoprotein B (ApoB) in the liver and intestine [19]. By blocking MTP, lomitapide reduces the production of very low-density lipoproteins (VLDL) and chylomicrons, thereby lowering the low-density lipoprotein (LDL) cholesterol levels in the blood [19]. The novel identification of both the drugs targeting the IL-1β/IL1R1 signaling highlights their potential for therapeutic repurposing. Such repurposing of drugs enhances their translational process since their safety profiles are already well established.

The function of Radotinib and Lomitapide in protecting the endothelial barrier integrity can act as a key regulator in suppressing the disease progression. The effect of compounds on preservation of vascular integrity can lead to decrease in the severity of diseases such as atherosclerosis and sepsis where preservation of vascular integrity is paramount in its prevention [46,51–53]. Beyond this, the compounds can be relevant to chronic inflammatory disorders such as rheumatoid arthritis and inflammatory bowel disease, where IL-1β acts as central player in progression of disease phenotype [54,55].

Nevertheless, certain limitations need to be acknowledged. First, the experimental validation was largely confined to in vitro endothelial models. Validation through animal model is needed to confirm the efficacy, pharmacokinetics, and drug safety profile. Second, although computational studies strongly suggested direct binding of the drugs with the IL-1R1 receptor, experimental validation through methods such as surface plasmon resonance or isothermal titration calorimetry is necessary. Also, the broader off-target effects of these drugs need careful evaluation in context of long-term therapeutic use.

In conclusion, this study provides compelling evidence that both Radotinib and Lomitapide represent a promising small-molecule inhibitors potentially by its direct interaction with the IL-1R1 receptor and thereby preserving the endothelial integrity in response to IL-1β. As a repurposed molecule, these compounds could hold potential as a novel and cost-effective treatments for inflammatory and vascular diseases. These in silico combined with the in vitro work need to be translated to in vivo models to propose these compounds for its clinical application.

4.7. Conclusion

The study identified and characterized novel small molecule inhibitors, that effectively target the IL-1β signaling pathway. Our in silico and in vitro findings demonstrated that these compounds possess potent anti-inflammatory and endothelial protective effects by suppressing IL-1β-induced inflammatory mediators and preserving endothelial barrier integrity. These findings underscore the significant therapeutic potential of these novel small molecules as orally bioavailable agents for the treatment of a wide spectrum of IL-1β-mediated inflammatory diseases and conditions characterized by endothelial dysfunction. This research provides a strong foundation for future preclinical and clinical development, offering a promising new avenue for more accessible and effective anti-inflammatory therapies.

4.8. Bibliography

[1] K. Malekmohammad, E.E. Bezsonov, M. Rafieian-Kopaei, Role of Lipid Accumulation and Inflammation in Atherosclerosis: Focus on Molecular and Cellular Mechanisms, Front. Cardiovasc. Med. 8 (2021) 707529. https://doi.org/10.3389/fcvm.2021.707529.

[2] P. Libby, Interleukin-1 Beta as a Target for Atherosclerosis Therapy, Journal of the American College of Cardiology 70 (2017) 2278–2289. https://doi.org/10.1016/j.jacc.2017.09.028.

[3] B.W. Van Tassell, S. Toldo, E. Mezzaroma, A. Abbate, Targeting Interleukin-1 in Heart Disease, Circulation 128 (2013) 1910–1923. https://doi.org/10.1161/CIRCULATIONAHA.113.003199.

[4] W. Liu, Y. Yin, Z. Zhou, M. He, Y. Dai, OxLDL-induced IL-1beta secretion promoting foam cells formation was mainly via CD36 mediated ROS production leading to NLRP3 inflammasome activation, Inflamm. Res. 63 (2014) 33–43. https://doi.org/10.1007/s00011-013-0667-3.

[5] A. Roy, U. Saqib, K. Wary, M.S. Baig, Macrophage neuronal nitric oxide synthase (NOS1) controls the inflammatory response and foam cell formation in atherosclerosis, International Immunopharmacology 83 (2020) 106382. https://doi.org/10.1016/j.intimp.2020.106382.

[6] A. Roy, U. Saqib, M.S. Baig, NOS1-mediated macrophage and endothelial cell interaction in the progression of atherosclerosis, Cell Biology International 45 (2021) 1191–1201. https://doi.org/10.1002/cbin.11558.

[7] X. Jiang, F. Wang, Y. Wang, A. Gisterå, J. Roy, G. Paulsson-Berne, U. Hedin, A. Lerman, G.K. Hansson, J. Herrmann, Z. Yan, Inflammasome-Driven Interleukin-1α and Interleukin-1β Production in Atherosclerotic Plaques Relates to Hyperlipidemia and Plaque Complexity, JACC: Basic to Translational Science 4 (2019) 304–317. https://doi.org/10.1016/j.jacbts.2019.02.007.

[8] D.J. Rader, IL-1 and atherosclerosis: a murine twist to an evolving human story, J. Clin. Invest. 122 (2012) 27–30. https://doi.org/10.1172/JCI61163.

[9] P. Theofilis, E. Oikonomou, C. Chasikidis, K. Tsioufis, D. Tousoulis, Inflammasomes in Atherosclerosis—From Pathophysiology to Treatment, Pharmaceuticals 16 (2023) 1211. https://doi.org/10.3390/ph16091211.

[10] W. Mai, Y. Liao, Targeting IL-1β in the Treatment of Atherosclerosis, Front. Immunol. 11 (2020) 589654. https://doi.org/10.3389/fimmu.2020.589654.

[11] X. Wang, G.Z. Feuerstein, J.-L. Gu, P.G. Lysko, T.-L. Yue, Interleukin-1β induces expression of adhesion molecules in human vascular smooth muscle cells and enhances adhesion of leukocytes to smooth muscle cells, Atherosclerosis 115 (1995) 89–98. https://doi.org/10.1016/0021-9150(94)05503-B.

[12] K. Kanno, Y. Hirata, T. Imai, M. Iwashina, F. Marumo, Regulation of inducible nitric oxide synthase gene by interleukin-1 beta in rat vascular endothelial cells, American Journal of Physiology-Heart and Circulatory Physiology 267 (1994) H2318–H2324. https://doi.org/10.1152/ajpheart.1994.267.6.H2318.

[13] P.M. Ridker, B.M. Everett, T. Thuren, J.G. MacFadyen, W.H. Chang, C. Ballantyne, F. Fonseca, J. Nicolau, W. Koenig, S.D. Anker, J.J.P. Kastelein, J.H. Cornel, P. Pais, D. Pella, J. Genest, R. Cifkova, A. Lorenzatti, T. Forster, Z. Kobalava, L. Vida-Simiti, M. Flather, H. Shimokawa, H. Ogawa, M. Dellborg, P.R.F. Rossi, R.P.T. Troquay, P. Libby, R.J. Glynn, Antiinflammatory Therapy with Canakinumab for Atherosclerotic Disease, N Engl J Med 377 (2017) 1119–1131. https://doi.org/10.1056/NEJMoa1707914.

[14] D.D. Arnold, A. Yalamanoglu, O. Boyman, Systematic Review of Safety and Efficacy of IL-1-Targeted Biologics in Treating Immune-Mediated Disorders, Front. Immunol. 13 (2022) 888392. https://doi.org/10.3389/fimmu.2022.888392.

[15] E. Lazarou, C. Koutsianas, P. Theofilis, G. Lazaros, D. Vassilopoulos, C. Vlachopoulos, C. Tsioufis, M. Imazio, A.

Brucato, D. Tousoulis, Interleukin-1 Blockers: A Paradigm Shift in the Treatment of Recurrent Pericarditis, Life 14 (2024) 305. https://doi.org/10.3390/life14030305.

[16] Y.-S. Ma, R. Xin, X.-L. Yang, Y. Shi, D.-D. Zhang, H.-M. Wang, P.-Y. Wang, J.-B. Liu, K.-J. Chu, D. Fu, Paving the way for small-molecule drug discovery, Am J Transl Res 13 (2021) 853–870.

[17] H. Wei, J.A. McCammon, Structure and dynamics in drug discovery, Npj Drug Discov. 1 (2024) 1. https://doi.org/10.1038/s44386-024-00001-2.

[18] M.S. Zabriskie, N.A. Vellore, K.C. Gantz, M.W. Deininger, T. O'Hare, Radotinib is an Effective Inhibitor of Native and Kinase Domain-Mutant BCR-ABL1, Leukemia 29 (2015) 1939–1942. https://doi.org/10.1038/leu.2015.42.

[19] A.J. Berberich, R.A. Hegele, Lomitapide for the treatment of hypercholesterolemia, Expert Opin Pharmacother 18 (2017) 1261–1268. https://doi.org/10.1080/14656566.2017.1340941.

[20] T.A. Halgren, R.B. Murphy, R.A. Friesner, H.S. Beard, L.L. Frye, W.T. Pollard, J.L. Banks, Glide: A New Approach for Rapid, Accurate Docking and Scoring. 2. Enrichment Factors in Database Screening, J. Med. Chem. 47 (2004) 1750–1759. https://doi.org/10.1021/jm030644s.

[21] O. Trott, A.J. Olson, AutoDock Vina: Improving the speed and accuracy of docking with a new scoring function, efficient optimization, and multithreading, J Comput Chem 31 (2010) 455–461. https://doi.org/10.1002/jcc.21334.

[22] D.A. Case, T.E. Cheatham, T. Darden, H. Gohlke, R. Luo, K.M. Merz, A. Onufriev, C. Simmerling, B. Wang, R.J. Woods, The Amber biomolecular simulation programs, J Comput Chem 26 (2005) 1668–1688. https://doi.org/10.1002/jcc.20290.

[23] J.A. Maier, C. Martinez, K. Kasavajhala, L. Wickstrom, K.E. Hauser, C. Simmerling, ff14SB: Improving the Accuracy of Protein Side Chain and Backbone Parameters from ff99SB, J. Chem. Theory Comput. 11 (2015) 3696–3713. https://doi.org/10.1021/acs.jctc.5b00255.

[24] J. Wang, R.M. Wolf, J.W. Caldwell, P.A. Kollman, D.A. Case, Development and testing of a general amber force field, J Comput Chem 25 (2004) 1157–1174. https://doi.org/10.1002/jcc.20035.

[25] J. Wang, W. Wang, P.A. Kollman, D.A. Case, Automatic atom type and bond type perception in molecular mechanical calculations, Journal of Molecular Graphics and Modelling 25 (2006) 247–260. https://doi.org/10.1016/j.jmgm.2005.12.005.

[26] D.J. Price, C.L. Brooks, A modified TIP3P water potential for simulation with Ewald summation, The Journal of Chemical Physics 121 (2004) 10096–10103. https://doi.org/10.1063/1.1808117.

[27] T. Darden, D. York, L. Pedersen, Particle mesh Ewald: An $N \cdot \log(N)$ method for Ewald sums in large systems, The Journal of Chemical Physics 98 (1993) 10089–10092. https://doi.org/10.1063/1.464397.

[28] V. Kr□utler, W.F. Van Gunsteren, P.H. H□nenberger, A fast SHAKE algorithm to solve distance constraint equations for small molecules in molecular dynamics simulations, J. Comput. Chem. 22 (2001) 501–508. https://doi.org/10.1002/1096-987X(20010415)22:5%253C501::AID-JCC1021%253E3.0.CO;2-V.

[29] H.J.C. Berendsen, J.P.M. Postma, W.F. Van Gunsteren, A. DiNola, J.R. Haak, Molecular dynamics with coupling to an external bath, The Journal of Chemical Physics 81 (1984) 3684–3690. https://doi.org/10.1063/1.448118.

[30] R.J. Loncharich, B.R. Brooks, R.W. Pastor, Langevin dynamics of peptides: The frictional dependence of isomerization rates of *N*-acetylalanyl-*N*′-methylamide, Biopolymers 32 (1992) 523–535. https://doi.org/10.1002/bip.360320508.

[31] R.W. Pastor, B.R. Brooks, A. Szabo, An analysis of the accuracy of Langevin and molecular dynamics algorithms, Molecular Physics 65 (1988) 1409–1419. https://doi.org/10.1080/00268978800101881.

[32] D.R. Roe, T.E. Cheatham, PTRAJ and CPPTRAJ: Software for Processing and Analysis of Molecular Dynamics Trajectory Data, J. Chem. Theory Comput. 9 (2013) 3084–3095. https://doi.org/10.1021/ct400341p.

[33] A.W. Götz, M.J. Williamson, D. Xu, D. Poole, S. Le Grand, R.C. Walker, Routine Microsecond Molecular Dynamics Simulations with AMBER on GPUs. 1. Generalized Born, J. Chem. Theory Comput. 8 (2012) 1542–1555. https://doi.org/10.1021/ct200909j.

[34] R. Salomon-Ferrer, A.W. Götz, D. Poole, S. Le Grand, R.C. Walker, Routine Microsecond Molecular Dynamics Simulations with AMBER on GPUs. 2. Explicit Solvent Particle Mesh Ewald, J. Chem. Theory Comput. 9 (2013) 3878–3888. https://doi.org/10.1021/ct400314y.

[35] B.R. Miller, T.D. McGee, J.M. Swails, N. Homeyer, H. Gohlke, A.E. Roitberg, *MMPBSA.py* : An Efficient Program for End-State Free Energy Calculations, J. Chem. Theory Comput. 8 (2012) 3314–3321. https://doi.org/10.1021/ct300418h.

[36] P.A. Kollman, I. Massova, C. Reyes, B. Kuhn, S. Huo, L. Chong, M. Lee, T. Lee, Y. Duan, W. Wang, O. Donini, P. Cieplak, J. Srinivasan, D.A. Case, T.E. Cheatham, Calculating Structures and Free Energies of Complex Molecules: Combining Molecular Mechanics and Continuum Models, Acc. Chem. Res. 33 (2000) 889–897. https://doi.org/10.1021/ar000033j.

[37] S. Samanta, M.F. Sk, S. Koirala, P. Kar, Exploring molecular interactions of potential inhibitors against the spleen tyrosine kinase implicated in autoimmune disorders via virtual screening and molecular dynamics simulations, SAR and QSAR in Environmental Research 34 (2023) 869–897. https://doi.org/10.1080/1062936X.2023.2266364.

[38] S. Koirala, R. Roy, S. Samanta, S. Mahapatra, P. Kar, Plant derived active compounds of ayurvedic neurological formulation, Saraswatharishta as a potential dual leucine zipper kinase inhibitor: an *in-silico* study, Journal of Biomolecular Structure and

Dynamics 42 (2024) 11201–11214. https://doi.org/10.1080/07391102.2023.2260892.

[39] A. Roy, U. Saqib, M.S. Baig, NOS1-mediated macrophage and endothelial cell interaction in the progression of atherosclerosis, Cell Biology International 45 (2021) 1191–1201. https://doi.org/10.1002/cbin.11558.

[40] C.A. Schneider, W.S. Rasband, K.W. Eliceiri, NIH Image to ImageJ: 25 years of image analysis, Nat Methods 9 (2012) 671–675. https://doi.org/10.1038/nmeth.2089.

[41] J. Galea, J. Armstrong, P. Gadsdon, H. Holden, S.E. Francis, C.M. Holt, Interleukin-1β in Coronary Arteries of Patients With Ischemic Heart Disease, ATVB 16 (1996) 1000–1006. https://doi.org/10.1161/01.ATV.16.8.1000.

[42] A. Qamar, D.J. Rader, Effect of interleukin 1β inhibition in cardiovascular disease:, Current Opinion in Lipidology 23 (2012) 548–553. https://doi.org/10.1097/MOL.0b013e328359b0a6.

[43] P.E. Auron, The Interleukin 1 Receptor: Ligand Interactions and Signal Transduction, Cytokine & Growth Factor Reviews 9 (1998) 221–237. https://doi.org/10.1016/S1359-6101(98)00018-5.

[44] Y. Wang, J. Wang, W. Zheng, J. Zhang, J. Wang, T. Jin, P. Tao, Y. Wang, C. Liu, J. Huang, P.Y. Lee, X. Yu, Q. Zhou, Identification of an IL-1 receptor mutation driving autoinflammation directs IL-1-targeted drug design, Immunity 56 (2023) 1485-1501.e7. https://doi.org/10.1016/j.immuni.2023.05.014.

[45] K. Solanki, R. Sharma, B. E, B. Ms, Small Molecule Inhibitors Targeting Endothelial IL-1β Receptor (IL-1R1): A Novel Approach to Atherosclerosis Therapy, Austinjpharmacolther 11 (2023). https://doi.org/10.26420/austinjpharmacolther.2023.1170.

[46] P. Rajendran, T. Rengarajan, J. Thangavel, Y. Nishigaki, D. Sakthisekaran, G. Sethi, I. Nishigaki, The Vascular Endothelium and Human Diseases, Int J Biol Sci 9 (2013) 1057–1069. https://doi.org/10.7150/ijbs.7502.

[47] P. Khanna, T. Yunkunis, H.S. Muddana, H.H. Peng, A. August, C. Dong, p38 MAP kinase is necessary for melanoma-mediated regulation of VE-cadherin disassembly, American Journal of Physiology-Cell Physiology 298 (2010) C1140–C1150. https://doi.org/10.1152/ajpcell.00242.2009.

[48] W. Nan, Y. He, S. Wang, Y. Zhang, Molecular mechanism of VE-cadherin in regulating endothelial cell behaviour during angiogenesis, Front. Physiol. 14 (2023) 1234104. https://doi.org/10.3389/fphys.2023.1234104.

[49] K. Hatanaka, M. Simons, M. Murakami, Phosphorylation of VE-cadherin controls endothelial phenotypes via p120-catenin coupling and Rac1 activation, American Journal of Physiology-Heart and Circulatory Physiology 300 (2011) H162–H172. https://doi.org/10.1152/ajpheart.00650.2010.

[50] C.A. Dinarello, A. Simon, J.W.M. van der Meer, Treating inflammation by blocking interleukin-1 in a broad spectrum of diseases, Nat Rev Drug Discov 11 (2012) 633–652. https://doi.org/10.1038/nrd3800.

[51] A. Galaup, E. Gomez, R. Souktani, M. Durand, A. Cazes, C. Monnot, J. Teillon, S. Le Jan, C. Bouleti, G. Briois, J. Philippe, S. Pons, V. Martin, R. Assaly, P. Bonnin, P. Ratajczak, A. Janin, G. Thurston, D.M. Valenzuela, A.J. Murphy, G.D. Yancopoulos, R. Tissier, A. Berdeaux, B. Ghaleh, S. Germain, Protection Against Myocardial Infarction and No-Reflow Through Preservation of Vascular Integrity by Angiopoietin-Like 4, Circulation 125 (2012) 140–149.
https://doi.org/10.1161/CIRCULATIONAHA.111.049072.

[52] R.R. McMullan, D.F. McAuley, C.M. O'Kane, J.A. Silversides, Vascular leak in sepsis: physiological basis and potential therapeutic advances, Crit Care 28 (2024) 97. https://doi.org/10.1186/s13054-024-04875-6.

[53] M. Murakami, M. Simons, Regulation of Vascular Integrity, J Mol Med (Berl) 87 (2009) 571–582. https://doi.org/10.1007/s00109-009-0463-2.

[54] I. Aggeletopoulou, M. Kalafateli, E.P. Tsounis, C. Triantos, Exploring the role of IL-1β in inflammatory bowel disease pathogenesis, Front Med (Lausanne) 11 (2024) 1307394. https://doi.org/10.3389/fmed.2024.1307394.

[55] C.A. Dinarello, Interleukin-1 in the pathogenesis and treatment of inflammatory diseases, Blood 117 (2011) 3720–3732. https://doi.org/10.1182/blood-2010-07-273417.

[56] C.A. Lipinski, F. Lombardo, B.W. Dominy, P.J. Feeney, Experimental and computational approaches to estimate solubility and permeability in drug discovery and development settings, Adv Drug Deliv Rev 46 (2001) 3–26. https://doi.org/10.1016/s0169-409x(00)00129-0.

[57] W.A. Muller, Mechanisms of Leukocyte Transendothelial Migration, Annu Rev Pathol 6 (2011) 323–344. https://doi.org/10.1146/annurev-pathol-011110-130224.

[58] R. Kaur, V. Singh, P. Kumari, R. Singh, H. Chopra, T.B. Emran, Novel insights on the role of VCAM-1 and ICAM-1: Potential biomarkers for cardiovascular diseases, Ann Med Surg (Lond) 84 (2022) 104802. https://doi.org/10.1016/j.amsu.2022.104802.

[59] T.M. Bui, H.L. Wiesolek, R. Sumagin, ICAM-1: A master regulator of cellular responses in inflammation, injury resolution, and tumorigenesis, J Leukoc Biol 108 (2020) 787–799. https://doi.org/10.1002/JLB.2MR0220-549R.

[60] J.M. Cook-Mills, M.E. Marchese, H. Abdala-Valencia, Vascular Cell Adhesion Molecule-1 Expression and Signaling During Disease: Regulation by Reactive Oxygen Species and Antioxidants, Antioxid Redox Signal 15 (2011) 1607–1638. https://doi.org/10.1089/ars.2010.3522.

CHAPTER 5

Novel peptide inhibitors targeting CD40 and CD40L interaction: a potential for atherosclerosis therapy

CHAPTER 5

Novel peptide inhibitors targeting CD40 and CD40L interaction: a potential for atherosclerosis therapy

5.1. Graphical Abstract

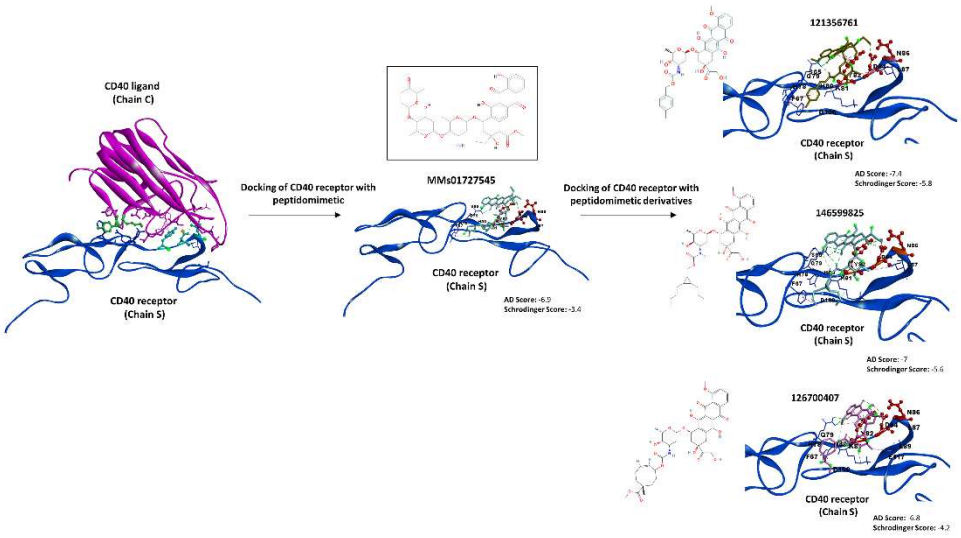

Figure 5.1. Graphical summary of binding of peptide and peptidomimetic inhibitors with the CD40 receptor. Figure depicting the binding of peptide, peptidomimetic and peptidomimetic derivatives with the active site of the CD40 receptor.

5.2. Summary:

Atherosclerosis is a chronic inflammatory disease characterized by plaque build-up in the arteries, leading to the obstruction of blood flow. Macrophages are the primary immune cells found in the atherosclerotic lesions and are directly involved in atherosclerosis progression. Macrophages are derived from extravasating blood monocytes. The monocytic CD40 receptor is important for monocyte recruitment on the endothelium expressing the CD40 ligand (CD40L). Thus, targeting monocyte/macrophage interaction with the endothelium by inhibiting CD40-CD40L interaction may be a promising strategy for attenuating atherosclerosis. Monoclonal antibodies have been used against this target but shows various complications. We used an array of computer-aided drug discovery tools and molecular docking approaches to design a therapeutic inhibitory peptide that could efficiently bind to the critical residues (82Y, 84D, and 86N) on the CD40 receptor; essential for the receptor's binding to CD40L. The initial screen identified a parent peptide with a high binding affinity to CD40, but the peptide exhibited a positive hepatotoxicity score. We then designed several novel peptidomimetic derivatives with higher binding affinities to CD40, good physicochemical properties, and negative hepatotoxicity as compared to the parent peptide. Furthermore, we conducted molecular dynamics simulations for both the apo and complexed forms of the receptor with ligand, and screened peptides to evaluate their stability. The designed peptidomimetic derivatives are promising therapeutics targeting the CD40-CD40L interaction and may potentially be used to attenuate atherosclerosis.

5.3. Introduction

Atherosclerosis is a chronic inflammatory disease in which plaque build-up due to the deposition of cholesterol, lipids, and fats as well as extravasation of immune cells in the arteries lead to an obstruction of blood flow. Atherosclerosis is a major cause of cardiovascular diseases (CVD) and is a risk factor for myocardial infarction (MI) and ischemic stroke [1]. Pharmacological treatments such as lipid-lowering therapies, anti-hypertensive agents, and anti-platelets drugs reduce the risk of CVD, but atherosclerosis-related complications remain persistent worldwide [2,3]. Thus far, several clinical trials have focused on targeting inflammatory molecules implicated in the progression of atherosclerosis [4–6]. Another strategy is to inhibit inflammation and/or to modulate the immune checkpoint proteins, promoting inflammation [7] . The CD40-CD40L dyad is an important immune checkpoint protein complex that is expressed on major immune cells, and its activation leads to the progression of atherosclerosis [8,9]

CD40L plays an important role in the pathogenesis of atherosclerosis[10]. Cells such as myeloid and lymphoid cells, platelets, endothelial cells and vascular smooth muscle cells (VSMCs) are known to express CD40L on their surfaces [11]. CD40L expression is primarily found on T-cells and platelets in atherosclerosis [12]. CD40L present on these cells would bind to CD40 receptor expressed on antigen presenting cells (APCs) to amplify the signaling [13] . Apart from CD40, CD40L also bind to other co-stimulatory receptor present on the cell surface to activate the inflammation response [9]. One of the major roles of CD40-CD40L interaction is the recruitment of monocytes and other immune cells to the site of inflammation during the initial phase of plaque formation. The endothelial cells are activated when the monocytic CD40 receptor binds the endothelial CD40L. This enhances the expression of cell adhesion molecules (CAMs) such as vascular cell adhesion molecule (VCAM)-1, intercellular cell adhesion molecule (ICAM)-1 and E-selectin on the endothelium [14]. Remarkably, high Ox-LDL

levels drive the expression of the CD40 receptor on monocytes/macrophages and CD40L on the endothelial cell, further enhancing the expression of CAMs on the endothelial cells and facilitating the recruitment and transmigration of monocytes into the arterial intima, critical steps of atherosclerosis progression [15] . Migration of monocytes into the intima leads to their differentiation into macrophages. These macrophages secrete various pro-inflammatory molecules and further enhance the inflammation process. Thus, inhibition of the CD40-CD40L interaction may be important for preventing chronic consequences of atherosclerosis. Indeed, studies have found that genetic or antibody-mediated inhibition of CD40 or CD40L reduces the inflammatory cell number within the plaque with a subsequent decrease in the lesion size and enhanced plaque stability [16–18]. CD40-TRAF6 interaction is present downstream of CD40-40L interaction [19]. Inhibition of CD40-TRAF6 with TRAF-STOP inhibitors have shown promising results [20]. Multiple antibodies have been developed to target the CD40-CD40L interaction [21] , but the strong immune response against the antibodies and thromboembolic complications limit their usage [22]. Thus, it is important to search for better therapeutic strategies that would have enhanced efficacy with limited side effects.

In the past few years, peptides and peptidomimetics have emerged as promising candidates to treat various diseases by modulating protein-protein interactions (PPIs) [23,24]. There are now peptides that successfully target certain biologically important protein complexes, such as transcription factors, which are traditionally considered as undruggable targets for small molecules because of their complex architecture and stability [25]. However, peptides possess certain characteristics that limit their usage as therapeutic candidates, such as low metabolic stability towards proteolysis in the gastrointestinal tract and serum, their poor absorption after oral ingestion, and their rapid excretion through the liver and kidneys [23]. Hence, advancements are necessary to meet the increased therapeutic demands. Recent technological advances in formulation,

delivery, and chemistry have driven the focus of drug discovery teams toward peptidomimetics [26–28] . Peptidomimetics are compounds whose essential elements (or pharmacophore) mimic a peptide or protein in their 3D space and which primarily tend to retain the ability to interact with the specified biological target and impart the same biological effect. Certain limitations of peptides can be compensated through creating peptidomimetics with increased stability against proteolysis, receptor selectivity or potency, among others. Hence, peptidomimetics have a great potential in drug discovery [24]. Also, designing/deriving compounds that contain the same backbone elements as peptidomimetic with few modifications in the side chains, which can increase the affinity of the compound with the target, can be a better therapeutic strategy against the target molecule [29].

Identification of the critical residues on the target protein is important for designing the molecules limiting the protein-protein interaction. *In-vitro* studies have identified three critical residues on the CD40 receptor (Y82, D84, and N86) having a key role in its interaction with CD40L [30]. In this study, we focused on designing peptides that may bind to these critical residues. Furthermore, we derived promising peptidomimetics and their derivatives with increased affinity to the CD40 receptor and improved physicochemical properties.

5.4. Methods

5.4.1. Analyses of CD40-40L interface and docking of CD40-CD40L

The crystal structure of CD40-CD40L interaction (**PDB ID:** 3QD6) was retrieved from RCSB Protein Data Bank (https://www.rcsb.org). The crystal structure was analysed by the X-Ray diffraction method with a resolution of 3.5Å. The complex contains a total of 4 CD40 receptor chains (Chain R, S, T, and U) interacting with 6 CD40L chains (Chain A, B, C, D, E, and F) in a ratio of 2:3 of receptor: ligand complex [31]. The complex was downloaded as a PDB file, and the monomer of the CD40 receptor (Chain S) interacting with the CD40L monomer (Chain C) was taken for further interaction studies. 4Å interacting residues

between the complex were analysed in UCSF Chimera [32]. Also, the individual monomers of both the receptor and the ligand were structurally minimized using Amber ff14SB [33] in the UCSF Chimera, and site-specific docking was done in PyDockWEB (https://life.bsc.es/pid/pydockweb) [34] providing the 4Å interacting residues between the complex.

5.4.2. In-silico mutational analysis of CD40-40L interaction

As the *in-vitro* mutational study had identified Y82, D84, and N86 as a critical residue on the CD40 receptor mediating the interaction with the ligand, we wanted to further confirm the result through *in-silico* study. Individual mutations on the CD40 receptor (Y82, D84, and N86) were done using the Rotamer option in UCSF Chimera [32], replacing key residues with alanine one at a time. The structure was then minimized using Amber ff14SB [33] in Chimera and docked with the CD40L (Chain C) in HDOCK (http://hdock.phys.hust.edu.cn/) [35] providing the 4Å interacting residues between the complex. Also, the triple mutations were done in CD40 before docking with wild type CD40L to compare the change in binding affinity with the individual mutations. Similar strategy was employed on CD40L by mutating the residues K143 and Y145 individually and by performing the double mutations (Chain C) and docked to CD40 in HDOCK (http://hdock.phys.hust.edu.cn/) [35]

5.4.3. The design and docking of the peptide

Four-amino acid peptide (*p-KGYY*) was designed against the critical residues on the receptor to block the receptor-ligand interaction. Stretch from residues 143-146 on the CD40L was used to design the peptide using the "*Build structure*" option in UCSF Chimera [32]. The designed peptide was then minimized using Amber ff14SB and docked with the CD40-receptor (Chain S) in PyDockWEB [34] and ZDOCK [36]. 4Å interacting residues between the complex were analysed in UCSF Chimera to find the critical residue(s) on the receptor involved in the binding with the peptide. Further, physicochemical and ADMET

analyses of the peptide were done using the pkCSM server (https://biosig.lab.uq.edu.au/pkcsm/) [37]. pkCSM uses graph-based signatures of the compounds to analyse the ADMET properties of the compounds by comparing them with the *in-vitro* data available on the server. The SMILES file of the compounds was generated on the pepSMI server (https://www.novoprolabs.com/tools/convert-peptide-to-smiles-string) and then analysed on the pkCSM server to optimize its ADMET properties.

5.4.4. The docking of peptidomimetic with the receptor

To address the limitations of the designed peptide, peptidomimetics that mimic the structure as well as the pharmacophore of the designed peptide were searched on the pep:MMs:MIMIC server (http://mms.dsfarm.unipd.it/pepMMsMIMIC/) [38]. pep:MMs:MIMIC is a server in which the 3D-similarity search of the peptides is possible among 3.9 million commercial compounds in the MMsINC database (http://mms.dsfarm.unipd.it/MMsINC/search/) [39]. Side chains of the lysine and tyrosine residue on the peptide were selected and fingerprint-based filtering of shape similarity and pharmacophoric similarity-based methods were used to provide the top 200 compounds from the database. All the compounds were downloaded in the 3D SDF format and docked to the CD40 receptor (Chain S; PDB 3QD6). Two docking platforms were used: AutoDock Vina (v1.2.0) [40,41] and the Glide module of the Schrodinger suite [42]. Preparation of the receptor for docking in AutoDock Vina (v1.2.0) was done by adding polar hydrogen bonds followed by the addition of Kolmann charges in AutoDock 4.2.6 [43]. A grid box was generated around the receptor covering the whole receptor molecule. For docking in Schrodinger, the protein preparation wizard of the Schrodinger suite [44] was used in which missing hydrogens were added, followed by the removal of heteroatoms and water molecules. The structure was then refined and optimized at pH 7.0 using PROPKA [45], followed by minimization using OPLS4 force-field [46]. The receptor grid was generated by selecting the 4Å residues on the CD40 receptor interacting with the ligand in the crystal structure.

The docked compounds were shortlisted based on the interaction of the peptidomimetic with all three critical residues (Y82, D84, and N86) in AutoDock Vina (v1.2.0) and Schrodinger. Further, physicochemical and ADMET analyses of the lead compounds were done on the pkCSM server [37].

5.4.5. The docking of peptidomimetic derivative

As the derived peptidomimetic had limitations in its ADMET property, we sought to find the derivatives of the lead compounds which can increase the binding affinity with the receptor as well as have good ADMET properties. A structural similarity search of the lead compounds was done in PubChem (https://pubchem.ncbi.nlm.nih.gov/) by uploading the SMILES ID of the peptidomimetic structure. The resulting compounds were downloaded as 2D SDF and converted to 3D by the LigPrep module of the Schrodinger suite [47]. 3D SDF files were converted into pdbqt in Open Babel and docked with the CD40 receptor (Chain S) in AutoDock Vina (v1.2.0) [40,41]. Compounds were then screened accordingly through their interaction with the three critical residues on the receptor. The shortlisted compounds were further docked in Glide [42] to find a similar interaction with the receptor. Physicochemical analysis of the top compounds in both platforms was done in the pkCSM server [37] to find the compound(s) with good ADMET properties.

5.4.6. Molecular dynamics simulation

To assess the stability of the screened peptide p-KGYY in complex with the CD40 receptor as well of peptidomimetic and peptidomimetic derivatives with the CD40 receptor, molecular dynamics simulations were performed using GROMACS 2025.4 [48] with the AMBER99-ILDN force field [49]. Each system was solvated in a cubic periodic box centred on the protein using the TIP3P water model, and counter-ions were added to neutralize the overall charge. After energy minimization, the systems were equilibrated under NVT at 300 K with

position restraints on the protein–ligand complex, followed by NPT at 1 bar to stabilize density. Long-range electrostatics were treated with the Particle Mesh Ewald (PME) method, and bond constraints were applied using the LINCS algorithm. Production simulations were then carried out for 200 ns with a 2 fs timestep under periodic boundary conditions. Trajectory analyses, including RMSD, RMSF, radius of gyration and solvent accessibility, were conducted using built-in GROMACS utilities and QtGrace software to evaluate conformational stability and dynamic behavior of the systems.

5.5. Results

5.5.1. Structural analysis and docking of the CD40 receptor with the CD40 ligand

To validate our computer modelling approach, we first analysed the crystal structure of the CD40-CD40L protein complex (RCSB: PDB 3QD6) to deduce the critical residues involved in the protein-protein interactions. The protein-protein interface of the CD40 receptor (Chain S) and CD40 ligand (Chain C) was scrutinized using UCSF Chimera [32] to identify all residues which are found within the range of ionic and hydrogen bonding interactions of 4Å (**Figure 5.2A and 5.2B**). Our analysis confirmed a previous study finding that there are three critical residues on the CD40 receptor (Y82, D84, and N86) and two critical residues on the CD40 ligand (K143 and Y145) contributing to the protein-protein interactions within the CD40R-CD40L protein complex [30]. The monomeric chains of the CD40 receptor (Chain S) and ligand (Chain C) were also docked using PyDockWEB [34] and then analysed for the 4Å range residues within the CD40R-CD40L complex. The docking results again showed the involvement of similar residues in mediating CD40R-CD40L interactions (**Figure 5.3**).

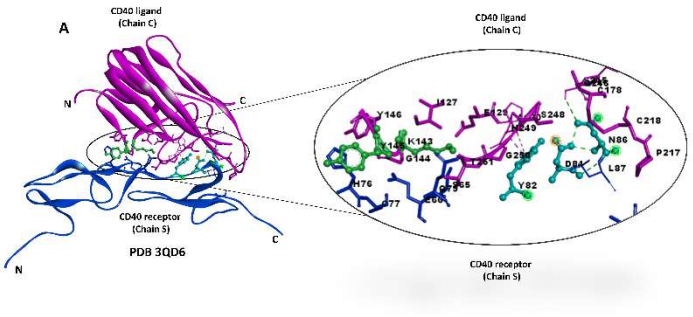

B

4Å residues	
CD40 receptor	CD40 ligand
65, 66, 76, 77, 79, **82**, **84**, **86**, 87, 119	127, 129, 130, **143**, 144, **145**, 146, 178, 217, 218, 245, 246, 248, 249, 250, 251

Figure 5.2. Analysis of the crystal structure of CD40-CD40L (PDB 3QD6): A.) Schematic representation of the CD40 receptor (Chain S) interacting with CD40L (Chain C). 4Å interacting residues between the complex have been highlighted in the circle. B) Table showing 4Å interacting residues between the CD40 receptor (Chain S) and CD40L (Chain C). Residues in bold indicate critical residues in the receptor and the ligand. CD40 is highlighted in blue, and CD40L is highlighted in pink.

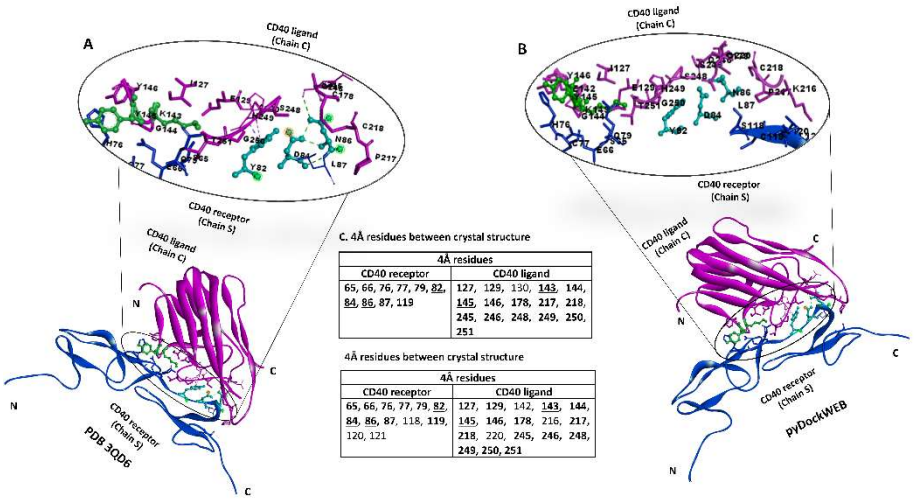

C. 4Å residues between crystal structure

4Å residues	
CD40 receptor	CD40 ligand
65, 66, 76, 77, 79, 82, 84, 86, 87, 119	127, 129, 130, 143, 144, 145, 146, 178, 217, 218, 245, 246, 248, 249, 250, 251

4Å residues between crystal structure

4Å residues	
CD40 receptor	CD40 ligand
65, 66, 76, 77, 79, 82, 84, 86, 87, 118, 119, 120, 121	127, 129, 142, 143, 144, 145, 146, 178, 216, 217, 218, 220, 245, 246, 248, 249, 250, 251

Figure 5.3. Comparison of the crystal structure and the docked structure: A.) Crystal structure of CD40 (Chain S) and CD40L (Chain C) along with 4Å residues highlighted in the circle. B.) Docking of CD40 (Chain S) and CD40L (Chain C) in PyDockWEB along with 4Å

residues highlighted in the circle. C.) Table showing 4Å interacting residues between crystal and docked structures of CD40-CD40L. Matching residues between the crystal and the docked structures are highlighted in bold and critical residues (82Y, 84D, and 86N) are underlined. CD40 is highlighted in blue, and CD40L is highlighted in pink.

5.5.2. In silico mutational analysis of the CD40 receptor and CD40L

To further decipher the importance of the critical residues on the receptor (Y82, D84, and N86) and the ligand (K143 and Y145), *in-silico* point mutational analysis was performed during which the critical residues on the CD40 receptor were individually replaced with alanine. Additionally, we created the CD40 receptor mutant in which all three critical residues were replaced with alanine. We then docked each *in-silico* created mutant of the CD40 receptor with the CD40 ligand using the HDOCK server (http://hdock.phys.hust.edu.cn/) [35] . Control docking of the wild type CD40 receptor (without mutations) with the CD40 ligand was performed to compare the docking scores among the wild type and mutated complexes. The results showed decreases in the docking scores of the individually mutated CD40 receptors compared to the wild type CD40 receptor used as a control, with the highest decrease in the mutated CD40 receptor where all three critical residues were replaced with alanine (**Figure 5.4**). Similarly, the critical residues on the CD40 ligand (K143 and Y145) were also mutated individually or together and then docked with the CD40 receptor using HDOCK [35]. The result again showed decreases in the binding affinity in the mutated structures compared to the control, with the highest decrease found in the combined mutated structures (**Figure 5.5**).

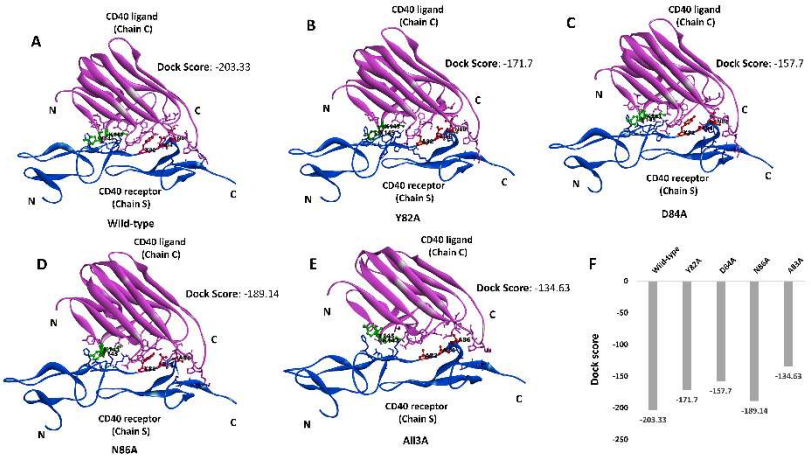

Figure 5.4. Effect of mutation(s) on the critical residue(s) on the receptor binding with the ligand: Figure showing the docking of CD40 (Chain S) and CD40L (Chain C) with individual mutation(s) along with the dock scores in HDOCK. A.) Wild-type (no mutation). B.) Y82A. C.) D84A. D.) N86A. E.) All three mutations. F.) Graph comparing the dock scores between all mutations. Residues 82, 84, and 86 in the receptor are highlighted in red, and residues 143 and 145 in the ligand have been highlighted in green. CD40 is highlighted in blue, and CD40L is highlighted in pink.

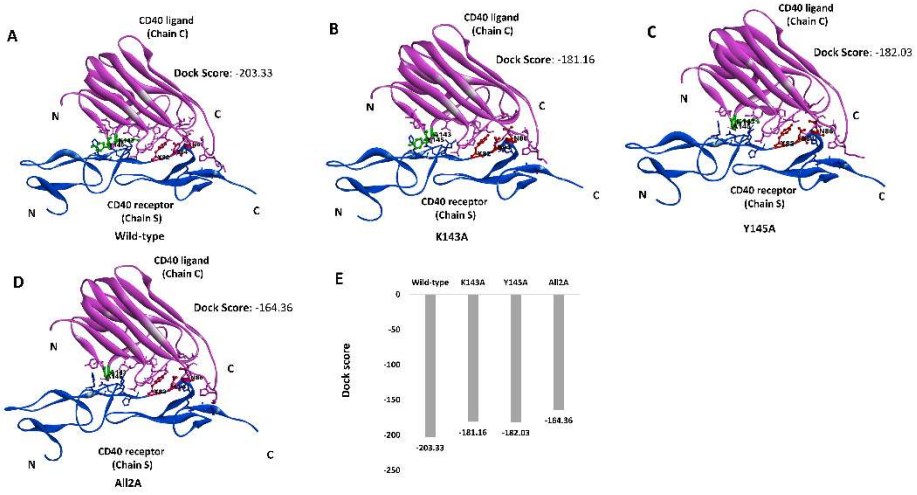

Figure 5.5. Effect of mutation(s) on the critical residue(s) on the binding of CD40L with CD40: Figure showing the docking of CD40 (Chain S) and CD40L (Chain C) with individual mutation(s) along with the dock scores in HDOCK. **A.)** Wild-type (no mutation). **B.)** K143A. **C.)** Y145A. **D.)** Both the mutations. **E.)** Graph comparing the dock scores between all the mutations. Residues 82, 84, and 86 in the receptor are highlighted in red, and residues 143 and 145 in the ligand are highlighted in green. CD40 is highlighted in blue, and CD40L is highlighted in pink

5.5.3. Designing of the inhibitory peptide and its docking to the CD40 receptor

Since the interaction of CD40 and CD40L is strongly implicated in atherogenesis, we next set out to design a small therapeutic inhibitory peptide capable of preventing the CD40-CD40L complex formation. A continuous stretch of residues in the CD40 ligand (143-146), critical for the interaction with CD40, was used as a template to design the therapeutic inhibitory peptide structure. The peptide (p-KGYY) was designed using UCSF Chimera [32] and then docked to the CD40 receptor (PDB 3QD6; Chain S) using PyDockWEB [34] and ZDOCK [36]. The residues within the 4Å range in the docked peptide-CD40 complex were analysed and compared with the interacting residues in the crystal structure of the CD40-CD40L complex. We found that the peptide-CD40 interface was very similar to that of the equivalent stretch in the CD40-CD40L crystal structure (**Figure 5.6**). However, while conducting the physicochemical and ADMET analyses of the peptide using the pkCSM server [37], we found that the designed peptide may

exhibit hepatotoxicity (**Table S5.1**). These urged us to search for a better therapeutic molecule with a safer profile.

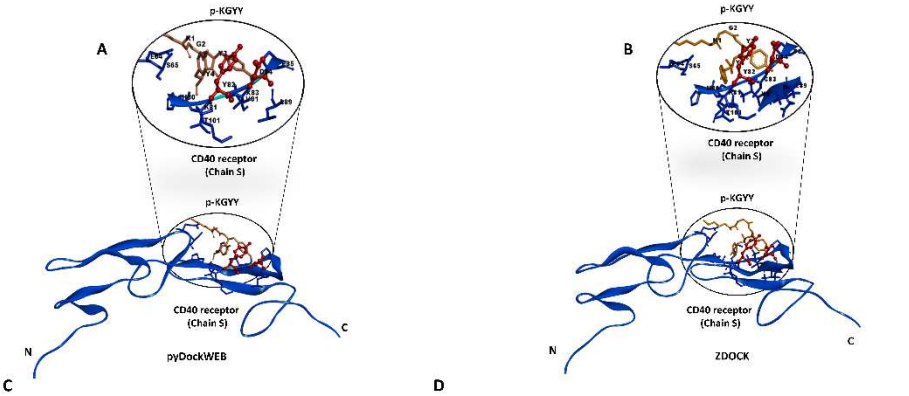

C

4Å residues	
CD40 receptor	CD40 ligand
65, 66, 76, 77, 79, **82**, **84**, **86**, 87, 119	127, 129, 130, **143**, 144, **145**, 146, 178, 217, 218, 245, 246, 248, 249, 250, 251

D

Sr. No.	Docking Platform	4A interacting residues
		Receptor
1	PyDOCK	E64, S65, H80, K81, Y82, C83, D84, P85, L89, V91, T101
2	ZDOCK	E64, S65, H80, K81, Y82, C83, D84, P85, L89, R90, V91, K94, T101

Figure 5.6. The docking of peptide (p-KGYY) with the CD40 receptor: A.) Diagrammatic representation of docking of the peptide with the CD40 receptor in PyDockWEB. 4Å̊ interacting residues are shown in a circle. B.) Diagrammatic representation of docking of the peptide with the CD40 receptor in ZDOCK. 4Å̊ interacting residues are shown in a circle. C.) 4Å̊ interacting residues in the crystal structure of CD40-CD40L (PDB 3QD6). D.) 4Å̊ interacting residues between the peptide and the receptor in PyDockWEB and ZDOCK. Similar residues in the docked structure and the crystal structure are highlighted in bold and critical residues on the receptor (82Y, 84, and 86N) are underlined. CD40 is highlighted in blue, and the peptide is highlighted in pink.

5.5.4. Peptidomimetics as a therapeutic strategy to block CD40-CD40L interactions

To address the limitations of the derived peptide structure, peptidomimetics were used as an alternative therapeutic strategy. The peptidomimetic pep:MMs:MIMIC server (http://mms.dsfarm.unipd.it/pepMMsMIMIC/) was used to derive the best peptidomimetic structures from the publicly available database. pep:MMs:MIMIC utilizes a 3D-similarity search of the peptide among

17 million available conformers of 3.9 million commercially available compounds in the MMsINC database [39] and provides the top 200 molecules. The resultant molecules were individually docked to the CD40 receptor using AutoDock Vina (v1.2.0) [40] and the Glide module of the Schrodinger suite [42] and were then shortlisted based on their interaction with all the three critical residues (Y82, D84, and N86) on the CD40 receptor. One molecule (MMs01727545) was found to be interacting with all the three critical residues on CD40 along with the good docking score in both platforms (**Figure 5.7**). However, the physicochemical and ADMET analyses still flagged a positive hepatotoxicity value for this compound (**Table S5.2**). Therefore, we next set out to search for the derivatives of our peptidomimetic structure (MMs01727545) with a comparable or greater binding affinity to CD40 and a negative hepatotoxicity value.

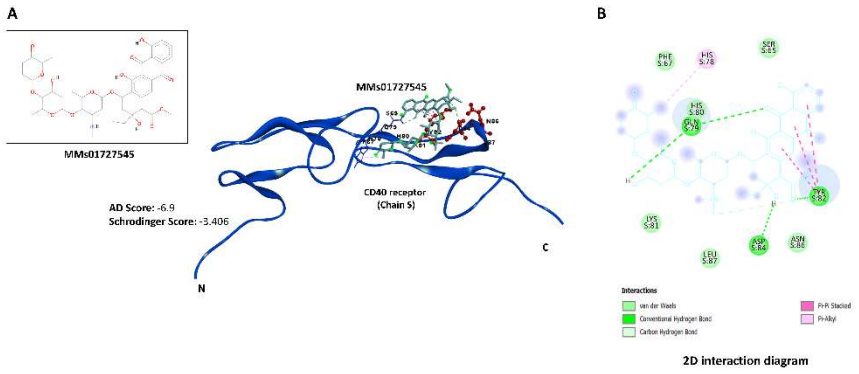

Figure 5.7. The docking of peptidomimetic (MMs01727545) with the CD40 receptor: A.) Diagrammatic representation of the docking of the peptidomimetic (MMs01727545) with the CD40 receptor. Docking scores for AutoDock Vina and Schrodinger are indicated **B.)** 2D interaction diagram of the interacting residues between the receptor and the peptidomimetic structure (MMs01727545).

5.5.5. Designing the peptidomimetic derivatives and their docking to CD40

In this case, we utilized PubChem (https://pubchem.ncbi.nlm.nih.gov/) to identify the peptidomimetic derivatives. We performed a similarity search of the molecules by uploading SMILES ID of our lead peptidomimetic structure (MMs01727545) and downloading 1000 structurally identical molecules. The docking of these molecules was performed using AutoDock Vina (v1.2.0) [41] and Schrodinger Software [42]. Three molecules were identified (PubChem ID 121356761, 146599825, and 126700407) that were able to bind to all three critical residues of CD40 in both docking platforms (**Figure 5.8**). Excitingly, the physicochemical and ADMET analyses of these molecules yielded negative hepatotoxicity values. In summary, these three derivatives interacted with all three critical residues on CD40 (Y82, D84, and N86), exhibited a higher binding affinity to CD40 as compared to the original peptidomimetic structure, and possessed good physicochemical and ADMET properties (**Table 5.1**).

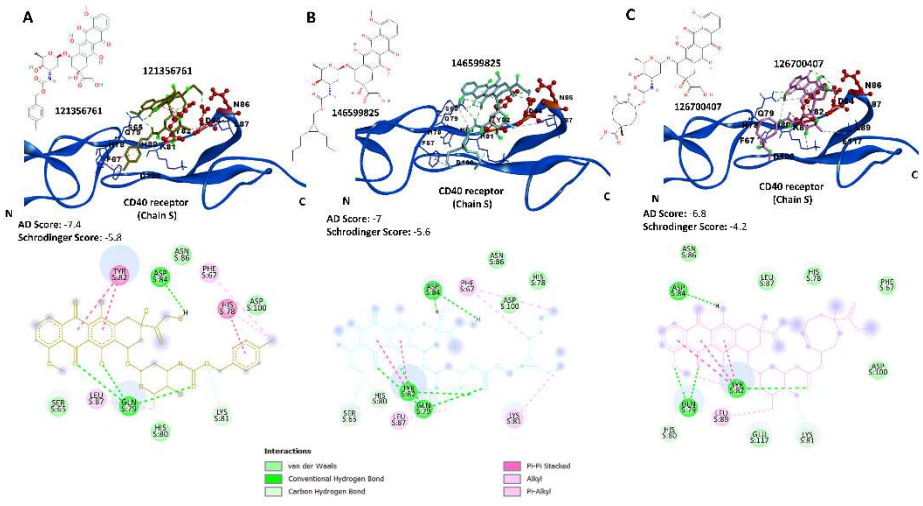

Figure 5.8. The docking of the peptidomimetic derivatives with the CD40 receptor: Diagrammatic representation of the docking of individual peptidomimetic derivatives with the CD40 receptor in AutoDock Vina and Schrodinger along with the 2D interaction diagram. A) 121356761, B) 146599825, and C) 126700407. Individual docking scores have been indicated. Interacting residues between the complex

have been highlighted. CD40 is highlighted in blue, and peptidomimetics are highlighted in pink

Table 5.1: Summary of docking of peptidomimetics and their derivatives:

A.) Dock Scores and residual interaction of peptidomimetic (MMs01727545) and their derivatives (PubChem ID: 121356761, 146599825 and 126700407).

Parameters		MMs01727545	121356761	146599825	126700407
Dock Scores	Autodock Vina	-6.9	-7.4	-7	-6.8
	Interaction	82: h-bond, C-H bond; 84: h-bond; 86: VdW	82: pi-pi; 84: H-bond; 86: VdW	82: H-bond; pi-pi; 84: H-bond; 86: VdW	82: H-bond; pi-pi; 84: H-bond; 86: VdW
	Schrodinger	-3.406	-5.8	-5.6	-4.2
	Interaction	82: pi-pi; 84: h-bond; 86: VdW	82: H-bond; pi-pi; 84: H-bond; 86: VdW	82: H-bond; pi-pi; 84: H-bond; 86: VdW	82: H-bond; pi-pi; 84: H-bond; 86: VdW

.

Parameters		p-KGYY	MMs01727545	121356761	146599825	126700407
Physicochemical properties	M.W.	531.61	812.8	691.686	737.799	767.781
	LogP	-1.92	1.7	2.27742	3.3973	2.4469
	Rotatable bond	15	9	8	13	8
	Acceptor bond	6	15	13	13	15
	Donor bond	8	5	6	6	6
Absorption	Water Solubility	-3.086	-3.073	-3.255	-3.392	-3.045
	Caco2 permeability	-0.26	0.368	0.281	0.391	0.314
	Intestinal absorption	6.574	71.983	78.598	66.907	70.84
	Skin permeability	-2.735	-2.735	-2.735	-2.735	-2.735
Distribution	Fraction unbound	0.39	0.173	0	0.067	0.1
	BBB permeability	-0.692	-1.925	-1.883	-1.826	-2.184
	CNS permeability	-4.368	-4.195	-4.31	-4.052	-4.351
Metabolism	CYP2D6 substrate	No	No	No	No	No
	CYP2D6 inhibitor	No	No	No	No	No
Excretion	Total Clearance	1.094	1.274	-0.392	-0.13	-0.466
Toxicity	AMES toxicity	No	No	No	No	No
	Hepatotoxicity	Yes	Yes	No	No	No
	Skin sensitization	No	No	No	No	No

B.) Comparison of physiochemical and ADMET properties of the peptide (p-KGYY), peptidomimetics and their derivative

5.5.6. Molecular Dynamic simulation

The peptide as well as peptidomimetic derivative compounds demonstrate pronounced structural stability and coherent binding to the CD40 receptor, as revealed by the 200 ns molecular dynamics simulations. In comparison to the native CD40R–CD40L complex (RMSD: 0.451 ± 0.103 nm; Rg: 2.276 ± 0.057 nm; SASA: 91.83 ± 2.04 nm^2), the designed derivatives consistently exhibit lower backbone deviations (RMSD: 0.312–0.348 nm), reflecting reduced conformational drift and enhanced stability of the receptor–ligand interface (**Figure S5.2-S5.5 and Table S5.3**). The radius of gyration values remained tightly clustered (2.14–2.22 nm), indicating that the global compactness of the receptor is preserved across all systems, while solvent-accessible surface area values (86.78–89.71 nm^2) are reduced relative to the native ligand, suggesting a more restrained solvent exposure and stabilized packing of the protein surface **(Figure S5.2-S5.5 and Table S5.3).** Residue-level RMSF analysis further supports this stabilization, with fluctuations across the CD40 backbone remaining below 0.4 nm and consistently lower than those observed in the apo state, highlighting dampened local flexibility and reduced dynamic perturbations at critical binding regions. Taken together, these quantitative metrics provide strong evidence that the peptidomimetic derivatives engage CD40 with superior structural stability and dynamic control compared to its natural ligand, thereby reinforcing their mechanistic potential as rationally designed inhibitors with therapeutic relevance.

5.6. Discussion

Computer-aided drug design approaches are powerful tools for drug discovery. In this study, we used these tools for *in silico* design of inhibitory peptides that could potentially disrupt the interaction between the CD40 receptor and CD40 ligand. The CD40-CD40L complex formation is implicated in the pathogenesis of atherosclerosis [9]. The CD40-CD40L interaction is critical during the rolling and adhesion of CD40 bearing monocytes on the CD40L positive endothelium, promoting monocytes extravasation and then transformation to macrophages that may later become foam cells after engulfing oxidized LDL [10]. Macrophage accumulation in plaques causes atherosclerosis progression [50]. Mechanistically, interaction of CD40 with the CD40L triggers the recruitment of Tumor necrosis factor receptor-associated factors (TRAFs) such as TRAF-2, -3, -5 and -6 [19]. Interaction of CD40-TRAF6 has found to play an important in plaque formation while, interaction with TRAF-2, -3 and -5 plays a minor role in the disease progression [19,51]. Indeed, targeting CD40-TRAF6 interaction by TRAF-STOP inhibitor was found to attenuate the formation of atherosclerosis plaque in *Apoe*$^{-/-}$ mice [20] . Atherosclerosis is a major CVD and a risk factor for myocardial infarction and stroke. Although lipid-lowering therapies, anti-hypertensive agents, and anti-platelets drugs are helpful in reducing the risk of CVD and save patient lives, novel alternative pharmacological tools are still needed. Thus, blocking CD40-CD40L interactions with a targeted peptide would reduce macrophage accumulation in atherosclerotic lesions, and this may lead to the regression of atherosclerosis [8]. The current study identified peptide and its peptidomimetic derivative which binds to the critical residues on the CD40 receptor involved in its interaction with the ligand and can block the receptor-ligand interaction, thus attenuating the disease progression.

5.6.1. The docking of the CD40 receptor to the CD40 ligand

The crystal structure of CD40-CD40L was downloaded from RCSB PDB (PDB 3QD6), and the monomeric chains of the CD40 receptor (Chain S) and CD40 ligand (Chain C) were studied to identify the interacting partners for each residue within the 4Å range known to characterise ionic and hydrogen bonding in protein complexes. Analyses of the 4Å residues between the complex is crucial as it dictates the involvement of critical residues involved in the interaction between the complex. We used UCSF Chimera [32] to perform this task. *In-vitro* mutational study established the critical role of residues Y82, D84, and N86 on CD40 and K143 and Y145 on CD40L in mediating the interaction within the protein-protein complex [30]. Our analysis of the 4Å interacting residues using the published crystal structure atomic coordinates also found the involvement of the same residues on the receptor as well as in the ligand, validating our computer modelling approach. We further validated our ability to identify critical residues in CD40 (Chain S) docked to CD40L (Chain C) by using PyDockWEB server [34]. PyDockWEB is a user-friendly server which allow the use of PyDOCK rigid-body protein-protein docking and scoring is performed based on electrostatics and desolvation energy [34,52]. Again, the 4Ǻ interacting residues were successfully identified in the docked structure. We found the maximum similarity of residues between the docked and the crystal structure (**Figure 5.2**), which further confirms the importance of these residues in mediating the receptor-ligand interaction.

5.6.2. The mutational analysis of CD40 and CD40L

After confirming *in silico* the importance of residues Y82, D84, and N86 on CD40 as well as K143 and Y145 residues on CD40L [30], we next aimed to perform the *in-silico* mutational analysis by replacing these critical residues with alanine which can impede the binding within the CD40-CD40L complex, resulting in the decrease in the binding affinity of CD40L to CD40. Replacement of critical residues using site-directed mutagenesis can help in deciphering the importance of that residue(s) in

the interaction with the ligand. Alanine is the most common residue used as it is a simpler amino acid. Our result indeed indicated a decrease in the binding affinity of the receptor with the ligand in individually mutated complexes. The binding affinity was further decreased when the combined all three mutations were done in the CD40 receptor binding domain, further confirming the importance of these residues in the interaction with CD40L (**Figure 5.4**). Vice versa, the replacement with alanine of the residues K143 and Y145 in the CD40L binding domain, individually or combined also resulted in a decrease in the binding affinity of the mutated CD40L to CD40 with a maximum decrease found when both residues were mutated simultaneously (**Figure 5.5**). These results again confirmed the importance of the CD40L binding site residues for the interaction of the receptor and ligand, targeting which can help in the inhibition of the interaction between these two proteins.

5.6.3. Designing the blocking peptide and its docking to CD40

CD40L is important for the interaction of the immune cells and the platelets. Various cells involved in the plaque pathogenesis expresses CD40L on their surfaces[11]. CD40L expression by cells such as T-cells and platelets plays an important role in their activation and disease progression [12] . Also, CD40L present on the platelets plays a major role in the stabilization of thrombus [53]. Notably, monoclonal antibody against CD40L has shown adverse side effects, such as thromboembolic events in humans and primates [54,55]. Therefore, in our study, we used the CD40 receptor as a therapeutic target. Another study has also targeted the CD40 receptor in atherosclerosis and found positive results in limiting the disease progression [19]. Thus, a therapeutic peptide was designed against the CD40 receptor to limit its interaction with CD40L. Designing a therapeutic peptide is a well-known strategy to limit the protein-protein interaction (PPI) [56]. Due to large and shallow interfaces of PPIs and the lack of binding pockets, PPIs is mostly regarded “undruggable” by small molecule inhibitors, while peptides designed against the critical residues involved in PPI serves as a good

antagonist which can limit their interaction [57,58]. Our peptides mimic the residues in the binding site of CD40, thus limiting the binding affinity of CD40L to CD40. Also, the usage of peptides as a therapeutics has several advantages over proteins or antibodies, such as low cost, lower toxicity, lower accumulation in tissues, high biological and chemical diversity, and high potency [59].

To identify the similarity of the involved residues between the docked structure of receptor-peptide complex and the crystal structure, the 4Å interacting residues between the docked CD40 receptor-peptide (pKGYY) complex were analysed and compared with the interacting residues in the crystal structure. We found similarity in some of the interacting residues between the CD40 receptor-peptide (pKGYY) and the crystal structure of CD40-CD40L (**Figure 5.6**). This result suggested that the peptide was interacting at the interface site of the receptor known for its interaction with the ligand and thus can limit the interaction of the receptor with the ligand. Therapeutic peptides have been successfully used as an antagonist for various cell-surface receptors [60]. Although Y82 and D84 interacted with the p-KGYY, N86 was not involved in the interaction. To analyse the ADMET properties of the peptide, we used pkCSM server [37]. pkCSM relies on the distance-based graph signature of the molecule to predict the pharmacokinetic and toxicity profiles. Many others studies have also reported the use of pkCSM for predicting the pharmacokinetics and toxicity profile of the molecule(s) [61–65]. For ADMET analysis, following parameters where chosen. In absorption parameter, water solubility, CaCo2 permeability, intestinal absorption and skin permeability were considered. Water solubility reflects the solubility of the molecule in the water at 25° C. Higher the negative value, better the solubility. CaCo2 permeability is used as an in-vitro model of human intestinal mucosa to predict the absorption of orally administered drugs. $LogP_{app}$ greater than 0.9 suggest high CaCo2 permeability. Intestinal absorption predicts the percentage of compound absorbed through human intestine. Compound with value less than 30% considered poorly absorbed. Skin permeability predicts whether given compound is skin

permeable for transdermal delivery. logKp > 2.5 considered low skin permeable. In distribution parameter, fraction unbound, blood-brain barrier (BBB) permeability and central nervous system (CNS) permeability were considered. Fraction unbound predicts the fraction of the drug free from binding with the serum proteins. More the binding with the serum proteins, less efficiently it can diffuse. It predicts the value on scale of 0-1. BBB permeability is the ability of compound to cross the blood-brain barrier. logBB value above 0.3 is considered readily crossable, while value below -1 suggest poor distribution in brain. logPS value > -2 considered penetrable for CNS permeability while logPS < -3 considered impenetrable. In metabolism parameter, substrate and inhibitor for isoform of cytochrome P450 (CYP450) and total clearance were considered. Cytochrome P450 is a detoxifying enzyme in the liver which deactivates the drug. Cytochrome P450 substrate suggest whether the compound is substrate for CYP450 isoforms CYP2D6 and CYP3A4 for effective clearance. Cytochrome P450 inhibitor predicts whether compounds act as an inhibitor for isoforms of CYP450. Total clearance predicts the bioavailability of the drug and to suggest the dosing rates to achieve steady-state concentration. It combines hepatic and renal clearance. Positive value corresponds to high clearance. In toxicity parameter, ames toxicity, hepatotoxicity and skin sensitization were considered. Ames Toxicity indicates the mutagenic potential of the compound. Positive value suggest compound is mutagenic and potential carcinogenic. Hepatotoxicity predicts whether the compound likely to associate with the disrupted normal functioning of the liver. Skin sensitization predicts whether the compound induce allergic contact dermatitis when encountered by skin. *In silico* physicochemical and ADMET analyses of the peptide revealed hepatotoxicity to be positive (**Table S5.1**). Hepatoxicity/ Drug-induced liver injury (DILI) is one of the most frequent cause for the termination of drug development programs [66]. Therefore, we further focused on the modifications of the parent peptide to improve its ADMET properties.

5.6.4. Peptidomimetic as a therapeutic strategy against CD40

There are several limitations associated with the natural peptides which limit their use, such as low oral bioavailability, short half-life, rapid clearance, and low metabolic stability, among others [23]. We found that our designed peptide was not interacting with all the three critical residues in CD40 as well as the ADMET analysis predicted positive hepatotoxicity of the peptide. To address these drawbacks, peptidomimetics were used as a therapeutic option. Peptidomimetic has been sought as an improved therapeutic option compared to the peptide. Peptidomimetics mimics the original structure of the peptide with increased stability, improved target specificity, and good membrane permeability due to the addition of unnatural amino acids, backbone amide modification, and/or the addition of hydrophobic residues [24,67]. Several reports had found improved outcomes when peptidomimetics were used as a therapeutic option [68–71]. Peptidomimetics utilizes 3D conformations and pharmacophoric properties of the input peptide to provide resultant peptidomimetic structures present in the database. We used peptidomimetic server pep:MMs:MIMIC (http://mms.dsfarm.unipd.it/pepMMsMIMIC/) [38] to find the best peptidomimetic structures in the database. The resultant molecules were docked to CD40 in AutoDock Vina (v1.2.0) [40] and Glide module of the Schrodinger suite [42]. After analysing the top 200 molecules, one molecule (MMs01727545) was found to be interacting with all three critical residues (Y82, D84, and N86) along with the good dock score in both platforms (**Figure 5.7**). Further, physicochemical and ADMET properties of the compound were analysed in pkCSM server. The peptidomimetic MMs01727545 still showed positive hepatotoxicity (**Table S5.2**). Therefore, we resorted to identifying the derivatives of MMs01727545 which would preserve its backbone elements with slight modification in the side chains, that can increase the binding affinity of it to the receptor and may reduce the molecule hepatotoxicity.

We used PubChem server (https://pubchem.ncbi.nlm.nih.gov/) for conducting the similarity search of the parent peptidomimetic molecule using 3D conformers by uploading SMILES ID of the peptidomimetic structure (MMs01727545). This resulted in the identification of 1000 structurally identical molecules from the database. After docking these molecules using AutoDock Vina (v1.2.0) [41] and Schrodinger, we were able to narrow the number of hits to three molecules (PubChem ID 121356761, 146599825, and 126700407). These three modified peptidomimetics interacted with all three critical residues of CD40 in both docking platforms (**Figure 5.8**). Interestingly, analysis of the ADMET properties of these molecules predicted no hepatotoxicity in pkCSM server (**Table 5.1).** In conclusion, our similarity search for the better modified peptidomimetics led us to the three best derivatives that were found to be interacting with the critical residues on CD40 receptor (Y82, D84, and N86) with higher binding affinity compared to the original peptidomimetic structure and had better physicochemical and ADMET properties compared to its counterpart (**Table 5.1**). Thus, we successfully identified peptidomimetics inhibitors capable of blocking the interaction between CD40 and CD40L. Such peptidomimetic inhibitors may potentially be useful for treating various autoimmune diseases such as atherosclerosis where CD40-40L interaction plays an important role in the progression of the disease.

5.6.5. Molecular Dynamic simulation of CD40-peptide and peptidomimetics derivatives

Molecular dynamics simulation was carried out for period of 200ns for all the apo and complex systems. The MD results were evaluated to understand the conformational changes and structural deviations. For the analysis of macromolecular structures and their dynamic changes, the root-mean-square deviation (RMSD) stands out as a widely accepted measure of similarity. This examination helps us assess whether the simulation has reached a state of equilibrium and there were minimal disturbances towards the end of the simulation. It determines the change in selection of atom from a particular frame with respect to the reference

frame. Compared to the CD40-40L complex, the peptide as well as the peptidomimetic derivatives showed better stability metrics suggesting that the peptide as well as peptidomimetic derivatives were having stable interaction with the receptor.

RMSF measures the variation or fluctuation in the positions of atoms over the course of an MD simulation. High RMSF values at specific regions of the molecule indicate that those areas are highly flexible and undergo significant fluctuations during the simulation. Conversely, low RMSF values suggest rigidity or minimal atomic movements. There was no significant difference observed in the RMSF values of the receptor with the peptide and peptidomimetics compared to CD40L. This suggests that the residue-wise fluctuations were not significant in all the complexes.

Radius of gyration plot indicates the compactness of the protein. Smaller Rg values indicate a more compact and tightly folded structure, while larger Rg values suggest a more extended and less compact structure [72] . There was no significant difference observed in the Rg values of the receptor with the peptide and peptidomimetics compared to CD40L. This suggests the compactness of all the receptor-ligand complex.

SASA, or solvent-accessible surface area, comes in handy during molecular dynamics (MD) simulations. It acts as our guide to discerning how much of a molecule's surface is available for interaction with the surrounding solvent molecules, offering valuable insights into the molecule's overall structure and behaviour. High SASA values imply that a larger portion of the molecule's surface is exposed to solvent, suggesting greater flexibility and conformational changes while low SASA values suggest that the molecule is more compact and buried within its own structure or is shielded from solvent molecules [73]. Monitoring SASA can help identify conformational changes in proteins. Increased SASA may indicate the opening of a protein's binding pocket, while decreased SASA can signal pocket closure. It was found that the

SASA values were slightly better for peptide and peptidomimetics derivatives compared to CD40-40L complex.

5.7. Conclusion

The current study identified three compounds that can bind to the critical residues on the CD40 receptor and can potentially inhibit the interaction of CD40 and CD40L. The compounds possess good physicochemical and ADMET properties with higher binding affinity compared to the parent compound. Interaction of CD40 and CD40L is implicated in atherosclerosis progression. Based on the molecular dynamics analysis, the CD40-peptide complex is relatively stable than the CD40-CD40L complex based on RMSD, RMSF, radius of gyration, SASA, and H-bonds. Therefore, the designed molecule may potentially help reduce atherosclerosis. Although this *in-silico* study has its limitations, *in-vitro* testing of these compounds should be done to validate the computational findings.

5.8. Bibliography

[1] A.J. Lusis, Atherosclerosis, Nature 407 (2000) 233–241. https://doi.org/10.1038/35025203.

[2] A. Peikert, K. Kaier, J. Merz, L. Manhart, I. Schäfer, I. Hilgendorf, P. Hehn, D. Wolf, F. Willecke, X. Sheng, A. Clemens, M. Zehender, C. Von Zur Mühlen, C. Bode, A. Zirlik, P. Stachon, Residual inflammatory risk in coronary heart disease: incidence of elevated high-sensitive CRP in a real-world cohort, Clin Res Cardiol 109 (2020) 315–323. https://doi.org/10.1007/s00392-019-01511-0.

[3] A.W. Aday, P.M. Ridker, Targeting Residual Inflammatory Risk: A Shifting Paradigm for Atherosclerotic Disease, Front. Cardiovasc. Med. 6 (2019) 16. https://doi.org/10.3389/fcvm.2019.00016.

[4] P.M. Ridker, B.M. Everett, A. Pradhan, J.G. MacFadyen, D.H. Solomon, E. Zaharris, V. Mam, A. Hasan, Y. Rosenberg, E. Iturriaga, M. Gupta, M. Tsigoulis, S. Verma, M. Clearfield, P. Libby, S.Z. Goldhaber, R. Seagle, C. Ofori, M. Saklayen, S. Butman, N. Singh, M. Le May, O. Bertrand, J. Johnston, N.P. Paynter, R.J. Glynn, Low-Dose Methotrexate for the Prevention of Atherosclerotic Events, N Engl J Med 380 (2019) 752–762. https://doi.org/10.1056/NEJMoa1809798.

[5] J.-C. Tardif, S. Kouz, D.D. Waters, O.F. Bertrand, R. Diaz, A.P. Maggioni, F.J. Pinto, R. Ibrahim, H. Gamra, G.S. Kiwan, C. Berry, J. López-Sendón, P. Ostadal, W. Koenig, D. Angoulvant, J.C. Grégoire, M.-A. Lavoie, M.-P. Dubé, D. Rhainds, M. Provencher, L. Blondeau, A. Orfanos, P.L. L'Allier, M.-C. Guertin, F. Roubille, Efficacy and Safety of Low-Dose Colchicine after Myocardial Infarction, N Engl J Med 381 (2019) 2497–2505. https://doi.org/10.1056/NEJMoa1912388.

[6] P.M. Ridker, B.M. Everett, T. Thuren, J.G. MacFadyen, W.H. Chang, C. Ballantyne, F. Fonseca, J. Nicolau, W. Koenig, S.D. Anker, J.J.P. Kastelein, J.H. Cornel, P. Pais, D. Pella, J. Genest, R. Cifkova, A. Lorenzatti, T. Forster, Z. Kobalava, L. Vida-Simiti, M. Flather, H.

Shimokawa, H. Ogawa, M. Dellborg, P.R.F. Rossi, R.P.T. Troquay, P. Libby, R.J. Glynn, Antiinflammatory Therapy with Canakinumab for Atherosclerotic Disease, N Engl J Med 377 (2017) 1119–1131. https://doi.org/10.1056/NEJMoa1707914.

[7] P.J.H. Kusters, E. Lutgens, T.T.P. Seijkens, Exploring immune checkpoints as potential therapeutic targets in atherosclerosis, Cardiovascular Research 114 (2018) 368–377. https://doi.org/10.1093/cvr/cvx248.

[8] L.A. Bosmans, L. Bosch, P.J.H. Kusters, E. Lutgens, T.T.P. Seijkens, The CD40-CD40L Dyad as Immunotherapeutic Target in Cardiovascular Disease, J. of Cardiovasc. Trans. Res. 14 (2021) 13–22. https://doi.org/10.1007/s12265-020-09994-3.

[9] M. Lacy, C. Bürger, A. Shami, M. Ahmadsei, H. Winkels, K. Nitz, C.M. Van Tiel, T.T.P. Seijkens, P.J.H. Kusters, E. Karshovka, K.H.M. Prange, Y. Wu, S.L.N. Brouns, S. Unterlugauer, M.J.E. Kuijpers, M.E. Reiche, S. Steffens, A. Edsfeldt, R.T.A. Megens, J.W.M. Heemskerk, I. Goncalves, C. Weber, N. Gerdes, D. Atzler, E. Lutgens, Cell-specific and divergent roles of the CD40L-CD40 axis in atherosclerotic vascular disease, Nat Commun 12 (2021) 3754. https://doi.org/10.1038/s41467-021-23909-z.

[10] E. Lutgens, D. Lievens, L. Beckers, M. Donners, M. Daemen, CD40 and Its Ligand in Atherosclerosis, Trends in Cardiovascular Medicine 17 (2007) 118–123. https://doi.org/10.1016/j.tcm.2007.02.004.

[11] F. Mach, U. Schönbeck, G.K. Sukhova, T. Bourcier, J.-Y. Bonnefoy, J.S. Pober, P. Libby, Functional CD40 ligand is expressed on human vascular endothelial cells, smooth muscle cells, and macrophages: Implications for CD40–CD40 ligand signaling in atherosclerosis, Proc. Natl. Acad. Sci. U.S.A. 94 (1997) 1931–1936. https://doi.org/10.1073/pnas.94.5.1931.

[12] N.A. Michel, A. Zirlik, D. Wolf, CD40L and Its Receptors in Atherothrombosis—An Update, Front. Cardiovasc. Med. 4 (2017) 40. https://doi.org/10.3389/fcvm.2017.00040.

[13] S.A. Quezada, L.Z. Jarvinen, E.F. Lind, R.J. Noelle, CD40/CD154 Interactions at the Interface of Tolerance and Immunity, Annu. Rev. Immunol. 22 (2004) 307–328. https://doi.org/10.1146/annurev.immunol.22.012703.104533.

[14] K. Kotowicz, G.L.J. Dixon, N.J. Klein, M.J. Peters, R.E. Callard, Biological function of CD40 on human endothelial cells: costimulation with CD40 ligand and interleukin-4 selectively induces expression of vascular cell adhesion molecule-1 and P-selectin resulting in preferential adhesion of lymphocytes, Immunology 100 (2000) 441–448. https://doi.org/10.1046/j.1365-2567.2000.00061.x.

[15] A. Roy, U. Saqib, M.S. Baig, NOS1-mediated macrophage and endothelial cell interaction in the progression of atherosclerosis, Cell Biology International 45 (2021) 1191–1201. https://doi.org/10.1002/cbin.11558.

[16] E. Lutgens, K.B.J.M. Cleutjens, S. Heeneman, V.E. Koteliansky, L.C. Burkly, M.J.A.P. Daemen, Both early and delayed anti-CD40L antibody treatment induces a stable plaque phenotype, Proc. Natl. Acad. Sci. U.S.A. 97 (2000) 7464–7469. https://doi.org/10.1073/pnas.97.13.7464.

[17] D. Engel, T. Seijkens, M. Poggi, M. Sanati, L. Thevissen, L. Beckers, E. Wijnands, D. Lievens, E. Lutgens, The immunobiology of CD154–CD40–TRAF interactions in atherosclerosis, Seminars in Immunology 21 (2009) 308–312. https://doi.org/10.1016/j.smim.2009.06.004.

[18] U. Schönbeck, F. Mach, G.K. Sukhova, M. Herman, P. Graber, M.R. Kehry, P. Libby, CD40 Ligation Induces Tissue Factor Expression in Human Vascular Smooth Muscle Cells, The American Journal of

Pathology 156 (2000) 7–14. https://doi.org/10.1016/S0002-9440(10)64699-8.

[19] E. Lutgens, D. Lievens, L. Beckers, E. Wijnands, O. Soehnlein, A. Zernecke, T. Seijkens, D. Engel, J. Cleutjens, A.M. Keller, S.H. Naik, L. Boon, H.A. Oufella, Z. Mallat, C.L. Ahonen, R.J. Noelle, M.P. De Winther, M.J. Daemen, E.A. Biessen, C. Weber, Deficient CD40-TRAF6 signaling in leukocytes prevents atherosclerosis by skewing the immune response toward an antiinflammatory profile, Journal of Experimental Medicine 207 (2010) 391–404. https://doi.org/10.1084/jem.20091293.

[20] T.T.P. Seijkens, C.M. Van Tiel, P.J.H. Kusters, D. Atzler, O. Soehnlein, B. Zarzycka, S.A.B.M. Aarts, M. Lameijer, M.J. Gijbels, L. Beckers, M. Den Toom, B. Slütter, J. Kuiper, J. Duchene, M. Aslani, R.T.A. Megens, C. Van 'T Veer, G. Kooij, R. Schrijver, M.A. Hoeksema, L. Boon, F. Fay, J. Tang, S. Baxter, A. Jongejan, P.D. Moerland, G. Vriend, B. Bleijlevens, E.A. Fisher, R. Duivenvoorden, N. Gerdes, M.P.J. De Winther, G.A. Nicolaes, W.J.M. Mulder, C. Weber, E. Lutgens, Targeting CD40-Induced TRAF6 Signaling in Macrophages Reduces Atherosclerosis, Journal of the American College of Cardiology 71 (2018) 527–542. https://doi.org/10.1016/j.jacc.2017.11.055.

[21] M. Croft, C.A. Benedict, C.F. Ware, Clinical targeting of the TNF and TNFR superfamilies, Nat Rev Drug Discov 12 (2013) 147–168. https://doi.org/10.1038/nrd3930.

[22] B. Leader, Q.J. Baca, D.E. Golan, Protein therapeutics: a summary and pharmacological classification, Nat Rev Drug Discov 7 (2008) 21–39. https://doi.org/10.1038/nrd2399.

[23] C. Recio, F. Maione, A.J. Iqbal, N. Mascolo, V. De Feo, The Potential Therapeutic Application of Peptides and Peptidomimetics in Cardiovascular Disease, Front. Pharmacol. 7 (2017). https://doi.org/10.3389/fphar.2016.00526.

[24] J. Vagner, H. Qu, V.J. Hruby, Peptidomimetics, a synthetic tool of drug discovery, Current Opinion in Chemical Biology 12 (2008) 292–296. https://doi.org/10.1016/j.cbpa.2008.03.009.

[25] P.J. Seo, S.-Y. Hong, S.-G. Kim, C.-M. Park, Competitive inhibition of transcription factors by small interfering peptides, Trends in Plant Science 16 (2011) 541–549. https://doi.org/10.1016/j.tplants.2011.06.001.

[26] Z. Antosova, M. Mackova, V. Kral, T. Macek, Therapeutic application of peptides and proteins: parenteral forever?, Trends in Biotechnology 27 (2009) 628–635. https://doi.org/10.1016/j.tibtech.2009.07.009.

[27] J. Audie, C. Boyd, The Synergistic Use of Computation, Chemistry and Biology to Discover Novel Peptide-Based Drugs: The Time is Right, CPD 16 (2010) 567–582. https://doi.org/10.2174/138161210790361425.

[28] P. Timmerman, J. Beld, W.C. Puijk, R.H. Meloen, Rapid and Quantitative Cyclization of Multiple Peptide Loops onto Synthetic Scaffolds for Structural Mimicry of Protein Surfaces, ChemBioChem 6 (2005) 821–824. https://doi.org/10.1002/cbic.200400374.

[29] G. Li Petri, S. Di Martino, M. De Rosa, Peptidomimetics: An Overview of Recent Medicinal Chemistry Efforts toward the Discovery of Novel Small Molecule Inhibitors, J. Med. Chem. 65 (2022) 7438–7475. https://doi.org/10.1021/acs.jmedchem.2c00123.

[30] J. Bajorath, N.J. Chalupny, J.S. Marken, A.W. Siadak, J. Skonier, M. Gordon, D. Hollenbaugh, R.J. Noelle, H.D. Ochs, A. Aruffo, Identification of Residues on CD40 and Its Ligand Which Are Critical for the Receptor-Ligand Interaction, Biochemistry 34 (1995) 1833–1844. https://doi.org/10.1021/bi00006a003.

[31] H.-J. An, Y.J. Kim, D.H. Song, B.S. Park, H.M. Kim, J.D. Lee, S.-G. Paik, J.-O. Lee, H. Lee, Crystallographic and Mutational Analysis of the CD40-CD154 Complex and Its Implications for Receptor

Activation, Journal of Biological Chemistry 286 (2011) 11226–11235. https://doi.org/10.1074/jbc.M110.208215.

[32] E.F. Pettersen, T.D. Goddard, C.C. Huang, G.S. Couch, D.M. Greenblatt, E.C. Meng, T.E. Ferrin, UCSF Chimera—A visualization system for exploratory research and analysis, J Comput Chem 25 (2004) 1605–1612. https://doi.org/10.1002/jcc.20084.

[33] J.A. Maier, C. Martinez, K. Kasavajhala, L. Wickstrom, K.E. Hauser, C. Simmerling, ff14SB: Improving the Accuracy of Protein Side Chain and Backbone Parameters from ff99SB, J. Chem. Theory Comput. 11 (2015) 3696–3713. https://doi.org/10.1021/acs.jctc.5b00255.

[34] B. Jiménez-García, C. Pons, J. Fernández-Recio, pyDockWEB: a web server for rigid-body protein–protein docking using electrostatics and desolvation scoring, Bioinformatics 29 (2013) 1698–1699. https://doi.org/10.1093/bioinformatics/btt262.

[35] Y. Yan, H. Tao, J. He, S.-Y. Huang, The HDOCK server for integrated protein–protein docking, Nat Protoc 15 (2020) 1829–1852. https://doi.org/10.1038/s41596-020-0312-x.

[36] B.G. Pierce, K. Wiehe, H. Hwang, B.-H. Kim, T. Vreven, Z. Weng, ZDOCK server: interactive docking prediction of protein–protein complexes and symmetric multimers, Bioinformatics 30 (2014) 1771–1773. https://doi.org/10.1093/bioinformatics/btu097.

[37] D.E.V. Pires, T.L. Blundell, D.B. Ascher, pkCSM: Predicting Small-Molecule Pharmacokinetic and Toxicity Properties Using Graph-Based Signatures, J. Med. Chem. 58 (2015) 4066–4072. https://doi.org/10.1021/acs.jmedchem.5b00104.

[38] M. Floris, J. Masciocchi, M. Fanton, S. Moro, Swimming into peptidomimetic chemical space using pepMMsMIMIC, Nucleic Acids Research 39 (2011) W261–W269. https://doi.org/10.1093/nar/gkr287.

[39] J. Masciocchi, G. Frau, M. Fanton, M. Sturlese, M. Floris, L. Pireddu, P. Palla, F. Cedrati, P. Rodriguez-Tomé, S. Moro, MMsINC: a large-scale chemoinformatics database, Nucleic Acids Research 37 (2009) D284–D290. https://doi.org/10.1093/nar/gkn727.

[40] J. Eberhardt, D. Santos-Martins, A.F. Tillack, S. Forli, AutoDock Vina 1.2.0: New Docking Methods, Expanded Force Field, and Python Bindings, J. Chem. Inf. Model. 61 (2021) 3891–3898. https://doi.org/10.1021/acs.jcim.1c00203.

[41] O. Trott, A.J. Olson, AutoDock Vina: Improving the speed and accuracy of docking with a new scoring function, efficient optimization, and multithreading, J Comput Chem 31 (2010) 455–461. https://doi.org/10.1002/jcc.21334.

[42] R.A. Friesner, J.L. Banks, R.B. Murphy, T.A. Halgren, J.J. Klicic, D.T. Mainz, M.P. Repasky, E.H. Knoll, M. Shelley, J.K. Perry, D.E. Shaw, P. Francis, P.S. Shenkin, Glide: A New Approach for Rapid, Accurate Docking and Scoring. 1. Method and Assessment of Docking Accuracy, J. Med. Chem. 47 (2004) 1739–1749. https://doi.org/10.1021/jm0306430.

[43] G.M. Morris, R. Huey, W. Lindstrom, M.F. Sanner, R.K. Belew, D.S. Goodsell, A.J. Olson, AutoDock4 and AutoDockTools4: Automated docking with selective receptor flexibility, J Comput Chem 30 (2009) 2785–2791. https://doi.org/10.1002/jcc.21256.

[44] G. Madhavi Sastry, M. Adzhigirey, T. Day, R. Annabhimoju, W. Sherman, Protein and ligand preparation: parameters, protocols, and influence on virtual screening enrichments, J Comput Aided Mol Des 27 (2013) 221–234. https://doi.org/10.1007/s10822-013-9644-8.

[45] M.H.M. Olsson, C.R. Søndergaard, M. Rostkowski, J.H. Jensen, PROPKA3: Consistent Treatment of Internal and Surface Residues in Empirical p K_a Predictions, J. Chem. Theory Comput. 7 (2011) 525–537. https://doi.org/10.1021/ct100578z.

[46] C. Lu, C. Wu, D. Ghoreishi, W. Chen, L. Wang, W. Damm, G.A. Ross, M.K. Dahlgren, E. Russell, C.D. Von Bargen, R. Abel, R.A. Friesner, E.D. Harder, OPLS4: Improving Force Field Accuracy on Challenging Regimes of Chemical Space, J. Chem. Theory Comput. 17 (2021) 4291–4300. https://doi.org/10.1021/acs.jctc.1c00302.

[47] N.M. O'Boyle, M. Banck, C.A. James, C. Morley, T. Vandermeersch, G.R. Hutchison, Open Babel: An open chemical toolbox, J Cheminform 3 (2011) 33. https://doi.org/10.1186/1758-2946-3-33.

[48] M.J. Abraham, T. Murtola, R. Schulz, S. Páll, J.C. Smith, B. Hess, E. Lindahl, GROMACS: High performance molecular simulations through multi-level parallelism from laptops to supercomputers, SoftwareX 1–2 (2015) 19–25. https://doi.org/10.1016/j.softx.2015.06.001.

[49] K. Lindorff-Larsen, S. Piana, K. Palmo, P. Maragakis, J.L. Klepeis, R.O. Dror, D.E. Shaw, Improved side-chain torsion potentials for the Amber ff99SB protein force field, Proteins 78 (2010) 1950–1958. https://doi.org/10.1002/prot.22711.

[50] K.J. Moore, F.J. Sheedy, E.A. Fisher, Macrophages in atherosclerosis: a dynamic balance, Nat Rev Immunol 13 (2013) 709–721. https://doi.org/10.1038/nri3520.

[51] M.M.P.C. Donners, L. Beckers, D. Lievens, I. Munnix, J. Heemskerk, B.J. Janssen, E. Wijnands, J. Cleutjens, A. Zernecke, C. Weber, C.L. Ahonen, U. Benbow, A.C. Newby, R.J. Noelle, M.J.A.P. Daemen, E. Lutgens, The CD40-TRAF6 axis is the key regulator of the CD40/CD40L system in neointima formation and arterial remodeling, Blood 111 (2008) 4596–4604. https://doi.org/10.1182/blood-2007-05-088906.

[52] T.M. Cheng, T.L. Blundell, J. Fernandez-Recio, pyDock: Electrostatics and desolvation for effective scoring of rigid-body

protein–protein docking, Proteins 68 (2007) 503–515. https://doi.org/10.1002/prot.21419.

[53] P. André, K.S.S. Prasad, C.V. Denis, M. He, J.M. Papalia, R.O. Hynes, D.R. Phillips, D.D. Wagner, CD40L stabilizes arterial thrombi by a β3 integrin–dependent mechanism, Nat Med 8 (2002) 247–252. https://doi.org/10.1038/nm0302-247.

[54] D.T. Boumpas, R. Furie, S. Manzi, G.G. Illei, D.J. Wallace, J.E. Balow, A. Vaishnaw, on behalf of the BG9588 Lupus Nephritis Trial Group, A short course of BG9588 (anti–CD40 ligand antibody) improves serologic activity and decreases hematuria in patients with proliferative lupus glomerulonephritis, Arthritis & Rheumatism 48 (2003) 719–727. https://doi.org/10.1002/art.10856.

[55] T. Kawai, D. Andrews, R.B. Colvin, D.H. Sachs, A.B. Cosimi, Thromboembolic complications after treatment with monoclonal antibody against CD40 ligand, Nat Med 6 (2000) 114–114. https://doi.org/10.1038/72162.

[56] L.J. Draeger, G.P. Mullen, Interaction of the bHLH-zip domain of c-Myc with H1-type peptides. Characterization of helicity in the H1 peptides by NMR, J Biol Chem 269 (1994) 1785–1793.

[57] X. Wang, D. Ni, Y. Liu, S. Lu, Rational Design of Peptide-Based Inhibitors Disrupting Protein-Protein Interactions, Front. Chem. 9 (2021) 682675. https://doi.org/10.3389/fchem.2021.682675.

[58] L. Sillerud, R. Larson, Design and Structure of Peptide and Peptidomimetic Antagonists of Protein- Protein Interaction, CPPS 6 (2005) 151–169. https://doi.org/10.2174/1389203053545462.

[59] J. Thundimadathil, Cancer Treatment Using Peptides: Current Therapies and Future Prospects, Journal of Amino Acids 2012 (2012) 1–13. https://doi.org/10.1155/2012/967347.

[60] L. Wang, N. Wang, W. Zhang, X. Cheng, Z. Yan, G. Shao, X. Wang, R. Wang, C. Fu, Therapeutic peptides: current applications and

future directions, Sig Transduct Target Ther 7 (2022) 48. https://doi.org/10.1038/s41392-022-00904-4.

[61] H.M. Abd El-Lateef, A.A. Elmaaty, L.M.A. Abdel Ghany, M.S. Abdel-Aziz, I. Zaki, N. Ryad, Design and Synthesis of 2-(4-Bromophenyl)Quinoline-4-Carbohydrazide Derivatives *via* Molecular Hybridization as Novel Microbial DNA-Gyrase Inhibitors, ACS Omega 8 (2023) 17948–17965. https://doi.org/10.1021/acsomega.3c01156.

[62] A.R. Das Neves, D.B. Carvalho, F. Silva, R.F. Rosalem, B.I. Pelizaro, P.F. Castilho, K.M.P. Oliveira, N.S. Cassemiro, L.R. Pessatto, E.J. Paredes-Gamero, E.M. Piranda, D.B. Silva, C.C.P. Arruda, A.C.M. Baroni, In Vivo Antileishmanial Effect of 3,5-Diaryl-isoxazole Analogues Based on Veraguensin, Grandisin, and Machilin G: A Glance at a Preclinical Study, ACS Infect. Dis. 9 (2023) 1150–1159. https://doi.org/10.1021/acsinfecdis.3c00090.

[63] N. Georgiou, E. Chontzopoulou, A. Cheilari, A. Katsogiannou, D. Karta, K. Vavougyiou, D. Hadjipavlou-Litina, U. Javornik, J. Plavec, D. Tzeli, S. Vassiliou, T. Mavromoustakos, Thiocarbohydrazone and Chalcone-Derived 3,4-Dihydropyrimidinethione as Lipid Peroxidation and Soybean Lipoxygenase Inhibitors, ACS Omega 8 (2023) 11966–11977. https://doi.org/10.1021/acsomega.2c07625.

[64] N. Khamto, K. Utama, S. Tateing, P. Sangthong, P. Rithchumpon, N. Cheechana, A. Saiai, N. Semakul, W. Punyodom, P. Meepowpan, Discovery of Natural Bisbenzylisoquinoline Analogs from the Library of Thai Traditional Plants as SARS-CoV-2 $3CL^{Pro}$ Inhibitors: *In Silico* Molecular Docking, Molecular Dynamics, and *In Vitro* Enzymatic Activity, J. Chem. Inf. Model. 63 (2023) 2104–2121. https://doi.org/10.1021/acs.jcim.2c01309.

[65] M.H. Presa, M.J.D. Rocha, C.S. Pires, K.N.B. Ledebuhr, G.P.D. Costa, D. Alves, C.F. Bortolatto, C.A. Brüning, Antidepressant-like Effect of 1-(2-(4-(4-Ethylphenyl)-1 *H* -1,2,3-triazol-1-yl)phenyl)ethan-1-one in Mice: Evidence of the Contribution of the Serotonergic System,

ACS Chem. Neurosci. 14 (2023) 2333–2346. https://doi.org/10.1021/acschemneuro.3c00108.

[66] S. David, J.P. Hamilton, Drug-induced Liver Injury, US Gastroenterol Hepatol Rev 6 (2010) 73–80.

[67] L. Gentilucci, A. Tolomelli, F. Squassabia, Peptides and Peptidomimetics in Medicine, Surgery and Biotechnology, CMC 13 (2006) 2449–2466. https://doi.org/10.2174/092986706777935041.

[68] C.M.I. Ahmed, J. Larkin, H.M. Johnson, SOCS1 Mimetics and Antagonists: A Complementary Approach to Positive and Negative Regulation of Immune Function, Front. Immunol. 6 (2015). https://doi.org/10.3389/fimmu.2015.00183.

[69] M.J.A. Amar, W. D'Souza, S. Turner, S. Demosky, D. Sviridov, J. Stonik, J. Luchoomun, J. Voogt, M. Hellerstein, D. Sviridov, A.T. Remaley, 5A Apolipoprotein Mimetic Peptide Promotes Cholesterol Efflux and Reduces Atherosclerosis in Mice, The Journal of Pharmacology and Experimental Therapeutics 334 (2010) 634–641. https://doi.org/10.1124/jpet.110.167890.

[70] A. Chattopadhyay, M. Navab, G. Hough, F. Gao, D. Meriwether, V. Grijalva, J.R. Springstead, M.N. Palgnachari, R. Namiri-Kalantari, F. Su, B.J. Van Lenten, A.C. Wagner, G.M. Anantharamaiah, R. Farias-Eisner, S.T. Reddy, A.M. Fogelman, A novel approach to oral apoA-I mimetic therapy, Journal of Lipid Research 54 (2013) 995–1010. https://doi.org/10.1194/jlr.M033555.

[71] A.T. Remaley, F. Thomas, J.A. Stonik, S.J. Demosky, S.E. Bark, E.B. Neufeld, A.V. Bocharov, T.G. Vishnyakova, A.P. Patterson, T.L. Eggerman, S. Santamarina-Fojo, H.B. Brewer, Synthetic amphipathic helical peptides promote lipid efflux from cells by an ABCA1-dependent and an ABCA1-independent pathway, Journal of Lipid Research 44 (2003) 828–836. https://doi.org/10.1194/jlr.M200475-JLR200.

[72] M.I. Lobanov, N.S. Bogatyreva, O.V. Galzitskaia, [Radius of gyration is indicator of compactness of protein structure], Mol Biol (Mosk) 42 (2008) 701–706.

[73] E. Durham, B. Dorr, N. Woetzel, R. Staritzbichler, J. Meiler, Solvent accessible surface area approximations for rapid and accurate protein structure prediction, J Mol Model 15 (2009) 1093–1108. https://doi.org/10.1007/s00894-009-0454-9.

CHAPTER 6

Summary, Conclusion and Future prospects

CHAPTER 6

Summary, Conclusion and Future prospects

6.1. Graphical Summary

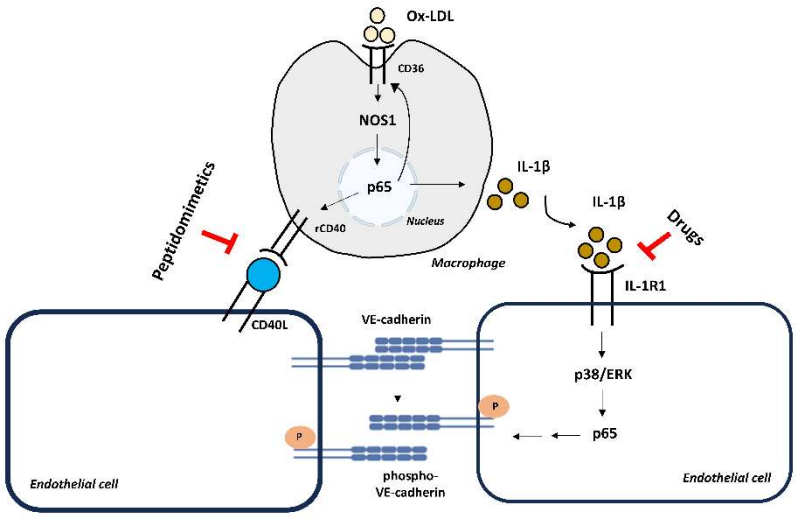

Figure 6.1. Overall summary of the work. Figure depicting the overall summary of the work. Uptake of Ox-LDL leads to the activation of NOS1 which further leads to activation of p65 and other inflammatory mediators such as IL-1β and CD40 receptor on the macrophage. The figure illustrates the targeting of IL-1β/IL-1R1 and CD40-40L interaction by small molecule inhibitors and therapeutic peptide, thereby reducing the disease pathogenesis.

6.2. Concluding points:

1. Nitric Oxide Synthase -1 (NOS1) plays an important role in mediating the foam cell formation and generation of nitric oxide in the macrophage in response to OxLDL stimulation. Ox-LDL stimulation in the RAW264.7 macrophage led to phosphorylation of NOS1 and translocation of p65 into the nucleus at 2-hour time point. TRIM treatment led to decrease in the NOS1 phosphorylation and p65 translocation, confirming the central role played by NOS1 in mediating the disease progression

2. Phosphorylation of NOS1 and subsequent translocation of p65 into the nucleus led to increase in the expression of pro-inflammatory cytokines such as TNF-α and IL-1β. It also led to increase in the inflammatory markers such as CD36 and CD40 receptor on the surface of the macrophage. This leads to the conclusion that NOS1 mediated p65 activation and translocation into the nucleus leads to expression of inflammatory mediators, further aggravating the disease progression.

3. Secretion of IL-1β by the macrophage binds to the IL-1R1 receptor present on the endothelial cell. Activation of IL-1R1 signalling axis further leads to changes in the membrane permeability of the endothelial cells as observed by the IL-1β induced VE-cadherin degradation and decrease in the electrical resistance of the membrane.

4. IL-1β induced IL-1R1 activation leads to activation of signalling cascade including of MAPK Cascade such as ERK and p38. These leads to downstream phosphorylation and activation of p65 which further is involved in pathway mediating the VE-cadherin degradation.

5. Computational analyses for the therapeutic inhibitors targeting the interaction between IL-1β and IL-1R1 led to identification of Radotinib and Lomitapide as a key inhibitor which might be involved in the inhibition of this interaction. Experimental analyses indicated increased electrical resistance and increase in the cell surface VE-cadherin expression in response to the drugs and IL-1β co-treatment. Also, lomitapide led to decrease in the ERK and p38 activation and subsequent decrease in the p65 activation. These results suggest that both radotinib and lomitapide can be a useful therapeutic entity targeting the IL-1β/IL-1R1 signalling axis.

6. Analyses of the CD40-40L interaction led to identification of key residues involved in the interaction. This led to designing of therapeutic peptide inhibiting this interaction by binding to the key residues on the CD40 receptor. Further refinement to increase the binding efficiency and better ADMET properties led to identification of three peptidomimetics derivatives with improved binding affinity and physicochemical characteristics. Furthermore, molecular dynamics simulation showed better stability with the receptor, thus confirming the peptidomimetic derivatives as a useful therapeutic strategy against the CD40-40L interaction.

6.3. Conclusion:

The current study deals with the identification of NOS1 as a central regulator for the Ox-LDL induced p65 activation and subsequent activation of pro-inflammatory mediators such as IL-1β, CD40 and CD36 receptor on the macrophage. Furthermore, it also deals with the identification of the therapeutic entities targeting the IL-1β/IL-1R1 and CD40-40L interactions by repurposed small molecule inhibitors and peptidomimetic derivatives respectively to ameliorate the disease progression.

Macrophage plays an important role in mediating the atherosclerosis disease progression. Oxidation of low-density lipoproteins (LDL) in the intimal region of the arteries leads to generation of oxidised LDL species (Ox-LDL). Ox-LDL binds to the scavenger receptor present on the macrophage such as CD36 receptor, further leading to its phagocytosis and engulfment inside the macrophage. Nitric oxide plays an important role in the pathogenesis of the disease. Nitric oxide produced from Nitric oxide synthase (NOS) plays an important role in vascular diseases. In that regard, the current study explored the role of NOS1-derived Nitric oxide production and its effect on the macrophage in foam cell formation. The study identified that ox-LDL led to production of NOS1-derived NO with increase in the NOS1 phosphorylation and ox-LDL uptake by the macrophage. Uptake of ox-LDL led to translocation of p65 into the nucleus, which further led to expression of pro-inflammatory cytokines and inflammatory mediators such as IL-1b, CD36 and CD40 receptor. Expression of these pro-inflammatory mediators further enhanced the disease progression by acting on the endothelial cell, leading to various physiological consequences such as recruitment of immune cells (via CD40 receptor), endothelial permeability (via IL-1β) and uptake of ox-LDL by the macrophage (via CD36 receptor).

Furthermore, the study explored the intrinsic role played by IL-1β on the endothelial cell. Release of IL-1β by the macrophage leads to its binding

with the IL-1R1 receptor present on the endothelial cell. These receptor-ligand interaction leads to activation of inflammatory signalling cascade such as MAPK cascade containing p38 and ERK, which further lead to activation of p65 in the endothelial cell. Activation of p65 leads to signalling events leading to phosphorylation of VE-cadherin on the surface. VE-cadherin phosphorylation leads to its internalisation inside the cells, thereby reducing the VE-cadherin expression on the surface and leading to permeability of membrane on the endothelial cell. Therefore, inhibiting the IL-1β/IL-1R1 interaction might be beneficial in the context of reducing the pathogenesis of the disease.

Therefore, to inhibit the IL-1β/IL-1R1 interaction, we explored for the therapeutic entities which can inhibit this interaction. Screening of FDA-approved and plant natural compound libraries led to identification of two molecules (i.e. Radotinib and Lomitapide) which bounded to the active site of the receptor, thereby inhibiting the receptor-ligand interaction. Further in-silico analyses found better stability and binding efficiency with the receptor compared to positive control. In-vitro analyses of the compounds showed reduction in the permeability of the endothelial cell, with increase in the surface expression of the VE-cadherin. Also, lomitapide showed decrease in the activation of MAPK cascade molecules such as ERK and p-38, which further led to decrease in the p65 activation. These led to conclude that the compounds were effective in neutralising the IL-1β mediated effect on the endothelial cell.

CD40-40L interaction also plays an important role in mediating the interaction between immune cells and endothelial cells. This leads to expression of cell adhesion molecule leading to invasion of immune cell into the intima and disease progression. Therefore, to target the CD40-40L interaction, we designed therapeutic peptide against the CD40 receptor. The peptide showed good binding with the critical residues of the receptor, but the ADMET analyses showed hepatoxicity associated with it. Therefore, we identified peptidomimetic with improved ADMET properties compared to peptide. To further increase the binding

affinity and ADMET properties, we identified peptidomimetic derivatives which had better binding efficiency and better ADMET properties compared to peptidomimetic structure. The identified peptidomimetics also possessed good stability with the receptor. Thus, these peptidomimetics derivatives need to be further validated through in-vitro and in-vivo analyses to identify as a therapeutic entity against the CD40-40L interaction

6.4. Future Prospects

Although the current study identified the novel role of NOS-1 in mediating the foam cell formation in the macrophage and therapeutic entities targeting IL-1β/IL-1R1 and CD40-40L axis, certain limitations remain which can be further explored:

6.4.1. Signalling intermediates involved in NOS1 induced foam cell formation and p65 activation

Although the study identified the role of NOS1 in foam cell formation and p65 activation, signalling intermediates involved in the activation of NOS1 and the mechanism of NOS1 mediated p65 activation remains to be explored. Identifying this signalling mechanism might provide a clear view of the involvement of the NOS1 in the disease pathogenesis.

6.4.2. Experimental validation of the effect of NOS1 in ApoE KO mice

The limitation with the current study is the identification of NOS1-mediated mechanism in the in-vitro cell culture model. Further replicating the same results in the ApoE KO mice model will justify the crucial role played by NOS1 in the disease pathogenesis of atherosclerosis.

6.4.3. Precise identification of the binding mechanism of the IL-1R1 inhibitors

Although, the study identified the therapeutic entities targeting the IL-1β/IL1R1 interaction, certain limitations still remain. Firstly, the experimental validation was largely confined to in vitro endothelial models. Validation through animal model is needed to confirm the efficacy, pharmacokinetics, and safety profile of the drug. Second, although computational studies strongly suggested direct binding of the drugs with the IL-1R1 receptor, experimental validation through methods such as surface plasmon resonance or isothermal titration calorimetry is necessary. Also, the broader off-target effects of these drugs need careful evaluation in context of long-term therapeutic use.

6.4.4. Experimental validation of the therapeutic peptide and peptidomimetic inhibitors against the CD40-40L interaction

In-silico analyses of the therapeutic peptide and peptidomimetic inhibitor showed good binding efficiency with the receptor with better ADMET properties. Although the current study was limited to in-silico analyses, further in-vitro and in-vivo studies remains to be explored to better characterise the therapeutic peptide and peptidomimetic inhibitor as a CD40-40L inhibitors.

APPENDIX

Supplementary Figures and Tables

APPENDIX

Appendix A: Supplementary Figures

Chapter 4: NOS1 mediated IL-1β activation and small molecule inhibitors targeting IL-1β and IL-1R1 interaction

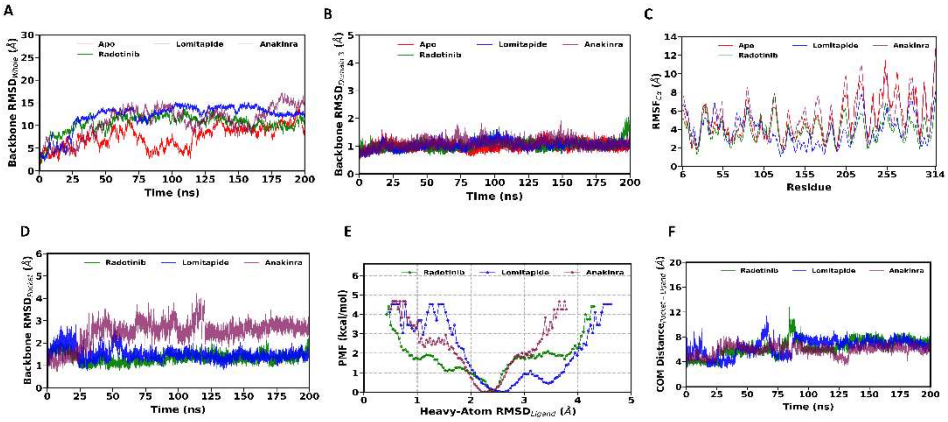

Supplementary figure S4.1. Structural and energetic analysis of IL-1R1 in complex with radotinib, lomitapide, and anakinra. (A) Backbone RMSD of whole protein backbone, (B) Backbone RMSD of domain 1 and 2, C.) Cα-RMSF of residues across the protein, (D) Backbone RMSD of binding pocket region, (E) Potential of mean force (PMF) versus heavy-atom RMSD of the ligands, (F) Distance between the center of mass (COM) of the binding pocket and the ligand

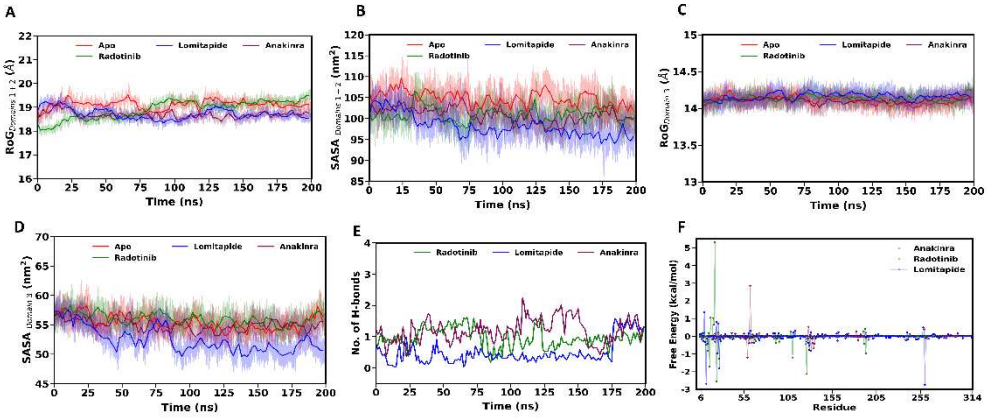

Supplementary figure S4.2. Structural and energetic analysis of IL-1R1 in complex with radotinib, lomitapide, and anakinra. (A) Radius of gyration (RoG) of domain 1 and 2, (B) Solvent-accessible surface area (SASA) of domain 1 and 2, (C) Radius of gyration (RoG) of domain 3, (D) Solvent-accessible surface area (SASA) of domain 3, (E) Number of hydrogen bonds formed between protein and ligands over time, (F) Per-residue free energy decomposition showing contributions of key residues to ligand binding

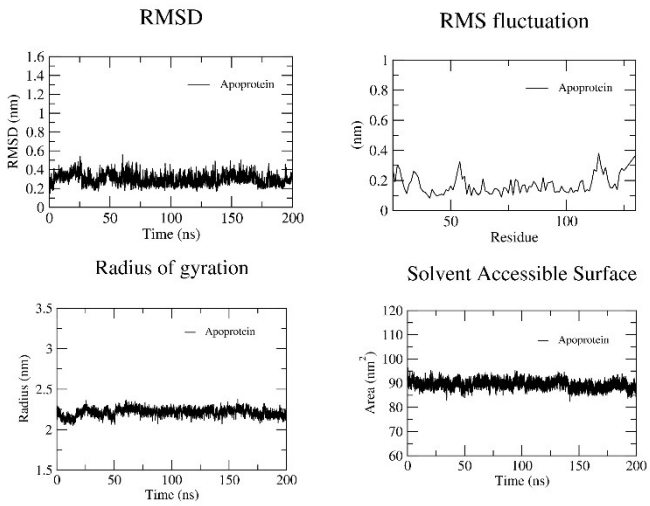

Supplementary Figure S5.1. Molecular Dynamic Simulation of the CD40 receptor (apo protein). Figure depicting the RMSD, RMSF, Rg and SASA values of the apo CD40 receptor.

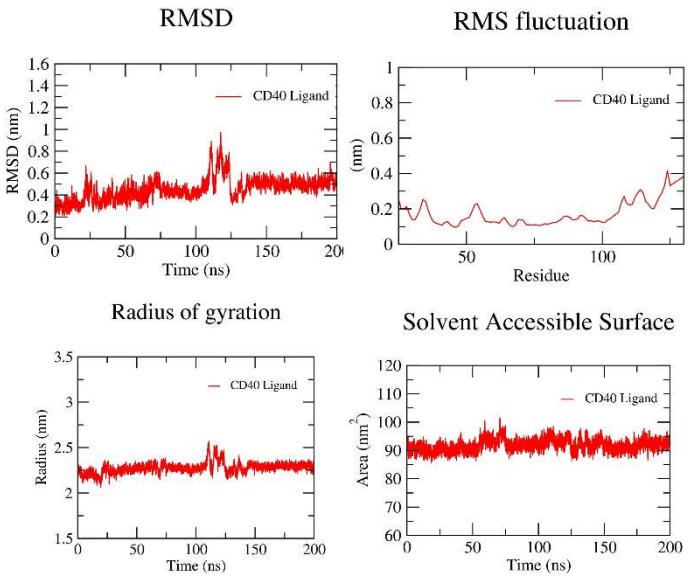

Supplementary Figure S5.2. Molecular Dynamic Simulation of the CD40 receptor with CD40 ligand. Figure depicting the RMSD, RMSF, Rg and SASA values of the CD40 ligand with the CD40 receptor.

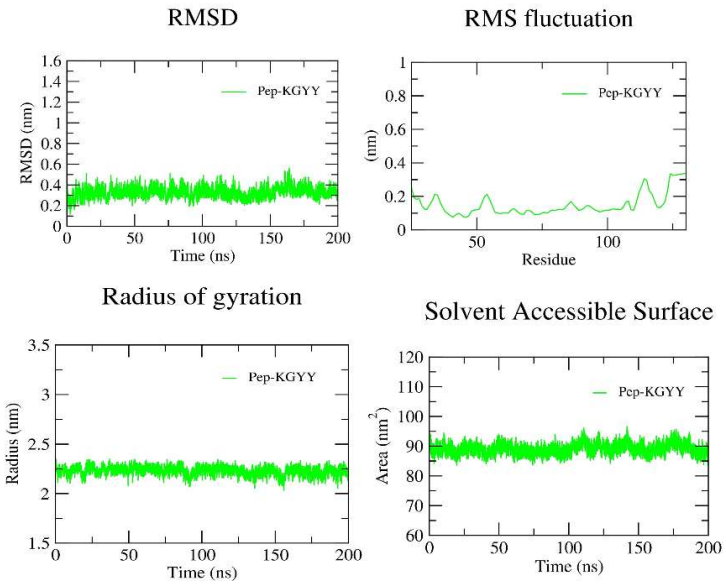

Supplementary Figure S5.3. Molecular Dynamic Simulation of peptide (p-KGYY) with the CD40 receptor. Figure depicting the RMSD, RMSF, Rg and SASA values of the peptide (p-KGYY) with the CD40 receptor.

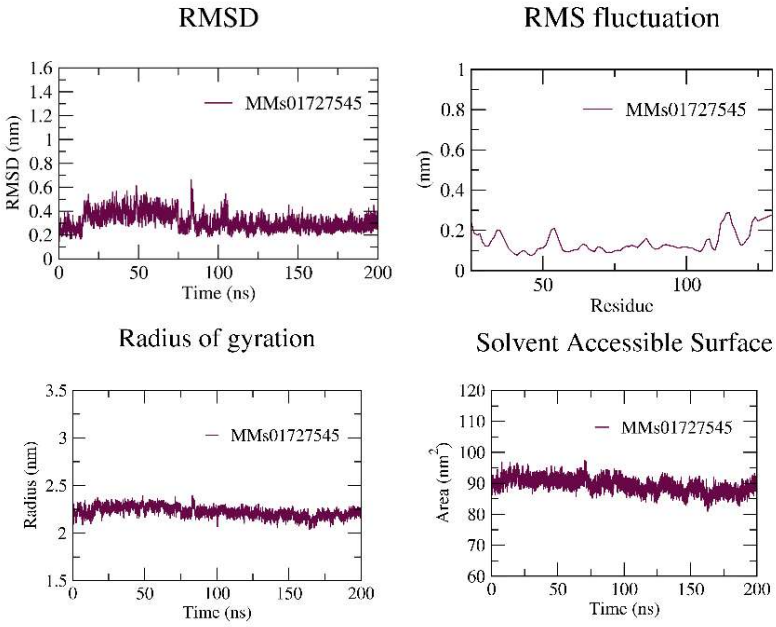

Supplementary Figure S5.4. Molecular Dynamic Simulation of peptidomimetic (MMs01727545) with the CD40 receptor. Figure depicting the RMSD, RMSF, Rg and SASA values of the peptide (MMs01727545) with the CD40 receptor.

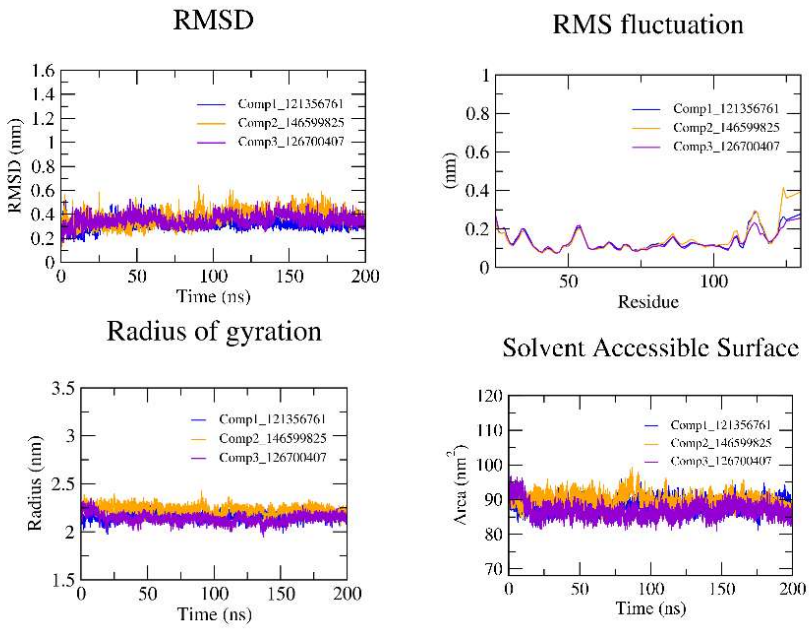

Supplementary Figure S5.5. Molecular Dynamic Simulation of the three peptidomimetic derivatives with the CD40 receptor. Figure depicting the RMSD, RMSF, Rg and SASA values of the three peptidomimetic derivatives with the CD40 receptor.

Appendix B: Supplementary Tables

Chapter 3: Role of NOS1 in different diseases and macrophage foam cell formation in atherosclerosis

Supplementary Table S3.1. Primers sequences used for qRT-PCR

Primers	Forward primer	Reverse primer
GAPDH	5'-GCACAGTCAAGGCCGAGAAT-3'	5'-GCCTTCTCCATGGTGGTGAA-3'
IL-1β	5'-TGCCACCTTTTGACAGTGATG-3'	5'-AAGGTCCACGGGAAAGACAC-3'
TNF-α	5'-AGGCACTCCCCCAAAAGATG-3'	5'-CCACTTGGTGGTTTGTGAGTG-3'

Table S4.1: Average metrics from the last 100 ns of production trajectories across all systems, with standard deviations in parentheses.

Metric	Apo	Radotinib Complex	Lomitapide Complex	Anakinra Complex
Backbone RMSD (Whole) (Å)	8.81 (2.06)	10.84 (0.99)	13.49 (0.81)	12.21 (2.12)
Backbone RMSD (Domains 1+2) (Å)	1.98 (0.30)	2.46 (0.21)	2.09 (0.18)	1.99 (0.22)
Backbone RMSD (Domain 3) (Å)	1.02 (0.11)	1.08 (0.16)	1.07 (0.12)	1.11 (0.14)
Backbone RMSD (Binding Pocket) (Å)	-	1.40 (0.18)	1.43 (0.15)	2.66 (0.31)
Ligand-Protein Distance (Å)	-	7.97 (0.79)	7.19 (0.53)	5.61 (0.98)
Radius of Gyration (Domains 1+2) (Å)	19.16 (0.17)	19.20 (0.17)	18.69 (0.19)	18.65 (0.15)
Radius of Gyration (Domain 3) (Å)	14.08 (0.07)	14.13 (0.07)	14.17 (0.07)	14.10 (0.06)
Solvent-Accessible Surface Area (Domains 1+2) (nm^2)	104.24 (2.42)	100.89 (2.31)	96.84 (2.35)	99.91 (2.23)
Solvent-Accessible Surface Area (Domain 3) (nm^2)	54.81 (1.47)	55.59 (1.34)	51.14 (1.39)	54.56 (1.29)

Table S4.2: MM/PBSA-based binding free energy components of the simulated complexes in kcal/mol. The standard errors of the mean are listed in parentheses alongside the average values.

System	ΔE_{vdW}	ΔE_{elec}	ΔG_{pol}	ΔG_{np}	ΔG_{bind}
Anakinra Complex	-43.00 (0.09)	-19.62 (0.39)	47.81 (0.37)	-4.34 (0.01)	-19.15 (0.13)
Radotinib Complex	-56.76 (0.10)	-14.63 (0.10)	48.31 (0.13)	-5.31 (0.01)	-28.38 (0.11)
Lomitapide Complex	-50.11 (0.08)	-124.97 (0.43)	143.03 (0.36)	-5.34 (0.01)	-37.39 (0.15)

ΔE_{vdW}, ΔE_{elec}, ΔG_{pol}, and ΔG_{np}, respectively, indicate the van der Waals, electrostatic, polar solvation free energy, and non-polar solvation free energy components of the binding free energy, while ΔG_{bind} represents the binding free energy. The entropy calculations have been avoided due to high computational cost.

Table S4.3: Analysis of hydrogen bond formation through the molecular dynamics' simulations. Only hydrogen bonds with an occupancy greater than 10% are shown.

Acceptor	Donor	Dist.	Angle	Occupancy (%)
Anakinra Complex				
Lig@O2	Asn136@N	2.89	151.55	22.03
Lys132@O	Lig@N2	2.85	152.45	26.79
Radotinib Complex				
Gly122@O	Lig@N3	2.84	156.97	16.03
Lomitapide Complex				
Glu11@OE2	Lig@N1	2.74	162.53	10.48

Table S4.4: Residue-wise binding free energy (kcal/mol) decomposition of the crucial contributing residues.

Residue	E_{vdW} (kcal/mol)	E_{elec} (kcal/mol)	G_{pol} (kcal/mol)	G_{np} (kcal/mol)	G_{total} (kcal/mol)
Anakinra Complex					
Hie60	-3.02	-1.63	3.44	0	-1.20
Lys132	-1.86	-2.76	3.81	0	-0.82
Asn135	-0.52	-1.35	1.18	0	-0.69
Radotinib Complex					
Arg25	-3.12	-9.66	10.23	0	-2.56
Tyr127	-4.13	0.58	1.42	0	-2.13
Ser17	-1.67	-1.15	1.11	0	-1.71
Pro28	-1.98	-1.19	1.90	0	-1.27
Phe111	-1.49	-0.35	0.64	0	-1.20
Arg194	-1.75	-2.51	3.28	0	-0.98
Leu15	-1.09	-0.18	0.46	0	-0.81
Phe130	-0.61	-0.32	0.42	0	-0.51
Lomitapide Complex					
Tyr261	-3.55	-1.18	1.98	0	-2.75
ILe13	-2.78	0.15	-0.06	0	-2.68
Pro28	-2.84	0.39	0.63	0	-1.82
Pro26	-1.62	-1.30	1.96	0	-0.97
Phe130	-1.02	0.28	-0.02	0	-0.76

Chapter 5: Novel peptide inhibitors targeting CD40 and CD40L interaction: a potential for atherosclerosis therapy

Supplementary Table S5.1. Physicochemical and ADMET analysis of peptide

Parameters		KGYY
Physiochemical parameters	M.W.	531.61
	LogP	-1.92
	Rotatable bond	15
	Acceptor bond	6
	Donor bond	8
Absorption	Water Solubility	-3.086
	Caco2 permeability	-0.26
	Intestinal absorption	6.574
	Skin permeability	-2.735
Distribution	Fraction unbound	0.39
	BBB permeability	-0.692
	CNS permeability	-4.368
Metabolism	CYP2D6 substrate	No
	CYP2D6 inhibitor	No
Excretion	Total Clearance	1.094
Toxicity	AMES toxicity	No
	Hepatotoxicity	Yes
	Skin sensitization	No

Water solubility (logS)- defines solubility in water at 25 °C; Skin permeability- $\log kp > -2.5$ classifies low skin permeability; Fraction unbound- defines unbound state in plasma protein remaining for pharmacological action; BBB permeability- $\log BB < -1$ classifies poorly distributed to the brain; CNS permeability- $\log PS > -2$ classifies CNS penetration and $\log PS < -3$ classifies no CNS penetration; Total clearance- includes both hepatic and renal clearance

Supplementary Table S5.2. ADMET analysis of peptidomimetic (MMs01727545)

Parameters		MMs01727545
Physiochemical parameters	M.W.	812.8
	LogP	1.7
	Rotatable bond	9
	Acceptor bond	15
	Donor bond	5
Absorption	Water Solubility	-3.073
	Caco2 permeability	0.368
	Intestinal absorption	71.983
	Skin permeability	-2.735
Distribution	Fraction unbound	0.173
	BBB permeability	-1.925
	CNS permeability	-4.195
Metabolism	CYP2D6 substrate	No
	CYP2D6 inhibitor	No
Excretion	Total Clearance	1.274
Toxicity	AMES toxicity	No
	Hepatotoxicity	Yes
	Skin sensitization	No

Water solubility (logS)- defines solubility in water at 25 °C; Skin permeability- logkp > -2.5 classifies low skin permeability; Fraction unbound- defines unbound state in plasma protein remaining for pharmacological action; BBB permeability- logBB < -1 classifies poorly distributed to the brain; CNS permeability- logPS > -2 classifies CNS penetration and logPS < -3 classifies no CNS penetration; Total clearance- includes both hepatic and renal clearance

Supplementary Table S5.3. Average metrics calculated using the 200 ns of production run trajectories, with standard deviations in parentheses.

Metric	Apo	CD40L	peptide	peptido mimetic	Comp 1	Comp2	Comp3
Protein RMSD (nm)	0.297636 (0.0554002)	0.450865(0.102845)	0.324422 (0.0518505)	0.31285 (0.0709637)	0.316812 (0.041539 1)	0.377597 (0.0641409)	0.348178 (0.0470708)
Radius of Gyration (nm)	2.21312 (0.0463692)	2.27648 (0.0573152)	2.22748 (0.0432464)	2.22366 (0.0518362)	2.16855 (0.039985)	2.23019 (0.0439244)	2.13952 (0.044533)
Solvent-Accessible Surface Area (nm^2)	89.4292 (1.67674)	91.825 (2.04208)	89.0813 (1.77758)	89.3604 (2.26223)	88.3128 (1.70471)	89.7115 (1.94118)	86.7775 (2.17026)

Thesis

ORIGINALITY REPORT

2%	1%	2%	1%
SIMILARITY INDEX	INTERNET SOURCES	PUBLICATIONS	STUDENT PAPERS

PRIMARY SOURCES

1	dspace.iiti.ac.in:8080 Internet Source	1%
2	Systems Biology of Free Radicals and Antioxidants, 2014. Publication	1%
3	Sajjan Rajpoot, Ashutosh Kumar, Vadim Gaponenko, Teresa LM Thurston et al. "Dorzolamide suppresses PKCδ -TIRAP-p38 MAPK signaling axis to dampen the inflammatory response", Future Medicinal Chemistry, 2023 Publication	1%

Exclude quotes	On	Exclude matches	< 1%
Exclude bibliography	On		